



UNIVERSITY OF
BIRMINGHAM

**Design and Synthesis of *N*-Containing Bicyclic
Scaffolds for Library Generation**

By

Órla M. Conway

A thesis submitted to University of Birmingham for a degree of

DOCTOR OF PHILOSOPHY

School of Chemistry

College of Engineering and Physical Sciences

University of Birmingham

March 2022

UNIVERSITY OF
BIRMINGHAM

University of Birmingham Research Archive

e-theses repository

This unpublished thesis/dissertation is copyright of the author and/or third parties. The intellectual property rights of the author or third parties in respect of this work are as defined by The Copyright Designs and Patents Act 1988 or as modified by any successor legislation.

Any use made of information contained in this thesis/dissertation must be in accordance with that legislation and must be properly acknowledged. Further distribution or reproduction in any format is prohibited without the permission of the copyright holder.

Abstract

In recent years, the field of drug discovery has begun to move away from targets which have traditionally been deemed “druggable” and has placed a focus on the exploration of novel areas of chemical space. However, efforts to access these challenging targets have been continually afflicted with low hit rates in early-stage discovery and subsequently high rates of attrition during clinical trials. Numerous studies have found that a lack of scaffold diversity coupled with poor physiochemical properties regarding bioavailability are major factors contributing to the high compound failure rates.

In order to circumvent these issues, drug discovery strategies such as lead- and diversity-orientated synthesis approaches have been developed to control and direct the molecular properties of compounds within a screening library to occupy relevant, under-explored areas of chemical space while synthesising structurally complex and diverse compound collections.

This thesis reports the development of a step-efficient and robust synthetic route for the synthesis of bicyclic, *N*-heterocycle-containing scaffolds with stereochemical control. The designed methodology takes stereochemically controlled 2,4-*cis*-azetidine rings and through a series of high-yielding transformations gives rise to two distinct bicyclic scaffolds; a 4,6-fused system and a 5,6-bridged system (**Figure (i)**). In silico library enumeration was carried out on these novel scaffolds using data analytics software to yield large sets of virtual compounds which were filtered based on their molecular properties to great small diverse sets for the creation of drug-like screening libraries.

The novel scaffold systems were decorated using a diversity-orientated synthesis approach to access 177 compounds which display a high degree of structural diversity and three

dimensionality and possess inherently drug-like molecular properties. The resultant compounds have been submitted for early-stage biological screening and preliminary results show that several members of the novel compound libraries display a biologically significant effect on the rate of bacterial growth.

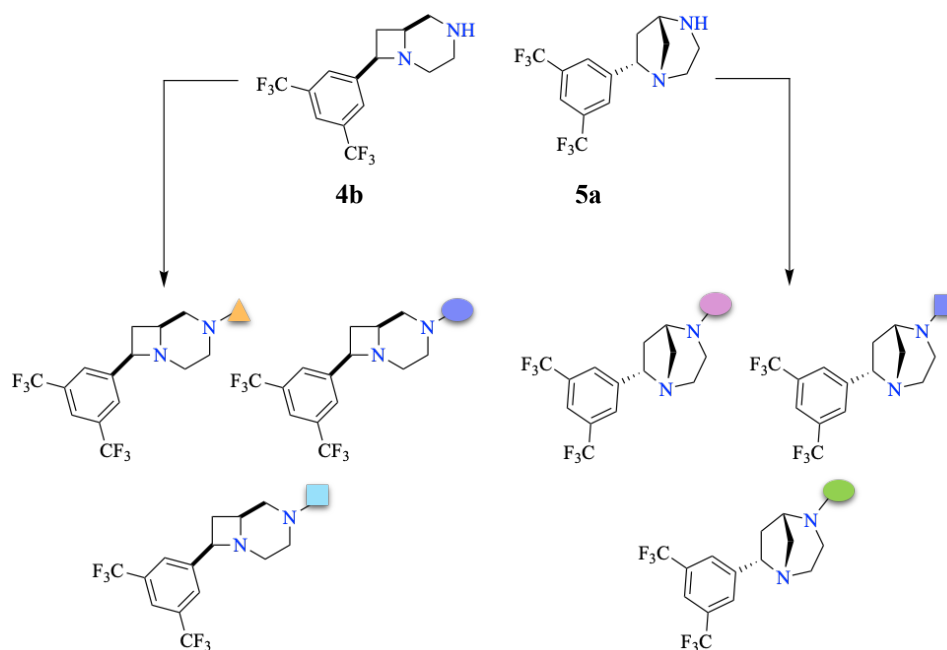


Figure (i). Two novel scaffold moieties, the 4,6-fused and the 5,6-bridged scaffold, have been synthesised and have been decorated to create two diverse compound libraries which are structurally complex and stereochemically diverse to populate underexplored areas of chemical space. The resultant novel compound libraries have been designed to be inherently drug-like with a high degree of three-dimensionality to explore under-utilised areas of chemical space.

Acknowledgements

Firstly, I would like to thank Prof. John. S. Fossey, for giving me the opportunity to undertake this PhD under his supervision and for offering his advice and support over the last three and a half years. I would also like to thank Marjon Bolster for sharing her extensive chemistry knowledge and offering unwavering support throughout this project, in particular, during my time in The Netherlands. I would also like to mention Dr. Paul Davies who supported me through the viva process, without your help that upsetting and confusing time would have been significantly harder to navigate.

Thank you to Dr. Liam Cox, for overseeing and co-ordinating such a varied and challenging programme, your work was greatly appreciated by us all. I would like to thank Dr. Jorg Benningshof for managing the industrial portion of this project. A special thanks to Dr. Phil Craven and Luke Jones for working so closely with the iDesign project in order to keep it running smoothly and for always being a friendly face when needed.

To my fellow iDesign students, thank you all for the making the last few years and all of the experiences within incredibly memorable. In particular, Ale and Sam, without you both my time in The Netherlands would have been significantly less enjoyable – thank you for the lunch breaks, the late-night lab music and the excel induced breakdowns, somehow, we survived it all.

My thanks go out all the members of the Fossey Group, past and present, who have always gone above and beyond to offer advice and guidance in the lab. Huy, who always had a smile and some form of confectionary to brighten up the toughest of days, thank you for every word of encouragement. Fernanda, Yixin and Yiming, thank you for friendliness during my first

weeks, it was massively appreciated. Thanks to Holly for all your feedback and for all your work supporting the project. Harry, thank you for joining the azetidine club, your commiserations when yet another reaction failed in those early days were welcomed and needed, I'm still not convinced they exist. Alex, thank you for becoming one of my most valued friends, for making me laugh daily and for wholeheartedly supporting my tea dependency. George, thank you for being a truly fantastic postdoc, both your humour and your willingness to give honest and constructive feedback was truly appreciated.

To the Parallel Group at Symeres, in particular Dr. Rik Megens, Dr. Robin Doodeman and Wouter Nieuwstraten for your continued support, encouragement and innovative ideas. Stefan and Jarno, thank you for making my time in the lab significantly more fun and thank you to Floor for teaching me more about excel than I thought it possible to know. A special thanks to the analytical team, particularly Jan, Gijs, Ilonka and Eef for always being open to questions and for working so hard to get the necessary results.

To all of the wonderful people I met during my time at Birmingham, thank you for the toxic Büchi chats and for dragging me to the Staff House on Friday evenings, I needed it. A special mention to Izzy Barker for being a fantastic friend and for never talking me out of an online order.

Rose and Ailbhe, thank you for your unwavering support and love over the last few years. Lorna and Jen, thank you both for being such fantastic friends and for encouraging me when I needed it. Gemma, thank you for always being there, no matter what continent we're on, your constant support and willingness to listen to me complain about every little inconvenience is more appreciated than you could know. Shauna and Aoife, my glasgals, despite only knowing

you both for such a short amount of time I am forever grateful for our friendship. Thank you both for getting me through this write up, I think I would have gone mad somewhere along the way if we hadn't discovered the cathartic effect of an evening spent in Kothel.

Kyle, you have been a constant and unwavering source of support and reassurance throughout my PhD and I couldn't have done it without you by my side. Thank you for every encouraging word, hug and cup of tea, your support has been more appreciated than you could ever know. You are a truly incredible person, and I cannot wait to watch you achieve everything you set your mind to in the years to come.

Finally, to my family, thank you for all your support, throughout my life, but especially throughout these last few years. Thank you for always going above and beyond to support me and for being there when I needed it the most. Thank you for every phone call, every early morning trip to the airport, every welcome home (and every tail wag). I would not be the person I am today if I didn't have you all behind me.

“Everything is theoretically impossible until it is done”

Robert A. Heinlein

For John,

I wish you could have seen this thesis in its final form, and I can only hope you would be proud of how it turned out, hanging bonds and all.

Abbreviations

2D	two-dimensional
3D	three-dimensional
Ac	Acetyl
AcOH	Acetic acid
Aq.	Aqueous
Bn	Benzyl
CADD	Computer-aided drug design
Cald.	Calculated
DCM	Dichloromethane
dd	Doublet of doublets
ddd	Doublet of doublet of doublets
ddt	Doublet of doublet of triplets
DIAD	Diisopropyl azodicarboxylate
DMF	<i>N,N</i> -Dimethylformamide
DMSO	Dimethylsulfoxide
DOS	Diversity-orientated synthesis
Eq	Equivalents
FDA	Food and Drug Administration
h	Hours
HBA	Hydrogen Bond Acceptor
HBD	Hydrogen Bond Donor
HCA	Hierarchical cluster analysis
hept	Heptet
hERG	Human ether-à-go-go related gene
HMBC	Heteronuclear Multiple Bond Correlation
HPLC	High performance liquid chromatography
HSQC	Heteronuclear Single Quantum Coherence
HTS	High throughput screening
IC ₅₀	Half maximal inhibitory concentration
<i>J</i>	Coupling Constant
KOH	Potassium hydroxide

LAH	Lithium aluminium hydride
LCMS	Liquid chromatography-mass spectrometry
LiHMDS	Lithium bis(trimethylsilyl)amide
LQTS	Long QT syndrome
MIC ₉₉	Minimum inhibitory concentration
Ms	Methanesulfonyl
NBS	<i>N</i> -Bromosuccinimide
NCE	New Chemical Entity
NCS	<i>N</i> -Chlorosuccinimide
NIS	<i>N</i> -Iodosuccinimide
NOE	Nuclear overhauser effect
Ns	Nosyl (nitrobenzenesulfonyl)
PA	Picolinamide
PBF	Plane of Best Fit
PC	Principal component
PCA	Principal Component Analysis
PIDA	Phenyliodide(III) diacetate
PMI	Principal Moment of Inertia
q	Quartet
Ro5	Rule of Five
rt	Retention time
RT	Room temperature
s	Singlet
SDF	Spatial data file
SMILES	Simplified molecular-input line-entry system
STAB	Sodium triacetoxymethylborohydride
t	triplet
THF	Tetrahydrofuran
TPPO	Triphenylphosphine oxide
TPSA	Topological Polar Surface Area
Ts	Tosyl
TsOH	<i>p</i> -toluenesulfonic acid
UPLC	Ultra-performance liquid chromatography

Table of Contents

<i>Abstract</i>	<i>v</i>
<i>Acknowledgements</i>	<i>viii</i>
<i>Abbreviations</i>	<i>xiv</i>
Chapter 1: Introduction	xxi
1.1. Introduction to Azetidines	1
1.1.1. Structure and Properties of Azetidine Rings	1
1.1.2. Metal-catalysed Synthesis of Azetidines	3
1.1.3. Cyclisation <i>via</i> Nucleophilic Substitution	7
1.1.4. Intramolecular Cyclisation towards Azetidines	9
1.1.5. Iodine-mediated Heterocyclic Ring formation	13
1.2. Biological Applications of Azetidines	21
1.2.1. Azetidines in Natural Products	21
1.2.2. Azetidines in Pharmaceutical Agents	22
1.3. Challenges in the Pharmaceutical Industry	25
1.4. Drug-Likeness: Properties Necessary for Successful Hits	29
1.5. Compound Dimensionality: Importance and Analysis	33
1.5.1. Fraction of sp^3 Centres (F_{sp^3})	33
1.5.2. Plane of Best Fit (PBF).....	36
1.5.3. Principal Moments of Inertia (PMI)	38
1.5.4. Principal Component Analysis (PCA).....	39
1.6. Privileged Structures in Drug Discovery	40
1.7. Diversity Oriented Synthesis	42
1.8. Aims and Objectives	46
Chapter 2: Towards a Bicyclic Scaffold	49
2.1. Synthesis of Azetidines	50
2.1.1. Iodine Mediated Cyclisation of Homoallylic Amines	50
2.2.2. Synthesis of Amino Azetidines.....	59
2.2. Synthesis of a Bicyclic Scaffold	62
2.2.1. Palladium Chemistry	62
2.2.2. Ring Closing Metathesis	70
2.2.3. Reductive Amination	72
2.2.4. Fukuyama Mitsunobu Chemistry	77

2.2.5.	Appel-type Chemistry	82
2.2.6.	Increased Reaction Efficiency	90
2.2.7.	Isolation of the 5,6-Bridged Scaffold	94
Chapter 3: Library Design and Development		99
3.1.	Computational Tools in Library Design	100
3.1.1.	KNIME	100
3.1.2.	DataWarrior	108
3.2.	Library Development: Generation One Scaffolds	109
3.2.1.	CF ₃ Azetidine Library	110
3.2.2.	KNIME Pathway	110
3.3.3.	Synthesis and Outcome	114
3.3.4.	NO ₂ Azetidine Small Set	117
3.3.	Library Development: Generation Two Scaffolds	119
3.3.1.	4,6-Fused Scaffold: Decoration for Library Synthesis	119
3.3.2.	4,6-Fused Scaffold: Knime Pathway	120
3.3.3.	4,6-Fused Scaffold: Library Synthesis	124
3.3.4.	4,6-Fused Scaffold: Summary of Synthetic Results	129
3.3.5.	5,6-Bridged Scaffold: KNIME Pathway	132
3.3.6.	5,6-Bridged Scaffold: Library Synthesis	136
3.3.7.	5,6-Bridged Scaffold: Summary of Synthetic Results	138
3.4.	Biological Evaluation of Library Compounds	141
3.4.1.	hERG inhibition	141
3.4.2.	Anti-Tuberculosis Activity	145
3.5	Summary of Results	150
Chapter 4: Conclusion and Future Work		152
4.1.	Conclusion	153
4.2.	Future Perspectives	161
4.2.2.	Potential for Scaffold Variation	162
4.2.3.	Alternative Cyclisation Procedures	162
4.2.4.	Potential for Alternative Applications	163
Chapter 5: Experimental		164
5.1.	General Information	165
5.2.	General Procedures	169
5.2.1.	General Procedure A: Imine Synthesis	169
5.2.2.	General Procedure B: Homoallylic Amine Synthesis	169

5.2.3.	General Procedure C: Amino-azetidine Synthesis	169
5.2.4.	General Procedure D: <i>rac</i> -(6,8- <i>cis</i>)-8-phenyl-1,4-diazabicyclo[4.2.0]octane Synthesis (4,6-Fused Scaffold)	170
5.2.5.	General Procedure E: <i>rac</i> -(1,5- <i>cis</i> ,1,7- <i>trans</i>)-7-phenyl-1,4-diazabicyclo[3.2.1]octane Synthesis (5,6-Bridged Scaffold).....	171
5.2.6.	General Procedure F: Azetidine Library Synthesis	172
5.2.7.	General Procedure G: 4,6 Library Synthesis	172
5.2.8.	General Procedure H: 5,6 Library Synthesis	174
5.2.9.	General Procedure I: Inhibition of Bacterial Growth	175
5.3.	Characterisation Data	178
5.3.1.	Imines	178
5.3.2.	Homoallylic Amines.....	184
5.3.3.	Amino-Azetidines.....	195
5.3.4.	CF ₃ Amino-Azetidine Library.....	201
5.3.5.	NO ₂ Amino-Azetidine Set	208
5.3.6.	4,6-Fused Bicyclic Scaffolds	214
5.3.7.	4,6-Fused Scaffold Library.....	219
5.3.8.	5,6-Bridged Bicyclic Scaffolds.....	230
5.3.9.	5,6-Bridged Scaffold Library.....	234
5.3.	X-Ray Crystallography	246
5.4.1.	X-Ray Crystallography: General Information	246
5.4.2.	Crystal Data.....	246
6.	Bibliography.....	248
7.	Supplementary Information	259
7.1.	Representative NMR Spectra	259
7.1.1.	Representative NMR of Homoallylic Amine (Bis-Aryl)	259
7.1.2.	Representative NMR of Amino-Azetidine.....	261
7.1.3.	Representative NMR of Homoallylic Amine (Amino Ethanol)	263
7.1.4.	Representative NMR Spectra for 4,6-Fused Scaffold.....	265
7.1.5.	Representative NMR Spectra for Decorated 4,6-Fused Scaffold	267
7.1.6.	Representative NMR Spectra for 5,6-Bridged Scaffold	269
7.1.7.	Representative NMR Spectra of Decorated 5,6-Bridged Scaffold	271
7.2.	X-Ray Crystallography Tables.....	273
7.3.	Compounds Submitted for Biological Screening.....	280
7.4.	4,6 Fused Compound Library	300
7.5.	5,6-Bridged Compound Library	309

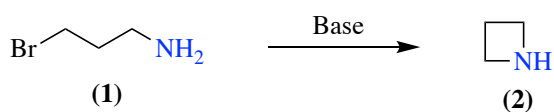
7.6. Knime Workflows.....	321
----------------------------------	------------

Chapter 1: Introduction

1.1.Introduction to Azetidines

1.1.1. Structure and Properties of Azetidine Rings

Azetidines are an important class of aza-heterocyclic scaffolds, with a polar-nitrogen atom embedded in a strained four-membered ring system, with a notable presence in both natural and synthetic products, displaying a range of biological activities.¹⁻³ While the ring strain associated with the azetidine ring (25.4 kcal/mol) is considerable,⁴ it lies between that of the three-membered aziridine derivative (27.7 kcal/mol), which are less stable and notably harder to handle, and the unreactive five-membered pyrrolidine ring (5.4 kcal/mol),^{4, 5} Azetidine **2** was first synthesised in towards the end of the 19th century by Gabriel and Weiner, through the cyclisation of γ -bromopropylamine under basic conditions as shown in **Scheme 1.1**.⁶



***Scheme 1.1.** The first reported synthesis of an azetidine ring was conducted through the cyclisation of γ -bromopropylamine under basic conditions.*

Azetidines were initially thought to be analogues of aziridines with limited practical usage, however, the difference in ring strain, geometry and general reactivity combined with the discovery of natural products such as azetidine-2-carboxylic acid resulted in a renewed interest in the four-membered ring system as a unique, under-utilised scaffold in organic synthesis and drug discovery. The structure and geometry of the azetidine ring was elucidated using electron diffraction⁷ and additional spectroscopic methods in the 1970s.⁸ Studies have shown the ring to be highly puckered with a dihedral angle (ϕ) of 33.1° (**Figure 1.1**).^{8, 9}

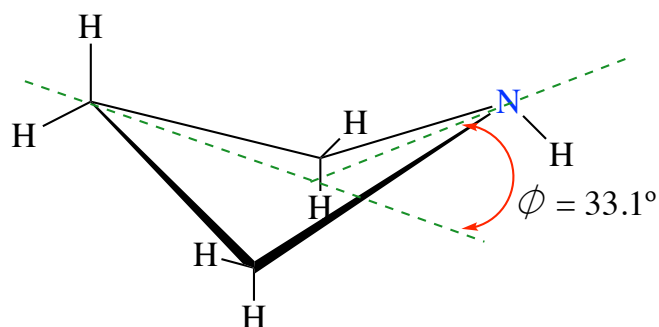
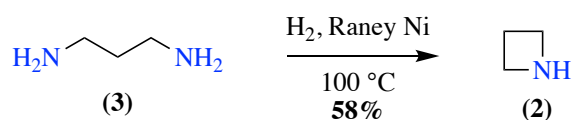


Figure 1.1. The structure and geometry of an azetidine ring was elucidated using electron diffraction techniques, the ring system was found to be highly strained with a dihedral angle (ϕ) of 33.1° .⁸

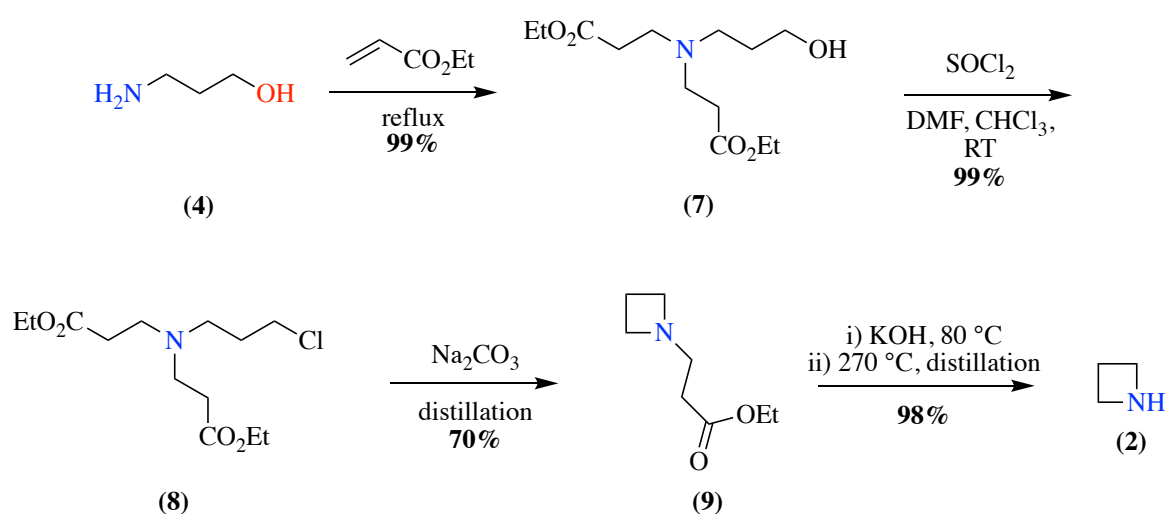
The dihedral angle of is comparable to that of cyclobutane ($\phi = \sim 35^\circ$), however, the azetidine ring displays a higher barrier to ring inversion (1.26 kcal/mol).⁸ The geometry of the ring can adopt either an axial or equatorial conformation with respect to the hydrogen on the nitrogen atom. It was found that while both confirmations are possible, the equatorial position with respect to the hydrogen is the most stable.⁸⁻¹⁰

Several more efficient methodologies towards the synthesis of azetidine rings have been developed since the initial account in the literature.⁶ Yasamura and co-workers reported an efficient transformation of 1,3-diamine **3** to azetidine **2** using Raney nickel as a catalytic source under catalytic hydrogenation conditions (**Scheme 1.2**).¹¹



Scheme 1.2. An azetidine ring was formed using 1,3-diamine with catalytic hydrogenation where Raney nickel was used as a catalyst.¹¹

A methodology for the conversion of 3-amino-1-propanol **4** to azetidine **2** in four high yielding steps was reported by Wadsworth.¹² Conversion of the alcohol **5** to 3-aminopropyl chloride **6** proceeded in high yields. A cyclisation reaction of compound **6** in the presence of sodium carbonate formed **7**, which was converted to azetidine **2** following the removal of the *N*-protecting group, 1-(2-carbethoxyethyl), with potassium hydroxide at elevated temperatures (Scheme 1.3).¹²

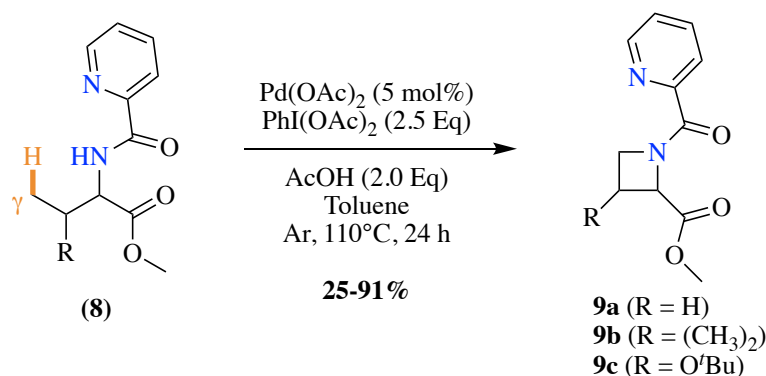


Scheme 1.3. An azetidine ring was produced using 3-amino-1-propanol as a starting material, following conversion to the corresponding 2-aminopropyl chloride, an *N*-protected azetidine was formed under basic conditions. Subsequent distillation at elevated temperatures gave rise to an azetidine ring in high yields.¹²

1.1.2. Metal-catalysed Synthesis of Azetidines

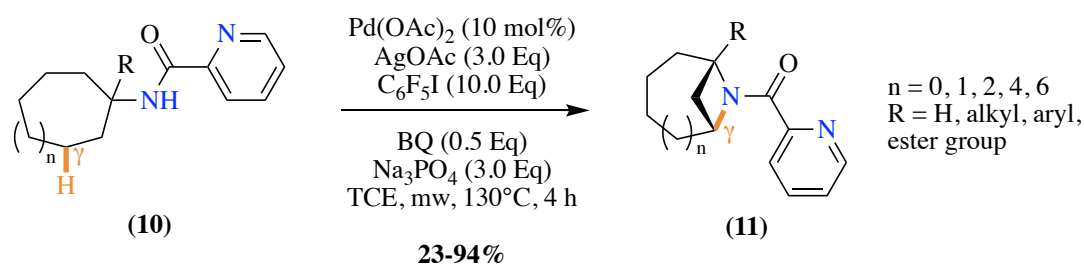
Chen and co-workers have published a methodology towards azetidines *via* palladium-catalysed intramolecular amination of $\gamma\text{-C}(\text{sp}^3)\text{-H}$ bonds of protected amine substrates.¹³ The picolinamide (PA) protecting group has been shown to display directing abilities enabling the transformation of $\gamma\text{-C}(\text{sp}^3)\text{-H}$ bonds with aryl iodides. Phenyl iodide(III) diacetate (PIDA) was found to be the best performing oxidant in terms of yield. Although the five-membered ring was initially thought to be the most likely product due to the kinetically favoured five-

membered palladacycle intermediate, the four-membered azetidine (**9a-c**) was obtained as the major product as a mixture of diastereoisomers. The final product was consistently obtained in yields greater than 78% with the exception of the **9a** which is unsubstituted at the β -position, giving a yield of 25% (**Scheme 1.4**).



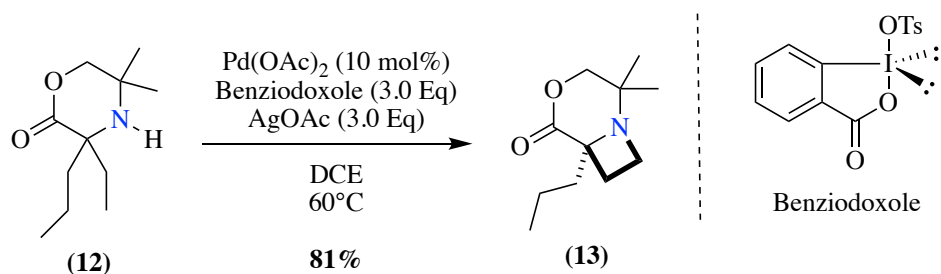
Scheme 1.4. A palladium-catalysed intramolecular amination of $\gamma\text{-C}(\text{sp}^3)\text{-H}$ bonds gave rise to substituted azetidines in moderate to excellent yields.¹³

As shown in **Scheme 1.5**, palladium catalysis for the amination of $\text{C}(\text{sp}^3)\text{-H}$ was also used by Wu *et al.* for the synthesis of polycyclic azetidines.¹⁴ PA protected aliphatic amine scaffolds (**10**) proceeded to the corresponding polycyclic *N*-containing heterocycles in generally good to excellent yields. Silver acetate was used as an additive for the palladium-catalysed C-H amination, successfully forming a Pd-Ag heterobimetallic intermediate species which allow the reaction to follow a lower energy pathway and display increased catalytic efficiency.¹⁵ Polycyclic azetidines (**11**) possessed a quaternary carbon allowing for the possible synthesis of non-canonical amino acids and the corresponding peptides.¹⁴



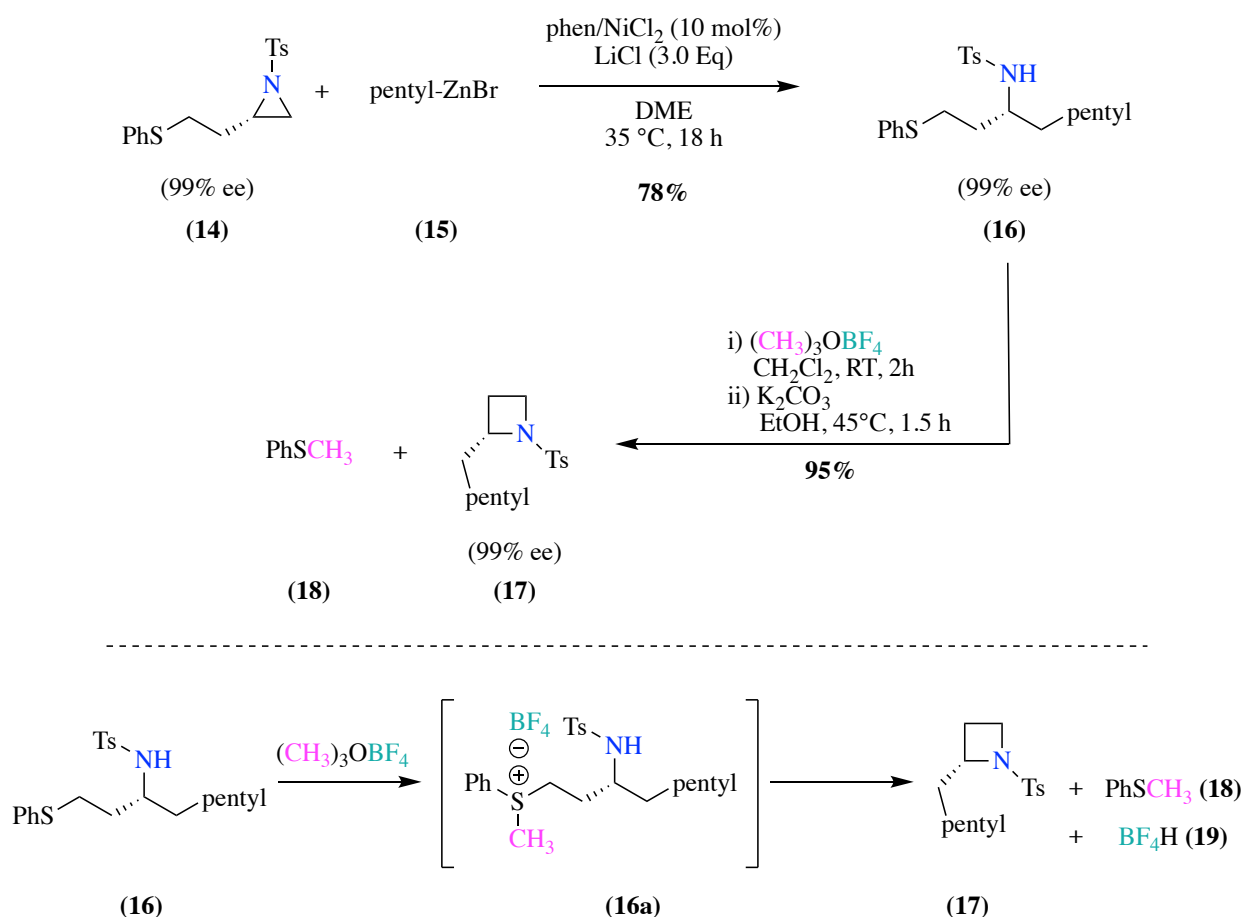
Scheme 1.5. Polycyclic azetidines were synthesised via a palladium-catalysed intramolecular amination of γ -C(sp³)-H bonds. Silver acetate was used as an additive to allow for increased catalytic activity during the cyclisation reaction.¹⁴

Cyclic alkyl amines were again used by Gaunt *et al.* for the synthesis of highly substituted azetidines.¹⁶ It was found that the combination of the oxidant, benziodoxole, and the additive, silver acetate, was essential to control the selective reductive elimination pathway to the desired azetidines. It was proposed that the C-H amination to the corresponding fused azetidine system was facilitated by a selective reductive elimination step within the catalytic cycle. This involved dissociative ionisation of the tosylate group present on the benziodoxole oxidant, with subsequent carboxylate binding to allow for the formation of an octahedral aminoalkyl-palladium(IV) complex. Nucleophilic attack of the tosyl group then formed a C-OTs bond, which was then displaced by the amino group to form the desired four-membered ring (**Scheme 1.6**).



Scheme 1.6. Highly substituted azetidines were synthesised via a palladium-catalysed amination in the presence of the oxidant, benziodoxole, with silver acetate as an additive to allow for selective reduction during the catalytic step.¹⁶

As displayed in **Scheme 1.7**, Jamison and co-workers used nickel catalysis for the transformation of three-membered aziridines to enantiomerically pure azetidines.¹⁷ An initial cross coupling reaction with 1,10-phenanthroline/nickel(II) chloride precatalyst occurred between the aziridine (**14**) and pentylzinc bromide (**15**), lithium chloride was found to be crucial for reactivity by forming a lithium organozincate intermediate with improved nucleophilicity. The resultant sulfonamide (**16**) underwent selective methylation to form the 2-substituted azetidine (**17**) in high yields, *via* a 4-*exo-tet*-cyclisation pathway. Further investigation showed this method to be robust when used with a series of aliphatic and aromatic organozinc reagents, giving the corresponding enantiomerically pure azetidine product in good yields.



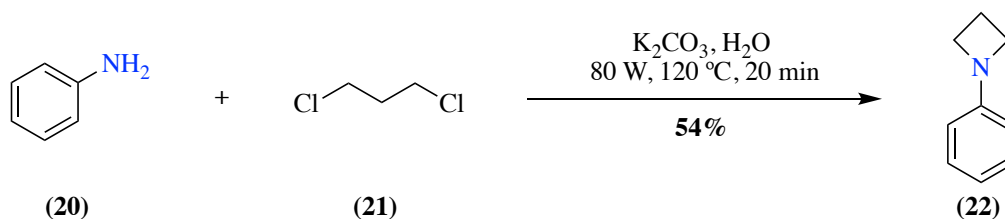
Scheme 1.7. Nickel-catalysed ring expansion of aziridine rings to enantiomerically pure azetidines was preformed through reaction with phenylzinc bromide and subsequent selective methylation via a 4-exo-tet cyclisation reaction pathway. Lithium chloride acts to improve nucleophilicity of the pentyl bromide reactant by forming a lithium organozincate intermediate.¹⁷

1.1.3. Cyclisation *via* Nucleophilic Substitution

Cyclisation of amines through nucleophilic displacement of a leaving group, most commonly halides, has long since been the most popular route towards the azetidine ring.^{2, 3}

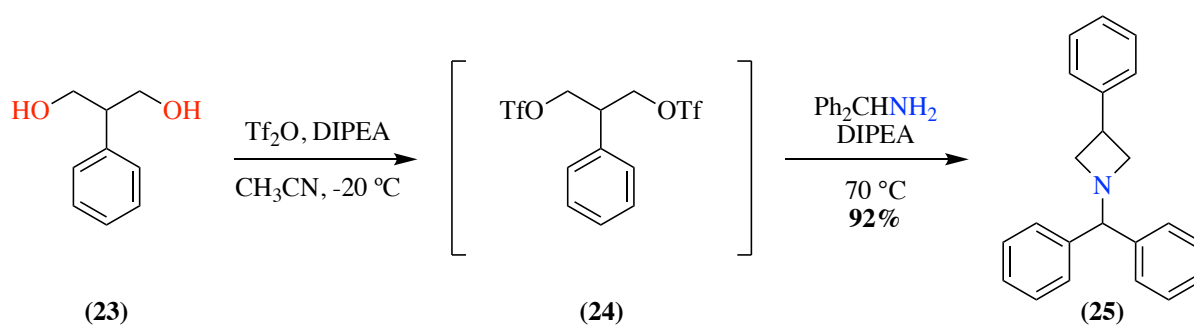
Nucleophilic displacement was employed by Ju *et al.* to form mono-substituted azetidines with simple reagents in a microwave assisted process.¹⁸ The cyclisation reaction of dihalides and

primary amines occurred in aqueous media in the presence of potassium carbonate to give an *N*-arylated azetidine **22** in moderate yields (**Scheme 1.8**).



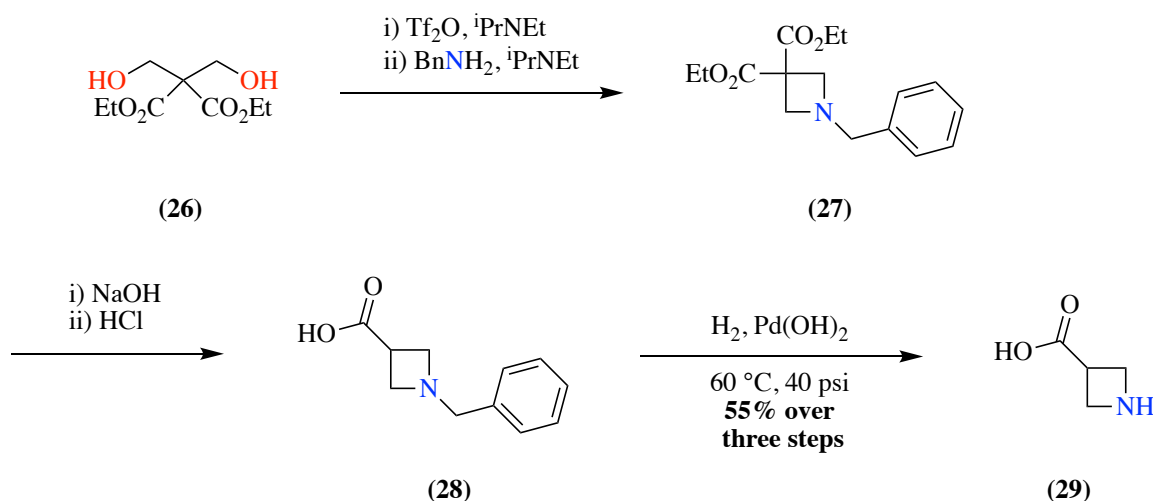
Scheme 1.8. Mono-substituted azetidines were formed from simple reagents in moderate yields using a microwave assisted process.¹⁸

While halides consistently remain the most popular choice of leaving group, triflates and sulfonate esters have also been shown to undergo base-mediated cyclisation. Hillier and co-workers have reported an efficient methodology for the synthesis of 1,3-disubstituted azetidines from a series of 1,3-propane diols in a single step.¹⁹ An example of this 1,3-disubstituted azetidine synthesis can be seen in **Scheme 1.9**, where the alkylation of primary amines by bistriflate **24** formed 1,3-disubstituted azetidine **25** in a yield of 92%.



Scheme 1.9. 1,3-propane diol was converted to the corresponding bis-triflate which was subsequently reacted with primary amine under basic conditions to synthesis the resultant 1,3-disubstituted azetidine.¹⁹

This methodology was applied by Miller *et al.* for the synthesis a novel β -amino acid **29**, which was later incorporated into several pharmaceutically active compounds, including CCR5 receptor modulators and protein inhibitors.²⁰ As shown in **Scheme 1.10**, malonate **26** was converted to the corresponding triflate **27**, which yielded azetidine (**28**) on reaction with benzylamine. Subsequent hydrolysis, decarboxylation, and removal of the benzyl group *via* catalytic hydrogenation yielded azetidine-3-carboxylic acid (**29**) in a 55% yield over three steps.

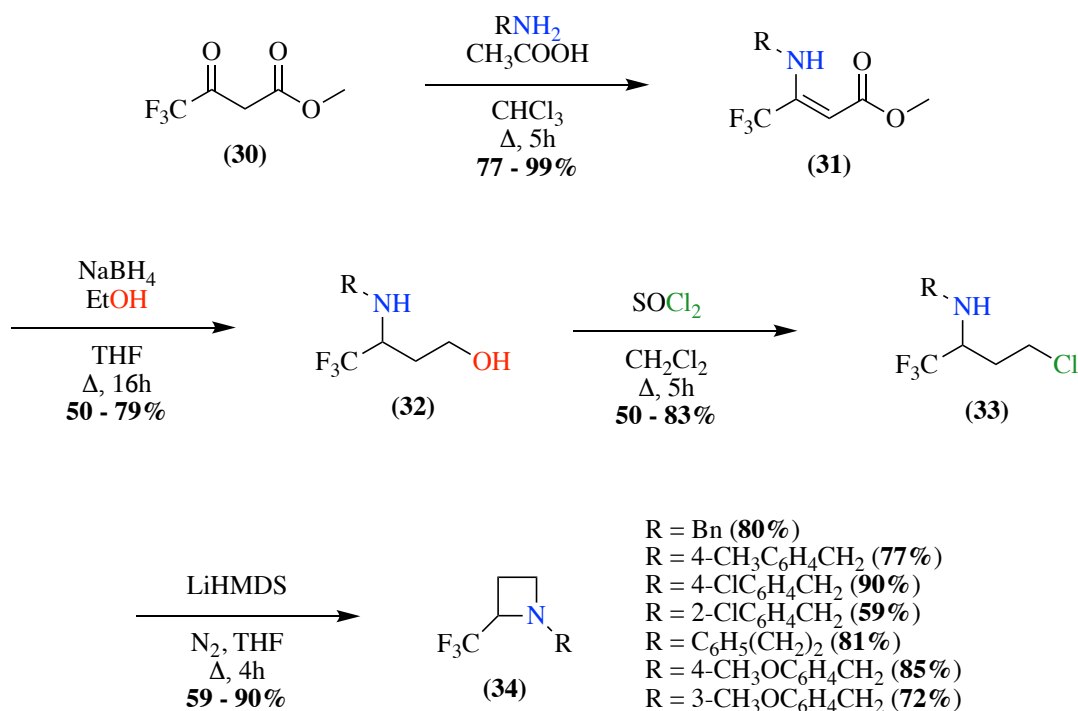


Scheme 1.10. A methodology to access a novel β -amino acid via nucleophilic substitution was reported. Under basic conditions a malonate was converted to the corresponding bis-triflate which yielded a 1,3-disubstituted azetidine upon alkylation with a primary amine. Following a series of hydrolysis, decarboxylation and deprotection reactions, the novel azetidine-containing β -amino acid was accessed with a yield of 55%.

1.1.4. Intramolecular Cyclisation towards Azetidines

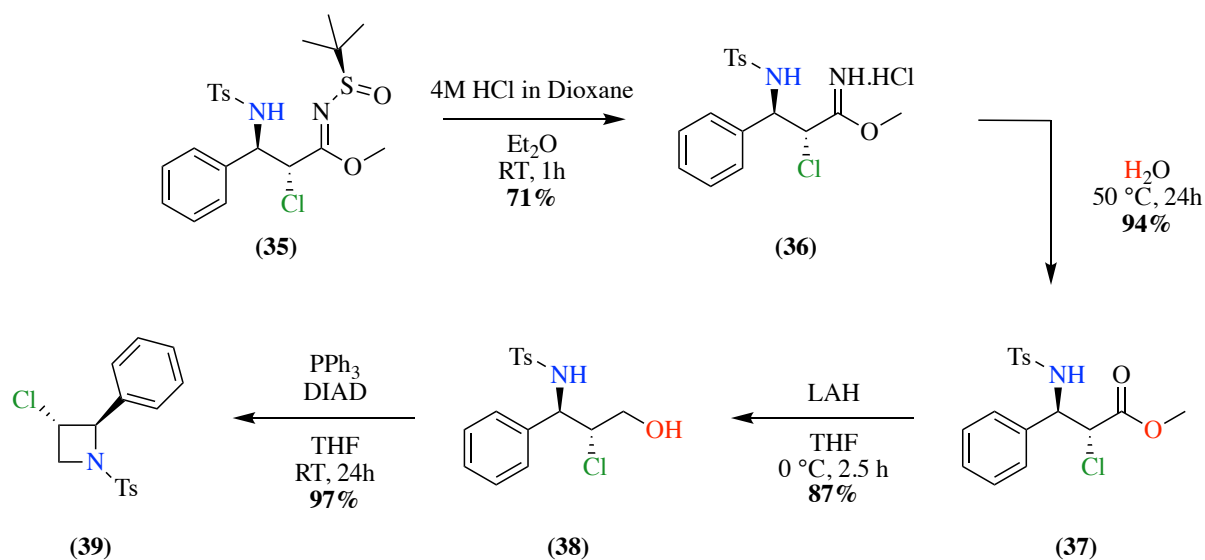
An intramolecular approach towards azetidine synthesis has frequently been reported in the literature.^{1, 3, 5} De Kimpe and co-workers have published a route towards 2-trifluoromethyl (CF₃) functionalised azetidines in moderate to excellent yields over a four-step synthesis

(Scheme 1.11).²¹ Reaction of trifluoroacetoacetate (**30**) with a primary amine under mildly acidic conditions yielded an enamine (**31**) which upon reduction with sodium borohydride afforded γ -amino alcohol (**32**). Treatment with thionyl chloride converted the alcohol group to a halide leaving group (**33**). Intramolecular cyclisation of **33** in the presence of lithium bis(trimethylsilyl)amide (LiHMDS) in THF resulted in 1-alkyl-2-(trifluoromethyl) azetidine (**34**). It was reported that the presence of the strong base, LiHMDS, was required to achieved intramolecular cyclisation as the electron-withdrawing nature of the trifluoromethyl group greatly reduced the nucleophilicity of the nitrogen atom. De Kimpe *et al.* have also reported a route towards enantiopure *trans*-2-aryl-3-chloroazetidines through the transformation of chiral α -chloro- β -amino-*N*-sulfinyl imidates.²²



Scheme 1.11. Trifluoroacetate was reacted with a primary amine to access the corresponding enamine, subsequent reduction with sodium borohydride yielded a γ -amino alcohol. Reaction with thionyl chloride allowed for the transformation of the alcohol group to a halide leaving group. Intramolecular cyclisation occurred in the presence of a strong base resulting in a 1,2-disubstituted azetidine in yields of over 70%, with the exception of $\text{R} = 2\text{-ClC}_6\text{H}_4\text{CH}_2$ which yielded the final product in 59% yield.²³

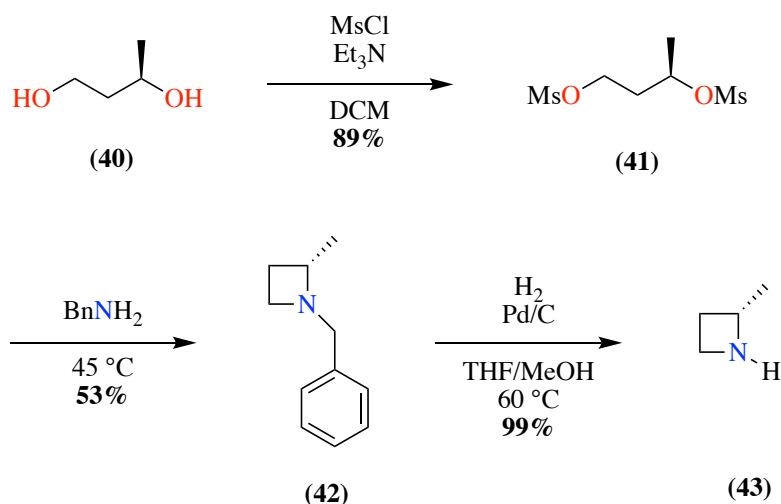
As shown in **Scheme 1.12**, deprotection of the imidate (**35**) occurs in the presence of 4 M hydrochloric acid in dioxane giving rise to (**36**), the corresponding imidate hydrochloride, which readily undergoes hydrolysis to access the ester functional group (**37**). Lithium aluminium hydride (LAH) was used as a reducing agent in anhydrous THF to produce the resultant β -chloro- γ -sulfonylamino alcohol (**38**) which then underwent intramolecular cyclisation yielding the trans-chloroazetidine (**39**) via classical Mitsunobu reaction conditions in excellent yields.



Scheme 1.12. An imidate was deprotected using 4 M hydrochloric acid to access the corresponding imidate hydrochloride which was subsequently hydrolysed to give rise to the resultant ester. Subsequent reduction with lithium aluminium hydride allowed for transformation to the resultant β -chloro- γ -sulfonylamino alcohol which underwent intramolecular cyclisation to the corresponding 1,3,4-trisubstituted azetidine via classical Mitsunobu conditions.

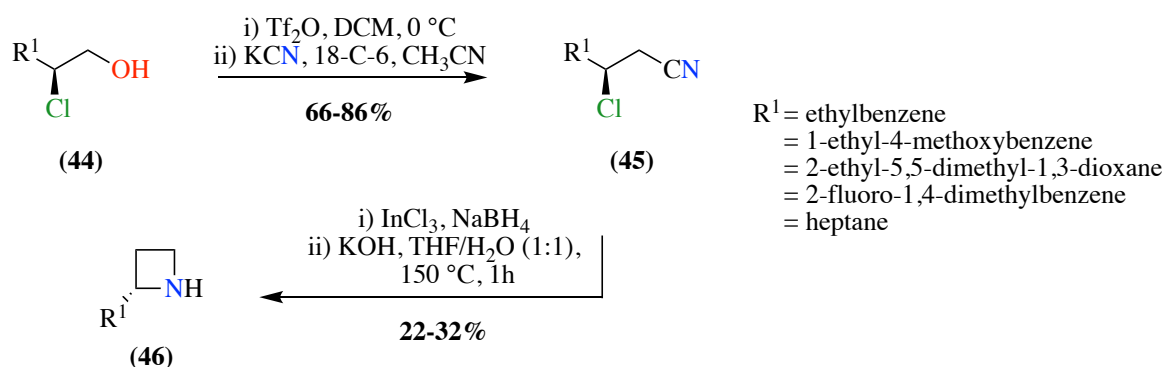
Smith and co-workers have reported a methodology to access (S)-2-methylazetidine(R)-(-)-camphorsulfonate from a simple 1,3-butanediol.²⁴ The 1,3-butanediol (**40**) underwent a mesylation reaction giving rise to the corresponding bis-mesylated product (**41**). Treatment with benzylamine at a relatively low temperature (45 °C) gave azetidine (**42**) in a yield of 54%

with 95% ee. Removal of the benzyl group was possible with hydrolysis using palladium on carbon as a catalytic source, allowing (S)-2-methylazetidine (**43**) to be isolated with a yield of 99% (**Scheme 1.13**).



Scheme 1.13. 1,3-butanediol was reacted with methanesulfonyl chloride to access the corresponding bis-mesylated product, subsequent reaction with benzylamine gave the corresponding 1,4-disubstituted azetidine. Subsequent palladium-catalysed hydrolysis to remove the benzyl protecting group yielded (S)-2-methylazetidine(R)-(-)-camphorsulfonate in a yield of 99%.²⁴

An alternative method for the synthesis of enantioselective functionalised azetidines was reported by Lindsley *et al.*²⁵ A readily available β -chloro-alcohol (**44**) was activated through conversion to the corresponding triflate, in the presence of 18-crown-6-ether (18-C-6), followed by displacement with potassium cyanide yielding the β -chloro-nitrile (**45**) in moderate to good yields. The nitrile compound was then reduced in the presence of indium(III)chloride-sodium borohydride, the resultant γ -chloro-amine was then cyclised to the corresponding 2-alkyl azetidine (**46**) in the presence of potassium hydroxide (KOH) in a 1:1 mixture of THF/H₂O using microwave irradiation. This methodology achieved high enantioselectivities (84-92% ee) but poor overall yields (22-32%) as shown in **Scheme 1.14**.



Scheme 1.14. Enantioselective mono-substituted azetidines were synthesised from β -chloro-alcohols. The alcohol group was activated by conversion to the corresponding triflate which was subsequently displaced using potassium cyanide to access the resultant β -chloro-nitrile. Reduction of the nitrile group with indium(III)chloride-sodium borohydride yielded the corresponding γ -chloro-amine which was then cyclised to a 2-alkyl azetidine in the presence of potassium hydroxide using microwave irradiation.

1.1.5. Iodine-mediated Heterocyclic Ring formation

Molecular iodine,²⁶ *N*-bromosuccinimide (NBS),²⁷ *N*-chlorosuccinimide (NCS),²⁸ *N*-iodosuccinimide (NIS)²⁹ have been employed as electrophilic halogen sources for the cyclisation of alkenes and alkynes to the corresponding nitrogen-containing heterocycles. Iodine-mediated cyclisation and functionalisation of heterocycles has been extensively reviewed by Mphahlele³⁰, Tilve and co-workers³¹ and Verma and co-workers,³² therefore only examples relevant to this work will be discussed in detail.

Over the past century, molecular iodine has gained recognition as an efficient,^{33, 34} non-toxic,³⁵ cost effective,³⁶ bench stable electrophilic reagent, which can be employed in halocyclisation reactions to produce novel iodo-functionalised heterocyclic compounds, which are employed as useful intermediate compounds in the synthesis of novel molecules.³⁷ Nitrogen-containing heterocycles and their analogues have remained popular in the medicinal chemistry community

due to their favourable pharmacological properties.³⁸ The general mechanism of halocyclisation for compounds with a double or triple bond proceeds through activation of the π -bond, either by a charge transfer or *via* the formation of an iodine-containing intermediate molecule.³⁹ This activation step is then quickly followed by an intramolecular nucleophilic attack, occurring in either an *endo*- or *exo*- fashion, in line with the substrate's respective geometry (**Figure 1.2**). There have been several examples of this synthetic route published in the literature.³⁰⁻³²

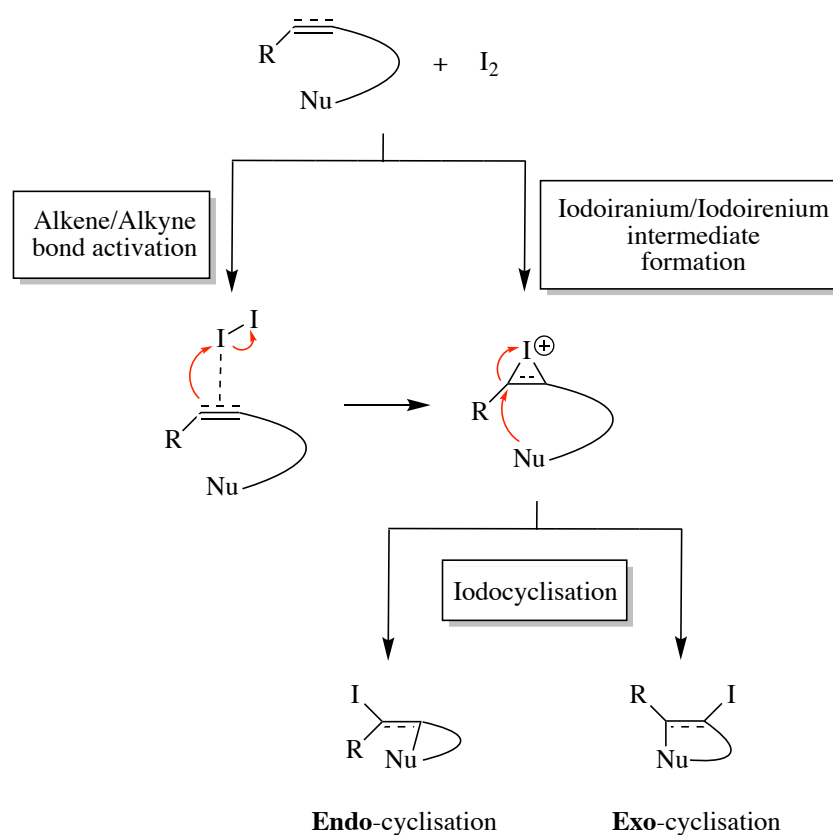
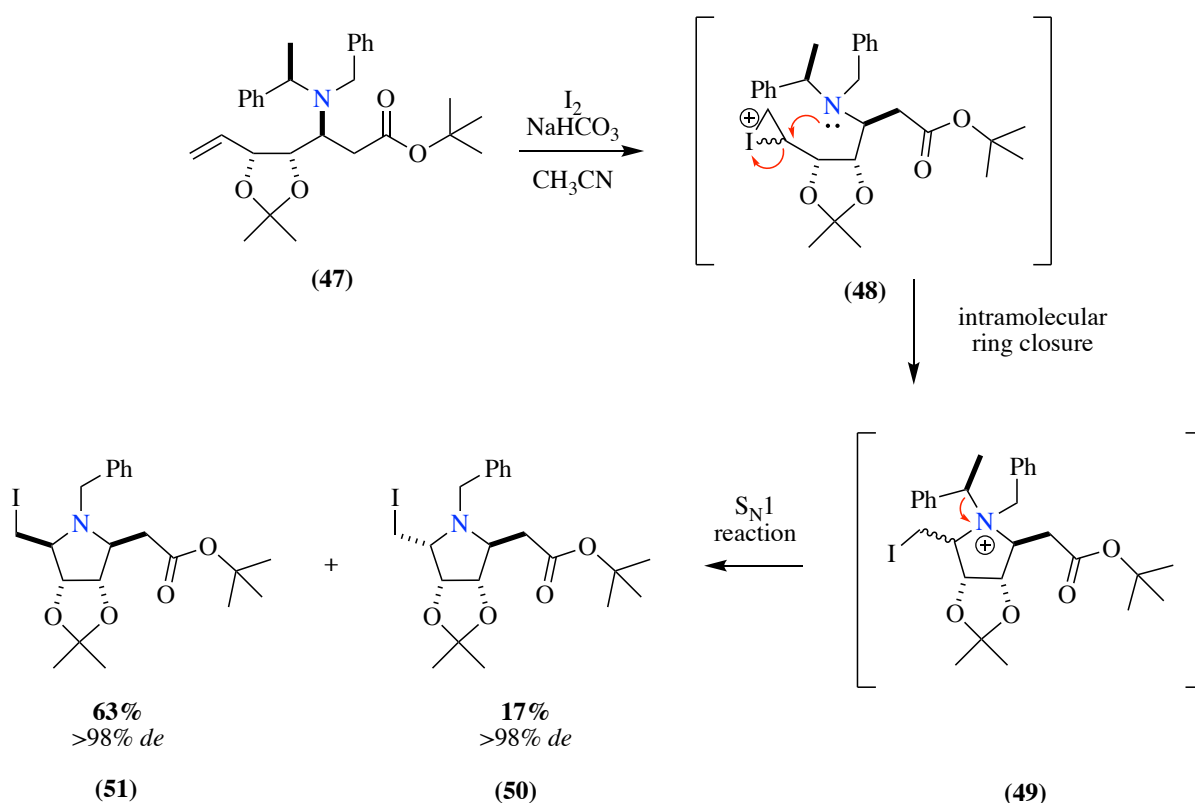


Figure 1.2. The general mechanism of iodine-mediated halocyclisation for compounds with a double or single bond proceeds via the activation of the π -bond, either by a charge transfer or through the formation of an iodine-containing intermediate molecule. Intramolecular nucleophilic attack then occurs in an *endo*- or *exo*- fashion in line with the geometry of the substrate resulting in the cyclised product.³⁹

Davies and co-workers described a method for the synthesis of polyhydroxylated pyrrolidines using an iodo-amination reaction to achieve intramolecular ring closure.⁴⁰ Treatment of **47** with an equivalent of molecular iodine in the presence of a base allowed for the formation of the iodonium ion (**48**) *in situ*, which was closely followed by a concerted intramolecular ring closure to give rise to a quaternary ammonium ion (**49**). Loss of the *N*- α -methylbenzyl protecting group in an S_N1 fashion gives the iodomethyl pyrrolidine compounds **50** and **51** as a racemic mixture. When acetonitrile was used as the reaction solvent, the formation of compound **51** was found to be stereochemically favourable, occurring in a ratio of almost 4:1 compared to compound **50**. It was hypothesised that this was either due to the stereoselective, irreversible formation of a single diastereomer of the iodonium ion (**48**), followed by the ring closure and deprotection, or through a reversible formation of the iodonium ion (**48**), which is then followed by the selective formation of a single diastereomer of the final pyrrolidine compound, with subsequent deprotection of the nitrogen group (**Scheme 1.15**). A solvent screen using a series of solvents with reducing polarity (toluene, tetrahydrofuran, and chloroform), was carried out to test the proposed hypothesis. Lower polarity solvents offered increased conversion to the final products but with a notable decrease in the stereoselectivity when compared to acetonitrile. This decrease in selectivity is consistent with a rapid equilibrium between both iodonium intermediates in polar acetonitrile, followed by the rate-determining intramolecular ring closure of one of the diastereomeric iodonium ions to the corresponding ammonium ion and deprotected pyrrolidine.

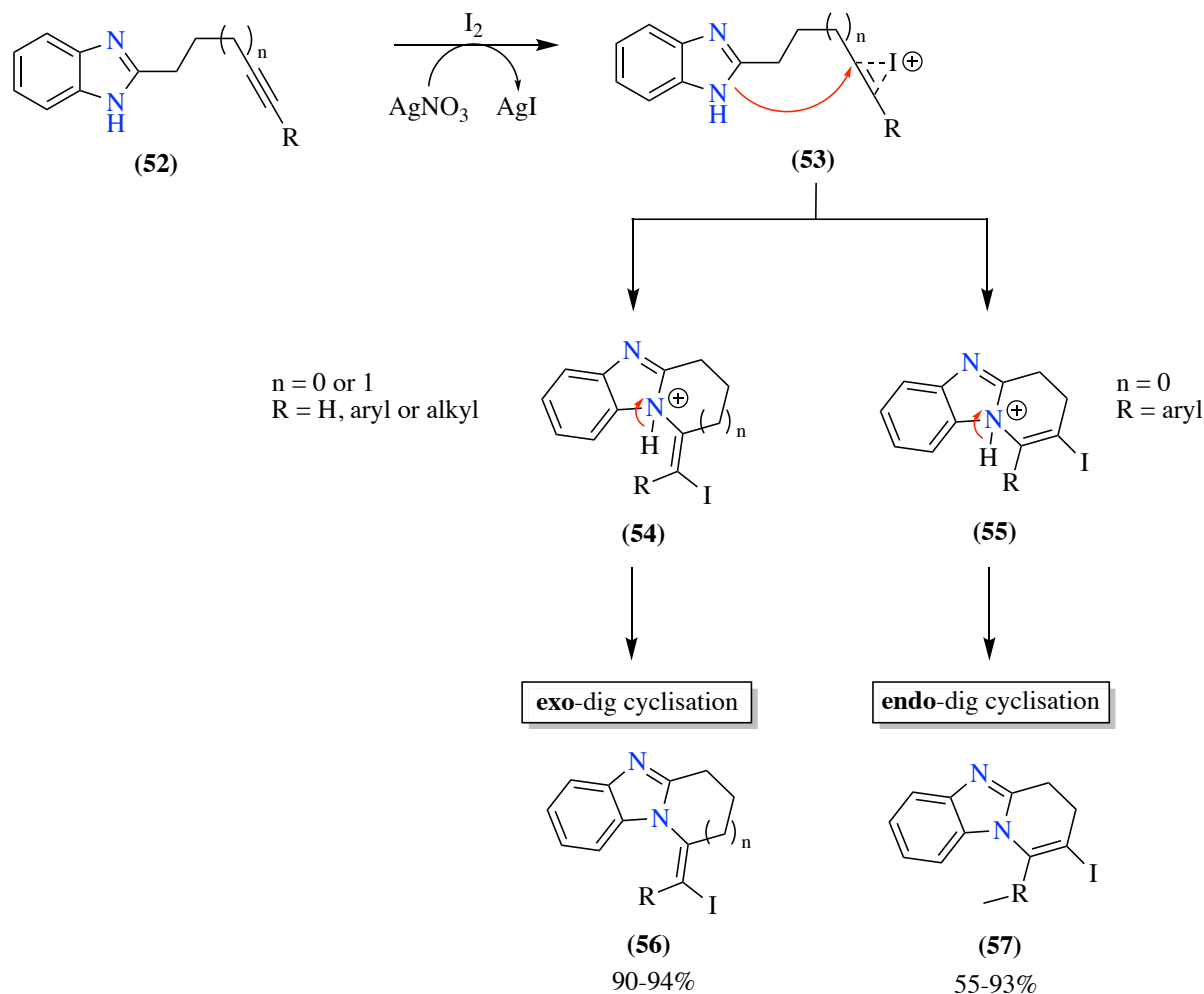


Scheme 1.15. Polyhydroxylated pyrrolidines were synthesised via an iodine-mediated intramolecular amination reaction.

Treatment of the alkene-containing starting material with iodine under basic conditions gave rise to a five-membered pyrrolidine intermediate. Subsequent removal of the *N*-α-methylbenzyl protecting group in an S_N1 fashion gave rise to two products, the *cis*- and *trans*-diastereomer in a 4:1 ratio.⁴⁰

Liu *et al.* published a route towards fused benzimidazoles from compounds containing terminal and substituted alkynes through an iodine-mediated pathway (**Scheme 1.16**).⁴¹ Iodine coordinates to the alkyne triple bond to form the iodonium complex (**53**). During the activation of the double bond, silver nitrate was added in order to boost the yield of the desired products through inhibition of bis-iodine biproducts, instead forming silver iodide.⁴² Intermediate compounds **54** and **55** were formed following nucleophilic attack of the activated bond by the nitrogen atom on the benzimidazole ring. This cyclisation reaction occurred *via* an *exo-dig* (**54**)

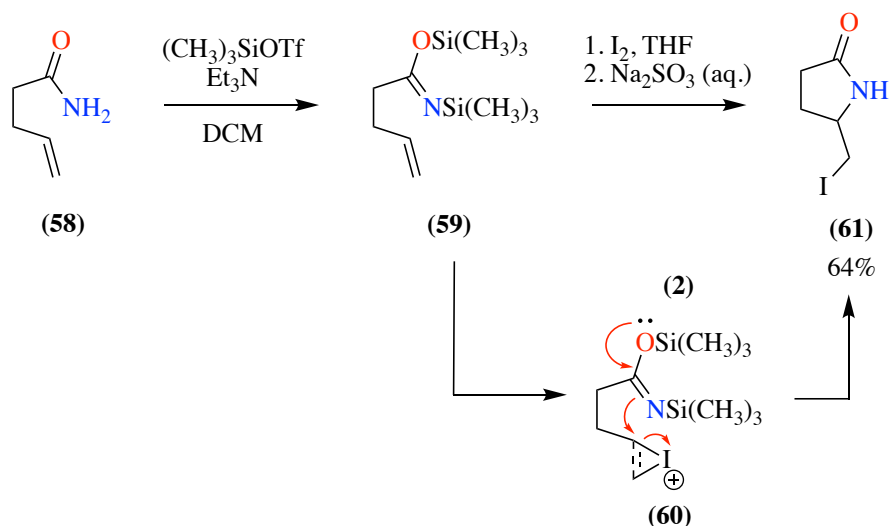
or an *endo-dig* (**55**) pathway, which was then followed by a rapid proton transfer resulting in formation of the final tricyclic products (**56** and **57**).



Scheme 1.16. Alkyne-containing compounds were used to access fused benzimidazoles using an iodine-mediated methodology. Molecular iodine co-ordinated with the alkyne triple bond in the presence of silver nitrate to form the resultant iodonium complex. Intermediate compounds were then formed through *endo-dig* and *exo-dig* nucleophilic attack of the nitrogen lone pair on the iodonium complex. Rapid proton transfer then occurred, giving rise to the corresponding, multicyclic final products.⁴¹

Knapp and co-workers reported a synthesis towards five-membered iodolactams *via* and iodine-mediated cyclisation of *N,O*-bistrimethylsilyl derivatives.⁴³ As shown in **Scheme 1.17**, the unsaturated amide (**58**) was initially converted to the corresponding imidate (**59**) through

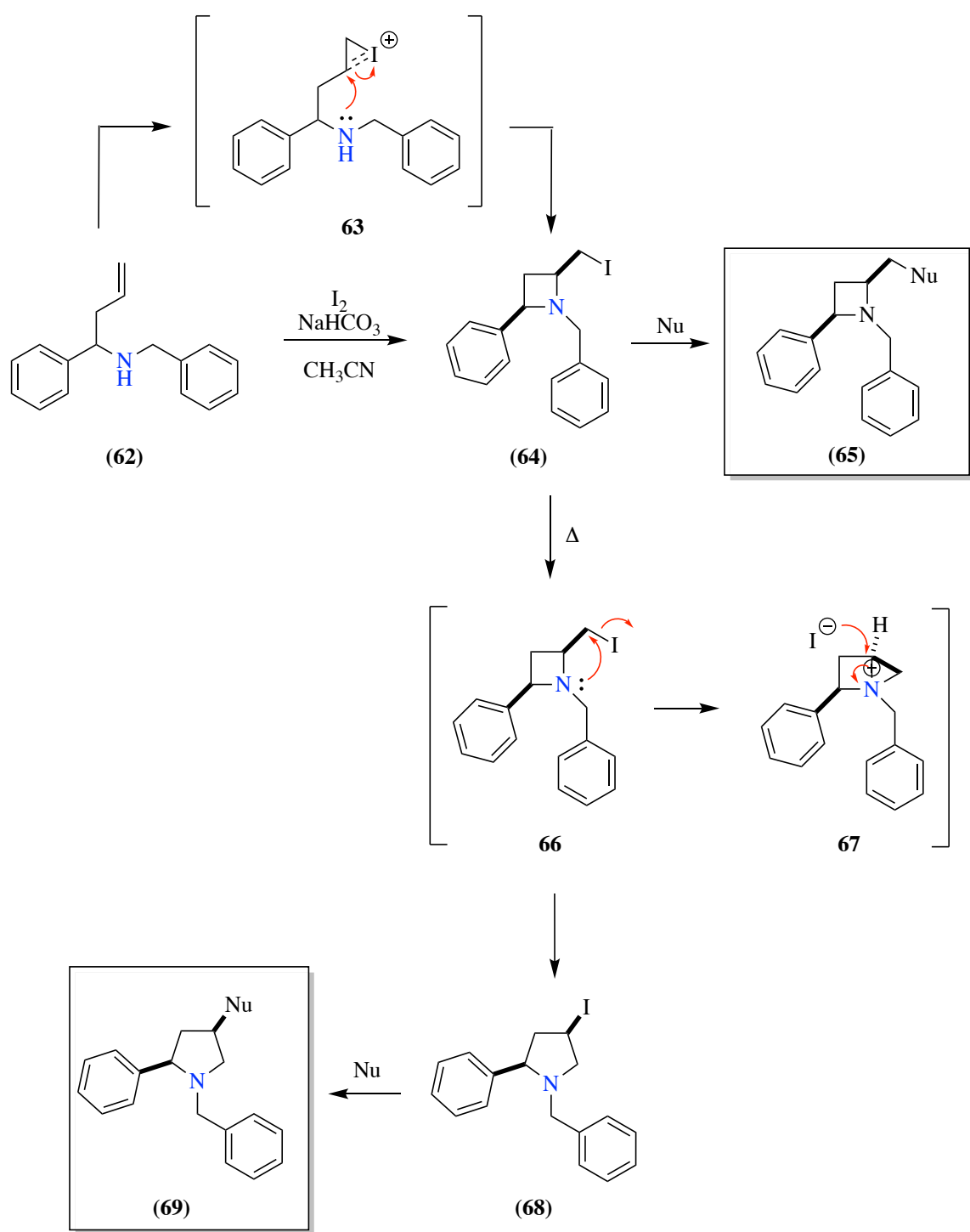
reaction with a triflate under basic conditions. The iodonium intermediate (**60**) was then created through coordination with the double bond. Following a quench with aqueous sodium sulfite, a rapid electron rearrangement occurred, restoring the original amide bond, and closing the ring to form the desired 5-(iodomethyl)pyrrolidin-2-one (**61**) in moderate yields.



Scheme 1.17. Iodine-mediated cyclisation was used for the creation of five-membered iodo-lactams. An unsaturated amide was reacted with a triflate to access the corresponding imidate which was subsequently reacted with molecular iodine to give rise to a cyclised iodonium intermediate. Rapid electron rearrangement allowed for the restoration of the amide bond, accessing the resultant 5-(iodomethyl)pyrrolidin-2-one with a yield of 64%.⁴³

Significant research has been carried out within the Fossey group towards iodine-mediated cyclisation. A diastereoselective methodology towards four-membered azetidines or five-membered pyrrolidines has been reported.^{44, 45} As shown in **Scheme 1.18**, activation of the homoallylic amine double bond occurred through coordination of an iodine molecule, resulting in the iodonium intermediate (**63**). Following the subsequent intramolecular attack, the 2,4-*cis*-iodo-azetidine (**64**) was formed which could be readily functionalised to the corresponding 2,4-*cis*-amino-azetidine (**65**) through nucleophilic attack. Alternatively, iodo-azetidine **64** could

undergo thermally controlled isomerisation to the corresponding 2,4-*cis*-iodo-pyrrolidine (**68**) when heated to around 50 °C which again can be converted to the corresponding amino-pyrrolidine (**69**) following a nucleophilic substitution reaction. This methodology yields both amino-azetidines and amino-pyrrolidines in a highly diastereoselective fashion in good yields. and forms the basis of this work discussed in this thesis.



Scheme 1.18. Reaction of homolallyc amines with molecular iodine under basic conditions gives rise to an iodo-azetidine intermediate which can be reaction with a nucleophile to create a 2,4-cis-azetidine compound in a diastereoselective fashion. Heating of the iodo-azetidine intermediate results in conversion to the corresponding iodo-pyrrolidine intermediate which can subsequently be reacted with a nucleophile to access the corresponding 2,4-cis-pyrrolidine product.

1.2. Biological Applications of Azetidines

1.2.1. Azetidines in Natural Products

The discovery of L-azetidine-2-carboxylic acid in 1956 by Fowden, sparked significant interest in azetidines within the medicinal chemistry community, due to their natural occurrence in many plants and as an analogue of the amino acid, L-proline (**70**).⁴⁶ The azetidine core is relatively rare, however some examples of it occurring in nature can be seen in **Figure 1.3**. Mugineic acid (**71**) can be readily extracted from the roots of the barley plant and is a phytosiderophore shown to promote the uptake of iron for chlorophyll biosynthesis.⁴⁷ Polyoxin A (**72**) is a peptide nucleoside antibiotic and is a potent inhibitor of chitin biosynthesis within cell walls, and also possesses additional anti-fungal properties.⁴⁸ Calydaphinone (**73**), an alkaloid, has been isolated from members of the plant species *Daphniphyllum*, which possesses an azetidine ring within its complex, polycyclic structure.⁴⁹ Azetidine alkaloid analogues have also been extracted from marine life forms, Penaresidin A and penaresidin B have shown significant activation of ATPase in actomycin, and were obtained from an aquatic sponge indigenous to the Pacific Ocean.^{2, 50}

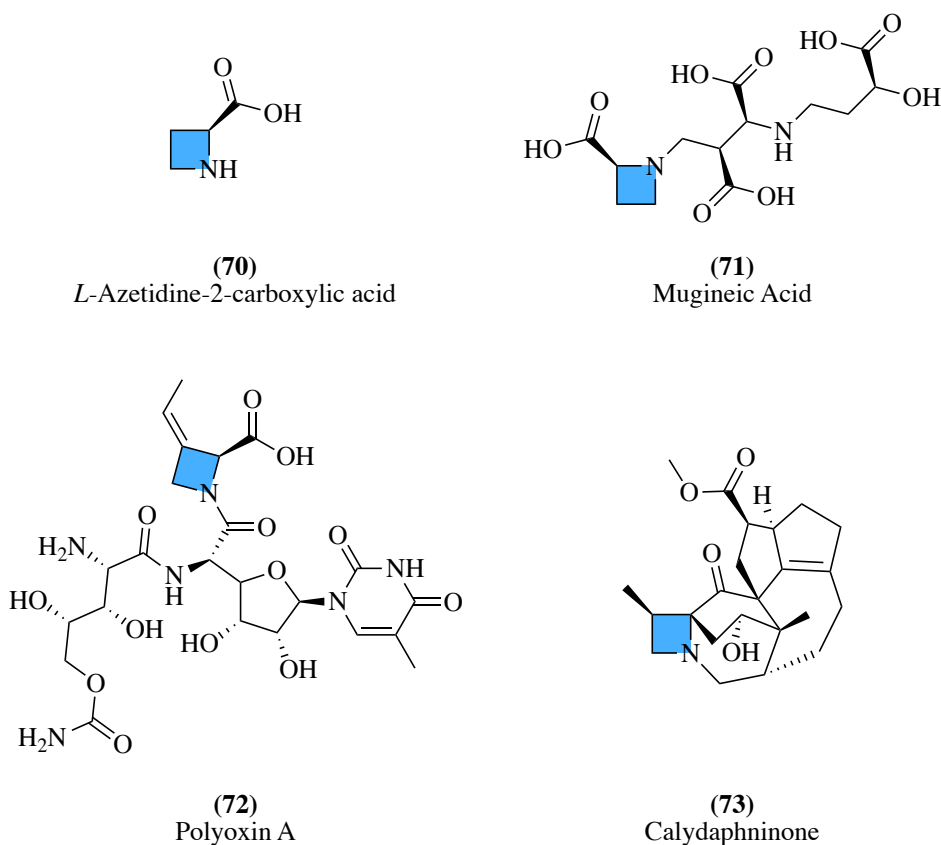
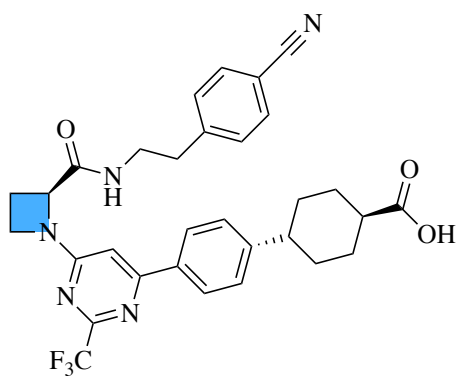


Figure 1.3. Azetidine rings commonly occur in natural products. L-azetidine-2-carboxylic acid was discovered in the later 1950's and is an analogue of the amino acid, L-proline. Mugineic Acid has been showed to promote the uptake of iron from soil by plants. Polyoxin A has inherently anti-fungal activity and is a nucleoside antibiotic. Calydaphninone is a naturally occurring alkaloid which has been successfully isolated.

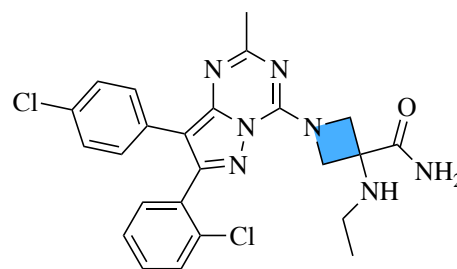
1.2.2. Azetidines in Pharmaceutical Agents

Despite the difficulties associated with its synthesis, the azetidine core has long since been, and continues to be, a popular motif in pharmaceutically relevant compounds.² These have found use as treatments for a variety of disorders, with some examples shown in **Figure 1.4**. Compounds with the azetidine moiety display a diverse range of pharmacological activities, such as anti-cancer,^{51, 52} anti-bacterial,⁵³ anti-microbial,⁵⁴ anti-schizophrenic,⁵⁵ anti-malarial,⁵⁶ anti-obesity,⁵⁷ anti-inflammatory,⁵⁸ anti-diabetic,⁵⁹ anti-viral,⁶⁰ anti-oxidant,⁶¹ analgesic,⁶² and dopamine antagonist activities,⁶³ and are also useful for the treatment of central nervous system

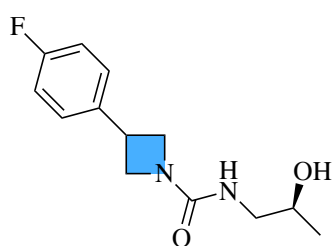
disorders.⁶⁴ Dipeptidyl peptidase-4 inhibitors are a relatively new class of oral diabetes therapy,⁶⁵ compound **74** was identified as a lead compound in both acute and chronic obesity models.⁶⁶ A selective endocannabinoid (CB₁) receptor antagonist (**75**) was developed by medicinal chemists at Pfizer and was patented for the treatment of certain metabolic disorders.⁶⁷ Compounds displaying anti-convulsant and anti-epileptic activity have also been studied, the azetidinecarboxamide **76** has been patented for the potential treatment of disorders of the central nervous system.⁶⁸ Studies revealed, the 3-substituted azetidine (**77**) as a potential treatment for depression, due to its' inhibitory activity towards several neurotransmitters.⁶⁹ Additionally, a novel benzodioxane **78** has been patented as a leukotriene hydrolase inhibitor, for use in the treatment of cardiovascular diseases.⁷⁰



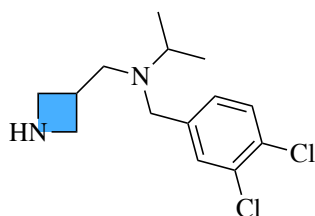
(74)
Diabetes treatment



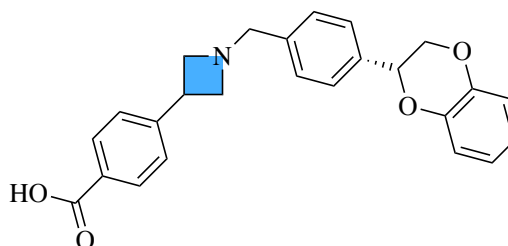
(75)
Metabolic Disorder
treatment



(76)
CNS Disorder
treatment



(77)
Antidepressant



(78)
Cardiovascular disease
treatment

Figure 1.4. Azetidine rings are a popular motif in pharmaceutical agents, Compounds with the azetidine moiety display a diverse range of pharmacological activities and have been used for treatment of diabetes, metabolic and central nervous system disorders. They have also been used to target cardiovascular disease and conditions such as depression.

Lowe and co-workers carried out a large-scale, diversity orientated library synthesis of azetidine-based polycyclic scaffolds for the treatment of central nervous system disorders.⁶⁴

Mykhailiuk *et al.* carried out a synthesis of spirocyclic azetidine compounds which were more potent and less toxic than the currently marketed anaesthetic drug, Bupivacaine.⁷¹

1.3. Challenges in the Pharmaceutical Industry

Over the previous three decades, the pharmaceutical industry has faced several challenges including a reduction in revenue, a decreased rate new chemical entities (NCE) advancing through the drug discovery pipeline and gaining approval, along with decreased innovation in terms of research and development.⁷²⁻⁷⁴ Clinical candidates proposed today are considerably more like to fail than in the 1970's when success rates were at approximately 40%,⁷⁵ today only 10% of candidates make it through the discovery and approval process.^{76, 77} There are many factors contributing to the decline of the pharmaceutical innovation and the resultant reduced revenue within the sector; the increasing cost of research and development has led to an increased aversion to risk taking when selecting new compounds for testing. Due to the high rate of attrition and complexity of the regulatory process coupled with an increasing research and production cost, several steps have been taken to increase the likelihood of a NCE advancing through the discovery pipeline and entering the pharmaceutical market.⁷⁸

The process of drug discovery is both lengthy and expensive and consists of multiple stages, typically taking between 12-15 years and cost over \$2.6 billion for each marketed NCE (**Figure 1.5**).⁷⁷⁻⁷⁹ A target must first be identified and validated before compound screening techniques can be employed to identify molecules with the desired activity against the chosen target, these active molecules are termed "hits". Once a number of hits have been identified, the selection is optimised by choosing the most potent and selective compounds in the set which possess pharmacokinetic properties suitable for *in vivo* biological testing.⁷⁷ This refined set of compounds are termed "leads" and are then further optimised to improve their activity and

drug-like molecular properties in order to create a set of preclinical candidate molecules with optimal pharmacodynamic and pharmacokinetic properties for biological testing.^{77, 80}

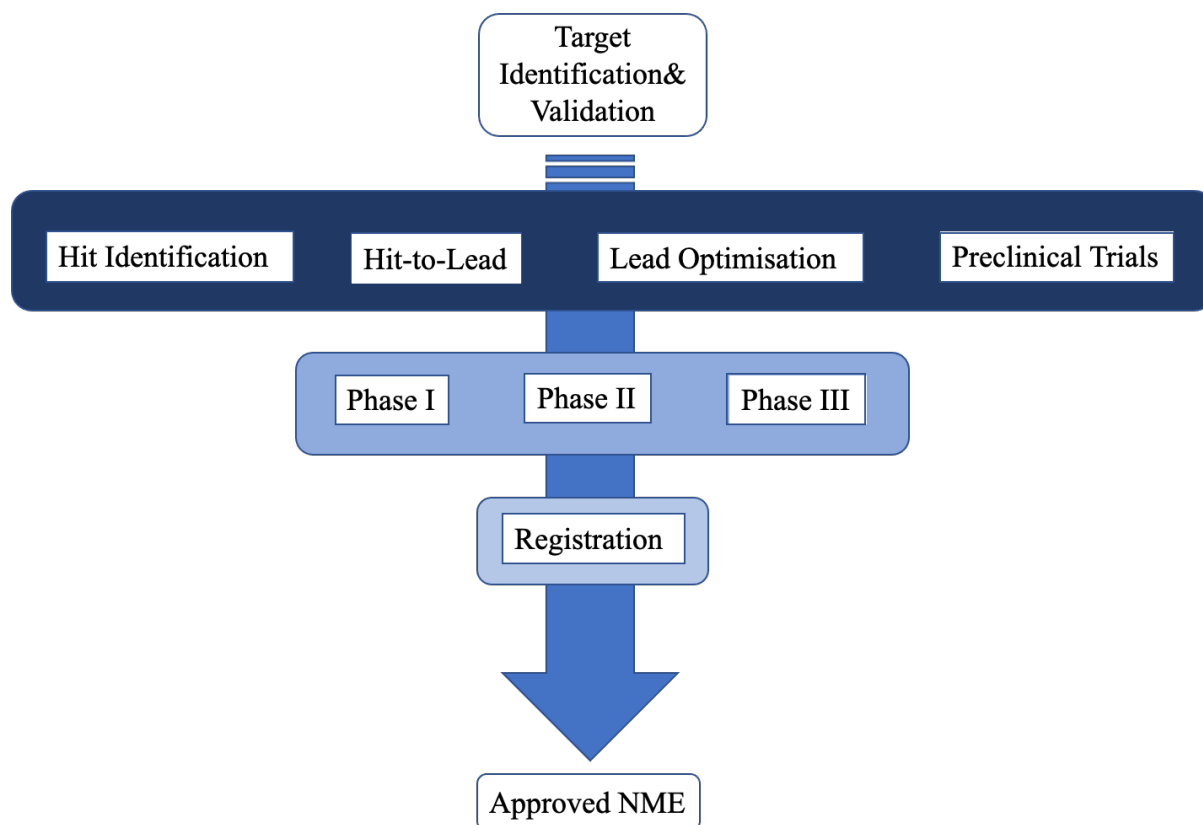


Figure 1.5. The drug discovery process typically extends over 12-15 years and is extremely financially demanding. Following on from the initial target validation compounds must be screened in order to find potential hits. The selected compounds are then optimised and undergo a series of pre-clinical trials to establish early safety and efficacy data. The drug candidate then enters clinical trials to establish the optimal dosage and possible safety concerns. If a candidate successfully progresses through each phase of clinical trial it is submitted for approval and registration before being marketed as a New Molecular Entity (NME).⁸⁰

Preclinical candidates then undergo a series of safety and efficacy tests using a combination of in silico modelling and in vivo animal trials prior to entering the clinical testing phase. Clinical trials are divided into a number of phases, beginning with Phase I which is primarily used to assess the safety and potential side effects of the NME in healthy individuals, while also

establishing the optimal dosage. If a candidate successfully progresses through Phase I it moves to the second stage, Phase II, and is tested in individuals with the targeted disease. Phase II is often viewed as a “proof of concept” study, designed to demonstrate the clinical efficacy or biological activity of the proposed candidate. Phase II studies are also used to further optimise the dose at which maximal activity is achieved with minimal side effects. Trial failure is most common during Phase II.⁸¹ The final stage of clinical testing, Phase III, is designed to assess the effectiveness of the candidate in large patient groups (300-3000 individuals) and are generally randomised and conducted across multiple centres to ensure a mixed testing population.⁸² Phase III trials are the most expensive and time-consuming to design and manage due to their scale and are commonly thought of as the “pre-marketing phase” as a consumer’s response to the product can be measured.⁸³

Once a candidate has been awarded regulatory approval for widespread distribution and use, it is registered and marketed, this stage of the process is commonly known as Phase IV or as a post-marketing surveillance and monitoring trial as the newly available drug is continually assessed in terms of its’ long-term safety and effectiveness in the general population.

As previously discussed, it can take between 12 to 15 years to progress a lead compound to the clinic. The attrition rate of compounds during this period is not insignificant; a study published in 2014 reports that over 92% of small molecule drugs that entered phase I clinical trials did not reach approval.⁸⁴ Due to this high rate of failure and the rapid development of drug resistance in many infective species, there is large amount of pressure on the pharmaceutical industry to identify and produce new pharmaceutical leads at a rapid rate.^{85, 86}

In answer to this pressure, many companies began to use high-throughput screening (HTS) methods to identify lead compounds in the 1990's, and it is still one of the most commonly employed methods of lead identification.^{80, 87} This process allows for large compound libraries, to be screened in a rapid and relatively inexpensive manner. HTS libraries can range in size, from hundreds to millions of compounds depending on the project requirements.⁸⁸ The cost-effective nature of the process, coupled with the speed at which screening can occur means that HTS has the potential to produce large numbers of potential lead compounds which can be progressed through the drug discovery pipeline with minimal financial burden. The HTS process is made up of several stages, as summarised in **Figure 1.6**, each of which plays an integral role in compound evaluation and selection. HTS is most commonly an automated process involving an operation platform, an advanced robotic system, a highly sensitive method of detection, a specific in vitro screening model and data acquisition and processing system.^{89,}
⁹⁰ Advances in technologies such as fluorescence, affinity chromatography and surface plasma on resonance it is now possible to screen upwards of 100,000 compounds per day in a single laboratory.⁹⁰

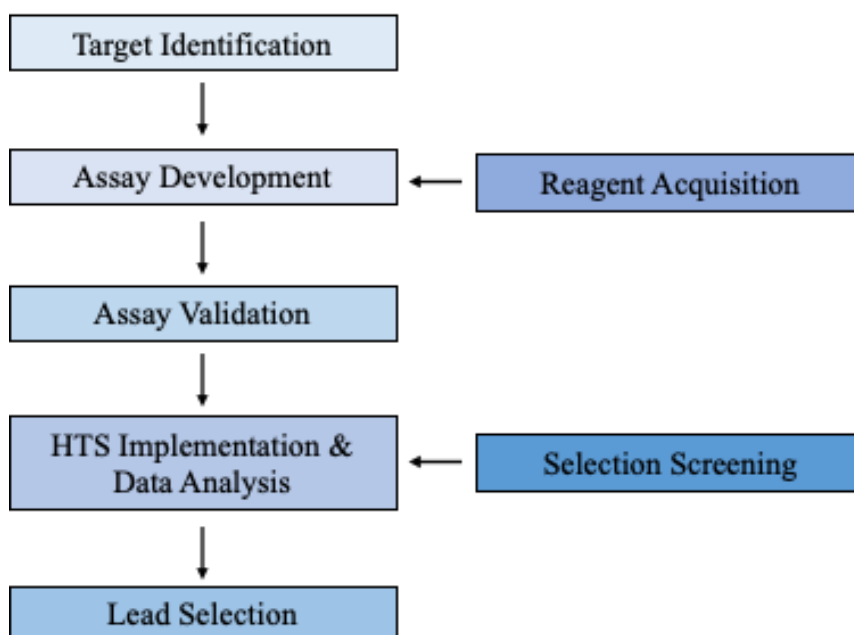


Figure 1.6. Following target identification, High-Throughput Screening (HTS) is used to screen large compound libraries to identify possible lead compounds. Initially assays are developed and validated on small sets of compounds before being employed to rapidly screen libraries containing hundreds to millions of compounds depending on the needs of the project. Screening data is analysed and the results are used to inform the selection of lead compounds which will be continued onto the next stage of the drug discovery pipeline.

1.4. Drug-Likeness: Properties Necessary for Successful Hits

There is an apparent link between the physiochemical properties and drug-likeness of a proposed drug candidate. In the early 1990's, Lipinski *et al.* studied the effects of physiochemical properties on solubility and permeability in the context of drug discovery through a number of experimental and computational approaches.⁹¹ As a result of this, the following four guidelines were proposed to maximise the oral bioavailability of proposed lead compounds:⁹² the compounds should possess no more than five H-bond donors, no more than H-bond acceptors, have a molecular weight below 500 Da and have a calculated LogP (cLogP) value of 5 or below (**Table 1.1**). cLogP is a calculated property derived from the log value of

the ratio of concentrations of a solute between two immiscible phases, octanol, and water (**Equation 1.1**).^{93, 94} If a drug is too lipophilic, it may have poor ADMET-related (absorption, distribution, metabolism, excretion, and toxicity) properties, and have issues binding to serum proteins, resulting in some undesirable off-target effects within the body.⁹⁵ Conversely, if the LogP value lies below 1, studies have shown increased problems with metabolic clearance and aqueous solubility, resulting in difficulty crossing cell membranes.^{96, 97} These guidelines have been termed the Rule of Five (Ro5).⁹¹

Equation 1.1. An equation used for the calculation of LogP values.

$$\text{Log}P_{\text{octanol}/\text{water}} = \log \left(\frac{[\text{solute}]_{\text{octanol}}}{[\text{solute}]_{\text{water}}} \right)$$

It was widely accepted that violating one or more of these guidelines leads to compounds with poor oral absorptions and in turn poor pharmacokinetic properties which would likely result in failure during early-stage clinical trials. The Ro5 guidelines, defined by Lipinski, were quickly adopted by the pharmaceutical community for designing high-throughput screening libraries and successfully reduced the rate of attrition due to poor ADMET-related properties from 40% to 10%.^{74, 93}

Table 1.1. A series of guidelines were proposed in order to optimise the oral bioavailability of pharmaceutical compounds.

These guidelines have been termed “The Rule of Five”.^{91, 92}

Physiochemical Properties	Ideal Value
Molecular Weight	≤500 Da
Hydrogen Bond Donors	≤10
Hydrogen Bond Acceptors	≤5
cLogP	≤5

Most compounds which are orally bioavailable are compliant with these guidelines and Lipinski has advised that an “ideal compound” which possesses such characteristics will have a higher chance of being successful throughout the drug discovery stages, and these criteria have been widely applied by medicinal chemists to predict the overall drug-likeness.⁹⁸ However, it is worth noting that there has been a departure from these guidelines in more recent times with studies showing that compounds with a significantly lower molecular weight and cLogP value have become increasingly favoured as compounds which lie close to the upper edge of the Lipinski limits have a lower probability of success.

During the optimisation of lead-like compounds, the drug candidate typically shows an increased molecular weight and becomes more lipophilic when compared to that initial lead compound, this occurs as the lead compound is decorated with additional substituents in order to enhance the compounds activity towards the desired target.^{99, 100} To facilitate this, the lead-compound will ideally possess physiochemical properties which when further optimised will allow them to move from the lead-like area of chemical space towards optimal drug-like space (**Figure 1.7**).^{99, 101, 102}

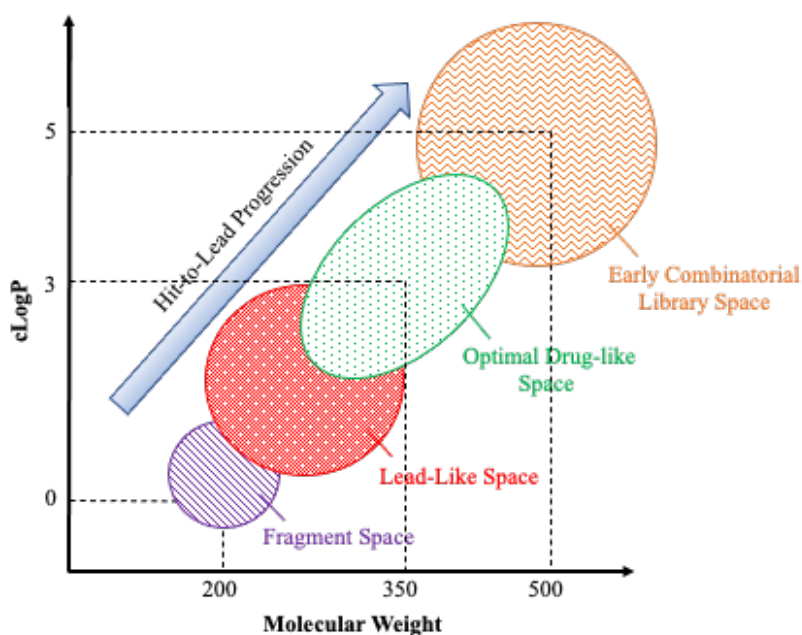


Figure 1.7. Compounds which are selected as leads following early target validation and HTS studies typically fall into the region of chemical space shown in the red circle and normally have a molecular weight of below 350 Da and a cLogP of less than 3. As lead compounds are optimised towards their intended target they move towards optimal drug-like space, typically becoming heavier and more lipophilic. This figure has been adapted from Nadin et al.⁹⁹

A molecule with molecular properties falling outside of lead-like chemical space prior to optimisation will have a greatly increased risk of failure during the later stages of discovery and development.⁹⁹ As lead-like compounds are optimised they move away from the initial Ro5 guidelines and begin to adopt properties to enhance their lead-likeness, these parameters are summarised in **Table 1.2**.

Table 1.2. Following the identification of potential lead compound, their physiochemical properties are increasingly refined to fall within lead-like chemical space.^{99, 103, 104}

Physiochemical Properties	Ideal Value
Molecular Weight	200 – 350 Da
Heavy Atom Count	14 – 26
Lipophilicity	$-1 \leq \text{cLogP} \leq 3$
Aromatic Ring Count	1 -3
Shape	3-D
Substructures	Absence of chemically-reactive or redox-active groups

1.5. Compound Dimensionality: Importance and Analysis

Assessment of compound shape has become increasingly more important for success at the discovery and development stage. Several methods have been developed to analyse compounds, computationally and experimentally, based on their shape and possible conformations. The importance of computational analysis in early-stage drug design has been highlighted by Bender and co-workers, by showcasing how the utilisation of novel computational methods can allow for a more efficient exploration of therapeutically relevant chemical space.¹⁰⁵ It has also been widely reported within the community that assessment of shape is one of the most effective methods for ensuring diversity in a set of compounds.¹⁰⁵⁻¹⁰⁷

1.5.1. Fraction of sp^3 Centres (F_{sp^3})

In 2009, Lovering and co-workers introduced a new method to evaluate the molecular complexity of molecules, using the number of sp^3 centres present in each molecule.¹⁰⁸ This approach was developed as a simplification of a method originally described by Badertscher

in 2001, which calculate the saturation in a given molecule through a mathematically demanding formula.¹⁰⁹ The degree of unsaturation (DU) can be calculated using **Equation 1.2** or through a structural representation of a molecule, itemising the contribution of each structure element (**Equation 1.3**).

Equation 1.2. An equation used to calculate the degree of unsaturation in a molecule.

$$DU = 1 + \frac{1}{2}(-q + \sum_i n_i (b_i - 2))$$

q = total molecular charge

n_i = number of atoms of element, i

b_i = standard number of bond electrons of i

Equation 1.3. An alternative equation for the calculation of the degree of unsaturation value.

$$DU = DB + 2 \bullet TB + RING + (1 - DIS) + \frac{1}{2}ELE$$

DB = number of double bonds

TB = number of triple bonds

RING = number of rings

DIS = number of disjoint parts

ELE = number of localised electrons

Both mathematical formulas are complex and require a large degree of input by the user, which is notably inefficient when compared to the formula (**Equation 1.4**) proposed by Lovering, which is a readily interpretable, user-friendly measure of saturation whereby the number of sp³ hybridised carbons is divided by the total number of carbons in a given molecule.¹⁰⁸ This measure is termed the fraction of sp³ (Fsp³).

Equation 1.4. An equation for the calculation fsp³ values.

$$\text{Fraction of } sp^3 = \frac{\text{number of } sp^3 \text{ hybridised carbons}}{\text{total number of carbons}}$$

Despite its popularity, this method has been criticised, primarily noting that F_{sp^3} poorly characterises whether the sp^3 carbons are connected to vectors which extend out of the main plane, therefore actively contributing to the structural diversity. Blagg and co-workers used two compounds, termed A and B, which have the identical F_{sp^3} values but have computationally-derived conformations which are different to each other to illustrate this point.¹⁰⁷ Both A and B have an F_{sp^3} of zero, suggesting that each compound should be planar. However, as can be seen in **Figure 1.8**, due to the presence of a pseudo- sp^3 carbon in compound B, it displays a “V-like” shape, whereas compound A is linear as expected through the calculation. This difference is likely to be detected by other shape analysis protocols which would be employed in tandem with F_{sp^3} calculations, meaning that it remains a valuable tool for the rapid analysis of molecular complexity, particularly in regards to large compound sets.

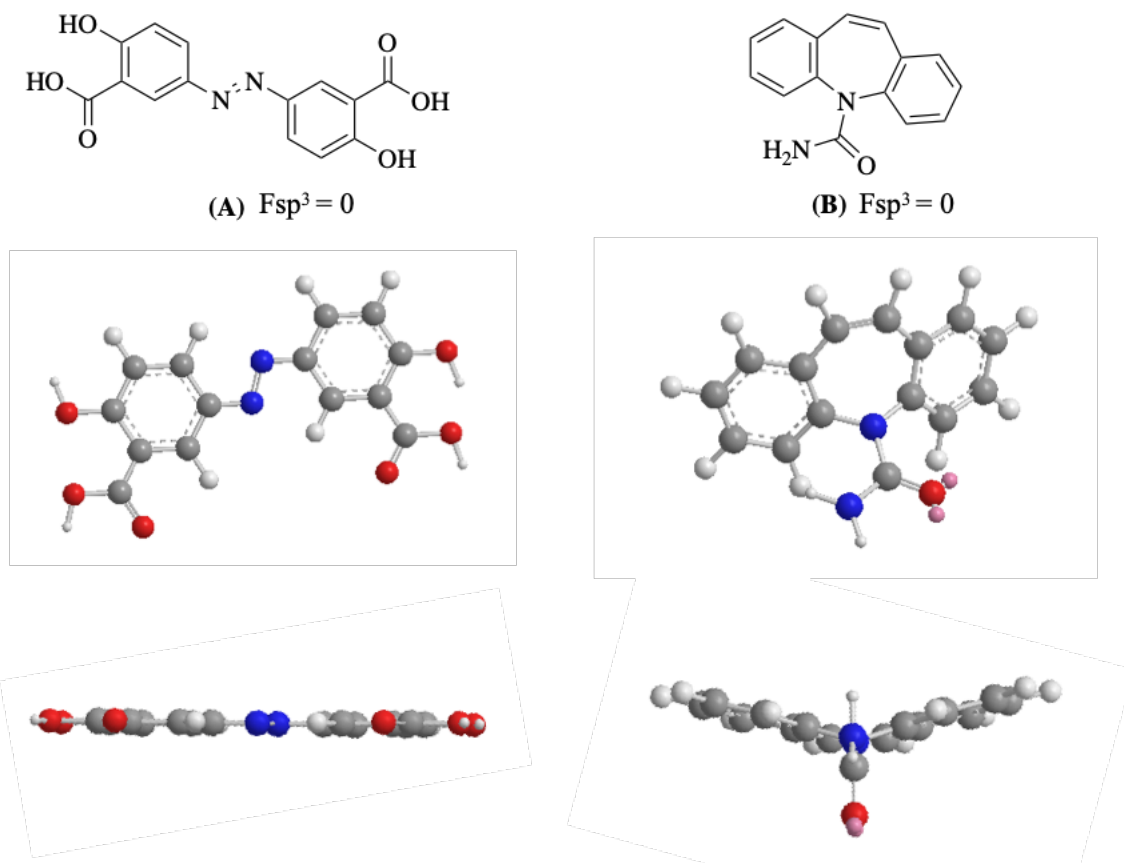


Figure 1.8. Two compounds, termed (A) and (B), have the same F_{sp^3} value of zero, suggesting that both compounds should be planar. However, both (A) and (B) possess different conformations which have been computationally-derived, the presence of a pseudo- sp^3 carbon in (B) causes it to have a “V-like” conformation whereas (A) is planar as would be expected. This figure has been adapted from Blagg and co-workers.¹⁰⁷

1.5.2. Plane of Best Fit (PBF)

Blagg *et al.* presented an alternative method of shape analysis, to quantify and characterise the three dimensionality of molecules in a rapid and unambiguous manner.¹⁰⁷ The method quantifies how far any molecule is removed from a two-dimensional plane, termed the plane of best fit (PBF). A two-dimensional plane was established across all the heavy atoms in a molecule in a given conformation. The averaged distances of each heavy atom away from this plane provides a quantitative measure of three dimensionality. For a given molecule, a conformation was computationally generated, using a literature standard method and software

CORINA.¹¹⁰ A single conformer of each molecule is used as a reference conformer, which is common in other shape analysis methods such as PMI analysis, although the method is amenable to the analysis of multiple conformers of a single molecule as required. The reference conformation is calculated computationally excluding salts and omitting hydrogen atoms, the PBF is then calculated using the “least squares” method from the generated conformers coordinates as shown in **Equation 1.5**.¹¹¹

Equation 1.5. An equation used for the calculation of the plane of best fit using the “least squares” method.

$$A_x + B_y + C_z = D$$

The equation of best fit is then used to calculate the distance, Δ , of each heavy atom in the molecule from the plane of best fit (**Equation 1.6**).

Equation 1.6. An equation used to calculate the distance of each heavy atom from the plane of best fit in a given molecule.

$$\Delta = \frac{|Ax_i + By_i + Cz_i + D|}{\sqrt{A^2 + B^2 + C^2}}$$

where $Ax + By + Cz = 0$

The solution of this equation is the average of these distances in angstroms, Å. The theoretical range of the PBF score is between 0 and ∞ , although most drug-like compounds have a score of less than 2.¹⁰⁷

As a means of testing the applicability of the PBF method, several sets of compounds were analysed and compared to alternative methods of shape analysis. In general, PBF performed well when compared to molecular globularity and PMI methods, but Fsp³ gave significantly different results. As previously discussed, Fsp³ is not an accurate descriptor of shape as the method cannot detect if the Fsp³ centre extends out of the plane. The PBF method is comparable

to the other methods available and offers a high-throughput methodology for rapid shape analysis.

1.5.3. Principal Moments of Inertia (PMI)

An additional method of shape and diversity analysis was developed by Sauer and Schwarz.¹⁰⁶ Normalised ratios of principal moments of inertia (PMI) were proposed as a descriptor of molecular shape. Molecular mechanics were used to computationally derive three principal moments of inertia from a three-dimensional structure. These PMI values were sorted to give I_1 , I_2 and I_3 in ascending size order. The values are then normalised, to give NPR1 (normalised PMI ratio 1) and NPR2, by dividing the lower values, I_1 and I_2 , by the largest value, I_3 , removing the dependence on size of the compounds under investigation (**Equation 1.7**).

Equation 1.7. An equation used for the calculation of normalised PMI ratios.

$$NPR1 = \frac{I_1}{I_3} \text{ and } NPR2 = \frac{I_2}{I_3}$$

Normalisation of these values reduces the need for decorrelation procedures when PMI is used along with additional, size dependant, molecular descriptors such as molecular weight and topological surface area.¹⁰⁶ Normalised values can be visualised on a two-dimensional, ternary plot, where the vertices (0,1), (0.5,0.5) and (1,1) represent a perfect rod (acetylene), a disc (benzene), and a sphere (adamantine). PMI plots allows the three-dimensionality of compounds to be readily visualised, compounds which are more spherical sit closer to the top right corner, whereas flatter compounds sit along the rod-disc axis on the left-hand side of the triangular plot. PMI can generate a value for each molecular conformer, making it a useful method for the comparison of both small and large sets of compounds.¹¹² The majority of approved drugs fall along the rod-disc axis, with relatively few populating the more three dimensional area of

chemical space, techniques such as fragment based drug discovery and diversity orientated synthesis can be used to create compound libraries which populate under explored areas of three dimensional chemical space (**Figure 1.9**).^{106, 113, 114}

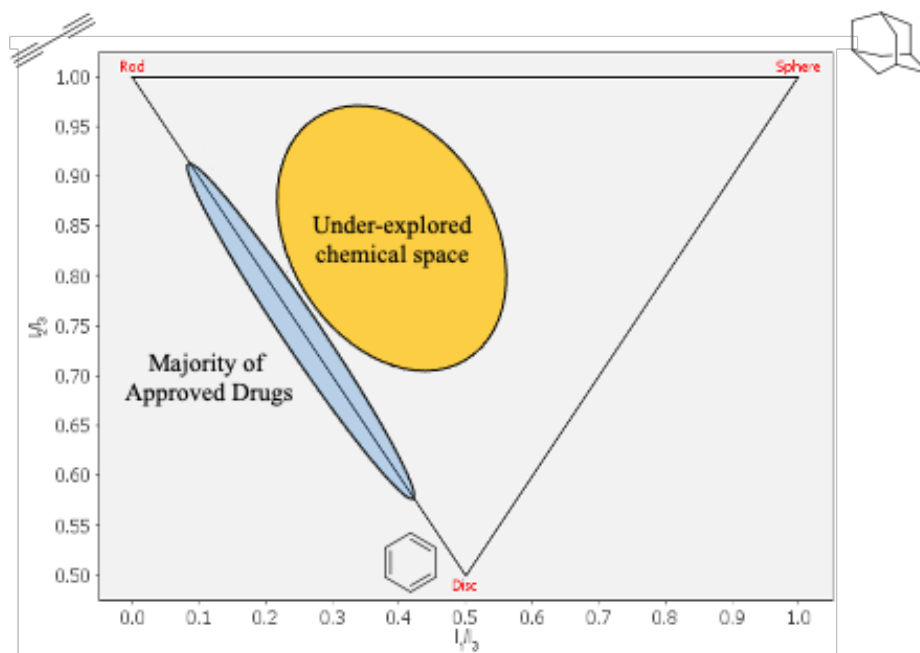


Figure 1.9. The majority of approved drugs fall along the rod-disc axis when visualised on a PMI plot with a relatively small percentage occupying a more three-dimensional region of chemical space. Techniques such as fragment-based drug design and diversity orientated synthesis allow for the creation of compound libraries which display a high degree of three-dimensionality and stereochemical diversity to enable the population of chemical space which is currently under-explored.^{106, 113, 114}

1.5.4. Principal Component Analysis (PCA)

Principal Component Analysis (PCA) works to simplify highly dimensional data while retaining as much information and as many patterns as possible, particularly when there are significant correlations between some, or all the variables present in the data set.¹¹⁵ PCA was initially introduced in 1901, and works by calculating a new, simpler, set of variables based on

the previously calculated molecular descriptors. New variables, termed principal components (PCs), explain much of the variance in the original set in a significantly simplified manner.¹¹⁶ PCA is commonly used to identify patterns in data with a high degree of dimensionality, making it a useful method for the assessment of chemical diversity. When used in the context of diversity orientated synthesis, PCA can be used to visualise the similarities and differences within compound collections, making it a useful tool for library design. Structural and physiochemical properties such as molecular weight, stereocentres, hydrophobicity and aqueous solubility are commonly included in such calculations allowing for an accurate comparison of diversity to be made.^{115, 117}

1.6. Privileged Structures in Drug Discovery

The term “privileged scaffold” was first introduced by Evans *et al.*,¹¹⁸ to describe molecular frameworks which could act as ligands towards a diverse series of receptors, however, the term has been used liberally over the past three decades. The ability to bind to multiple targets is no longer a definition strictly applied by the community, instead a privileged scaffolds is now considered as a biologically important pre-validated platforms for the design of compound libraries in the search for new drug candidates, by providing three-dimensional vectors which can be readily manipulated to enable for diversification.¹¹⁹ Such scaffolds should be accessible through established and robust methodologies. Although there are no specific set of characteristics that a compound must possess in order to be defined as privileged, generally, they are found to contain two or more ring systems which are fused or connected by a single bond.^{120, 121} Welsch and co-workers have stated that the key to successful construction of a privileged scaffold library is the development of a broad scope of reactions combined with intelligent library design and selection such that the final compounds possess molecular

properties which are suitably drug-like, examples of privileged scaffolds can be seen in **Figure 1.10**.¹¹⁹

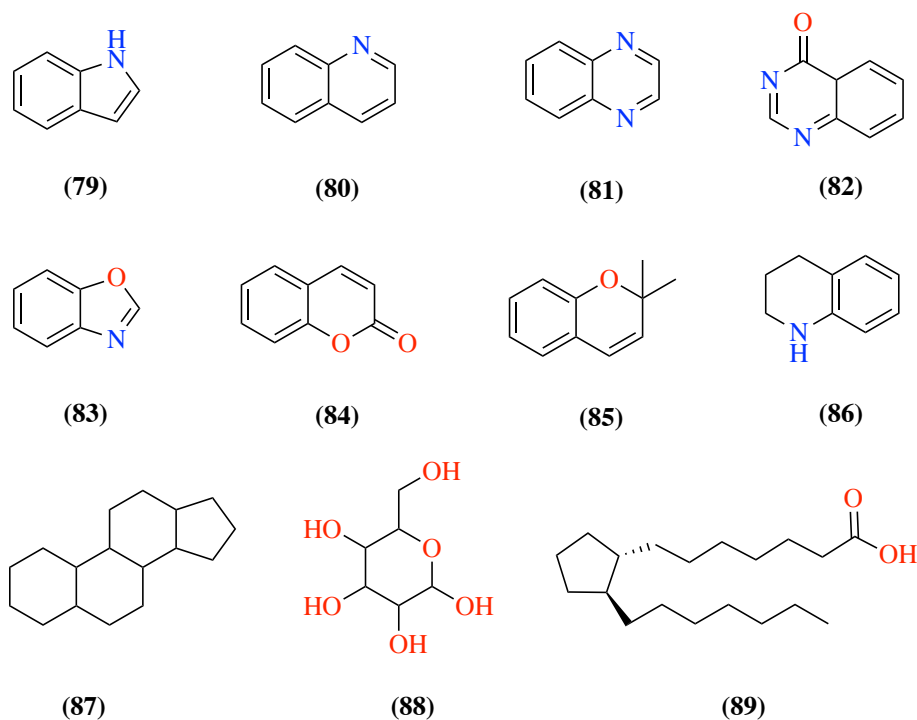
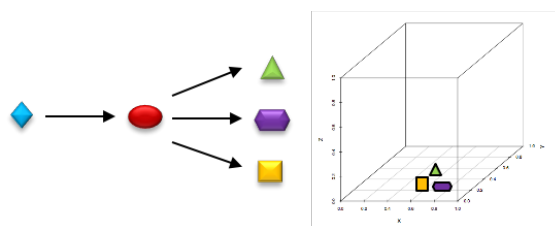


*Figure 1.10 . Privileged scaffolds are commonly derived from natural products and are thought to be pre-validated platforms for the creation of compound libraries which provide multiple vectors on which diversification can occur.*¹¹⁹

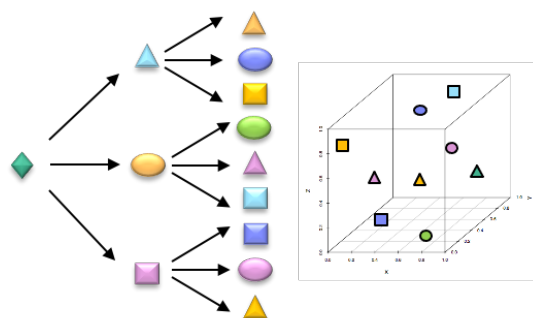
Heterocyclic rings are commonly observed in natural products and often have a low molecular weight, are non-planar and are conformationally robust, making them ideally suited to feature in newly designed privileged scaffolds. Heterocycles are commonly incorporated during early-stage drug discovery to create novel privileged scaffolds with favourable properties in terms of bioavailability.¹²² This has been demonstrated by Njarðarson and co-workers who reported over 80% of the top grossing pharmaceutical compounds of 2010 contained one or more heterocycles in their chemical structure.¹²³

1.7. Diversity Oriented Synthesis

It has been widely accepted that the synthesis of all theoretically stable carbon-based molecules is not realistically feasible,^{124, 125} therefore the ability to synthesise a molecular library which can achieve a wide coverage of chemical space is an important consideration during early-stage library design.¹²⁴ Diversity-oriented synthesis (DOS) was first introduced by Schreiber *et al.* and aims to explore chemical space through the preparation of large libraries of skeletally diverse compounds for use in HTS, with the hope of identifying hits towards biological targets.¹²⁶ The DOS approach aims to create a collection of structurally diverse, complex molecules with a wide variety of favourable physiochemical and biological properties in an efficient manner.¹²⁷ While there are some notable advantages to this library synthesis approach in terms of its exploration of chemical space to enable its use as a tool for the development of novel biologically active compounds,^{128, 129} the approach has also been criticised due to its lack of consideration in terms of molecular properties when constructing a compound library.¹²⁸ The DOS approach uses a branching pathway and aims to cover a wider, more diverse area of chemical space than can be achieved *via* traditional combinatorial library synthesis (**Figure 1.11**).¹²⁹



Combinatorial Approach



DOS Approach

Figure 1.11. Combinatorial library synthesis results in a complex library in which the compounds occupy a smaller, more defined area of chemical space. Alternatively, diversity-orientated synthesis results in a library with greater three-dimensionality and structural diversity owing to the creation and diversification from multiple scaffolds resulting in a compound library which populates a wide area of chemical space. This figure has been adapted from Galloway *et al.*¹²⁹

Two methods for the introduction of skeletal diversity are commonly used within the DOS methodology. The first is a reagent-based approach whereby a common substrate with the potential diversification is exposed to a variety of reaction conditions and co-substrates to access products with a varied stereochemical and skeletal diversity (**Figure 1.12**).^{124, 130} The alternative approach, a substrate-based pathway, gives rise to diverse molecular skeletons through the reaction of substrates which possess different appendages, termed σ -elements, which pre-inform skeletal information, in a combinatorial fashion.^{131, 132}

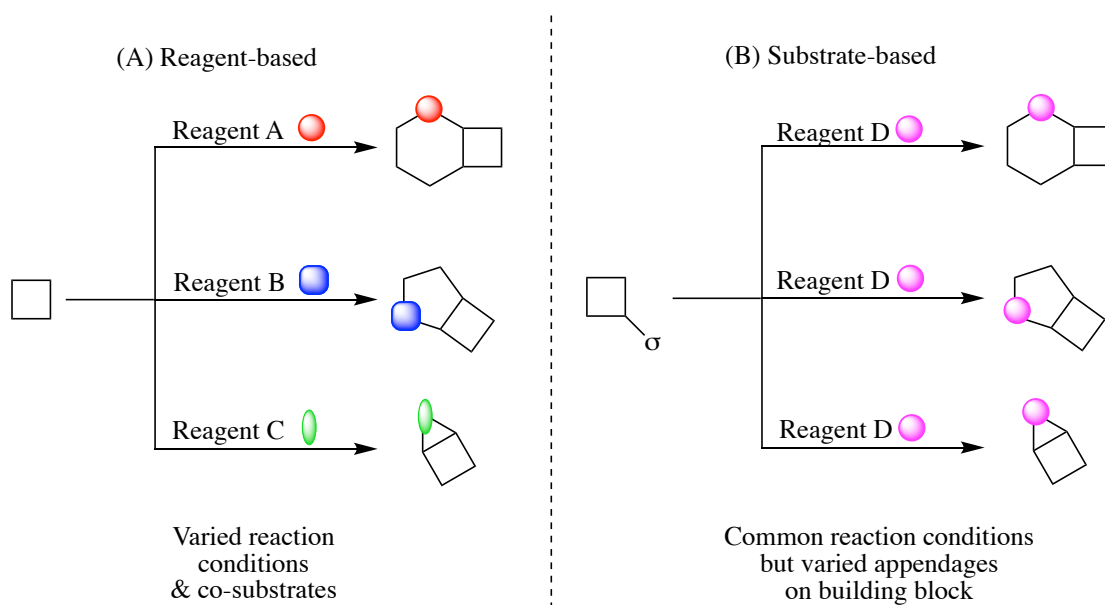


Figure 1.12. Two methods are used for the introduction of skeletal diversity in DOS libraries. The reagent-based approach uses a common substrate with diversification potential which is exposed to a series of co-substrates and reaction conditions to create several diverse scaffolds. Conversely, a substrate-based approaches requires the reaction of substrates which are decorated with various appendages which inform the final scaffold moiety.^{130, 131}

A three-step DOS strategy termed *build/couple/pair* (B/C/P) was described by Nielsen and Schrieber,¹³³ in which a collection of stereochemically-controlled, diverse compounds were prepared using chiral building blocks which possessed orthogonal points of diversity for subsequent coupling reactions. The *Build* phase involves the asymmetric synthesis of these chiral building blocks which when coupled provide a large degree of stereochemical diversity. The subsequent *Couple* phase, refers to the intermolecular coupling of these prepared building blocks, with the aim of having complete control of all possible stereochemical outcomes. The final stage, *Pair*, refers to functional group pairing reactions to provide an increased amount of skeletal diversity. A general example of the B/C/P approach can be seen in **Figure 1.13**.

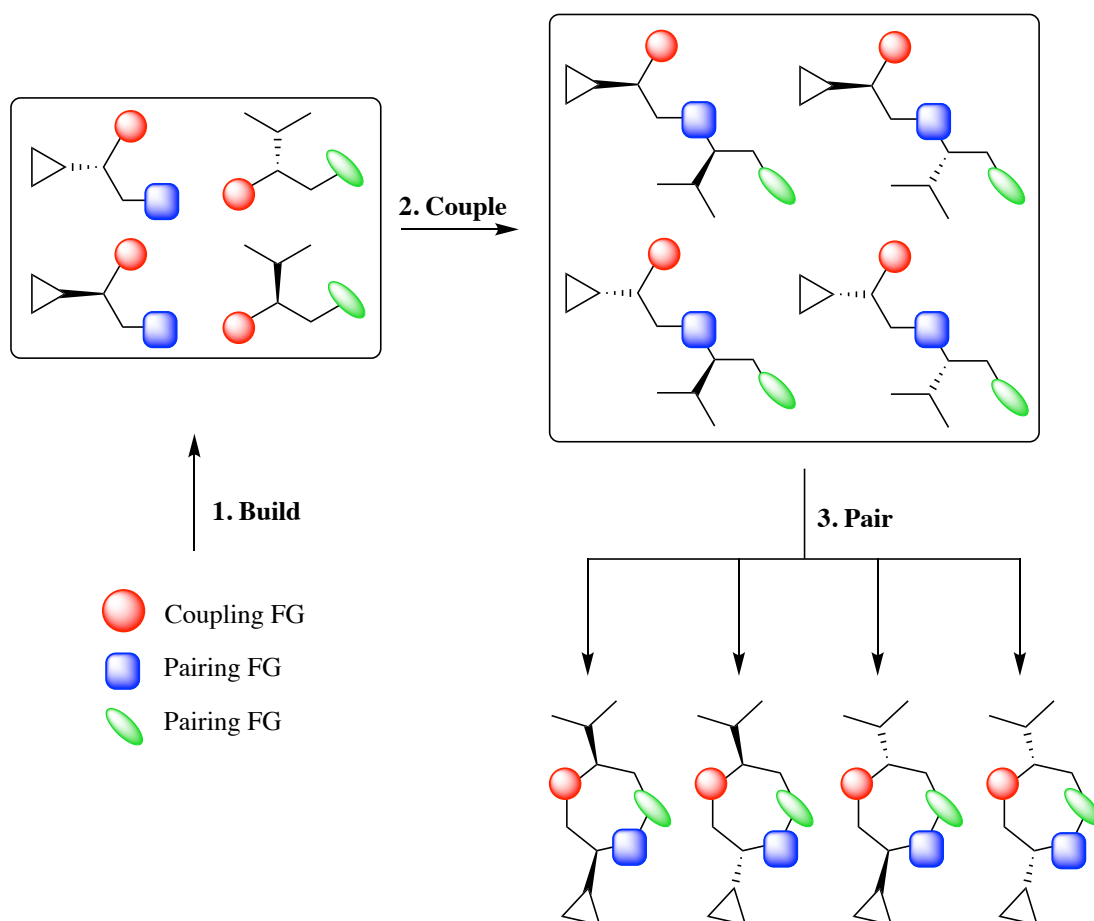


Figure 1.13. The Build/Couple/Pair approach is a commonly used approach to introduce diversity into DOS libraries. The Build phase involves the synthesis of chiral building blocks, each containing a coupling functional group and a pairing functional group. The Couple phase represents the coupling of the previously synthesised and aims to completely control the stereochemical outcomes. The Pair phase refers to the final pairing of functional groups to create scaffolds with increased skeletal diversity. This figure has been adapted from Nielsen et al.¹³³

Since its conception, DOS has had a significant impact on the scientific community, as it has addressed the deficiencies previously observed with compound collections and has allowed for sets of compounds, which display both stereochemical and skeletal diversity, to be synthesised in an efficient manner. Compounds which are created *via* a DOS methodology are typically employed in high-throughput and phenotypic screens, allowing for the identification of lead compounds towards targets of which very little was previously known

1.8. Aims and Objectives

The aim of this project is to populate unexplored and underutilised areas of chemical space through the design and synthesis of novel compound libraries with a high degree of three dimensionality.

To achieve this overarching goal, a series of aims were set out:

- i. Develop a robust method towards the synthesis of bicyclic, heterocycle-containing scaffolds
- ii. Carry out *in silico* scaffold decoration using open-source computational software
- iii. Generate a virtual compound collection with favourable molecular properties for drug discovery and with a high degree of structural diversity
- iv. Synthesise a selection of diverse compounds to create a reference library for use in biological studies

Firstly, using a methodology previously developed within the JSF group a series of azetidines will be synthesised and the synthetic scope of these molecules explored and expanded to allow for the creation of novel azetidine compounds. Newly synthesised azetidines will be employed as building blocks during the development of a robust and scalable methodology towards novel, bicyclic scaffold moieties which possess multiple points of diversification.

Following the generation of novel, synthetically enabled scaffolds, *in silico* screenings will be carried out to create a virtual compound collection spanning unpopulated areas of chemical space. Using a series of virtual screening techniques, this virtual compound collection will be filtered and refined to establish a diverse compound library with a high degree of structural diversity (**Figure 1.14**).

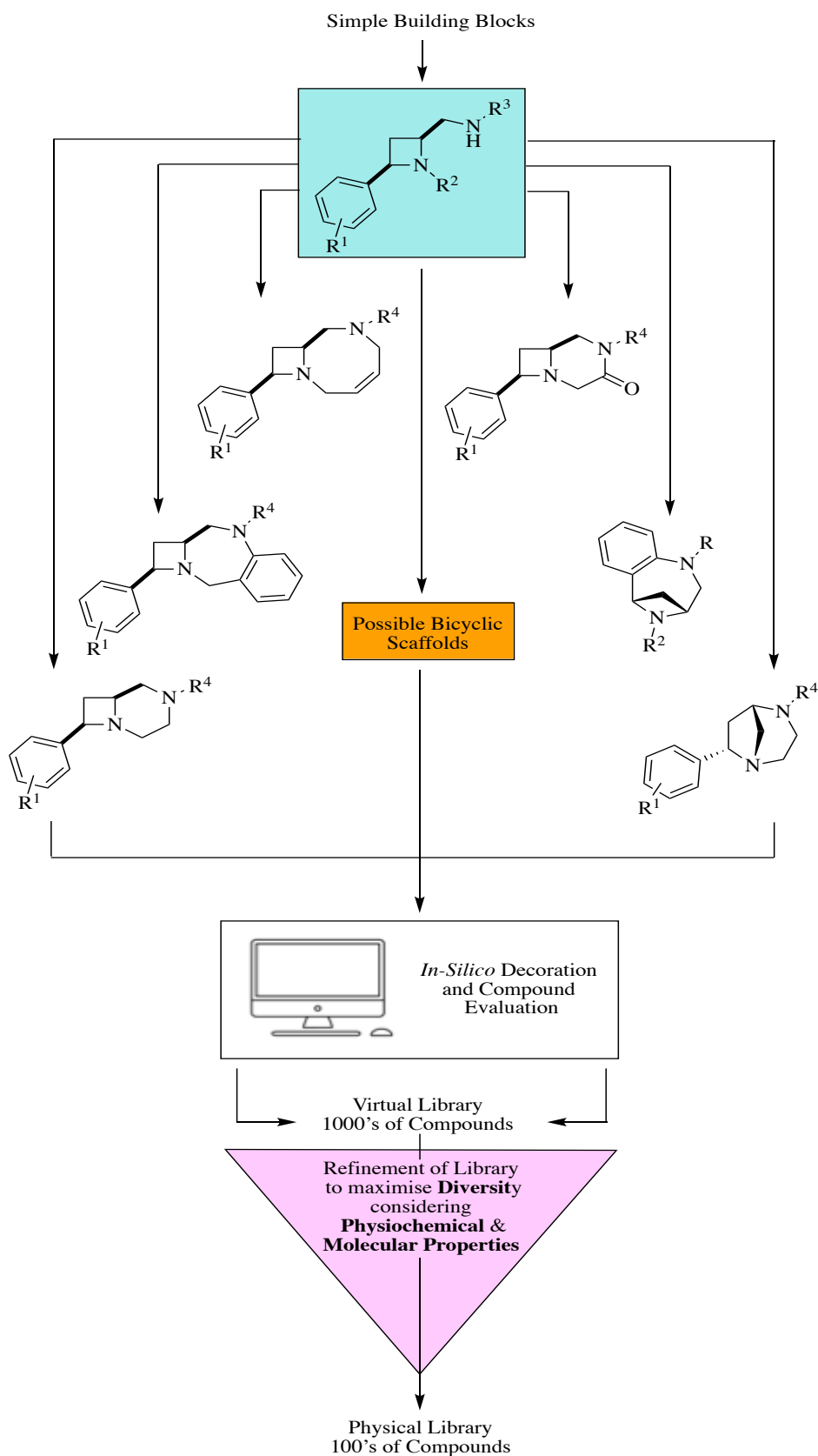


Figure 1.14. A general project overview whereby simple building blocks are used for the generation of structurally diverse, three-dimensional scaffolds. *In silico* scaffold decoration and library enumeration will be conducted to inform the selection of compound libraries which will subsequently be synthesised.

This refined set of compounds will then be synthesised using parallel synthetic methods to create a diverse set of library compounds containing the novel bicyclic core. This final set of compounds will display a large degree of structural diversity in order to occupy a large and varied area within chemical space in order to potentially establish new lead compounds for drug discovery.

Representative compounds from this library will be selected and submitted for biological testing against a number of disease models and will be evaluated based on their efficacy in these models to identify active compounds.

Chapter 2: Towards a Bicyclic Scaffold

2.1. Synthesis of Azetidines

A major aim of this research was to develop a novel method towards bicyclic, *N*-heterocycle containing scaffold moieties which possess multiple points of diversity for the population of chemical space. In order to achieve this aim, a series of diastereoselective 2,4-*cis*-amino-azetidine molecules were to be synthesised for use as building blocks towards the final scaffolds.

2.1.1. Iodine Mediated Cyclisation of Homoallylic Amines

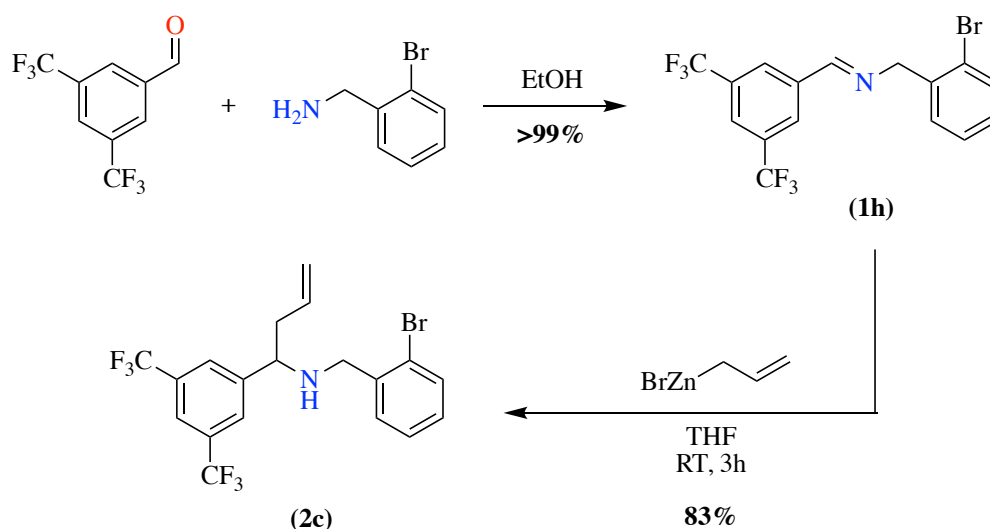
To facilitate the synthesis of the desired azetidine molecules, a series of imines were synthesised through the reaction of benzylamines and benzaldehydes using a well-established mechanism. The respective benzylamines (1.1 Eq) and benzaldehydes (1.0 Eq) were refluxed for one hour in ethanol (0.3 M), the resultant imines were isolated and progressed onto to next step without the need for further purification.

Numerous methodologies for the allylation of imines have been reported in the literature, lewis acids such as boron trifluoride, indium, magnesium, palladium, stannane chloride have all been used to activate imines for the synthesis of homoallylic amines.¹³⁴⁻¹⁴⁰ Zinc-mediated methodologies have also been widely quoted in the literature,¹⁴¹⁻¹⁴³ and extensive work has been done within the JSF group by previous members to establish a reliable route towards homoallylic amines.^{44, 45}

In accordance with the protocol previously established within the group, zinc metal was activated by stirring in 1.0 M HCl for thirty minutes at room temperature before filtration and washing with water, ethanol, acetone, and dry diethyl ether.¹⁴⁴ The required allylzinc bromide reagent was then prepared by stirring activated zinc powder with allyl bromide under an

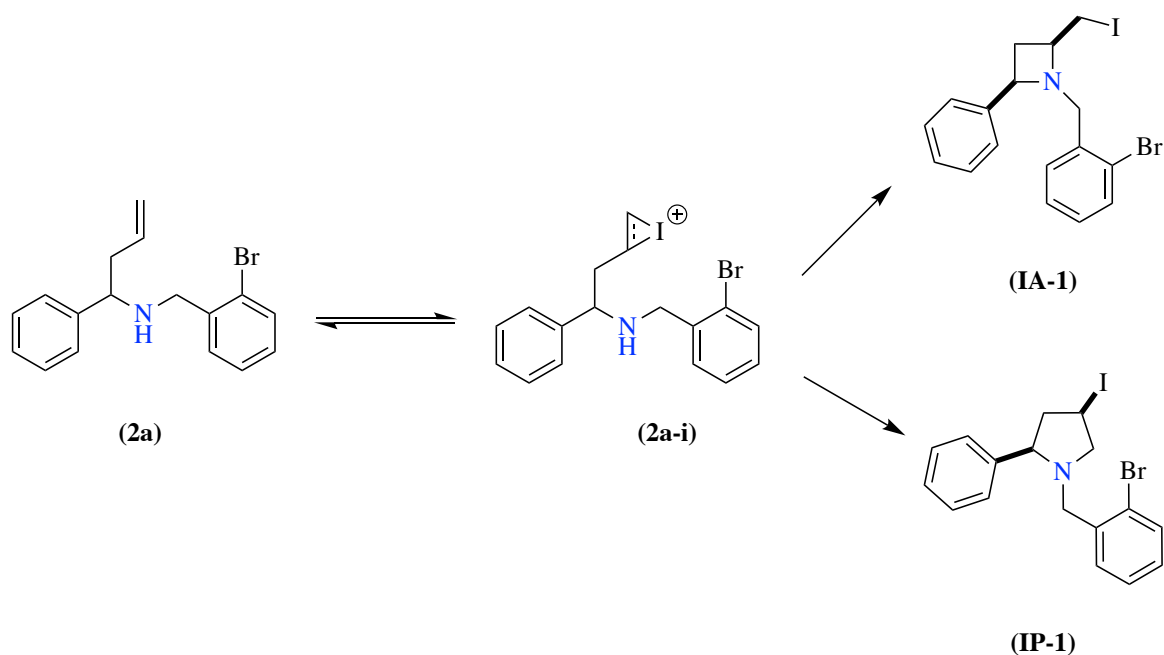
anhydrous atmosphere at room temperature in dry tetrahydrofuran for until all of the zinc metal (generally between 0.5 – 3 h, depending on reaction scale) had been consumed. Formation of the allylzinc reagent resulted in an exotherm within the reaction vessel which was easily controlled using a room temperature water bath.

Upon joining the industrial project partner, Symeres, additional studies were conducted to further enhance the homoallylic amine synthesis protocol to make it more amenable to industrial use. It was found that anhydrous conditions were not required for the allyl zinc bromide reagent to form in situ, in addition to this it was noted that zinc dust preformed equally well when not pre-activated with a hydrochloric acid wash. Most notably, the work-up procedure associated with the allylation reaction was modified to maximise yields. The reaction was quenched with a portion of saturated sodium bicarbonate resulting in the formation of a dense precipitate, in accordance with the original methodology the resultant precipitate was removed through gravity or vacuum filtration which was time consuming and resulted in significant loss of yield. It was found that washing the precipitate with ethyl acetate and decanting off the solution gave yields of up to 99% in a more time efficient manner, making the method suitable for use in an industrial setting as required. It was also found that by decantation of the solvent followed by a wash with water and brine often allowed for the desired homoallylic amine product to be collected without the need for additional purification. Using this method, the reaction was found to be readily scalable, with high yielding, multi-gram (≤ 12 g) reactions being carried out regularly in high yields. The synthetic route from starting materials to homoallylic amine is summarised in **Scheme 2.1**.



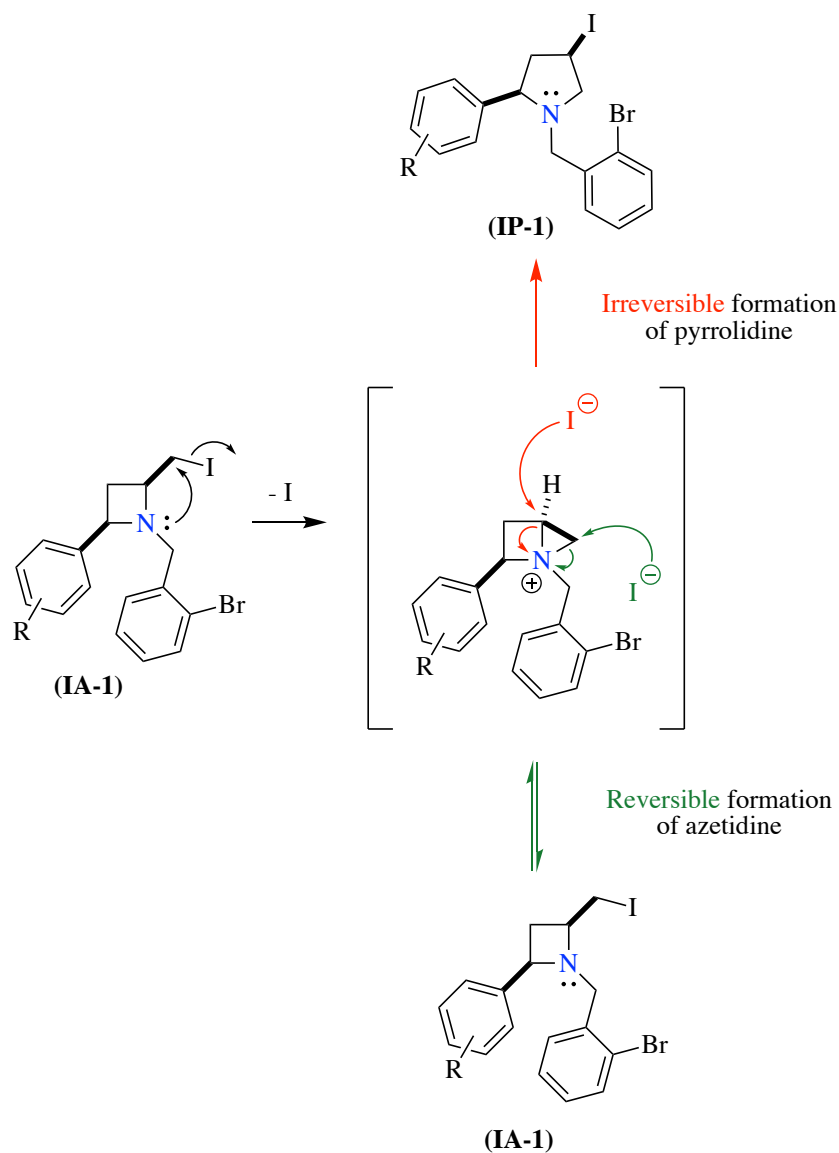
Scheme 2.1. Reaction of benzylaldehyde and benzylamine in ethanol gave rise to an imine in yields of greater than 99%, this was subsequently converted to the corresponding homoallylic amine through reaction with allyl bromide and zinc

Cyclisation of the homoallylic amine *via* the iodoiranium intermediate (**2a-i**) could result in either the four-membered iodo-azetidine (**IA-1**) or the corresponding five-membered iodo-pyrrolidine (**IP-1**) stereoisomer (**Scheme 2.2**). According to Baldwin's Rules, when a three-membered ring is open for the formation of a new cyclic system, the rules lie between those for tetrahedral and trigonal systems, with *exo* ring closure generally being preferred.¹⁴⁵⁻¹⁴⁸ With this in mind, 4-*exo-trig* and 4-*exo-tet* would be considered the more favoured ring closure process for the cyclisation of homoallylic amine (**2a**) with iodine to yield the iodo-azetidine (**IA-1**).



Scheme 2.2. Reaction of homoallylic amines with iodine can result in the formation of the corresponding iodo-azetidine or iodo-pyrrolidine intermediate via an iodoiranium intermediate.

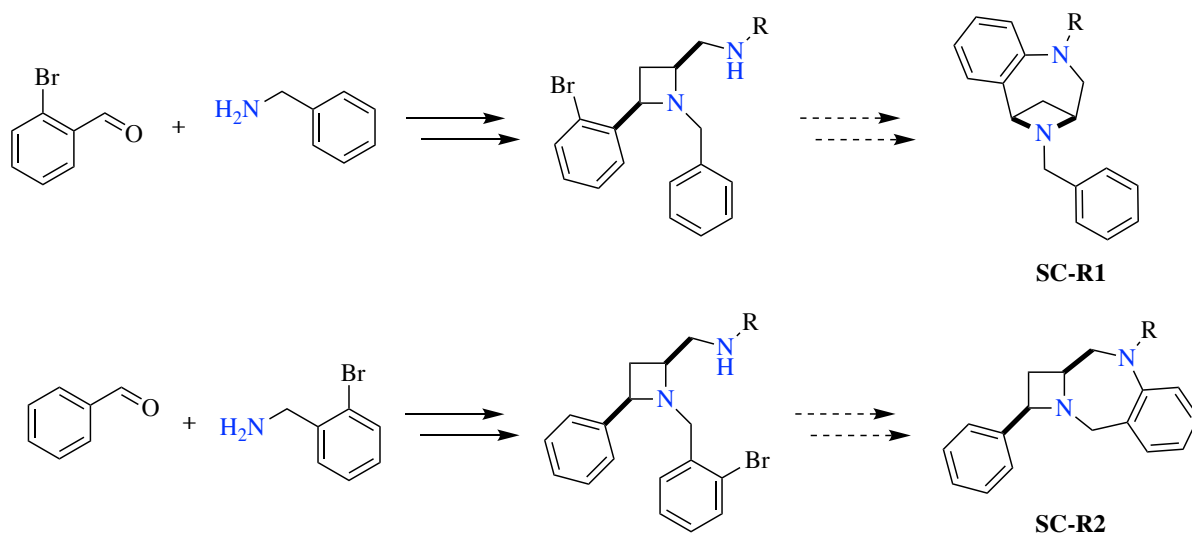
Iodo-azetidines were known to be unstable, even at low temperatures ($< 4\text{ }^{\circ}\text{C}$) and were prone to rapid isomerisation to the corresponding five-membered iodo-pyrrolidine ring system, this isomerisation was previously proven to occur in accordance with the literature.^{44, 149-151} A proposed mechanism for the expansion of the four-membered ring involves an intramolecular displacement of iodine by the nitrogen atom to give the resultant aziridinium intermediate structure. This unstable intermediate compound then underwent attack with the eliminated iodide, attack on the least hindered carbon atom would reform the *cis*-azetidine, making it a reversible reaction. However, attack by the iodide at the more hindered position would be an irreversible process and would result in the formation of the more thermodynamically favourable *cis*-pyrrolidine, relieving some of the torsional ring strain and creating a more stable ring system (**Scheme 2.3**). While this research was initially focussed on the application of the azetidine ring system, pyrrolidines were also utilised to further the aims of the project.



Scheme 2.3. Iodo-azetidine intermediate compounds are prone to rearrangement through iodine displacement, subsequent attack at the least hindered carbon results in the reformation of the iodo-azetidine (green pathway). Alternatively, attack by the iodide at the more hindered carbon results in the irreversible formation of the corresponding iodo-pyrrolidine intermediate compound (red pathway).

Previous work within the group suggested that only homoallylic amines where R = aryl or benzylic rings, on the nitrogen, could be converted to the corresponding azetidine under iodine-mediated cyclisation conditions. When considering this pre-established knowledge and the overarching aims of this work, the initial azetidine compounds were proposed, synthesised

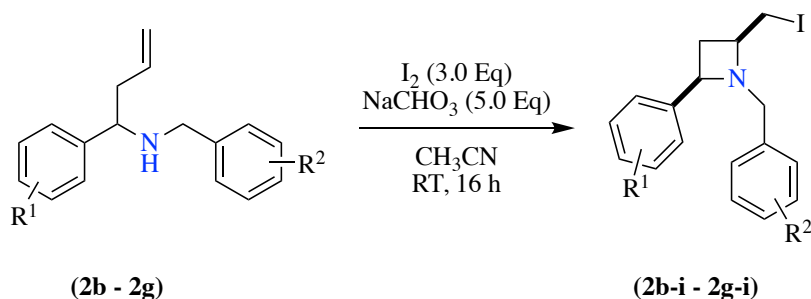
from simple aryl amines and benzaldehydes, and designed to be suitable for use in intramolecular cross-coupling at a later stage, the earliest proposed scaffold moieties can be seen in **Scheme 2.4**. The application of these azetidine molecules in C-N Buchwald-Hartwig amination is discussed in (**Section 2.2.1**). Homoallylic amine (**2a**) was stirred as a solution in acetonitrile with an excess of molecular iodine and sodium hydrogen carbonate at ambient room temperature to ensure the formation of the desired iodo-azetidine intermediate compound. Following several unsuccessful attempts at cyclising the homoallylic amine to the desired azetidine ring, it was decided to investigate the effects of electron-donating and electron-withdrawing substituents had on cyclisation.¹⁵²⁻¹⁵⁵ With this in mind, a series of homoallylic amines were synthesised with additional substitution present on the aryl rings. Trifluoromethyl groups and nitro groups were incorporated to investigate the effect of electron withdrawal on ring closure, while methoxy groups were used to donate electron density into the ring to monitor its effect. The newly synthesised homoallylic amines were treated as before, by stirring as a solution in acetonitrile with molecular iodide and sodium hydrogen carbonate at room temperature.



Scheme 2.4. A halide, generally bromine, was incorporated into the amino-azetidine building blocks using an appropriate benzaldehyde or benzylamine, the resulting compounds were cyclised to the corresponding iodo-azetidines and amine nucleophiles were used to create amino-azetidines which were theoretically capable of intramolecular C-N cross coupling

Inclusion of the electron donating group in the homoallylic amine appeared to have no effect on the cyclisation to the azetidine ring. Conversely, the azetidine ring was formed with a conversion of $\geq 96\%$ when electron withdrawing groups are present on the homoallylic amine compounds (**Table 2.1**). It was proposed that inclusion of electron withdrawing groups on the aryl ring of the homoallylic amine decreases the nucleophilicity of the nitrogen lone pair which allows the double bond of the allyl group to attack the iodine. Following the formation of the iodoaziridium intermediate, the nitrogen lone pair can then attack the three-membered ring to form the desired four-membered ring.

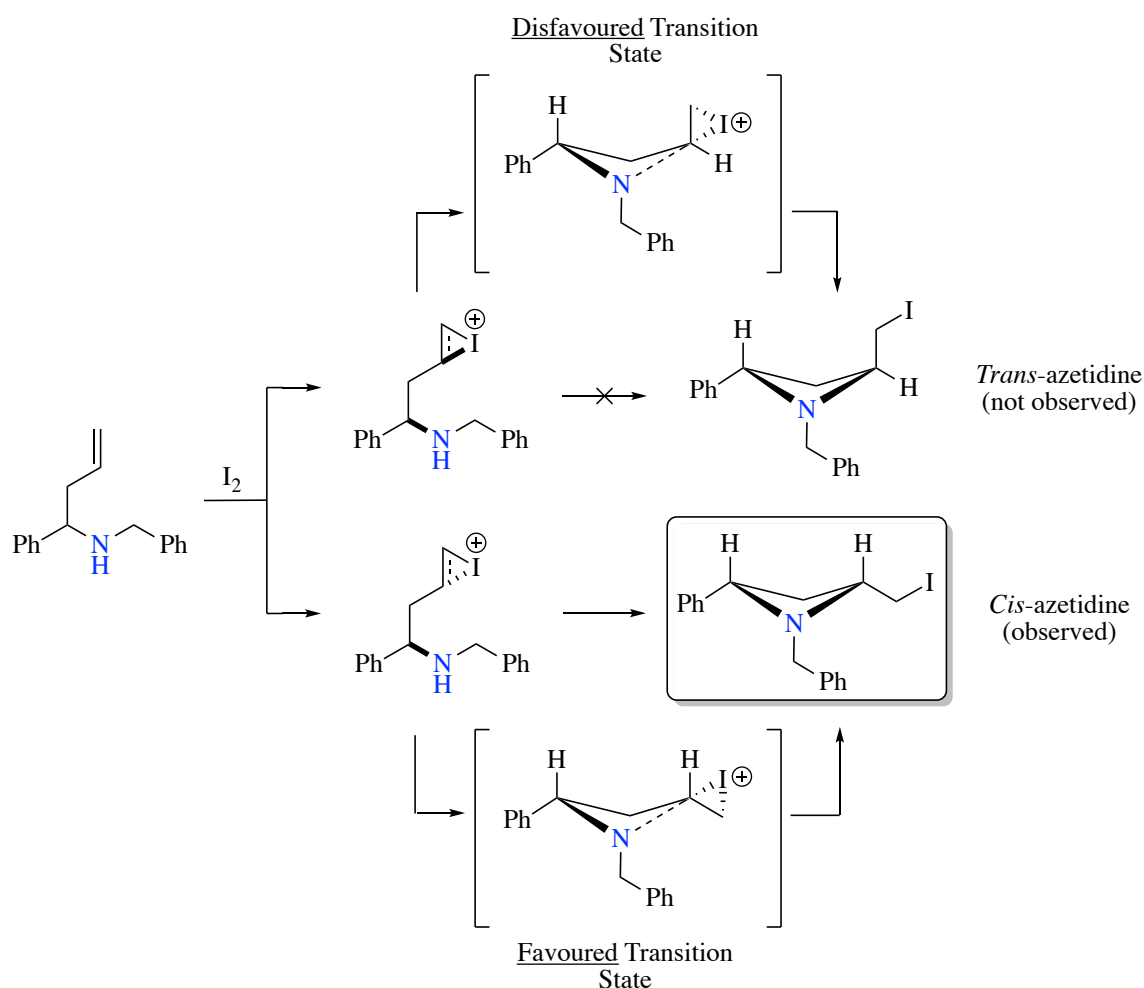
Table 2.3. Aromatic ring substitution screening, a series of homoallylic amines were synthesised and were reacted with molecular iodine under basic conditons at ambient room temperature to study the effect of electron-withdrawing and electron-donating groups on cyclisation to the corresponding iodo-azetidine intermediate compound.



	R^1	R^2	% Conversion
<i>2b-i</i>	<i>o</i> -Br	<i>m</i> -CF ₃ , <i>m</i> -CF ₃	98
<i>2c-i</i>	<i>m</i> -CF ₃ , <i>m</i> -CF ₃	<i>o</i> -Br	97
<i>2d-i</i>	<i>p</i> -NO ₂	<i>o</i> -Br	96
<i>2e-i</i>	<i>o</i> -NO ₂	<i>o</i> -Br	97
<i>2a-i</i>	H	<i>o</i> -Br	0
<i>2f-i</i>	<i>o</i> -Br	H	0
<i>1A-7</i>	H	<i>m</i> -OCH ₃ , <i>p</i> -OCH ₃	0
<i>1A-8</i>	<i>o</i> -Br	<i>m</i> -OCH ₃ , <i>p</i> -OCH ₃	0
<i>2g-i</i>	<i>o</i> -Br	<i>o</i> -OCH ₃ , <i>p</i> -OCH ₃	0

Iodo-azetidine intermediates were formed with an assumed *cis* relative stereochemistry which can be explained by examining the transition states for both the *cis* and *trans* products. The *cis* stereochemistry of the product was confirmed using 2D NMR techniques following the transformation of the iodo-azetidine intermediate to the corresponding amino-azetidine, which is discussed in **Section 2.2.2**. Banide and co-workers published an electrophile-induced cyclisation of homoallylic amino vinylsilanes towards enantiopure azetidines, in which NBS

is employed as the electrophile.¹⁵⁶ It was proposed that the cyclisation of homoallylic amines would proceed *via* a similar transition state. As seen in **Scheme 2.5**, attack of iodine on the alkene double bond gives rise to two possible diastereomeric iodoiranium intermediate species. In order for cyclisation to occur the lone pair of the nitrogen atom must attack the iodoiranium cation to create the desired four-membered ring *via* two possible transition states. The *cis*-azetidine is possible when the butterfly-shaped transition state proceeds with protons on both the 1- and 3-position occurring in a pseudo-axial position relative to each other, meaning the iodoiranium ion and phenyl groups lie pseudo-equatorially. This transition state is thought to be the most favoured as the alternative, disfavoured transition state would result in an increased 1,3-diaxial interaction within the molecule.

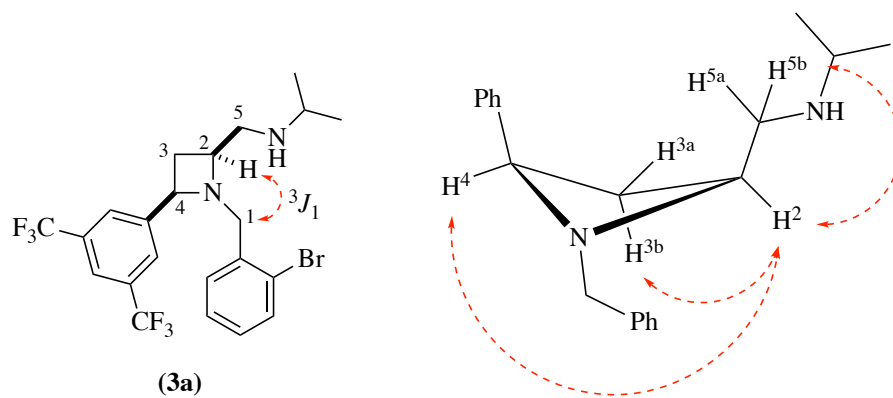


Scheme 2.5. Reaction of homoallylic amine with molecular iodine gives rise to two possible iodoiranium species, in order to form the desired azetidine ring, the iodoiranium must undergo nucleophilic attack by the nitrogen lone pair which can occur through two possible transition states. The *cis*-azetidine is formed when the butterfly-shaped transition state proceeds with protons on both the 1- and 3-position occurring in a pseudo-axial position relative to each other, meaning the iodoiranium ion and phenyl groups lie pseudo-equatorially. The alternative transition state would result in an increased 1,3-diaxial interaction within the molecule is disfavoured and the resulting *trans*-azetidine is not observed.¹⁵⁶

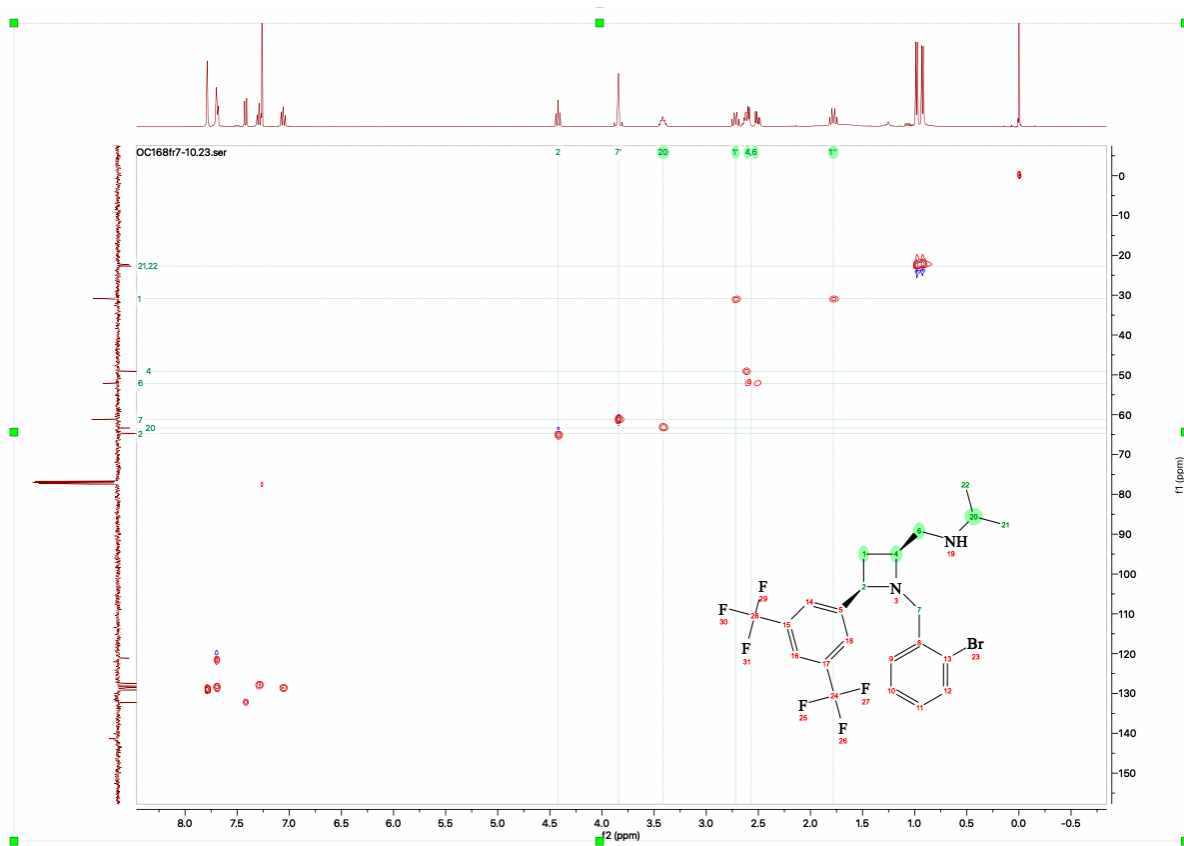
2.2.2. Synthesis of Amino Azetidines

Due to the thermal instability associated with the newly formed *cis*-iodo-azetidine ring, following the analysis of the crude ¹H NMR showing that only the desired product was observed with full conversion of starting material, was readily converted to the corresponding amino-azetidine without further purification. The iodo-azetidine (**2c-i**) was stirred in neat

isopropyl amine at ambient room temperature for 48 hours giving the amino-azetidine (**3a**) as the only observed product. Following purification by flash chromatography, the structure and conformation of the azetidine ring was confirmed using 2-D NMR spectroscopy, a HMBC (**H**eteronuclear **M**ultiple **B**ond **C**orrelation) experiment showed a through bond 3J_1 coupling between the carbon 1 atom and the proton of carbon 2, which was proven to be CH rather than a CH₂ using 1-D ¹³C Attached Proton Test (APT) experiments. The relative stereochemistry of the ring system was confirmed using 2-D NOESY (**N**uclear **O**verhauser **E**ffect spectroscopy) experiments to identify a through-space interaction between H², H^{3b} and H⁴, showing these to all sit on the same side of the ring indicating a *cis* conformation (**Figure 2.1**).



HMBC:



NOESY:

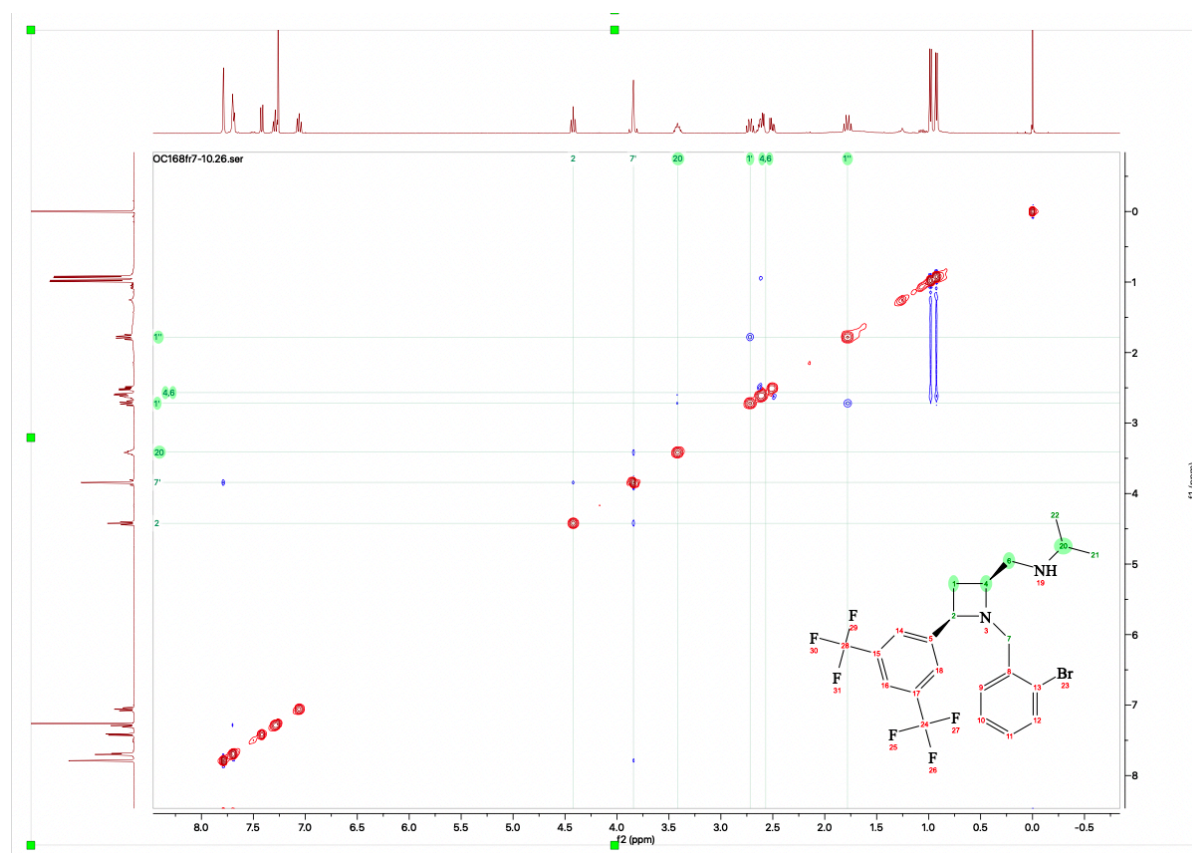


Figure 2.1. The structure of the *cis*-azetidine (AA-1) was confirmed using 2-D NMR spectroscopy, NOE interaction between H^2 , H^{3b} and H^4 confirmed the *cis*-stereochemistry of the ring.

2.2. Synthesis of a Bicyclic Scaffold

2.2.1. Palladium Chemistry

The overarching goal of this research was to further expand the scope of the azetidine chemistry which had previously been established by members of the JSF group, and to use these four-membered rings to create azetidine-containing bicyclic scaffold cores with pharmacologically favourable properties to explore new areas of chemical space. In order to achieve this aim, Buchwald-Hartwig C-N amination was proposed as a potential methodology to access the desired scaffold moieties due to its versatility and well explored scope in terms of aryl and amine coupling partners.¹⁵⁷⁻¹⁶⁰

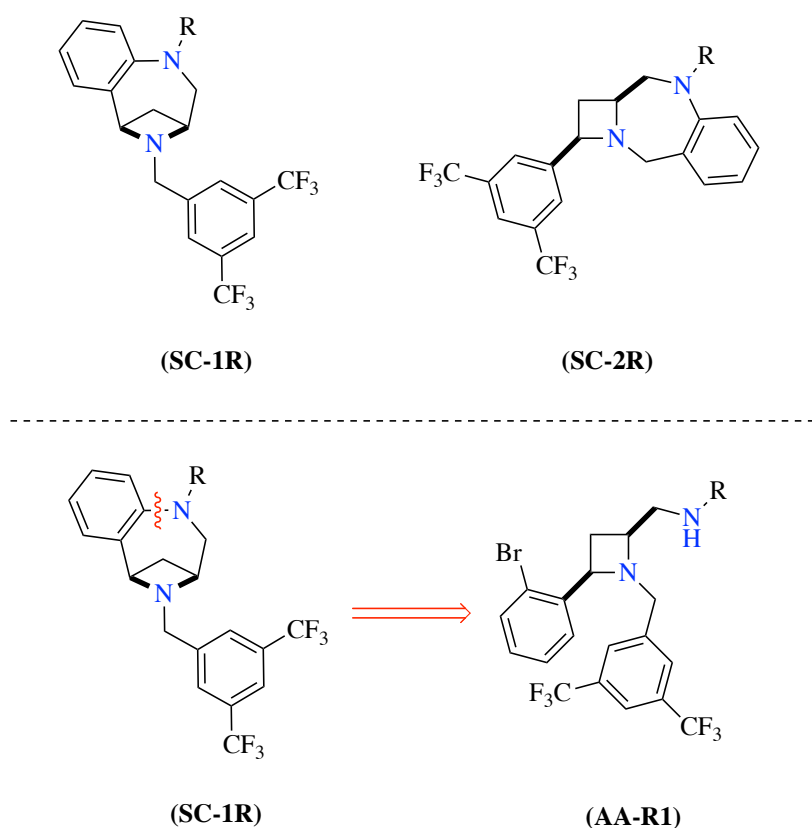


Figure 2.2. Intramolecular Buchwald-Hartwig C-N amination was proposed as a method to create bridged and fused azetidines-containing three-dimensional scaffolds.

As discussed in (Section 2.1.1.), previous work carried out within the group proposed that the presence of aryl or phenyl rings were required for cyclisation of the homoallylic amine to the azetidine ring to occur, in addition to this, it was found that the presence of electron withdrawing groups on these rings are also necessary for successful ring closure. Owing to these requirements, the earliest proposed scaffolds (**Figure 2.2**) were designed with this in mind, while also including a halide in the 2-position of on an aryl ring in order to facilitate Buchwald-Hartwig C-N amination reactions to create novel bicyclic scaffolds, examples of the homoallylic amine precursors (**2a – 2e**) can be seen in **Figure 2.3**. Following the synthesis of

the desired iodo-azetidine intermediates, the iodine was displaced with simple alkyl amines, such as isopropyl amine and propyl amine, to allow for cross-coupling to occur.

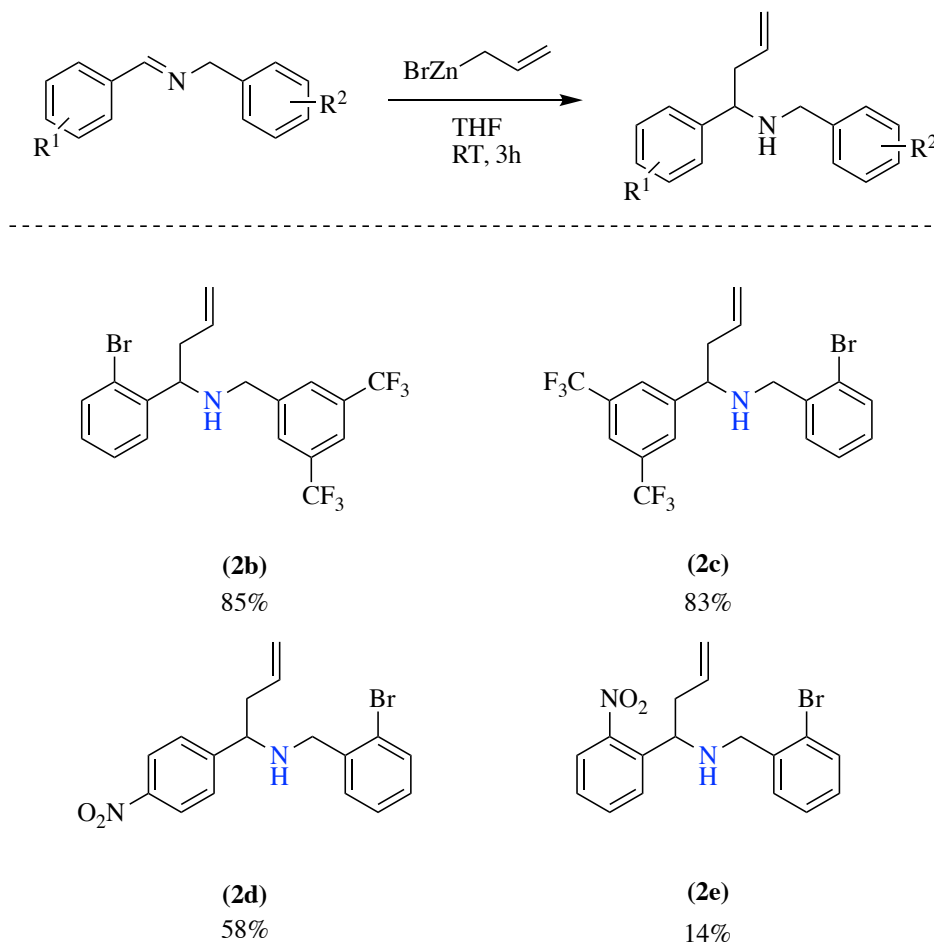
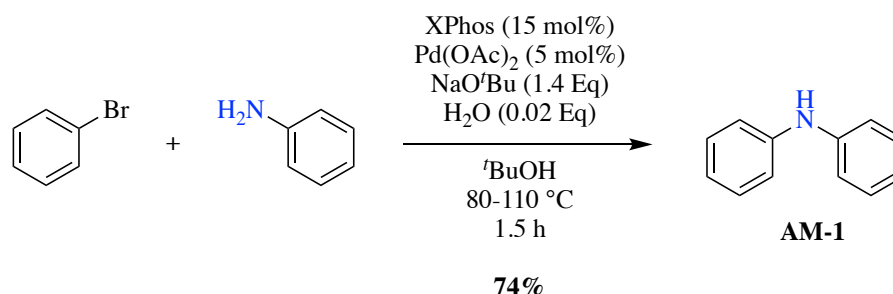


Figure 2.3. Examples of homoallylic amines used for the synthesis of amino-azetidines for the creation of novel multicyclic scaffolds.

In order to investigate potential reaction conditions for scaffold synthesis, a methodology developed by Buchwald and co-workers was used for initial test reactions.¹⁶¹ This approach proceeded via a water-mediated catalyst pre-activation step using biaryldialkylphosphine ligands. This method allowed for lower catalyst loading and did not require harsh additives such as triethylborane, in addition to this, the water-mediated activation step of the catalyst negated the requirement for dry solvent making the method more amenable to large scale parallel library synthesis. The air-stable crystalline XPhos ligand was chosen due to excellent

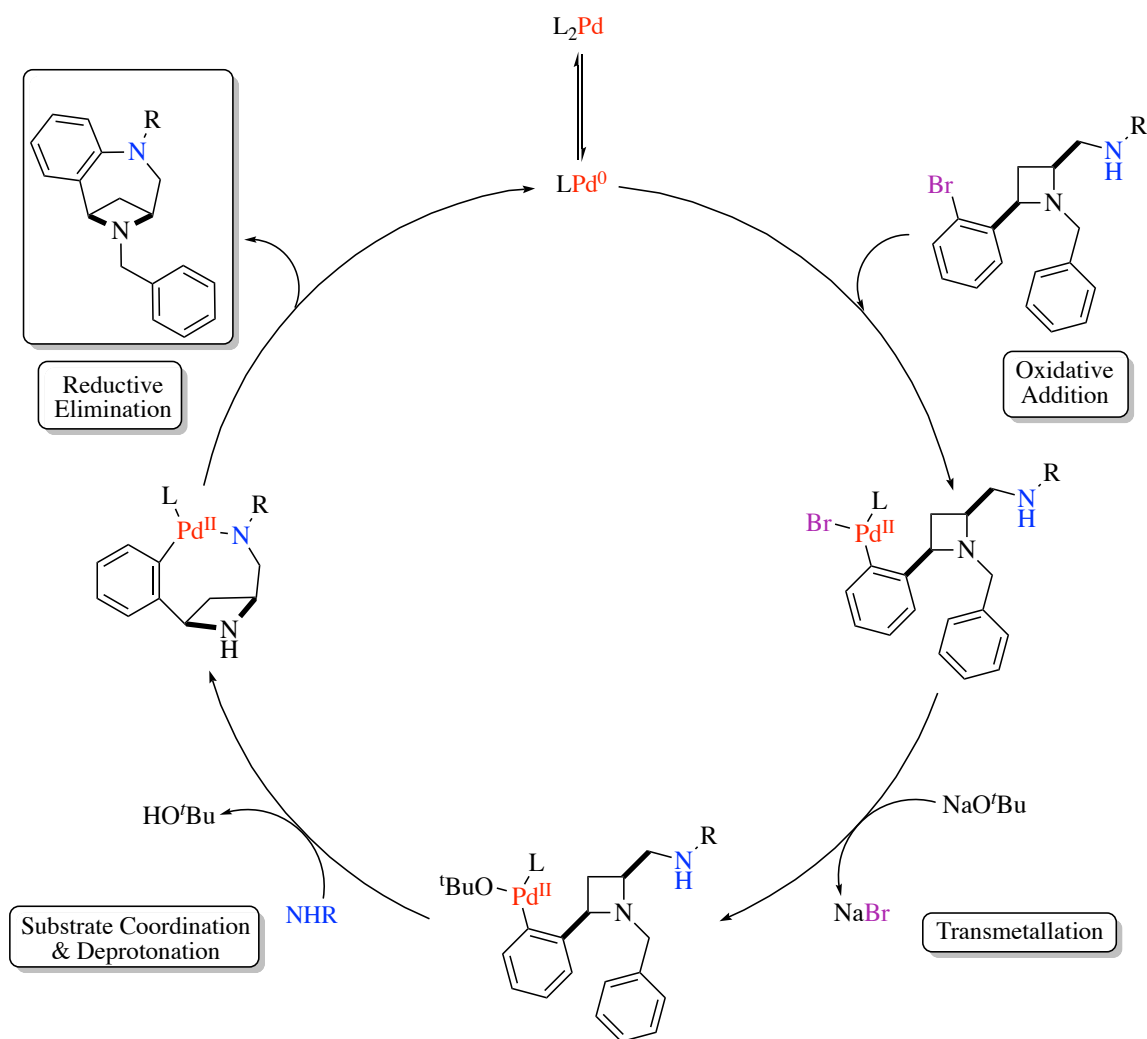
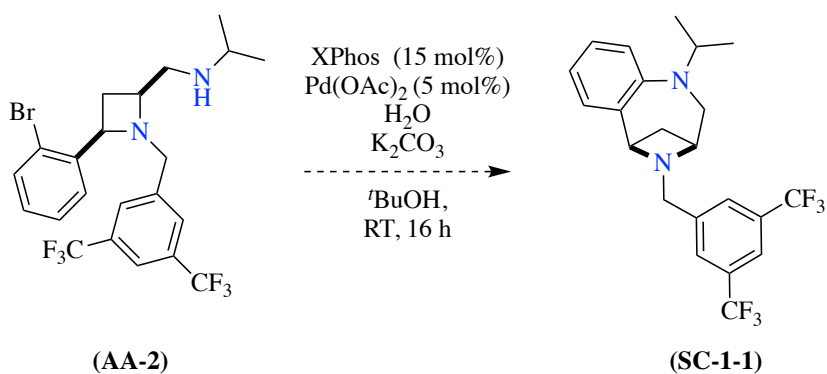
catalytic reactivity in C-N amination reactions and has been shown to be particularly successful in the coupling of secondary amines.^{162, 163}



Scheme 2.6. A small-scale test reaction conducted to probe conditions for Buchwald-Hartwig C-N cross coupling reactions, using a method proposed by Buchwald and co-workers, a simple aryl halide and aryl amine were coupled giving the biarylamine product with a yield of 74%.¹⁶¹

A series of small-scale test reactions were conducted with a simple aryl halide and aryl amine yielding the coupled product (**AM-1**) with a yield of 74% (**Scheme 2.6**). Following the successful coupling of the simple analogues, the reaction was trialled under the same conditions with azetidine (**3b**), on a small scale (10 mg), with 15 mol% of XPhos ligand along with 5 mol% catalyst loading. It was hypothesised that the reaction would follow the proposed catalytic cycle as seen in **Scheme 2.7**, resulting in the desired bicyclic scaffold moiety. Both the catalyst and the phosphine ligand were milled and added to a vial with tertbutyl alcohol as a solvent, the solution was degassed with argon and heated to 80 °C for three minutes to activate the catalyst. In a second vial, the azetidine (**3b**) was added as a solution in tertbutyl alcohol with potassium carbonate. The contents of both vials were combined under an argon atmosphere and the reaction mixture was heated to 110 °C overnight. After sixteen hours the reaction was cooled to room temperature and a colour change was noted, the reaction mixture had darkened to a deep green-brown colour overnight. TLC analysis confirmed that all the

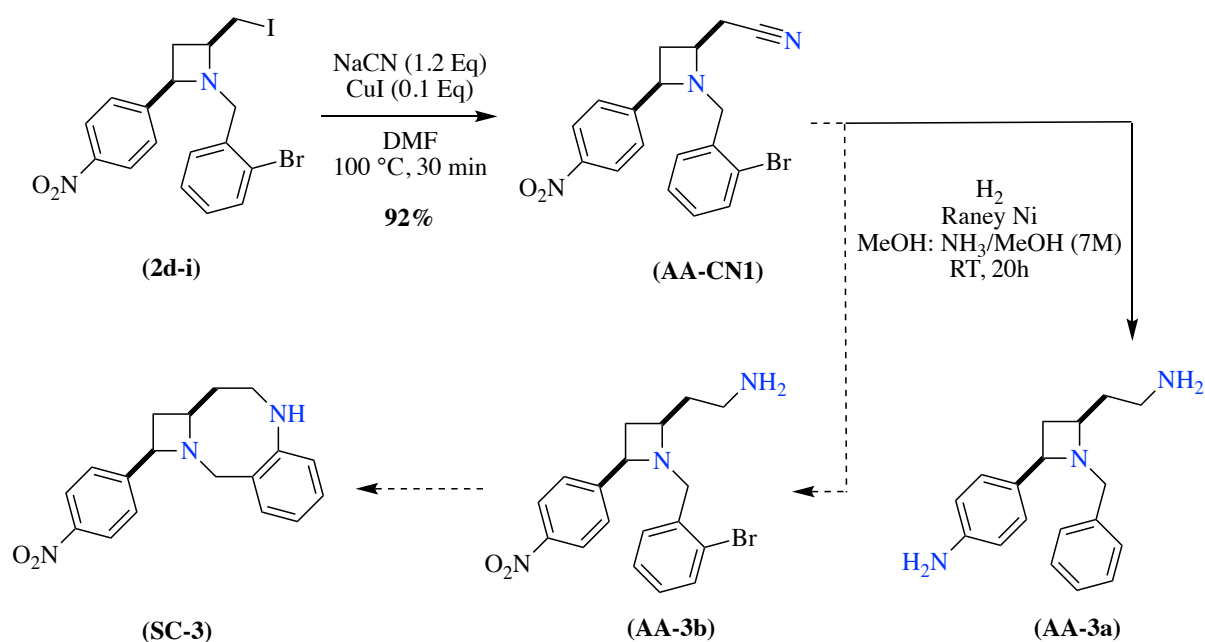
azetidine starting material had been consumed by the reaction and a new spot was visible on the analysis plate. Despite the identification of a newly formed spot on TLC the product was not successfully collected through flash chromatography. The reaction was repeated at a slightly larger scale (30 mg), with the catalyst loading at 20 mol% and the ligand loading adjusted to 60 mol% accordingly. It was hoped that this would allow the reaction to go to completion. Following the same procedure as described previously, the palladium catalyst was preactivated before addition to the reaction mixture containing azetidine (**3b**), the reaction was stirred for fourteen hours at 110 °C. Partial consumption of starting material was confirmed with TLC analysis. The crude reaction mixture was purified using flash chromatography, but the desired product was not obtained.



Scheme 2.7. A small-scale intramolecular C-N amination test reaction was conducted using a protocol described by Buchwald and co-workers.¹⁶¹ It was proposed that the reaction would follow a catalytic cycle whereby the amino-azetidine compound undergoes oxidative addition causing the activated palladium ligand to co-ordinate to the bromide substituent of the aryl ring. A subsequent transmetalation step with base allows for displacement of the bromine which is removed as NaBr. Intramolecular co-ordination of the amine with the palladium catalyst results in a highly strained intermediate structure. A final reductive elimination step causes the displacement and regeneration of the palladium catalyst to form the desired bicyclic structure.

After failing to isolate the coupled product it was hypothesised that the new spot formed on TLC was a palladium-azetidine complex which formed following the substrate coordination and deprotonation step of the catalytic cycle. Due to the ring strain attributed with the final bicyclic scaffold it was proposed that an intermediate complex was successfully forming but that the final product was too strained to access *via* this method.

In order to reduce strain on the ring and add an additional degree of flexibility into the final system it was decided to length the chain on the 4-position of the azetidine ring. By adding an additional carbon to the chain and by performing a Buchwald-Hartwig C-N amination, a 4,8-ring system (**SC-3**) would be created. Using a method previously described by Peters *et al.*,¹⁶⁴ copper iodide was used to catalyse the introduction of the nitrile group onto the azetidine molecule, which resulted in crude yields of up to 92% of the nitrile containing intermediate (**AA-CN1**). With the aim of accessing the free amine, (**AA-CN1**) was dissolved a 1:1 mixture of methanol and methanolic ammonia and was placed under an inert atmosphere, Raney nickel was added to the reaction mixture and the reaction was pressurised to 5 Bar using hydrogen gas. The reaction mixture was stirred vigorously over twenty hours at room temperature. Upon analysing the reaction mixture, it was noted that while the nitrile group had been hydrogenated to the corresponding free amine as desired the reaction had also resulted in the reduction of the 4-nitro group of the aryl ring and debromination of the phenyl ring (**Scheme 2.8**). Conditions were deemed too harsh to selectively reduce the nitrile group to access the desired product (**AA-3b**).

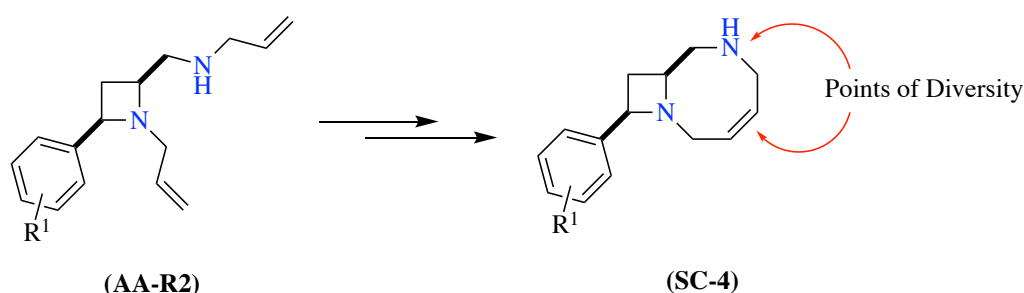


Scheme 2.8. Iodine was displaced from iodo-azetidine (2d-i) using sodium cyanide to introduce a nitrile group into the molecule. Raney Ni was used to reduce the triple bond of the nitrile group to access the free amine (AA-3b), the reduction method was non-selective and resulted in reduction of the 4-NO₂ group as well as total debromination of the molecule (AA-3a).

Following the debromination of the phenyl ring and reduction of the nitro group giving rise to (AA-3a), it was decided that Buchwald-Hartwig C-N amination was not the best approach towards the synthesis of the desired bicyclic scaffold moieties. This method required the reacting secondary amine to be incorporated into the azetidine ring prior to ring closure, at the iodine-replacement step, meaning that the scope for decoration at this point was relatively limited as it was theorised that the presence of bulky amines would prevent the catalytic cycle from going to completion thus preventing the formation of the second ring, thus making this an unsuitable route for the synthesis of a structurally diverse compound library.

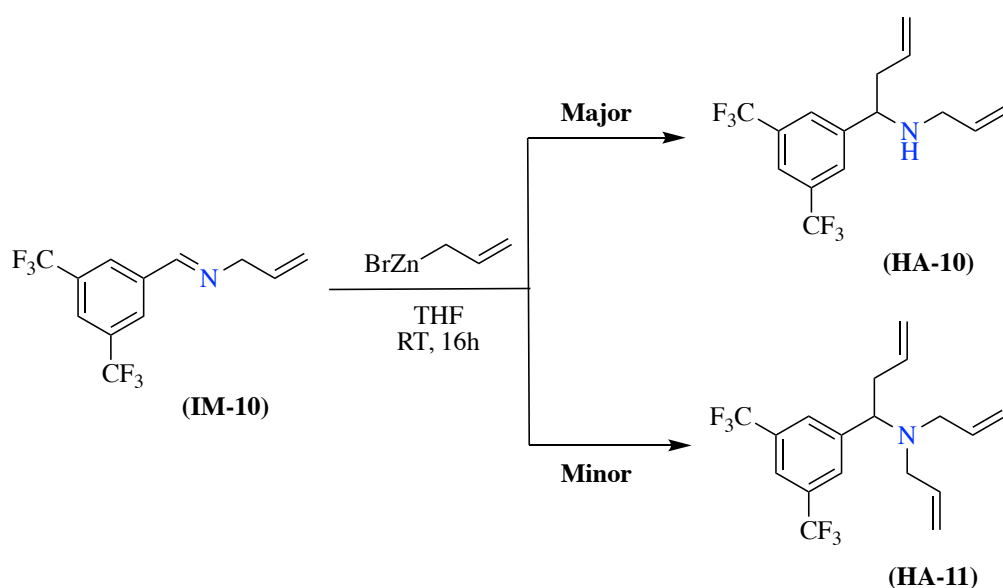
2.2.2. Ring Closing Metathesis

Due to the issues faced with cross coupling reactions, alternative methods of ring closure were investigated. Ring closing metathesis (RCM) has been widely reported in the literature as a means of creating multicyclic compounds.¹⁶⁵⁻¹⁶⁸ It was hypothesised that if an additional terminal alkene could be successfully introduced into the homoallylic amine starting material (**AA-R2**) then ring closing metathesis could be used to generate the desired bicyclic ring structure (**SC-4**) while simultaneously introducing an additional point of diversity as well as a free secondary amine into the final scaffold allowing for a wider range of diversification to occur (**Scheme 2.9**).



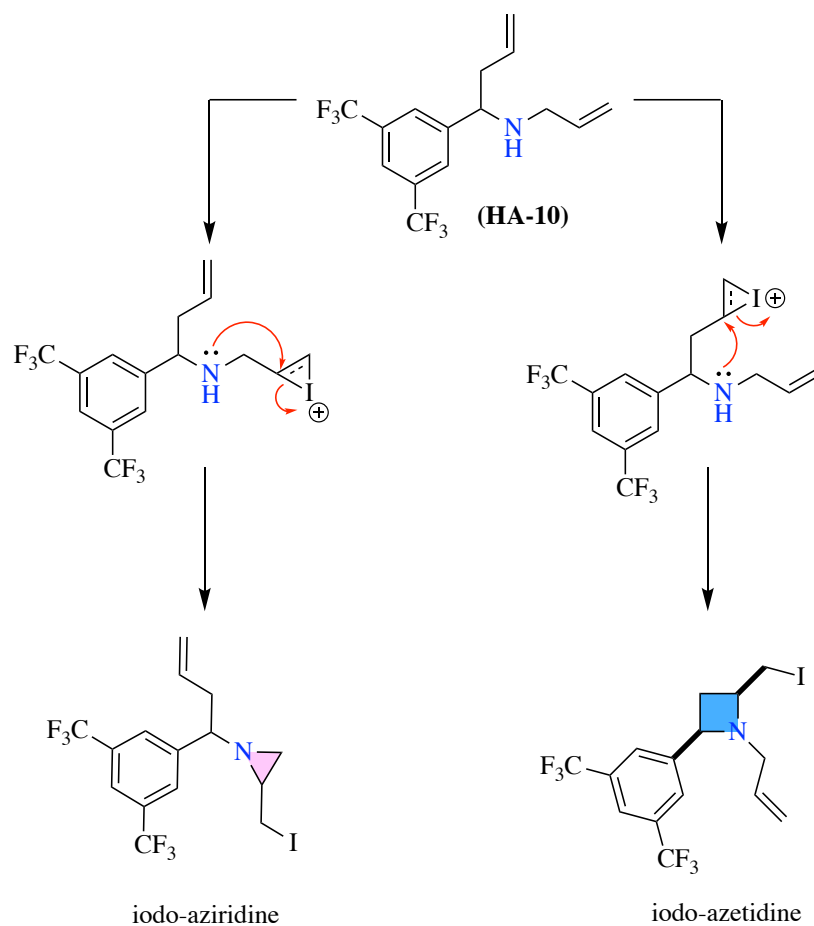
***Scheme 2.9.** Ring closing metathesis was proposed as a method which could be employed for the creation of novel bicyclic scaffolds with multiple points of diversity.*

To synthesise a bicyclic scaffold *via* this synthetic route, a homoallylic amine was synthesised through reaction of an *N*-allyl containing imine with allylzinc bromide using the methods as described previously in (**Section 2.1.1.**). Reaction was monitored by LCMS and proceeded well with the mono-allylated (**HA-10**) compound being the major reaction product in a ratio of approximately 3:1 with the bis-allylated amine (**HA-11**) (**Scheme 2.10**).



Scheme 2.10. Reaction of a *N*-allyl containing-imine with allylzinc bromide resulted in the formation of both the mono- and the bis-allylated homoallylic amine products.

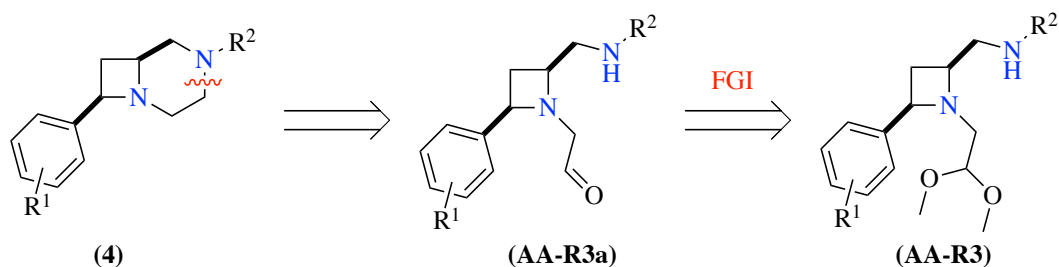
Although both the mono- and bis-allylated homoallylic amines were observed using LCMS analysis of the crude reaction mixture, both products appeared to be unstable and proved challenging to isolate upon quenching the reaction. It was also theorised that while RCM has the potential to yield scaffolds with multiple points for orthogonal diversification to occur, it may not be possible to form the four-membered azetidine ring in the presence of two terminal alkenes, due to the potentially favoured formation of a three-membered iodo-aziridine intermediate upon reaction with molecular iodine and base (**Scheme 2.11**). With this in mind, it was decided to investigate alternative routes towards bicyclic scaffolds.



Scheme 2.11. RCM was proposed as a methodology towards novel bicyclic scaffolds, however reaction of the mono-allylated product with molecular iodine could theoretically result in two possible iodoiranium ions. Subsequent nucleophilic attack of the nitrogen lone pair on the iodoiranium ion results in the formation of an iodo-aziridine and iodo-azetidine respectively. It was theorised that the formation of the iodo-aziridine may be favoured over the four-membered alternative.

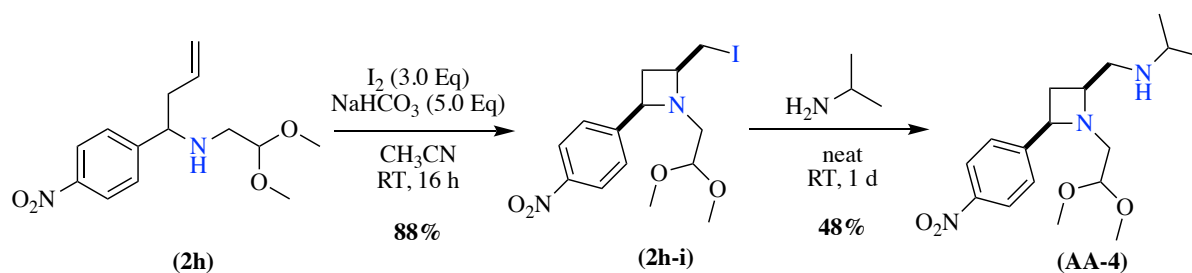
2.2.3. Reductive Amination

Reductive amination reactions have long since been used as a reliable method for the formation of C-N bonds due to robustness and scalability in a pharmaceutical setting.¹⁶⁹⁻¹⁷² It was theorised that reductive aminations could be used for the formation of 4,6-fused scaffolds (**4a** and **4b**) (Scheme 2.12).



Scheme 2.12. Reductive aminations are commonly employed for the synthesis of scaffold moieties in a pharmaceutical setting. It was proposed that reductive amination reactions could be used to create novel 4-6-fused scaffolds for use in drug discovery.

Further work was done to expand the scope the azetidine ring using dimethoxyethylamine in place of a decorated benzylamine during precursor synthesis, this dimethyl acetal group could act as a protecting group for a C=O carbonyl bond necessary for reductive amination to occur. Following the successful incorporation of the amine and cyclisation to the azetidine ring methodologies for the deprotection of the carbonyl group were investigated (**Scheme 2.13**).

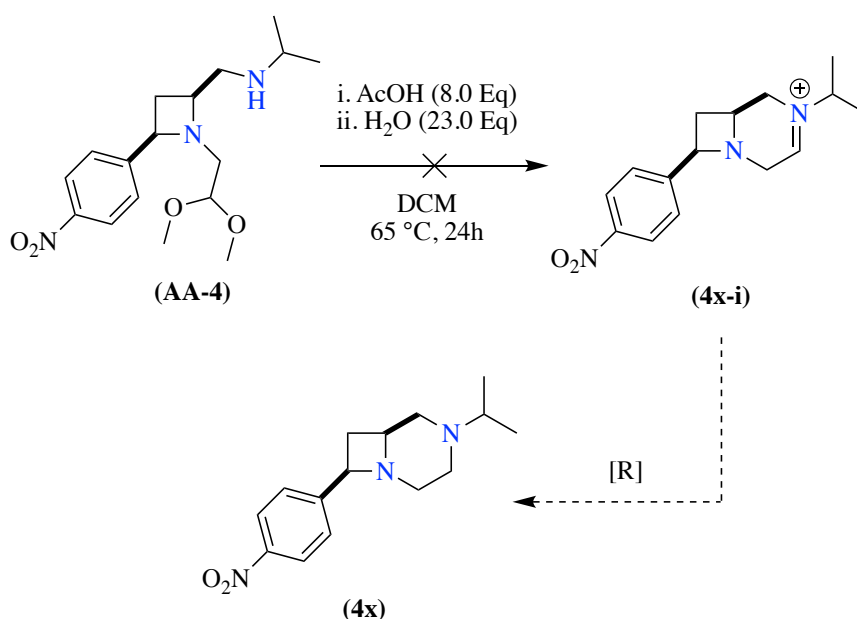


Scheme 2.13. A homoallylic amine (2h) was synthesised with an incorporated dimethyl acetal aldehyde protecting group, (2h) was cyclised using molecular iodine under basic conditions and subsequently underwent nucleophilic attack with N-isopropyl amines to access the corresponding amino-azetidine (AA-4) in a yield of 48%.

For reductive amination to be possible it was imperative that the dimethyl acetal protecting group be removed cleanly and efficiently. Initially a method originally described by Williams *et al.* was evaluated as a means of protecting group removal,¹⁷³ the amino-azetidine (AA-4)

was dissolved in a 2:1 solution of water and THF and heated to 80 °C over two hours without the presence of an additional additive or catalyst. Interestingly this method resulted in complete degradation of the azetidine ring despite its' relatively mild conditions. Acid-catalysed trans-acetalisation is a common method for the removal of dimethyl acetals, owing to this a catalytic amount of *p*-toluenesulfonic acid (TsOH) as reported by Smith *et al.*,¹⁷⁴ was stirred at room temperature in an excess of acetone over 48 hours, interesting this method has no effect on the starting material leaving both the dimethyl acetal protecting group and the azetidine ring, which was feared to be acid-labile, intact.

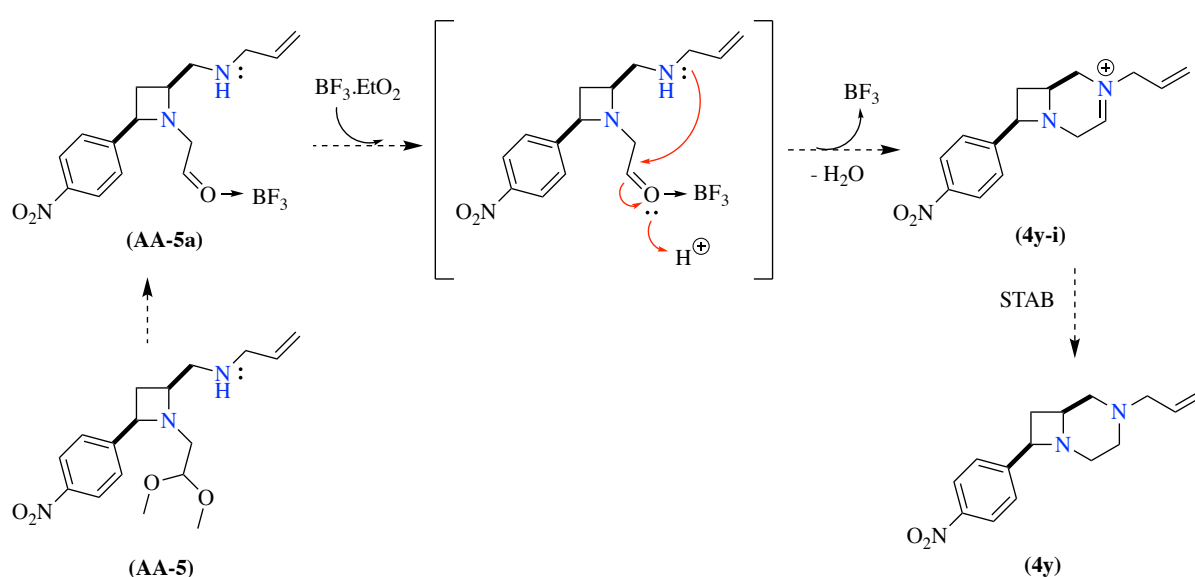
Acetic acid (AcOH) was used as an alternative to TsOH, the protected azetidine (**AA-4**) was stirred with an eight-fold excess of AcOH in dichloromethane and heated to reflux as described by Kita and co-workers.¹⁷⁵ No conversion to the deprotected product was observed using LCMS analysis after two hours, in order to promote deprotection and formation of the cyclised iminium ion an excess of water was added to the reaction mixture in a single portion. The reaction mixture was stirred overnight but protecting group cleavage was not observed (**Scheme 2.14**).



Scheme 2.14. Deprotection of the acid-labile dimethyl acetal group with excess acetic acid failed to access the aldehyde group which would allow for cyclisation to the intermediate 4,6-fused intermediate compound.

Boron trifluoride etherate (BF₃.Et₂O), an oxophilic lewis acid, was employed as a metal-free catalyst for reductive amination with a wide range of both primary and secondary amines and diversely substituted aldehydes to access secondary and tertiary amines with a wide functional group tolerance.¹⁷⁶ The protected azetidine (AA-5) was stirred as a solution in methanol at room temperature with a three-fold excess of BF₃.Et₂O and a two-fold excess of the mild reducing agent sodium triacetoxyborohydride (STAB). It was proposed that the dimethyl acetal protecting group could be cleaved through a series of proton transfer steps, using the solvent as a proton source, the newly uncovered aldehyde group could then coordinate to boron trifluoride oxygen of the carbonyl group, encouraging intramolecular nucleophilic attack of the secondary amine leading to the formation of an iminium ion which could then be reduced with STAB to the cyclised scaffold (**Scheme 2.15.**). After two hours, the starting material had been fully consumed with a new mass recorded which possibly corresponded to [M + 2Na-H] ion

of the desired product, suggesting that the reaction has been successful. However, the major isolated product of flash column chromatography had a mass of 263.1 and was unable to be identified with certainty. NMR analysis of the major product showed peaks relating to the azetidine starting material along with some new peaks which could be attributed to the newly formed six-membered ring of the bicyclic compound (**4y**), this suggested that ring closure was possible, but an unknown transformation had occurred during purification.



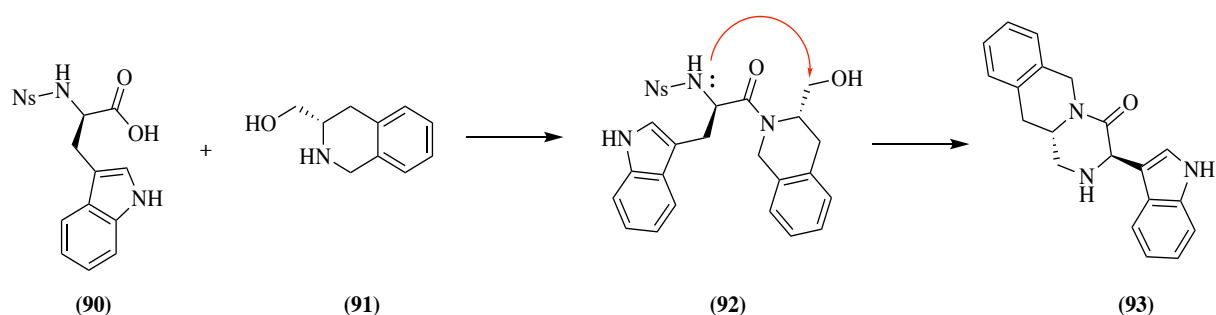
Scheme 2.15. Protected azetidine (**AA-5**) was stirred as a solution in methanol at room temperature with a three-fold excess of $\text{BF}_3 \cdot \text{Et}_2\text{O}$ and a two-fold excess of sodium triacetoxyborohydride to access the corresponding aldehyde (**AA-4a**) through a series of proton transfer steps. It was theorised that aldehyde group could co-ordinate with the BF_3 to encourage intramolecular nucleophilic attack of the amine to form the 4,6-fused intermediate ion which would be subsequently reduced to yield the desired final compound.

Although the reductive amination approach yielded some interesting results, the final scaffolds faced some of the same limitations seen before, namely decoration of the azetidine occurred prior to cyclisation to the bicyclic system resulting in compounds with a limited potential for diversification. However, it was decided to investigate methods towards the proposed 4,6-fused

system *via* an alternative approach, with hope of accessing the same fused system with a free amine on the six-membered ring to allowed for a varied diversification strategy.

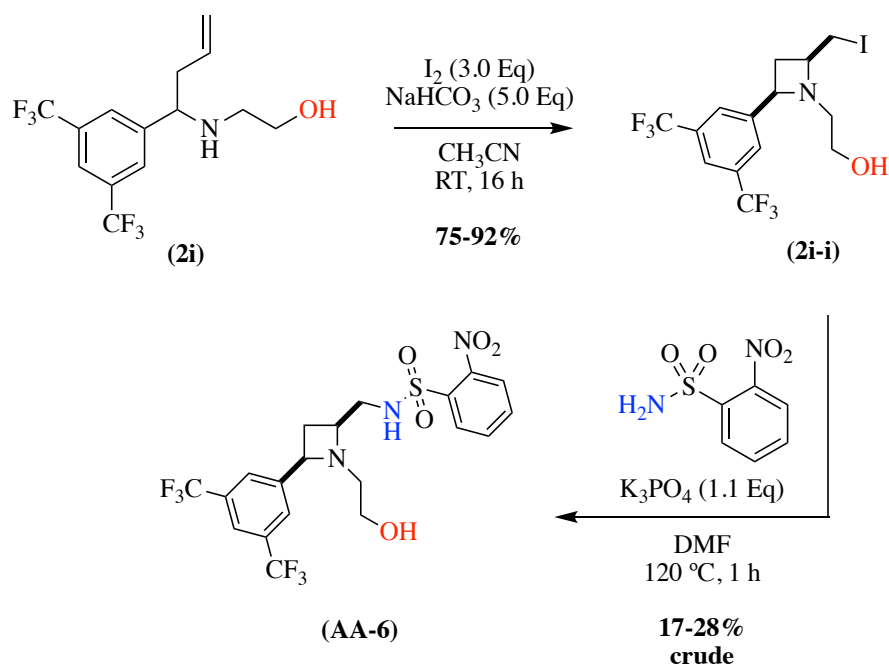
2.2.4. Fukuyama Mitsunobu Chemistry

Fukuyama and co-workers have previously shown a versatile and robust method for amine synthesis *via* a Mitsunobu reaction with nitrobenzenesulfonamides simultaneously acting as both a protecting and activating group on the molecule (**Scheme 2.16**).^{177, 178} In 2005, the Fukuyama-Mitsunobu reaction was utilised for the intramolecular synthesis of novel *N*-heterocycle containing scaffolds in moderate yields.¹⁷⁹



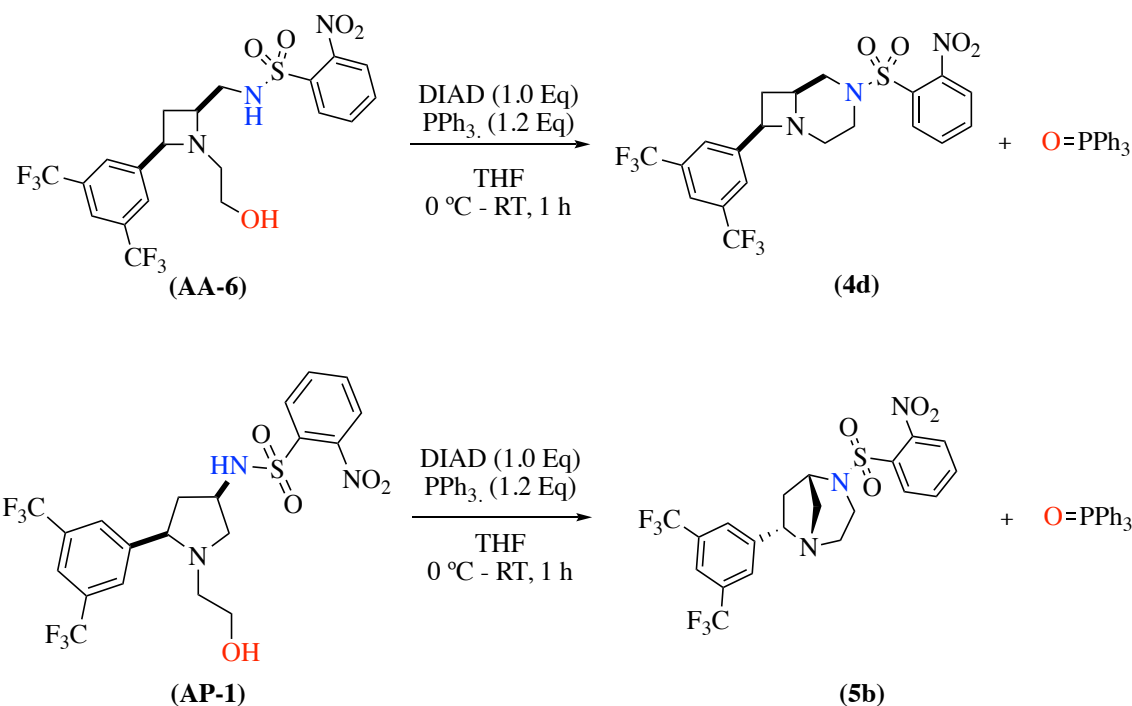
Scheme 2.16. The Fukuyama-Mitsunobu reaction was used to synthesise a novel scaffold. Saponification of *D*-tryptophan (90) with an alcohol containing amine (91) resulted in the formation of an amide (92) which underwent an intramolecular Fukuyama-Mitsunobu reaction to access the cyclised secondary amine (93) following the base-mediated removal of the Ns protecting group.

It was hypothesised that if the scope of the azetidine ring could be expanded to include an aliphatic alcohol then it may be possible to form the desired bicyclic scaffold using this method. Following the successful incorporation of an aliphatic alcohol in place of a benzylic ring into homoallylic amine (**2i**), cyclisation to the four-membered iodo-azetidine intermediate (**2i-i**) using the methodology detailed in (**Section 2.1.1.**) in good to excellent yields.



Scheme 2.17. Alcohol-containing homoallylic amine (HA-13) was cyclised using molecular iodine under basic conditions to yield the corresponding iodo-azetidine intermediate (IA-13). Subsequent nucleophilic attack with nitrobenzene sulfonamide results in iodine displacement to access the amino-azetidine (AA-6) as the final product ahead of Fukuyama-Mitsunobu cyclisation.

The iodo-azetidine intermediate (2i-i) was reacted with nitrobenzene sulfonamide and tripotassium phosphate (K_3PO_4) to form amino-azetidine (AA-6), introducing a protected -NH group into the molecule in one step (Scheme 2.17). Although the sulfonamide was successfully introduced into the molecule, the conditions required were notably harsh, requiring a temperature of $120\text{ }^\circ\text{C}$ and the reaction was consistently low yielding (17-28%).



Scheme 2.18. Fukuyama-Mitsunobu conditions were used to access the *Ns* protected 4,6-fused scaffold (**4d**), purification and isolation of the final product revealed that an additional scaffold, the 5,6-bridged system (**5b**), was also formed. It was theorised that interconversion from the iodo-azetidine intermediate to the corresponding iodo-pyrrolidine intermediate had occurred earlier in the reaction pathway.

A solution of the amino azetidine (**AA-6**) and triphenylphosphine was prepared in THF and cooled to 0 °C (**Scheme 2.18.**). To the reaction mixture, a 0.1 M solution of diisopropyl azodicarboxylate (DIAD) in THF was added slowly over 10 minutes. Following the addition of the DIAD solution, the reaction mixture was warmed to room temperature and stirred for a further 50 minutes. Subsequent work-up and purification yielded two products, both the 4,6-fused (**4d**) and the unexpected 5,6-bridged (**5b**) diazabicyclic ring systems. Isolation of the 5,6-bridged system suggested that some interconversion to the corresponding iodo-pyrrolidine stereoisomer had occurred, likely during the sulfonamide incorporation step, due to the high reaction temperature promoting conversion the five-membered ring. Isolation of both the fused and bridged ring systems proved that the synthesis of bicyclic ring systems was possible using

mild methods. As can be seen in **Figure 2.4**, NMR analysis of the isolated 4,6-fused system showed an NOE interaction between H_o, H_j, and H_g of the azetidine ring, proving that the cis stereochemistry of the azetidine ring was maintained. This correlation can also be visualised in the accompanying NOESY spectra

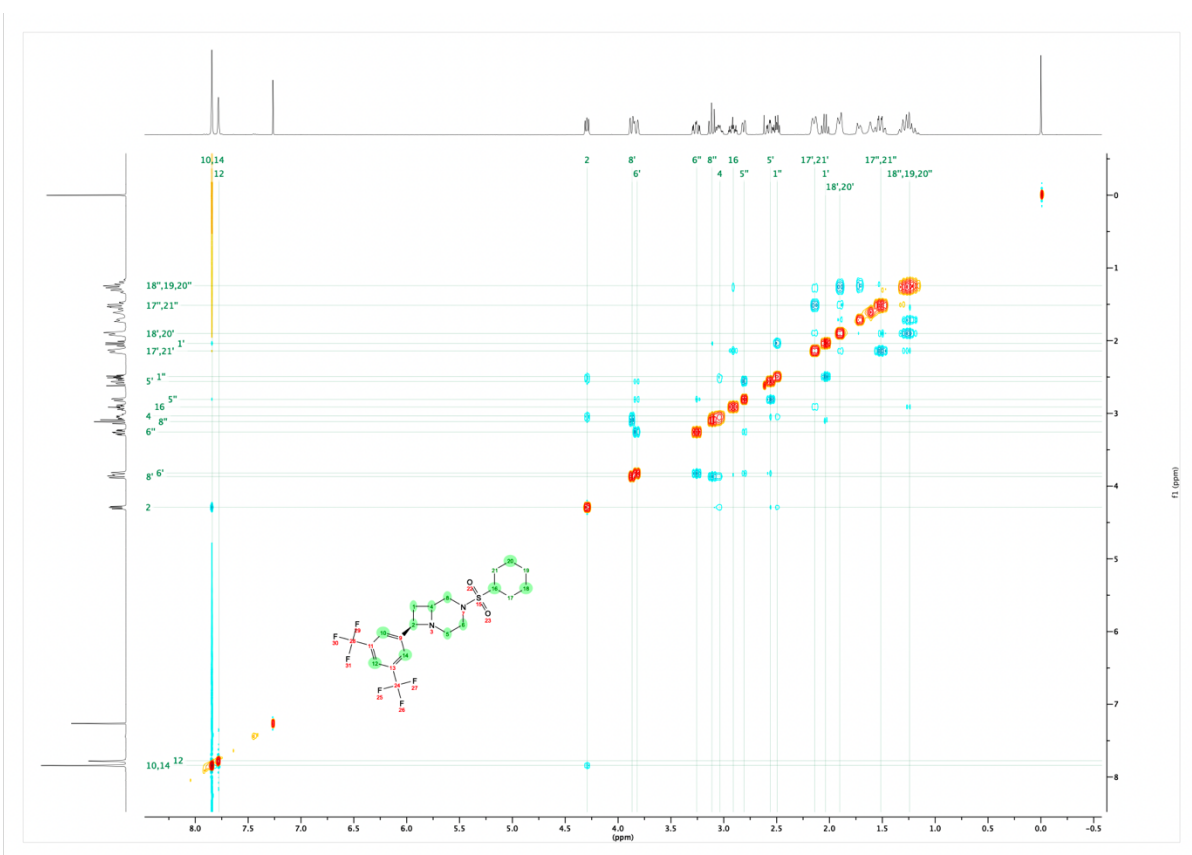
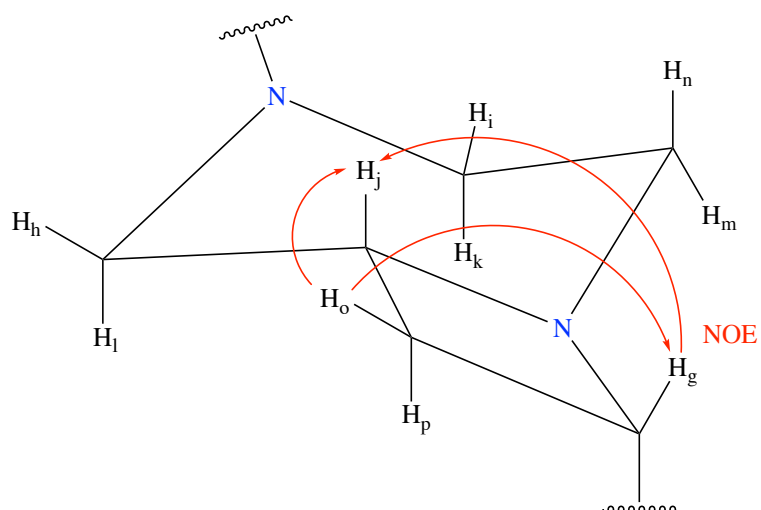


Figure 2.4. 2-D NMR spectroscopy confirmed the stereochemistry of the 4,6-fused scaffold, NOE interaction between *H_o*, *H_j*, and *H_g* of the azetidine ring, proving that the *cis* stereochemistry of the 2,4-azetidine ring was maintained.

Despite the initial success of the Mitsunobu pathway in terms of compound synthesis and overall proof of concept, the triphenylphosphine oxide reaction by-product co-eluted with the

cyclised product (**4d** and **5b**) using normal phase chromatography. Pure product was successfully isolated with a preparative column using 30-65% acetonitrile/water as an eluent system. However, isolated yields were poor, less than 20%, due to some co-elution and adherence to the column. To increase the isolated yields, methods of removing triphenylphosphine oxide (TPPO) from the reaction mixture before column chromatography were investigated. A methodology for the removal of TPPO using zinc chloride (ZnCl_2) in polar solvents was reported in 2017 by Weix *et al.*,¹⁸⁰ following the completion of the reaction volatile components were removed *in vacuo* and the resultant oil was redissolved in ethanol. A 1.8 M solution of ZnCl_2 was prepared in warm ethanol, using two equivalents of ZnCl_2 for each equivalent of PPh_3 used in the Staudinger reduction. The ethanolic solution of ZnCl_2 was added to the reaction mixture and stirred at room temperature overnight to allow for precipitation of a TPPO-Zn complex, the resultant complex was then collected using vacuum filtration, and washed with water, ethanol, and ether. Analysis of the filtrate showed that up to 70% of the TPPO was removed from the mixture. TPPO was also precipitated out of solution using cold hexanes and diethyl ether,^{181, 182} solid TPPO was removed from the reaction mixture using vacuum filtration and was washed with water, ethanol, and ether. Analysis of the filtrate showed that between 40-50% of TPPO had been removed from the reaction mixture. While both removal of TPPO has been shown to be possible using both precipitation and complexation methods, the percentage of by-product remaining in the reaction mixture was still relatively high (30-60%) and would require the step to be repeated, making the reaction pathway quite inefficient.

2.2.5. Appel-type Chemistry

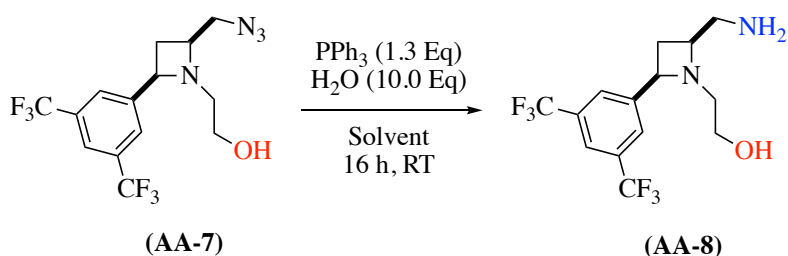
As a result of the low isolated yields from the Fukuyama-Mitsunobu cyclisation reaction and from the preceding sulfonamide introduction, an alternative protocol was investigated. The

Appel reaction, first reported by Lee and co-workers,¹⁸³ is a method of alcohol activation through transformation to an alkyl halide, the reaction is classically performed using either carbon tetrachloride or carbon tetrabromide with PPh₃.^{184, 185} Although traditional Appel chemistry has become less popular in recent years due to the use of toxic halogenating agents, the transformation of the alcohol group into a significantly better leaving group formed the basis of the next approach towards scaffold synthesis

Sodium azide was used as a means of introducing an eventual free amine into the molecule which could be more easily protected using methanesulfonyl chloride. Sodium azide was stirred with iodo-azetidine (**2i-i**) in DMF for 16 hours resulting in full conversion of to the azido-azetidine (**AA-7**). Standard Staudinger reduction conditions were used for the transformation of the azide group to a free amine (**AA-8**) using triphenylphosphine and water. A systematic solvent screen was carried to identify the solvent which allowed for both clean Conversion and simple isolation. As shown in **Table 2.2**, a series of non-polar, polar aprotic and polar protic solvents were investigated as reaction solvents. Polar protic solvents, methanol, and ethanol, both yielded product but triphenylphosphine was poorly soluble, making it unsuitable for larger scale reactions. Several non-polar solvents, 1,4-dioxane, diethyl ether and toluene, were also trialled. Product mass was not observed when 1,4-dioxane was used while both diethyl ether and toluene yielded product the isolated crude yield in both cases was low to moderate, 36% and 22% respectively. Polar aprotic solvents are most commonly used in Staudinger reactions,¹⁸⁶ acetone, ethyl acetate, dichloromethane, acetonitrile, *N,N*-dimethylformamide and tetrahydrofuran were all screened and the desired product was observed in all cases. Although the correct mass was observed when acetonitrile and dichloromethane were used as the reaction solvent, it was not the major component of the reaction mixture and therefore was not isolated. Ethyl acetate yielded a reaction mixture with

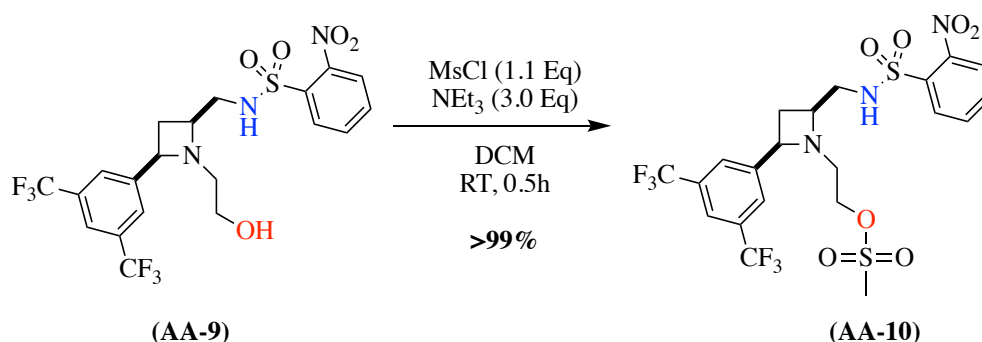
very few additional impurities; however, the rate of conversion was notably lower than with other solvent systems. Reactions in *N,N*-dimethylformamide (DMF) and tetrahydrofuran (THF) both proceeded well, giving moderate to good yields on a small scale, with few impurities, due to the difficulties associated with DMF removal THF was ultimately shown to be the best choice reaction solvent for the Staudinger azide reduction of (**AA-7**) to the corresponding amino-azetidine (**AA-8**).

Table 2.4. A systematic solvent screen was conducted to select the most optimum solvent for reduction of the azide of (AA-7) to the corresponding free amine-containing amino-azetidine (AA-8) under classic Staudinger reduction conditions.



	Solvent	Solubility	Product Observed	Product Isolated	Crude Yield (%)	Comments
1.	Methanol	Moderate	Yes	No	N/A	Initially reaction was a homogenous solution, PPH ₃ crashed out over time
2.	Ethanol	Moderate	Yes	No	N/A	Slow conversion to desired product, PPH ₃ crashed out of solution over time
3.	1,4-Dioxane	Poor	No	No	N/A	No product observed
4.	Diethyl Ether	Moderate	Yes	Yes	36	Low yielding reaction
5.	Toluene	Poor	Yes*	Yes	22	Desired product was the minority component of the reaction mixture after 16 h
6.	Acetonitrile	Good	No	No	N/A	Desired product was the minority component of the reaction mixture after 16 h
7.	Ethyl Acetate	Good	Yes	No	N/A	Slow conversion to the desired product
8.	DCM	Good	Yes	No	N/A	Desired product was the minority component of the reaction mixture after 16 h
9.	Acetone	Good	Yes	Yes	44	Slow conversion to desired product
10.	DMF	Good	Yes	Yes	58	Reaction proceeded well; solvent not chosen due to difficulties with removal
11.	THF	Good	Yes	Yes	67	Reaction proceeded well, chosen as optimal solvent

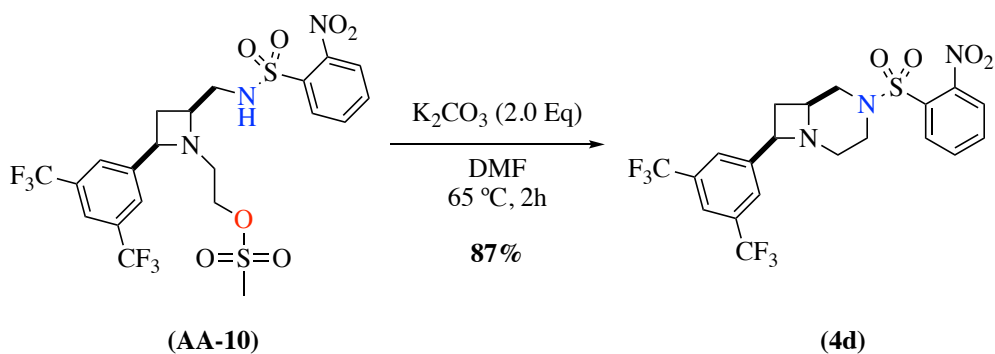
The amino-azetidine (**AA-8**) was isolated as a crude product and protected using 2-nitrobenzenesulfonyl chloride with triethylamine in DCM resulting in an average yield of 70%. This methodology was favoured over the original synthetic route utilising the sulfonamide due to the milder reaction conditions and higher yields. It was hypothesised that the nitro group would have the same activating effect as in the Fukuyama-Mitsunobu route, making it possible to close the ring. A methodology previously reported by Lowe and co-workers was employed to form the 4,6 system over two steps.⁶⁴ Amino-azetidine (**AA-9**) was dissolved in DCM at ambient room temperature and was stirred with methanesulfonyl chloride (MsCl) and triethylamine for 30 minutes to convert the hydroxyl group to a better leaving group (**AA-10**) (**Scheme 2.19**).



Scheme 2.19. Amino-azetidine (AA-9) was reacted with methanesulfonyl chloride at room temperature to convert the hydroxyl group to a better leaving group.

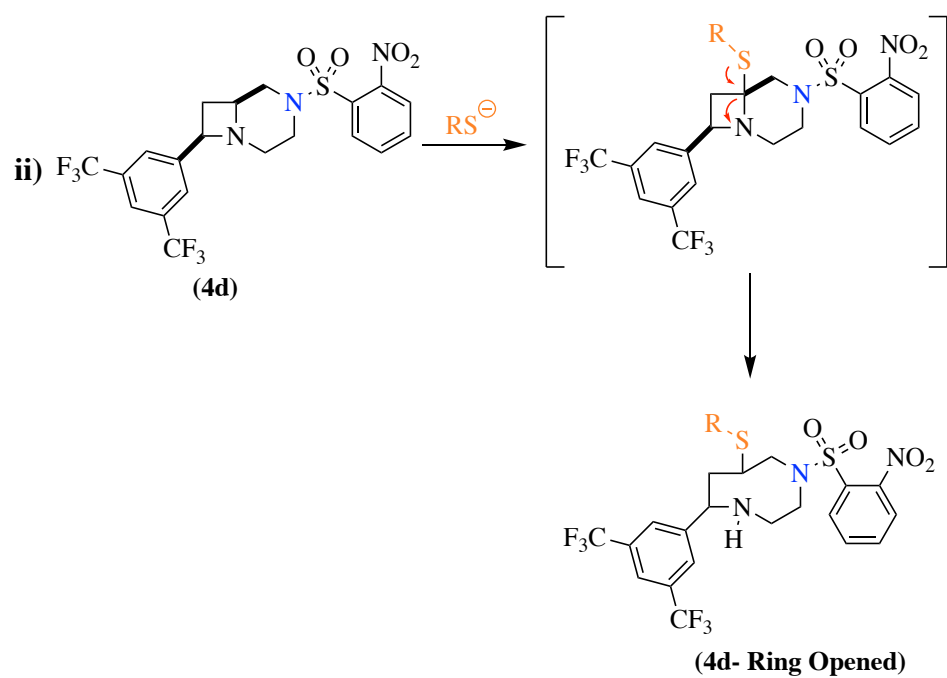
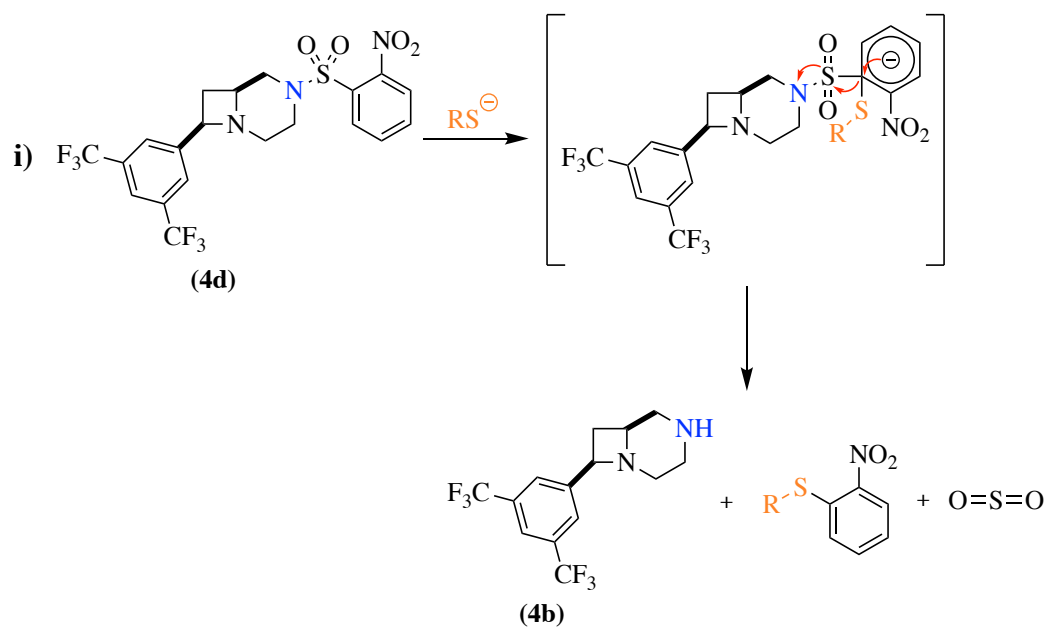
Following a quick work-up, DCM was removed *in vacuo* and the resultant crude sulfonate (**AA-10**) was redissolved in DMF and heated at 65 °C with potassium carbonate for two hours (**Scheme 2.20**). The reaction mixture was acidified to pH 2 using 1.0 M hydrochloric acid solution and washed with DCM which removed the triphenylphosphine oxide by-product, leaving only the desired product in the aqueous layer which was isolated as a salt by removing

the liquid under vacuum. The resultant salt was then triturated using ethanol and ethyl acetate in a 9:1 solution, the isolated solution was then concentrated yielding the desired cyclised product (**4d**) as a yellow oil, without need for further purification.



Scheme 2.20. The resulting amino-azetidine (AA-10) was subsequently reacted with potassium carbonate at elevated temperatures for two hours giving the protected 4,6-fused scaffold (SC-5-3) with an 87% yield.

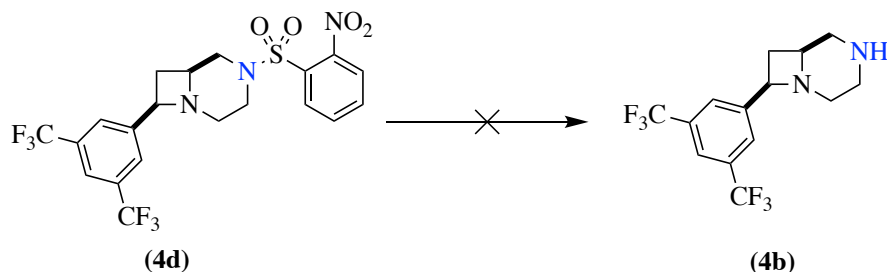
Deprotection of the nosylated amines has widely been reported with good yields using thiophenol with a base.¹⁸⁷ However, thiophenol with both potassium carbonate and caesium carbonate did not achieve clean deprotection, instead resulting in a 1:3 mixture of the free amine (**4b**) and an additional product suspected to be the 9-membered ring opened compound (**4b-Ring Opened**) based on LCMS analysis (Scheme 2.21).



Scheme 2.21. Deprotection of the Ns-protected 4,6-fused scaffold (4d) with thiophenol yielded two final products in a 1:3 ratio: (i) The deprotected scaffold (4b) is formed as the minor product by LCMS, (ii) the major product of the reaction corresponds to the 9-membered ring opened Ns-protected compound (4d – Ring Opened). It was theorised that the 4,6-fused scaffold underwent nucleophilic attack by the thiolate ion at the most hindered carbon to relieve ring strain.

As summarised in **Table 2.3**, several additional methodologies were trialled for the removal of the Ns protecting group. Mercaptoacetic acid (MAA) was utilised as an alternative thiolate nucleophile, the advantage being that the resulting cleavage side product of nitrophenylthioacetic acid could be washed away with NaHCO_3 .¹⁸⁸ MAA coupled with both triethylamine and caesium carbonate gave clean conversion, but the rate of rate of deprotection was very slow, even when the reaction temperature was raised from room temperature to 50 °C making it an unsuitable method of deprotection. Finally, magnesium turnings in methanol at 40 °C were trialled as a much harsher method of nosyl removal, which resulting in complete decomposition of starting material.

Table 2.3. Several methodologies were trialled for the removal of the *Ns* protecting group to yield the 4,6-fused scaffold at the major product.

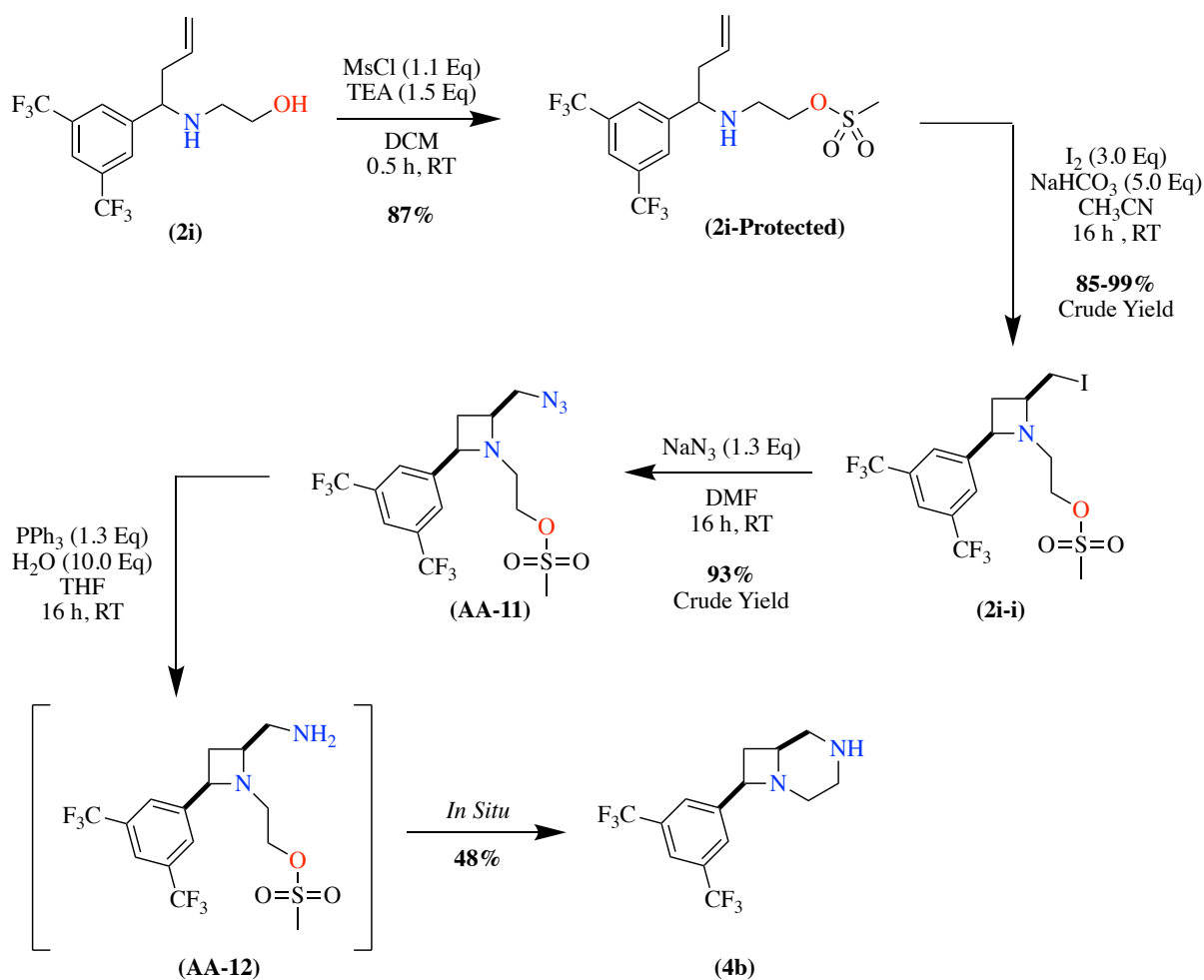


	Reagents	Solvent	Temp	Time (h)	Comments
1.	PhSH (3.0 Eq) K ₂ CO ₃ (2.0 Eq)	Acetonitrile	RT	3	Full consumption of starting material - product mass observed in a 1:3 ratio with compound of m/z 435.2 (suspected 4d – Ring Opened)
2.	PhSH (2.0 Eq) CsCO ₃ (2.0 Eq)	DMF	RT	1	Full consumption of starting material - product mass observed in a 1:3 ratio with compound of m/z 435.2 (suspected 4d – Ring Opened)
3.	PhSH (5.7 Eq) K ₂ CO ₃ (3.0 Eq)	DMF	RT	1	Full consumption of starting material - product mass observed in a 1:3 ratio with compound of m/z 435.2 (4d – Ring Opened)
4.	Mercaptoacetic Acid (1.3 Eq) TEA (2.0 Eq)	DMF	RT	2.5	No conversion to desired product
5.	Mercaptoacetic Acid (2.5 Eq) Cs ₂ CO ₃ (5.0 Eq)	DMF	RT	4 days	Very slow rate of conversion - 20% conversion to desired product after 4 days
6.	Mercaptoacetic Acid (2.5 Eq) Cs ₂ CO ₃ (5.0 Eq)	DMF	50	24	Reaction very slow, additional 2.5 Eq. of MAA added, no increase in rate of deprotection
7.	Mg (96.0 Eq)	MeOH	40	1	Starting material destroyed

2.2.6. Increased Reaction Efficiency

Due to the difficulties in removing the nosyl protecting group on (**4d**), several steps were taken to increase the efficiency of the route. Firstly, the activation of the hydroxyl group of the homoallylic amine (**2i**) was carried out at the beginning of the synthetic pathway. The reaction

sequence then proceeded as before, the modified homoallylic amine (**2i-Protected**) was cyclised using molecular iodine to access the iodo-azetidine intermediate (**2i-i**) which was then reacted with sodium azide to form the desired azido-azetidine (**AA-11**). It was hypothesised that potassium carbonate and heat would be required to close the ring as in a previous synthetic route. However, a fortuitous discovery revealed that the ring closure reaction occurred as a single step *in situ*. The azido-azetidine was reduced to the free amine in THF and near-total cyclisation to the fused ring system was observed within 16 hours of reaction initiation. The 4,6-fused scaffold (**4b**) was the major reaction product, a small amount of uncyclised amino azetidine was also observed (**Scheme 2.22**).



Scheme 2.22. To access the 4,6-fused scaffold, **(4b)** more efficiently, the homoallylic amine **(2i)** was first reacted with methanesulfonyl chloride to transform the hydroxyl group to a significantly better leaving group. The resulting protected homoallylic amine **(2i-Protected)** was cyclised using iodine under basic conditions yielded the corresponding iodo-azetidine intermediate **(2i-i)** which was reacted with sodium cyanide. The resultant azide-containing azetidine **(AA-11)** was reduced under classical Staudinger reaction conditions to give **(AA-12)** which underwent intramolecular cyclisation *in situ* to give the 4,6-fused scaffold **(4b)** on a multi-gram scale.

Isolation of the 4,6-fused scaffold **(4b)** from the reaction mixture was achieved through manipulation the pH. The neutral solution was acidified to pH 2 using 1.0 M HCl solution and extracted with ethyl acetate, the organic layer contained mainly the triphenylphosphine by-product with **(4b)** being the major product in the aqueous fraction. The pH of the aqueous layer was adjusted to pH 10 using 2.0 M NaHCO₃ solution to push the product of the aqueous layer

and was extracted with ethyl acetate before washing with brine. Purification of the free amine bicyclic system was easily achievable in good yields using normal phase chromatography with 5% MeOH in DCM with 1% triethylamine in yields of between 53% and 72% on a multigram scale. Having successfully identified a robust route towards a bicyclic, heterocycle-containing scaffold moiety, a series of test diversification reactions were carried out in preparation for library generation.¹ The pure product (**4f**) of one of these reactions was recrystallised from acetonitrile and an X-ray crystal structure was obtained (**Figure 2.5**).

¹ The diversification of 4,6-fused scaffold (**4b**) is discussed in detail in Chapter 3, Section 3.3.1 – Section 3.3.4.

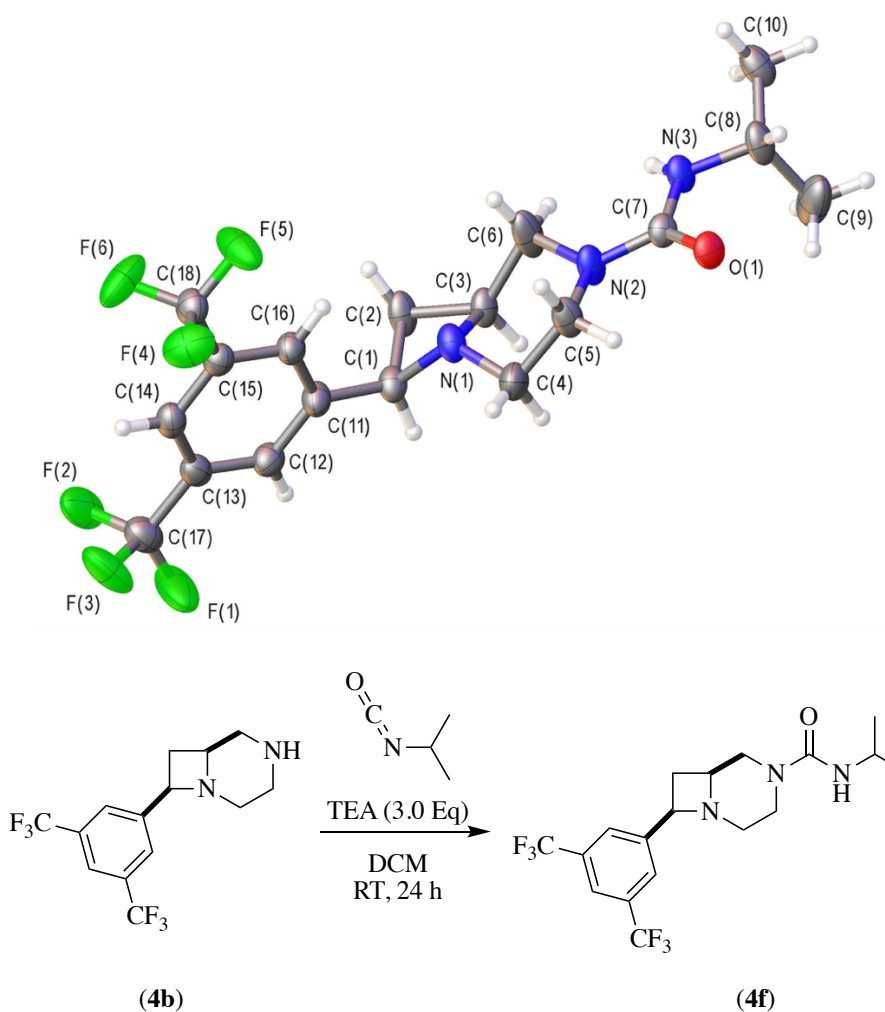
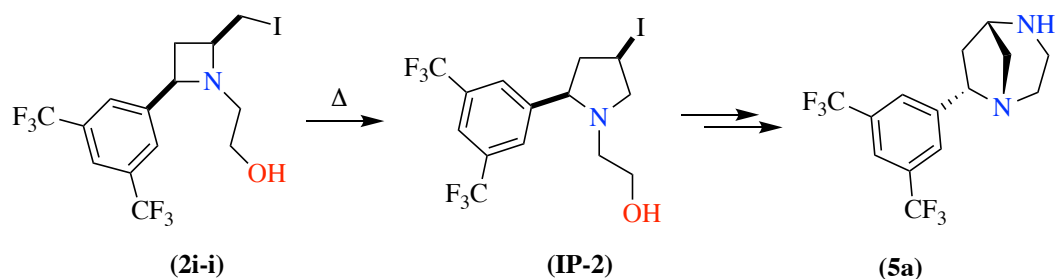


Figure 2.5. An X-ray crystal structure was obtained of **(4f)** with ellipsoids drawn at the 50 % probability level, to further confirm the structure and stereochemistry of the 4,6-fused scaffold.

2.2.7. Isolation of the 5,6-Bridged Scaffold

As discussed above (**Section 2.1.1.**), iodo-azetidines can be readily converted to the corresponding iodo-pyrrolidine stereoisomer by heating to 50 °C as a solution in acetonitrile. Using the same methodology as described in (**Section 2.2.6.**), the iodo-pyrrolidine intermediate (**IP-2**) was converted to the corresponding 5,6-bridged scaffold (**5a**) with final yields of between 32% and 67% on a multigram scale (**Scheme 2.23**).



Scheme 2.23. Iodo-azetidine intermediate (**2i-i**) was readily converted to the corresponding iodo-pyrrolidine intermediate (**IP-2**). Using the previously developed method towards the 4,6-fused scaffold, the iodo-pyrrolidine intermediate was converted to the corresponding 5,6-bridged scaffold (**5a**) to be used in library diversification.

The structure and conformation of the bridged system was confirmed using 2-D NMR experiments (**Figure 2.6** and **Figure 2.7**). NOE through-space proton interactions were observed were particularly useful in confirming the structure of the 5,6-fused scaffold; Hg interacts with both protons present on the carbon bridge, Hn and Hi, as well as Hp (**IV**). The NOE interaction between Ho with Hj and Hi proved that these protons sit in the same side of the molecule (**II**). HMBC (**H**eteronuclear **M**ultiple **B**ond **C**orrelation) showed through bond couplings between Ho and C8 (**VII**). Hi and Hg, as well as Hm and Hp display coupling to C2 (**V** and **VI**) adding further proof to the structure determination.

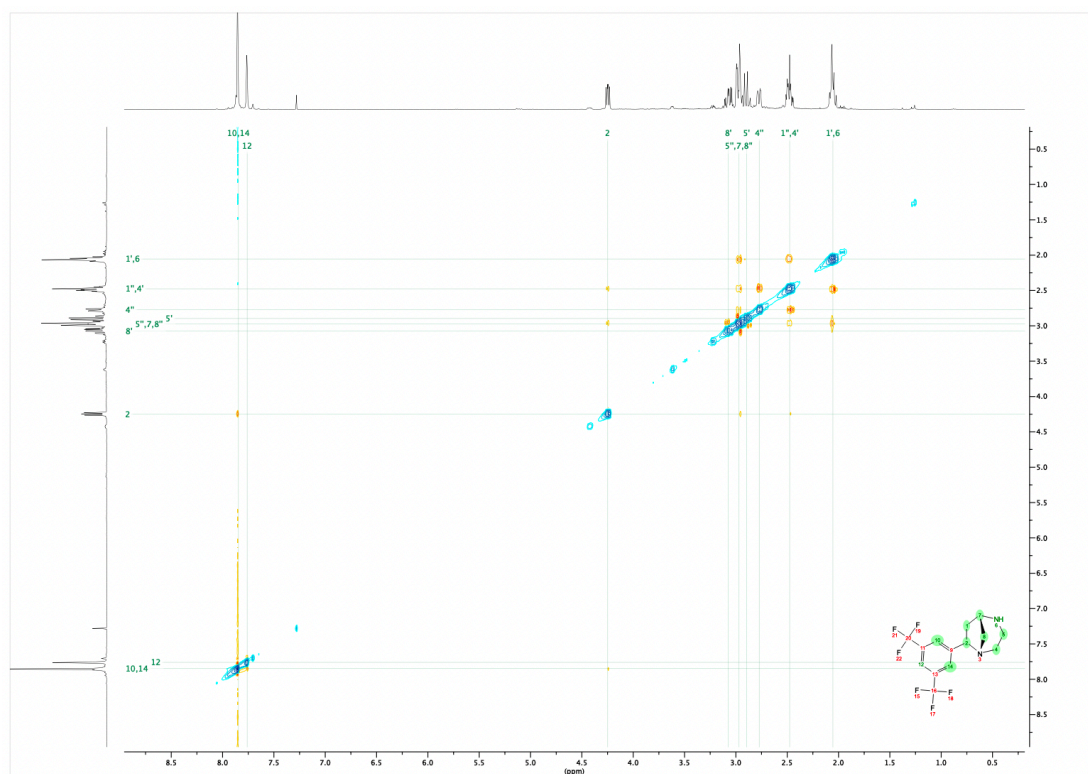
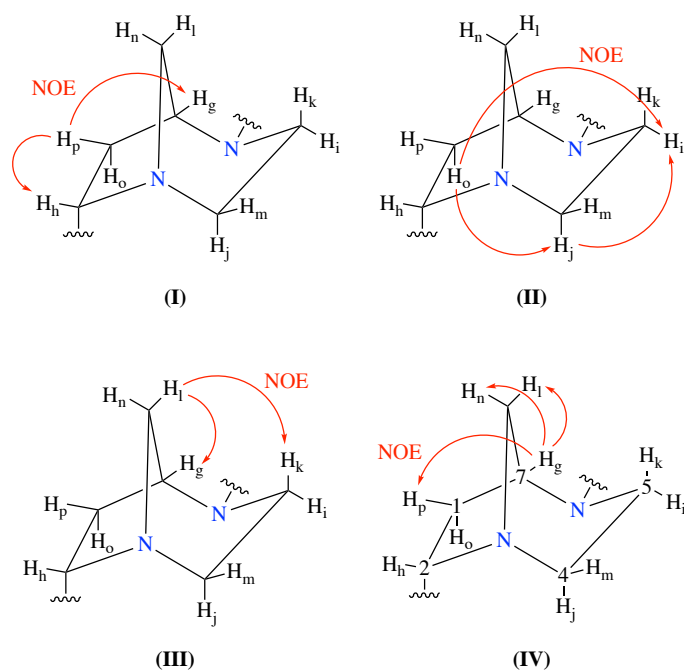


Figure 2.6. 2-D NMR spectroscopy was used to confirm the structure and conformation of the 5,6-bridged scaffold (SC-6-NH). NOE through-space proton interactions (red arrows) were observed were particularly useful in confirming the structure of the 5,6-fused scaffold; H_g interacts with both protons present on the carbon bridge, H_n and H_i, as well as H_p (IV). The NOE interaction between H_o with H_j and H_i proved that these protons sit in the same side of the molecule (II), confirming the *cis*-stereochemistry of the scaffold.

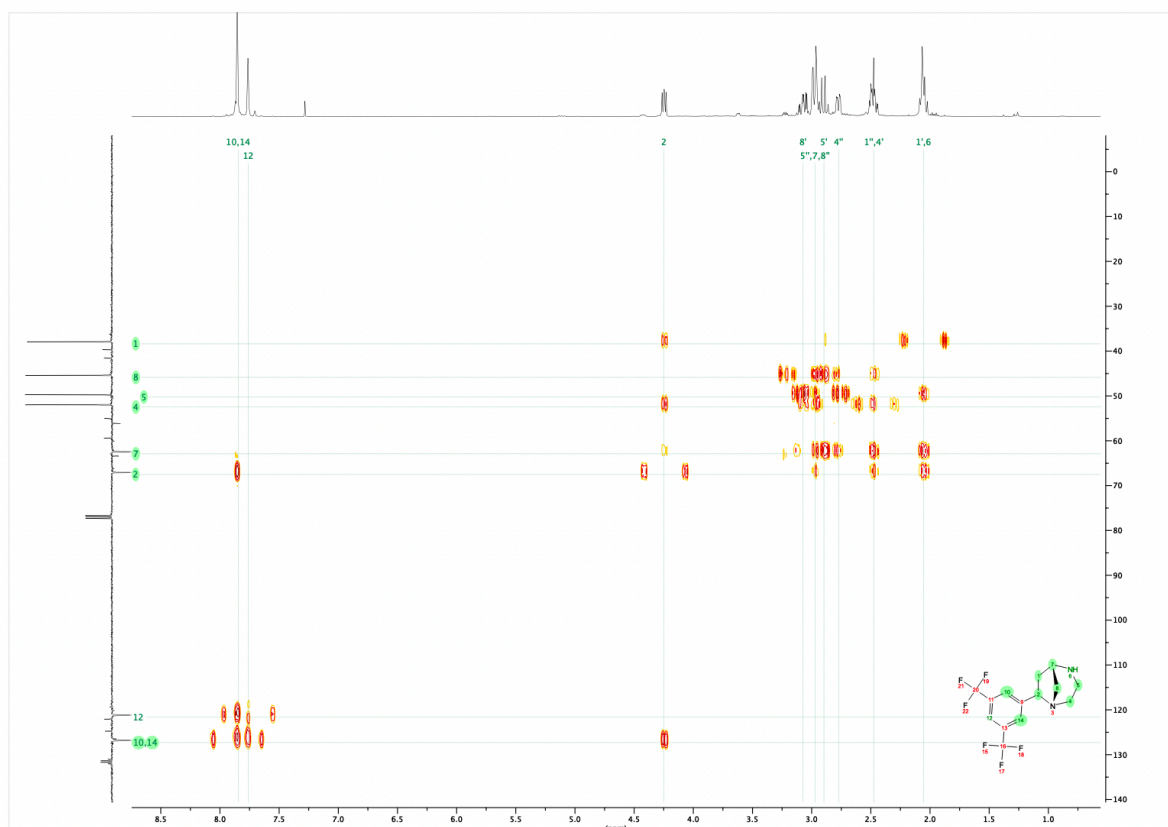
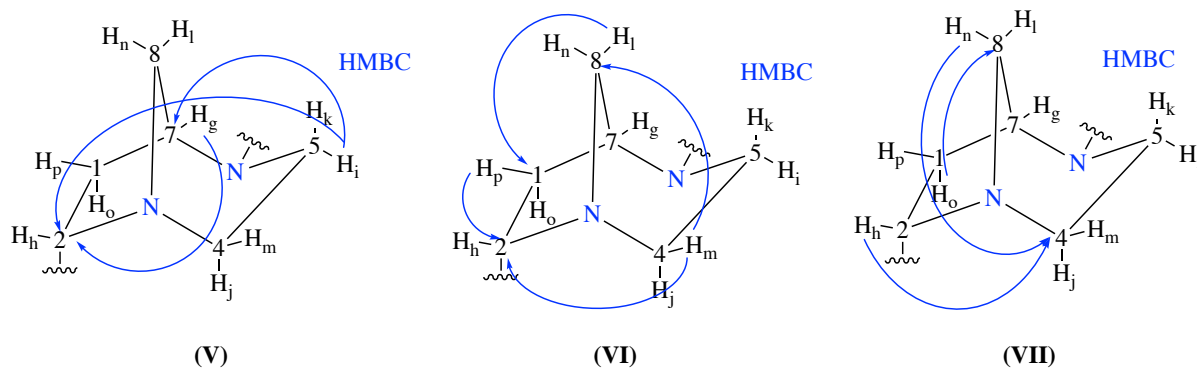


Figure 2.7. HMBC (Heteronuclear Multiple Bond Correlation) interactions (blue arrows) showed through bond couplings between H_o and $C8$ (VII). H_i and H_g , as well as H_m and H_p display coupling to $C2$ (V and VI).

Having successfully isolated and optimised the synthesis of the azetidine-containing 4,6-system (**4b**) and the corresponding pyrrolidine-containing 5,6 system (**5a**), it was decided that both scaffolds would be used for virtual library enumeration towards the generation of a physical compound library. Both the 4,6-fused and the 5,6-bridged system originated from the same starting material, iodo-azetidine intermediate (**2i-i**), however by exploiting a known

structural interconversion through temperature manipulation, two scaffolds which are structurally very different to each other have been generated in good yields. The azetidine containing system is a relatively flat and compact scaffold whereas the pyrrolidine-containing scaffold offers an additional degree of three-dimensionality to the scaffold due to the carbon bridge within the system, allowing for a greater area of chemical space to be covered. The effect of scaffold shape and dimensionality in terms of drug discovery and the process of library generation will be discussed in the proceeding chapter.

Chapter 3: Library Design and Development

3.1. Computational Tools in Library Design

Computational tools are widely employed throughout the drug discovery pipeline, such resources are commonly used to (i) design and select novel molecules *in silico*, (ii) filter large compound libraries based on specific molecular properties or physiochemical characteristics and (iii) virtually optimise and screen compounds to improve their pharmacokinetic properties. Computer-Aided Drug Design (CADD) methodologies are becoming increasingly important in drug discovery and are critical for the cost effective identification of new drug candidates with suitable pharmacological properties.¹⁸⁹

Open-source applications were used to aid the library design process, KNIME¹⁹⁰ was used to perform *in silico* reactions for the enumeration of compound collections, which were then visualised and evaluated in terms of three-dimensionality using DataWarrior.¹⁹¹

3.1.1. KNIME

KNIME, the Konstanz Information Miner, is an open-source data analysis platform which contains a large set of building blocks, termed nodes, and third-party tools to allow for the creation of detailed, interactive workflows to assist in the virtual screening of compounds. The software uses a combination of machine learning and data mining procedures to sort and manipulate data based on a particular set of parameters established by the user. The platform uses “nodes” to represent each task which can be carried out throughout the entirety of the workflow. KNIME inherently possesses many of the nodes necessary for basic data analysis, however, for analysis of the required level for this project, it is necessary to install additional open-source third-party extensions. Specifically, RDKit,¹⁹² ChemAxon,¹⁹³ and CDK¹⁹⁴ extensions were installed in order to carry out the work discussed throughout this chapter.

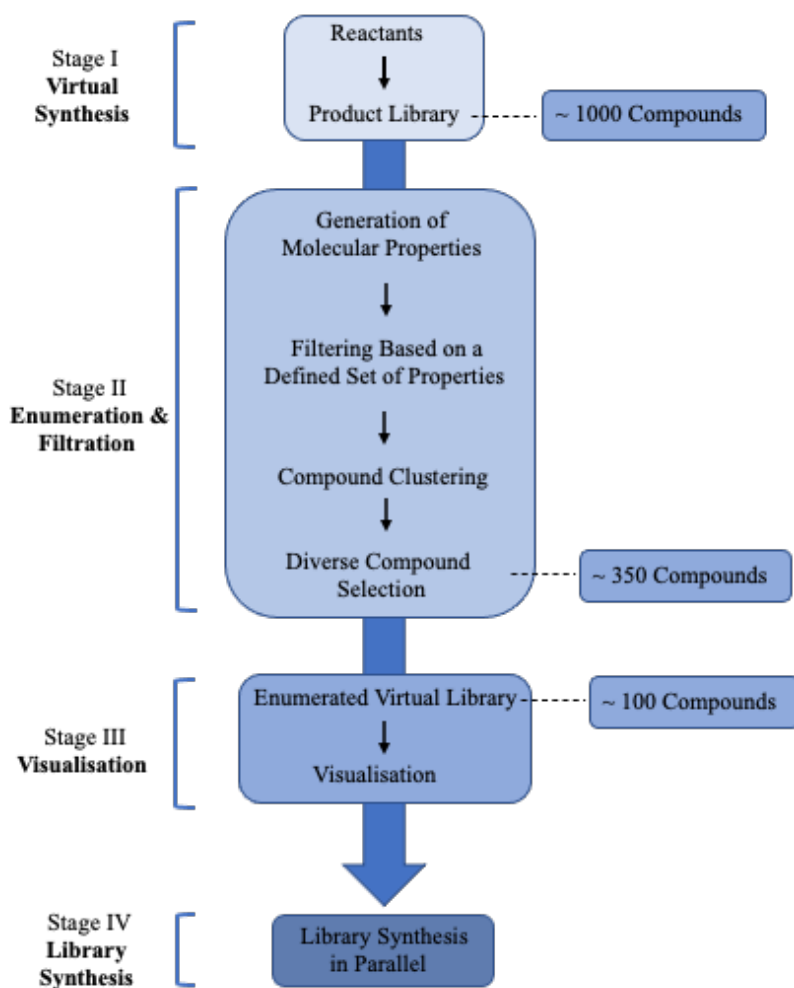


Figure 3.1. The process of designing a compound library and progressing it to market can be divided into four main stages.

Stage One involves the creation of large numbers of compounds through the *in silico* reaction of building blocks. The resultant virtual compounds are then virtually enumerated and selected (Stage Two) based on specific molecular properties and compound clustering to create a diverse virtual library set. Stage Three involves the visualisation of compounds to evaluate the spread of the library through chemical space to quantify the level of diversity within the selected library. Stage Four relates to the synthesis of the enumerated set to create a physical compound library, this synthesis process is typically conducted in parallel.

KNIME has been used in pharmaceutical research since 2006.¹⁹⁵ The process of creating a compound library using a data analysis software such as KNIME can be divided into four main stages (**Figure 3.1**). Stage I, termed “virtual synthesis” involves the *in silico* reactions of virtual

compounds, for example a scaffold moiety and all the possible reactants available, in a single or a series of in silico reactions to create a virtual product library which contains all the possible reaction outcomes. The reactants are imported as Structure Data Files (SDF) for ease of transfer between multiple platforms and in silico reactions can be composed in one of two ways. MarvinSketch is an advanced chemical editor developed by ChemAxon used to draw chemical structures, queries, or reactions. Alternatively, a form of line notation for describing the structure of molecules can be used: Simplified Molecular-Input Line-Entry System (SMILES), can be used to represent individual molecules and reactions. Importantly, the two can be readily interconverted using various nodes within KNIME. A reaction component node is used to join the reactants and generate the virtual products of the reaction, this virtual collection is usually very large, determined by the number of building blocks and reactive handles used (**Figure 3.2**). This data is present as a table, with each compound having a unique row and each property adding an additional column.

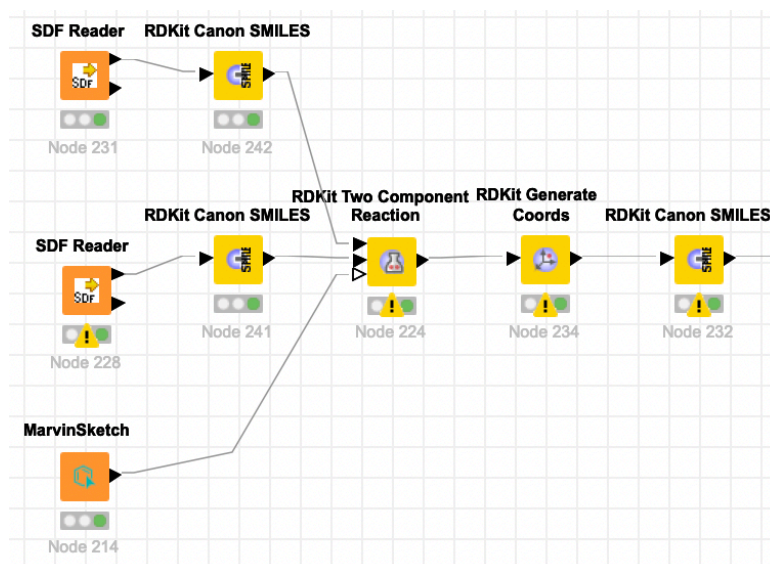


Figure 3.2. Reactants are imported as Structure Data Files (SDF) for ease of transfer between multiple platforms and in silico reactions are preformed using a “Two Component Reaction” node (Node 224) to create a set of virtual compounds.

Following the creation of a large virtual compound set, often containing thousands of items, the associated molecular properties of each compound are calculated, including but not limited to molecular weight, cLogP, topological polar surface area (TPSA), number of hydrogen bond donors (HBD) and hydrogen bond acceptors (HBA). A set of parameters are established to filter the whole compound set against, for example, using the guidelines set out by the Lipinski Ro5.⁹¹ This filter requires any compound with a molecular weight of greater than 500 Da, a cLogP greater than 5, more than 10 HBD and more than 5 HBA respectively will be removed from the table following processing with a “Row Filter” node to create a smaller set of compounds which sit inside the desired parameters.

To further reduce the size of the compound library and to create the most diverse set of compounds possible to ensure a broad exploration of chemical space, the compounds are clustered and sampled. Hierarchical Cluster Analysis (HCA) is an algorithm that groups similar objects into groups, termed clusters, each cluster is notably distinct from every other cluster, with the objects within each cluster being broadly similar. Within HCA, two modes of clustering are possible, divisive, and agglomerative. Divisive clustering, also known as top-down, starts the algorithm with all data points in one large cluster and the most dissimilar datapoints are divided into sub-clusters until each cluster consists of exactly one data point.¹⁹⁶ An alternative to this is agglomerative clustering or the bottom-up approach, which is used by KNIME. This method initially considers each data point as a unique cluster, also called a leaf. The distance is then calculated between each cluster and all the other clusters using a complete linkage strategy which defines the distance between two clusters, c_1 and c_2 , as the maximal distance between any two points, x and y , where x is in c_1 and y is in c_2 . Mathematically the complete linkage can be described by the following expression (**Equation 3.1**):

Equation 3.1. An equation to calculate the distance between two clusters.

$$D(c1, c2) = \max_{x \in c1, y \in c2} d(x, y)$$

where: $d(x, y)$ is the distance between elements $x \in c1$ and $y \in c1$

and $c1$ and $c2$ are two sets of elements (clusters)

The clusters with the shortest distance between them merge to form a new data point, termed a node. This process continues until all the data is assigned to a single, over-arching cluster termed a root. The progression for the clustering method can be visualised on tree-like plot called a dendrogram as visually represented in **Figure 3.3**. The number of clusters formed can be controlled by the user.

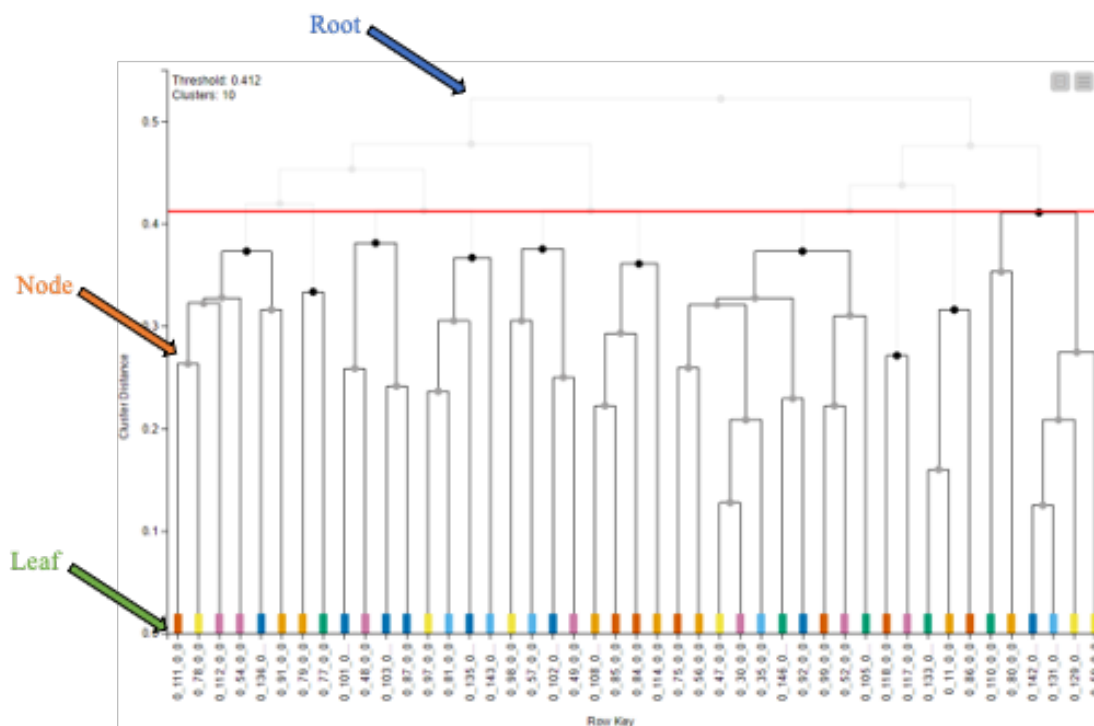


Figure 3.3. Hierarchical Cluster Analysis (HCA) is an algorithm that groups similar objects into groups, termed clusters, each cluster is notably distinct from every other cluster, with the objects within each cluster being broadly similar. An alternative to this is agglomerative clustering or the bottom-up approach, which is used by KNIME. This method initially considers each data point as a unique cluster, also called a leaf. The distance between each cluster is calculated, clusters are joined together in pairs based on their proximity in space to one another, these pairs are termed nodes. The process of joining clusters together continues until a single cluster group, called a root, remains.

Following the assignment of each virtual compound to its respective cluster, a “row sampling” node is employed to take a selection of compounds from each cluster to create a more refined, diverse set for synthesis. A linear sampling mode is used which takes the first and last row in each cluster and selected from the remaining rows in a linear fashion giving an even selection of the data at hand.

The third stage of library design involves the visualisation of the refined compound collection, this is commonly carried out using PMI plots, to visually represent the shape distribution and

diversity within the set.² Using a series of nodes, the geometry of each molecule is optimised, and its' PMI-derived properties are calculated. Three principal moment of inertia values are calculated, I_1 , I_2 , I_3 , ranging from smallest (I_1) to largest (I_3), subsequent normalisation of the resultant values is then carried out by dividing the lower values, I_1 and I_2 , by the highest, I_3 , to generate two characteristic values of normalised PMI ratios (NPRs) for each compound in the set. By calculating these values, I_1/I_3 and I_2/I_3 , the dependence on the size of the molecules in the chosen representation is completely removed, which reduced the need for decorrelation procedures¹⁰⁶, thus making the method less computationally demanding. The majority of approved drugs currently available fall along the rod-disc axis of the ternary PMI plot, with relatively few populating the more three dimensional area of chemical space, techniques such as fragment based drug discovery and diversity orientated synthesis can be used to create compound libraries which populate under explored areas of three dimensional chemical space (**Figure 3.4**).^{106, 113, 114}

² For a more detailed explanation of PMI plots and their applications please see Section 1.5.3.

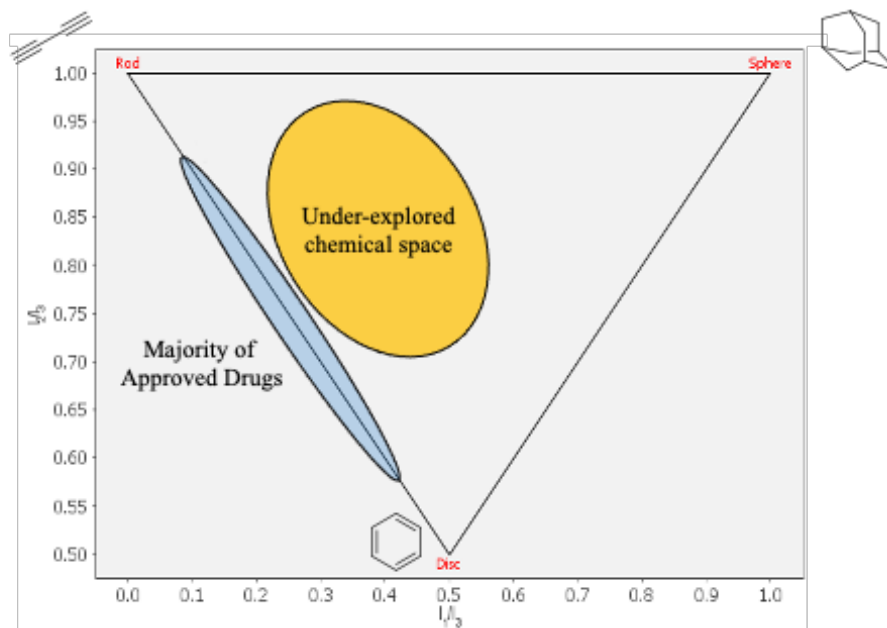


Figure 3.4. The geometry of each compound is calculated through the generation of normalised PMI ratios. The majority of approved drugs fall along the rod-disc axis when visualised on a PMI plot with a relatively small percentage occupying a more three-dimensional region of chemical space. Techniques such as fragment-based drug design and diversity orientated synthesis allow for the creation of compound libraries which display a high degree of three-dimensionality and stereochemical diversity to enable the population of chemical space which is currently under-explored.

These plotted values result in a triangular graph into which all the molecules in the collection are projected. The three corners of the graph are defined by the vector $[I_1/I_3, I_2/I_3]$ which translated to $[1,1]$, $[0.5, 0.5]$ and $[0,1]$ respectively.

The final step in the process, involves the translation of the enumerated virtual library into a physical compound collection which can be employed in biological assays. The process is usually carried as a series of reactions in parallel allowing for between 10's and 1000's of compounds to be synthesised at the same time.¹⁹⁷

3.1.2. DataWarrior

DataWarrior, is an open-source platform which can be used for the for the analysis and visualisation of data.^{191, 198} DataWarrior was primarily utilised for the visualisation and evaluation of the final compound collections compared to pharmaceutical compounds available on the market. Principal Component Analysis (PCA) is a widely used technique to convert many highly correlated variables into a smaller number of less correlated variables to allow for the creation of an easily interpretable visual representation of molecular diversity. Molecular descriptors are widely employed in cheminformatics,¹⁹⁹ and are a mathematical representation of a molecule and its associated molecular properties.²⁰⁰ Descriptors are commonly classified in accordance with their associated “dimensionality”, which is extrapolated from the properties being calculated. One-dimensional (1-D) descriptors relate to the bulk molecular properties such as molecular weight and LogP, two-dimensional (2-D) descriptors correspond to the properties such as Fsp³,²⁰¹ which are computed from 2-D representations of the molecules being studied and are represented as unique binary codes termed molecular fingerprints.²⁰² Three-dimensional (3-D) descriptors are calculated from 3-D molecular representations and may require the analysis of multiple geometric conformations in order to extrapolate descriptors such as principal moments of inertia and molecular topology,²⁰⁰ which are represented as mathematical vectors.²⁰³

DataWarrior possesses a series of options for the calculation of the descriptors associated with a particular molecule. The “SkeletonSphere” descriptor was chosen to assess compound similarity and to generate principal component data due to its accuracy when compared to other available descriptor calculations.^{204, 205} Following the calculation of the principal component data, the enumerated library was displayed in a three-dimensional plot in order to visualise the diversity of its’ components from one another (**Figure 3.5**).

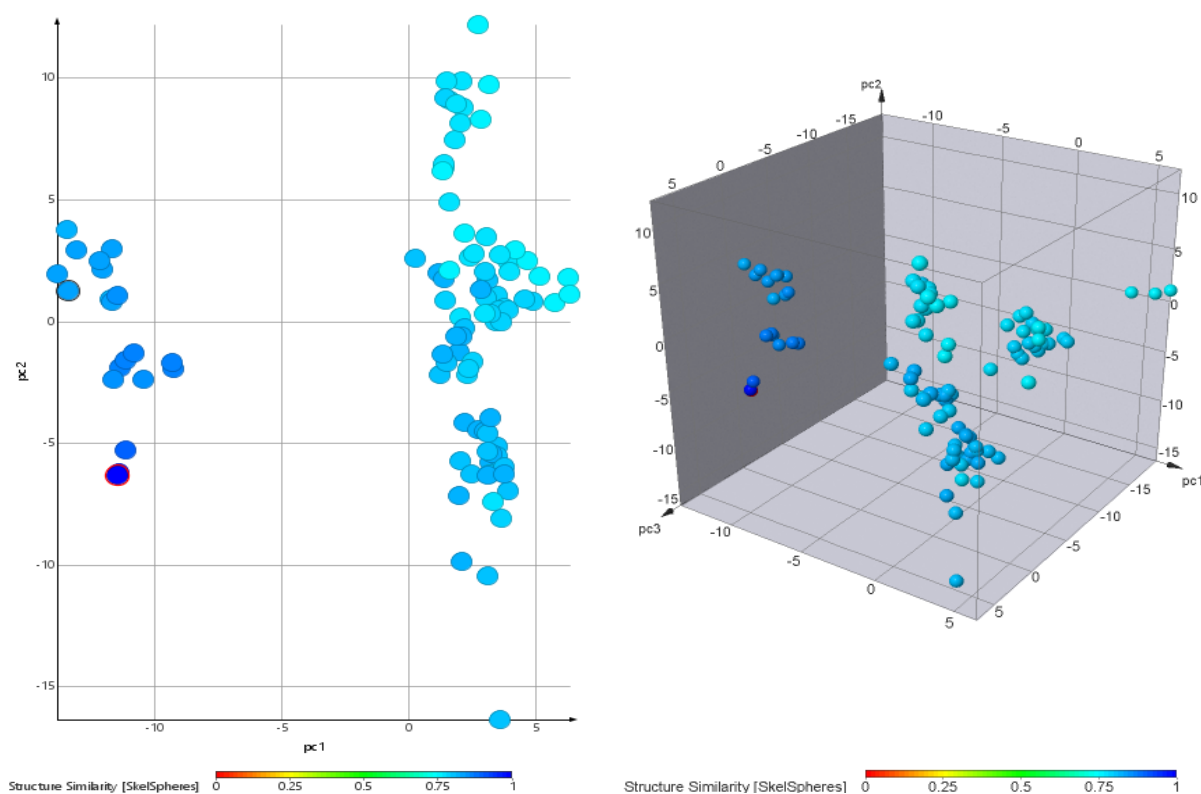


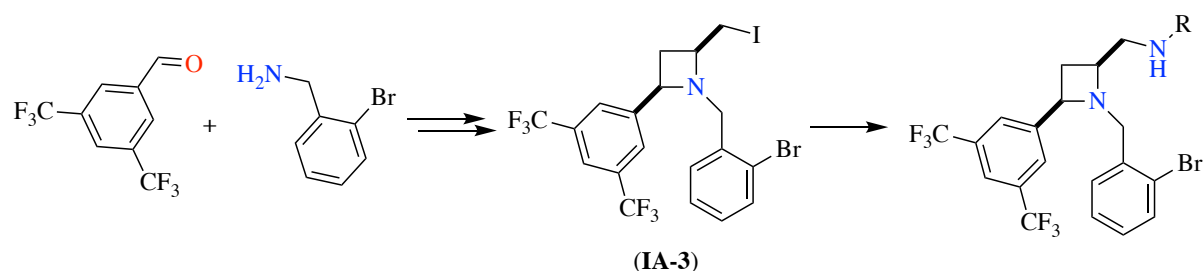
Figure 3.5. A two-dimensional and three-dimensional representation of 101 compounds based on the same core scaffold, compounds display a similarity score of between 0.7 and 0.8 owing to use of a common scaffold moiety. Decoration of the scaffold with a series of reactants has allowed for the creation of a library set which covered a wide range of chemical space.

3.2. Library Development: Generation One Scaffolds

An additional aim of this work, aside from the development of novel, bicyclic scaffolds, was to improve the scope of the azetidine ring formed via iodine-mediated cyclisation. The azetidine ring was viewed as a “Generation One” scaffold to be decorated accordingly for the exploration of chemical space.

3.2.1. CF₃ Azetidine Library

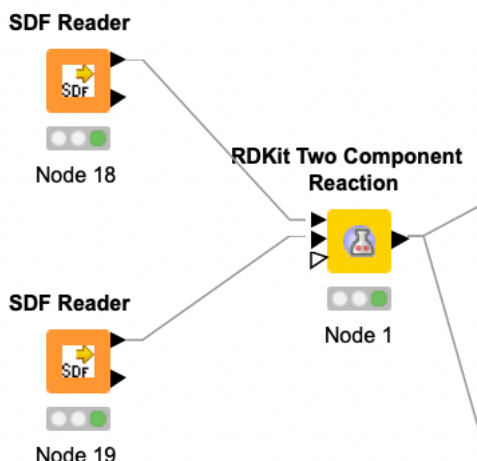
As discussed in Chapter Two, Buchwald-Hartwig amination was proposed as a method towards a bicyclic ring system. A small library of decorated azetidine rings was designed and synthesised to facilitate the creation of the final diverse *N*-heterocyclic-containing library via a late-stage cross-coupling reactions (**Scheme 3.1**).



Scheme 3.1. Simple benzylamine and benzaldehyde building blocks were used to synthesise an iodo-azetidine intermediate compound which was subsequently reacted with a series of pre-selected amines to create a diverse amino-azetidine library.

3.2.2. KNIME Pathway

Using KNIME, a basic workflow was constructed for the virtual enumeration of decorated azetidines *in silico*. Using “SDF Reader” nodes representations of the relevant starting materials, 2-bromobenzylamine and 3,5-bis-trifluorobenzaldehyde were imported to the workflow. A “Two-Component Reaction” node was used to virtually create the iodoazetidine intermediate and a SMILES string was used to represent the transformation of the simple aldehyde and amine starting materials to the corresponding cyclised azetidine ring system (**Figure 3.6**).



```
[c:1][C:2]=[O:3].[c:4][C:5][NX3;H2;!$(NC=O):6]>>[c:1][C:2]1CC(Cl)[N:6]1([C:5][c:4])
```

Figure 3.6. Building blocks were imported into the KNIME workflow using “SDF Reader” nodes and were virtually reacted using a “Two Component Reaction” node. SMILES notation was used to represent the reaction of building blocks to form the virtual iodo-azetidine intermediate compounds.

A selected set of aliphatic amines with a molecular weight of less than 175 Da (1300 compounds) was downloaded from the SigmaAldrich website²⁰⁶ as an SDF file which was uploaded to the workflow using a reader node. The contents of this node was connected to an additional “Two Component Reaction” node and reacted with the iodo-azetidine intermediate, with the reaction described using SMILES notation (**Figure 3.7**). This action created a virtual set of over 1,300 amino azetidines.

```
[C:1][C:2][I:3].[NX3;H2,H1;!$(NC=O):4][C:5]>>[C:1][C:2][N:4][C:5]
```

Figure 3.7. SMILES notation was used to represent the virtual reaction of the iodo-azetidine intermediate compounds with a selection of amines, this virtual reaction was carried out using an additional reaction “Two Component Reaction” node.

The LogP was calculated using a methodology developed by Lai and co-workers,²⁰⁷ and additional molecular properties were subsequently calculated. The virtual compound collection was then filtered based primarily on the Lipinski Ro5 guidelines,⁹¹ removing compounds with more than ten HBD, more than five HBA and a logP of greater than five. The upper limit for molecular weight was raised to 600 Da due to the presence of a bromide on the azetidine's benzylic ring adding significantly to the weight of the scaffold. Using the "Row Filter" node, this filtration process reduced the virtual library to 120 compounds (**Figure 3.8**).

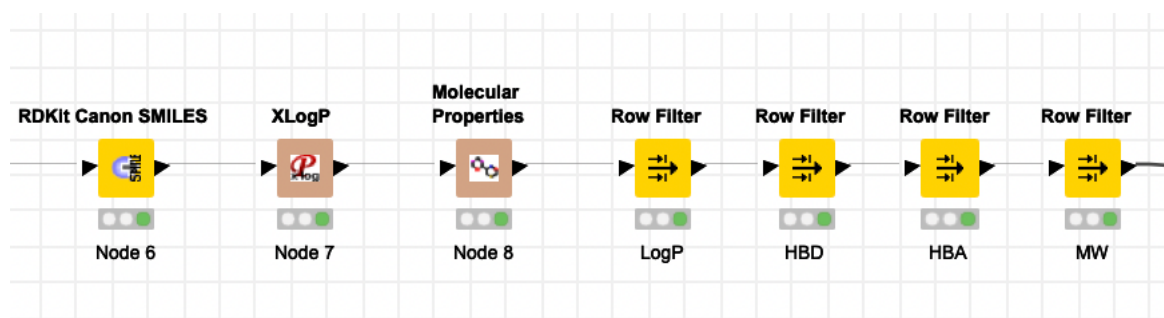


Figure 3.8. Following the creation of a virtual compound set, the molecular properties of each compound were calculated. The compound set was then filtered based on a pre-determined set of parameters using a series of "Row Filter" nodes.

The remaining compounds were clustered using a hierarchical agglomerative clustering method as discussed above (**Section 3.1.1**). Ten individual cluster groups were formed, and each group was linearly sampled to select a diverse group of virtual compounds.

The sampled collection contained 77 diverse amino-azetidines which were prepared for visualisation by optimising each compound's geometry in terms of energy/kcal and subsequently generating the PMI-derived properties associated with each molecule. As can be seen in **Figure 3.9**, the PMI plot of the enumerated library shows that the collection is

highly diverse, moving significantly away from the rod-disk line towards the centre of the plot, populating under-explored regions of chemical space.

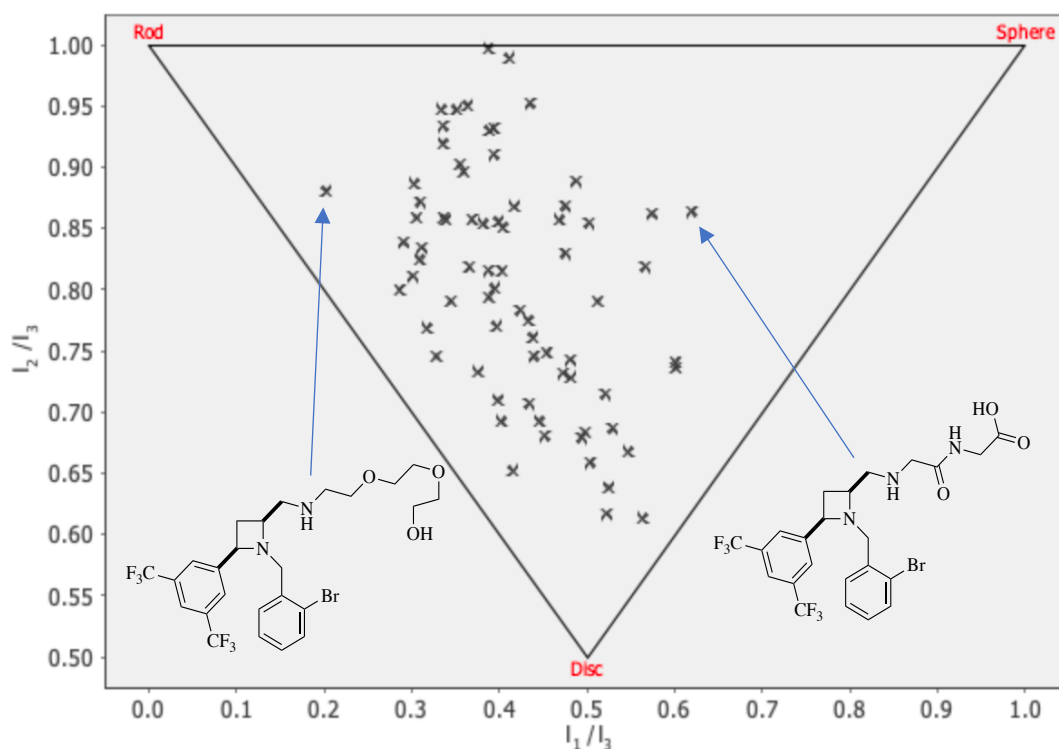


Figure 3.9. The PMI-derived properties were calculated for the amino-azetidine library and were visualised accordingly on using a triangular PMI plot where the three vertices of the plot represent the extremes of molecular geometry, it was noted that the compounds in the set had moved away from the rod-disk axis and were populating the centre of the plot, indicating a high degree of three-dimensionality within the library set.

Despite the degree of diversity observed on the PMI plot, it was decided to further reduce the size of the library to 40 compounds, which were in the original enumerated library, to focus on the major aim of the project, creation of a novel bicyclic-containing scaffold.

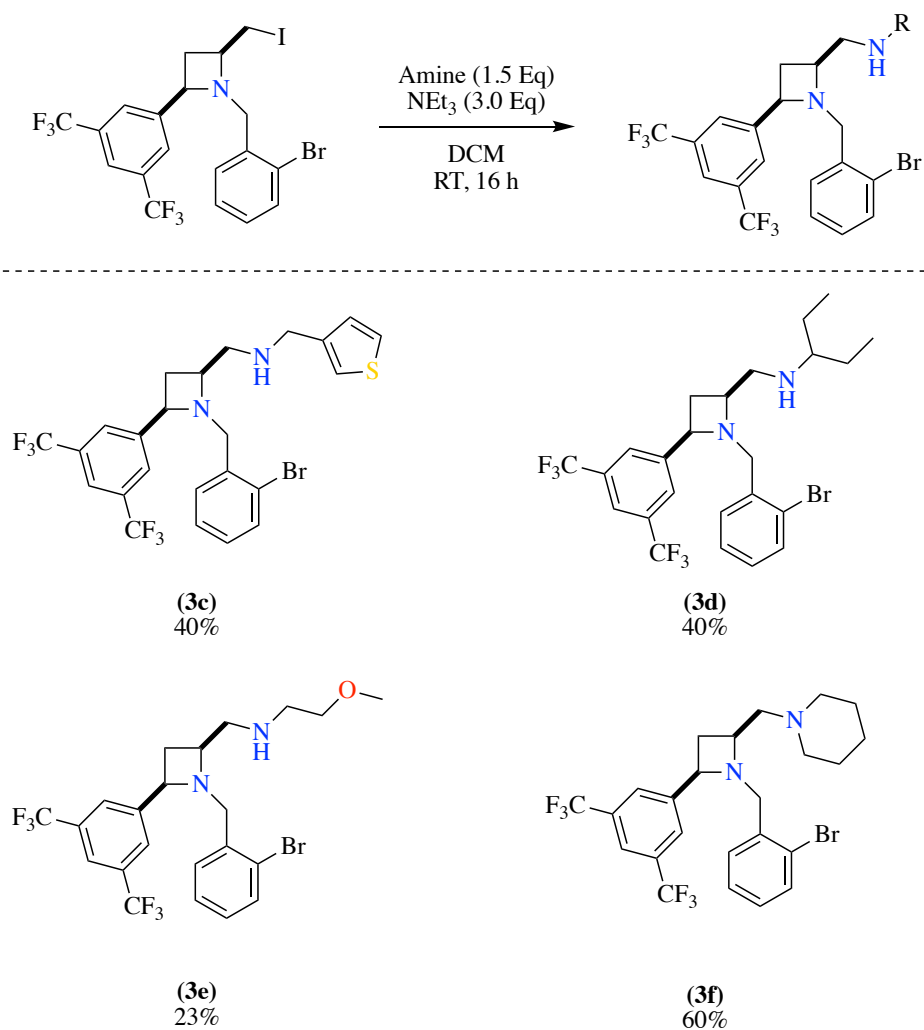
3.3.3. Synthesis and Outcome

Small-scale validation experiments were carried out to finalise conditions for both the parallel reactions and the final preparative purification of the resulting products. The reactions were carried out on a 20 mg scale with regards to the scaffold (**2c-i**) with DMF initially chosen as the reaction solvent due to its compatibility with the preparative high-pressure liquid chromatography (HPLC) purification system. However, after stirring at ambient temperature overnight, minimal conversion to the desired product was observed in all cases. Therefore, DCM was chosen as it has previously been employed as a reaction solvent in the concerted displacement of iodine and can be easily removed from the reaction mixture prior to preparative purification methods. The reaction was conducted with an excess of triethylamine to increase the nucleophilicity of the amine reactant towards the iodo-azetidine to increase the likelihood of reaction success (**Scheme 3.2**).

Purification of the validation set revealed that the product molecules did not move well on silica gel when purified under basic conditions,³ which was initially expected to be the most suited due to the number of basic centres in the final compounds. Unexpectedly, purification under acidic conditions⁴ resulted in significantly less streaking on the preparative column resulting in a more efficient purification process. Yields of the final products in the validation set were lower than would typically be expected but this was attributed to the initial difficulties faced during purification.

³ Basic conditions refer to the use of 10mM ammonium bicarbonate in water (pH 9.5) or 100mM ammonia in water being used as a eluent with acetonitrile for the preparative purification of compounds.

⁴ Acidic conditions refer to the use of 0.1% formic acid in water with acetonitrile for the preparative purification of compounds.



Scheme 3.5. A small scale validation experiment was conducted to establish conditions for library synthesis, the pre-prepared iodo-azetidine was reacted with a series of amines in a parallel fashion. The resultant compounds were purified using HPLC under basic conditions.

Preparation of the azetidine library was carried out in parallel, a solution of iodo-azetidine (**2c-i**) was prepared in DCM (45 mg/mL), the amount of starting material per reaction was increased from the original scale used in the validation set to increase the reaction concentration to boost the final isolated yields. The reaction mixture was added to labelled reaction vials with triethylamine and the amine reactant. Reactions were sealed and stirred overnight at room temperature. Reaction progress was monitored using ultra performance liquid chromatography (UPLC), after 16 hours reaction mixtures which did not contain the desired product were

discarded and DCM was removed from the remaining reactions within the set using centrifugal evaporation and were prepared for preparative purification. 34 compounds were successfully isolated, the final compounds were visualised using PMI-derived properties, I_1/I_3 and I_2/I_3 , and showed a similar spread of diversity to the larger enumerated library (**Figure 3.10**).

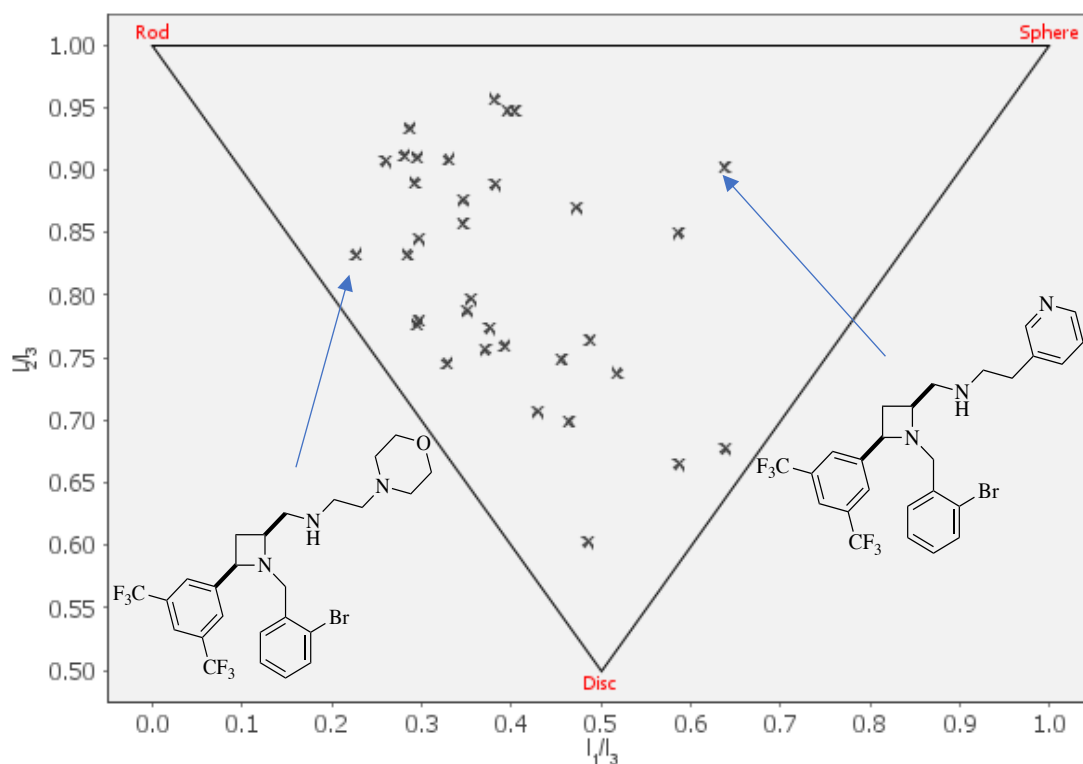
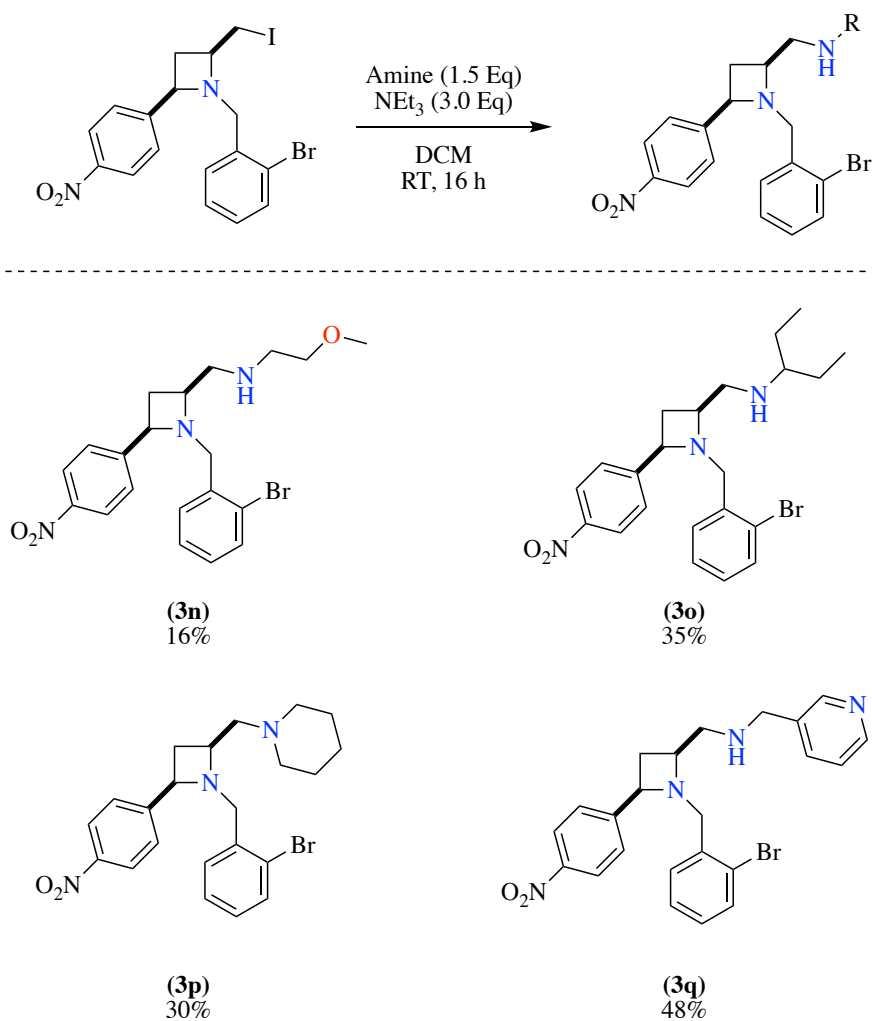


Figure 3.10. 34 amino-azetidines were successfully isolated following parallel library synthesis, the spread of three-dimensionality within the group is evident from the resultant PMI plot, the majority of compounds populate the centre of the plot indicating a high degree of shape diversity.

Yields of the isolated products were typically $\leq 30\%$, these low yields were thought to be related to the use of an intermediate product, which did not undergo flash chromatography prior to library synthesis, as a scaffold. A small selection of these uncyclised azetidine compounds were submitted for biological testing and showed interesting results towards anti-tuberculosis activity (discussed in **Section 3.4.2**).

3.3.4. NO₂ Azetidine Small Set

Additionally, a small set of nitro-containing amino-azetidines (6 compounds) was also prepared in parallel. A solution of iodo-azetidine (**2d-i**) was prepared in DCM (25 mg/mL) and subsequently partitioned between labelled reaction vials containing the amine nucleophile and three equivalents of triethylamine. The reactions were stirred overnight at ambient room temperature and monitored by UPLC. After 16 hours, all reactions contained the desired product and were prepared for preparative purification by removing the reaction solvent *via* centrifugal evaporation and resuspension in DMSO. As with the CF₃-containing set, it was found that acidic conditions were required to achieved good separation during purification, however, it was noted that there was still a significant loss of yield with the majority of products being collected with relatively low yields of less than 25% (**Scheme 3.3**).



Scheme 3.3. A small set of nitro-containing amino-azetidines were additionally synthesised in a parallel fashion to further diversify the final compound set.

The collection of compounds was visualised using the PMI-derived properties associated with each molecule, which showed that the set was quite diverse in terms of three-dimensionality. All compounds have moved significantly away from the rod-disc axis towards the centre of the plot, towards the traditionally underexplored areas of chemical space (**Figure 3.11**).

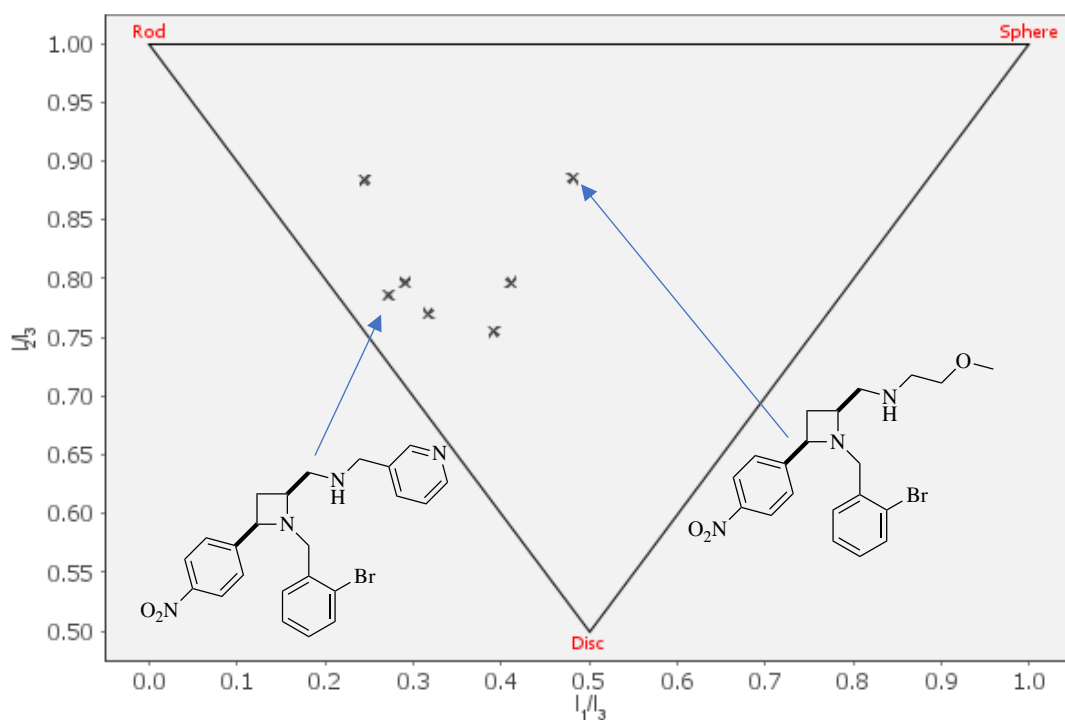
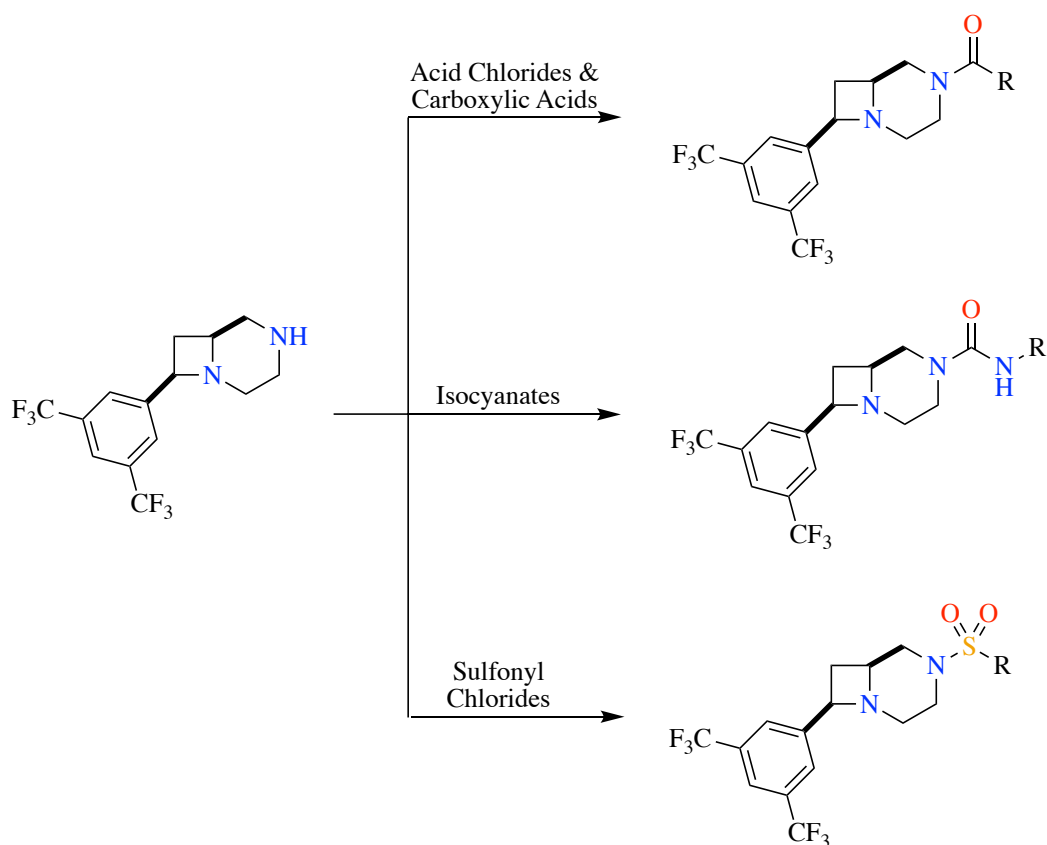


Figure 3.11. The nitro-containing amino-azetidine set was visualised using a PMI plot. The compounds possess a high degree of three-dimensionality relative to each other.

3.3. Library Development: Generation Two Scaffolds

3.3.1. 4,6-Fused Scaffold: Decoration for Library Synthesis

Following the successful synthesis of the desired heterocyclic containing “Generation Two” scaffold as discussed in Chapter Two, a workflow was designed using KNIME to enumerate a virtual compound collection for library synthesis. In order to achieve a reasonable level of diversity within the decorated library, it was decided that the scaffold would be decorated with acid chlorides, sulfonyl chlorides and isocyanates (**Scheme 3.4**).



Scheme 3.4. A schematic demonstrating the decoration of the 4,6-fused scaffold (SC-5-CF₃-NH) with acid chlorides, carboxylic acids, isocyanates and sulfonyl chlorides to create a diverse compound library

3.3.2. 4,6-Fused Scaffold: KNIME Pathway

For ease of data processing, it was decided to carry out each set of *in silico* reactions, between scaffold and reactant subgroup, separately and combine resultant data in a later step. SD files of selected acid chlorides, sulfonyl chlorides and isocyanates compiled by Sigma Aldrich were downloaded and uploaded to an “SDF Reader” node at the beginning of the workflow, the contents of the SD files were converted to their corresponding canonical SMILES strings to allow them to be processed by RdKit nodes at a later point. A second “SDF reader” node is used to introduce the 4,6-bicyclic scaffold (**4b**) to the workflow (**Figure 3.12**). A reaction query is generated using “Marvin Sketch” which was then fed into a “Two Component Reaction”

node to inform the in silico reaction between the scaffold moiety and the available reactants, resulting in a collection of 305 compounds. The reaction node (Node 234) generates a data table as the containing a row for each molecule and a new column for each additional property calculated.

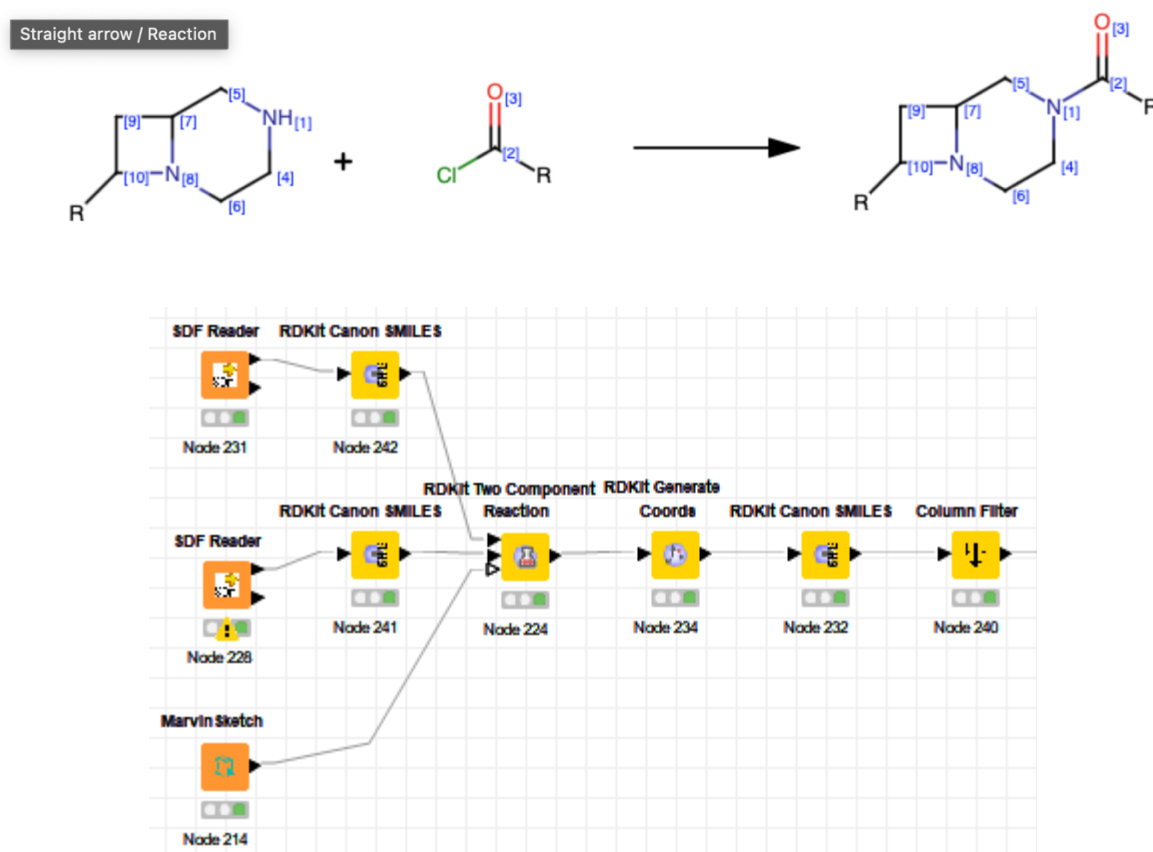


Figure 3.12. A Marvin Sketch node (Node 214) was used to generate a representation of the virtual reaction at the beginning of the workflow. This node, along with nodes containing a series of reactant building blocks and the scaffold moiety. Using a “Two Component Reaction” node (Node 224), a series of in silico reactions were conducted to generate a large set of decorated scaffolds, the corresponding SMILES notation is then generated for each virtual product.

Three-dimensional co-ordinates were generated for the resultant virtual product molecules, and unnecessary columns were removed from the data table using the “Column Filter” node to

reduce the computational load and create a simplified table containing only the starting materials and the resultant product molecules represented as SMILES with their 3-D coordinates.

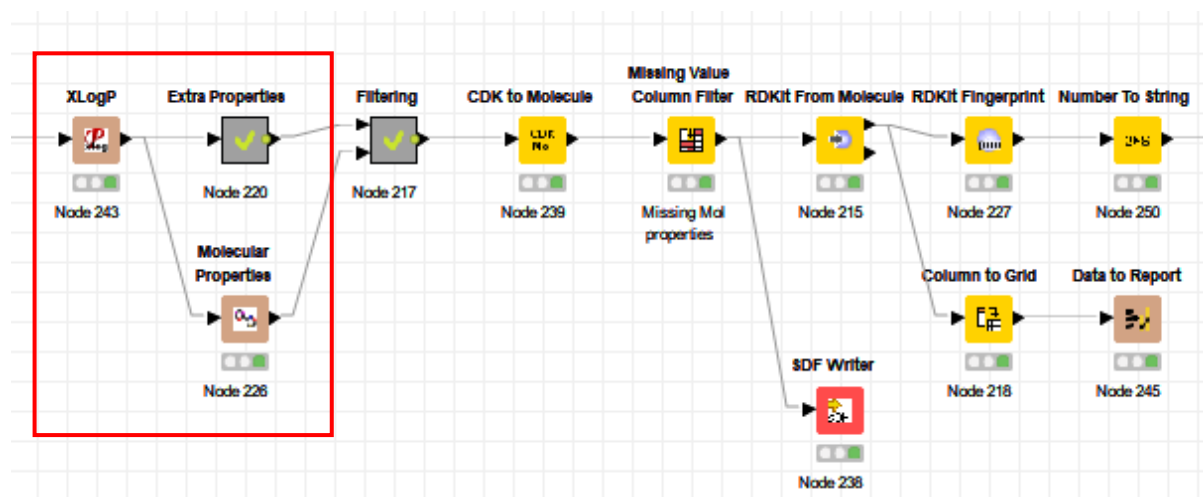


Figure 3.13. The molecular properties of virtual compounds generated by the in silico reactions were then generated using the “XLogP” (Node 243) and “Molecular Properties” (Node 226).

LogP values for each product molecule were calculated using an atom-type methodology called XLogP which was developed by Lai and co-workers.²⁰⁸ Selected molecular properties, including HBA, HBD, molecular weight, topological polar surface area (TPSA) and sp^3 character, were then calculated using a node developed by CDK (Figure 3.13).²⁰⁹ It was decided to employ Lipinski’s Ro5 guidelines, discussed in **Section 1.4.**, as a means of quickly removing compounds which fall outside the realms of lead-like chemical space. Using “row filter” nodes to apply the guidelines previously discussed, compounds which fell outside the pre-defined parameters were removed from the data table, reducing the number of compounds in the collection from 305 to 106 (Figure 3.14).

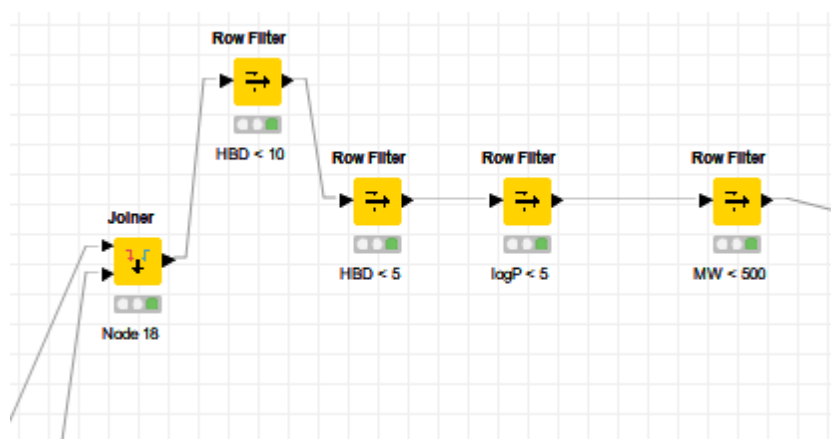


Figure 3.14. The virtual compounds were then filtered based on parameters previously defined by Lipinski.⁹¹ The filtration step was conducted so as to refine the library to include molecules with molecular properties to promote oral bioavailability.

Following this refinement in the virtual library, a molecular fingerprint is generated for each remaining virtual compound, allowing for rapid similarity comparisons to be carried out during the clustering step. The majority of molecular fingerprint methods have all been validated and used with low molecular weight compounds which fall within the limits described by Lipinski.^{210, 211} The Morgan fingerprint method, which was employed here, is one of the most popular methods available²¹² and is sometimes referred to as the extended-connectivity fingerprint (ECFP4).²¹³ ECFP4 was chosen as it has been found to perform well in benchmark drug analog studies and can readily encode highly complex structures.^{214, 215} The virtual library set was then clustered using a hierarchical, agglomerative clustering methodology as discussed above in **Section 3.1.1.**, which generated ten cluster groups, which were then linearly sampled. This gave rise to a collection of 82 virtual compounds which were prepared for visualisation. The geometry of each molecule was optimised and energy in terms of kcal/mol calculated, based on a particular force field, MMFF94 which was developed by Merck.²¹⁶ The PMI-

derived properties for each molecule were then calculated and the compound collection was then visualised on a triangular PMI scatter plot (**Figure 3.15**)

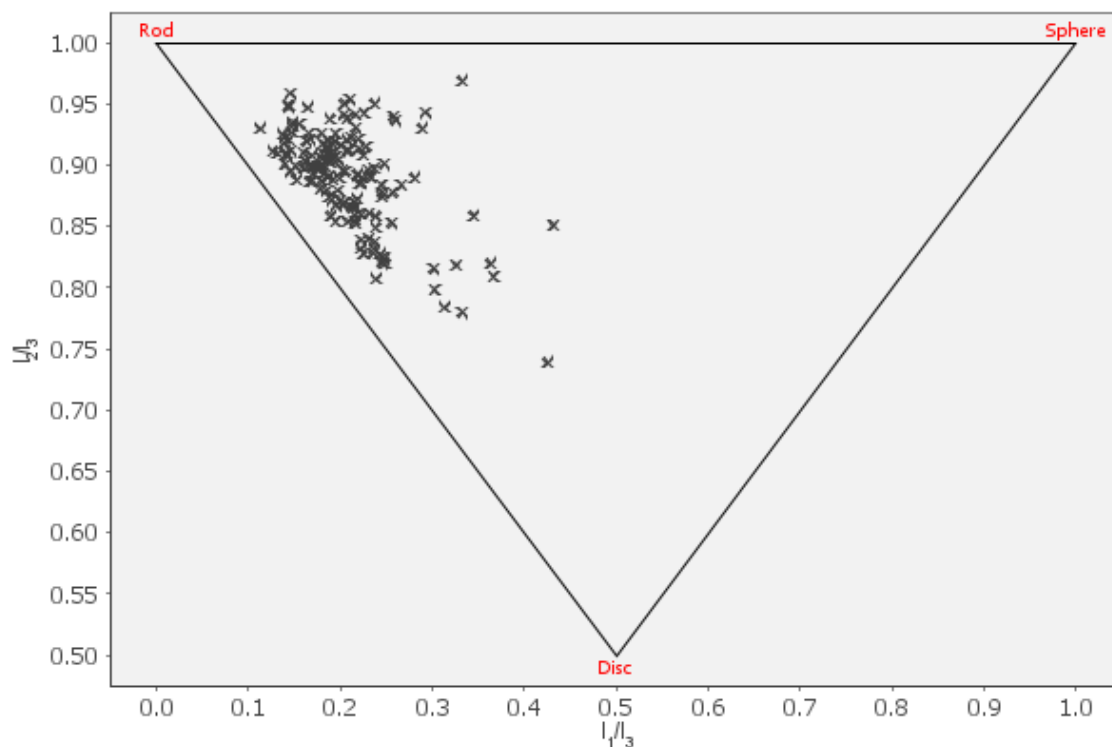
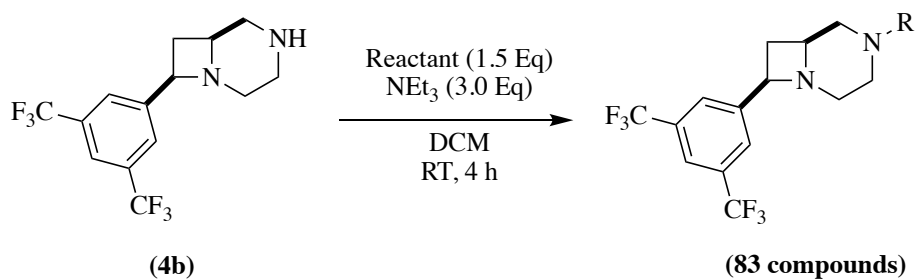


Figure 3.15. The enumerated library was visualised using a PMI scatter plot, the compounds within the selected set are positioned away from the rod-disc axis representing an increased degree of three-dimensionality within the set.

As visualised in a PMI plot, the enumerated library moved away from the rod-disk axis towards the centre of the plot, representing a more three-dimensional occupation of chemical space, which satisfies the aims of this project.

3.3.3. 4,6-Fused Scaffold: Library Synthesis

Following the virtual library enumeration of the 4,6-bicyclic scaffold, a series of small-scale validation reactions were conducted to establish conditions for parallel library synthesis (**Scheme 3.5**).



Scheme 3.5. The 4,6-fused scaffold (SC-5-CF₃-NH) was decorated with a series of amines to create a diverse compound collection.

Following purification, the compounds collected in moderate to good yields with a purity of greater than 95% (**Figure 3.16**). While preparing for library synthesis it was discovered that many of the building blocks using in the KNIME enumeration derived from the SigmaAldrich Selected Sets files were unavailable. Due to the vast collect of carboxylic acids available within the company, it was decided to carry out a validation reaction using a carboxylic acid and acid coupling reagents to further expand the scope of the scaffold decoration reactions.

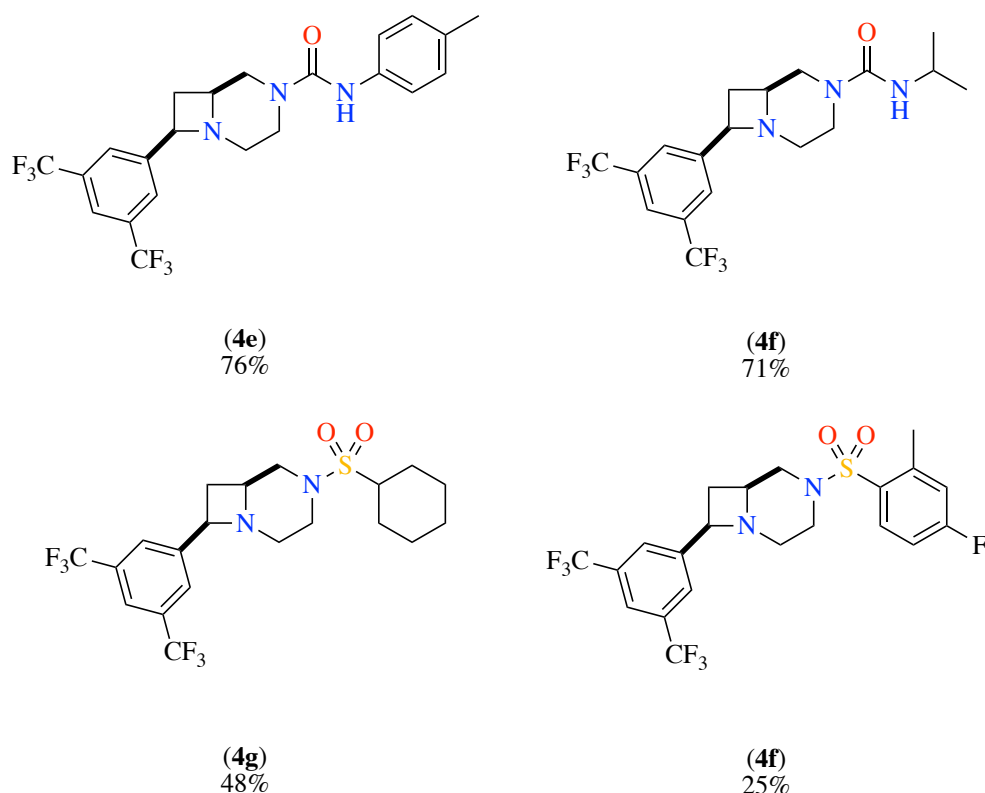
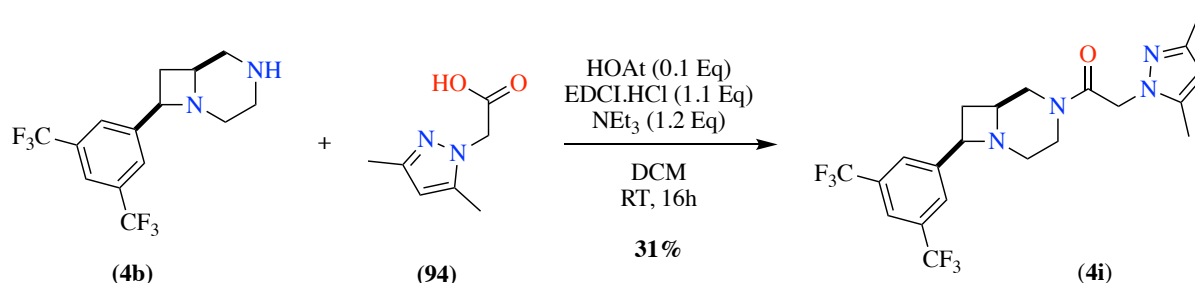


Figure 3.16. A validation experiment was conducted to establish suitable reaction conditions for the decoration of the 4,6-fused scaffold (SC-5-NH) with a series of building blocks.

Scaffold (**4b**) was dissolved in DCM along with carboxylic acid (**94**), the carbodiimide (EDC.HCl) and the peptide-coupling agent (HOAt) were added as solids along with triethylamine base, The reaction mixture was stirred at room temperature for 16 hours with good conversion to product observed, following purification the desired product was obtained in a moderate yield of 31% (**Scheme 3.6**).



Scheme 3.6. A test reaction was conducted to investigate the coupling of a carboxylic acid with the 4,6-fused scaffold to investigate the use of this reaction in library development.

Owing to the success of the acid coupling validation reaction, a series of available carboxylic acids (252 compounds) were enumerated, and 55 compounds were selected to be employed in library synthesis (**Figure 3.18**) alongside the available acid chlorides, isocyanates, and sulfonyl chlorides to expand the library and explore new chemical space.

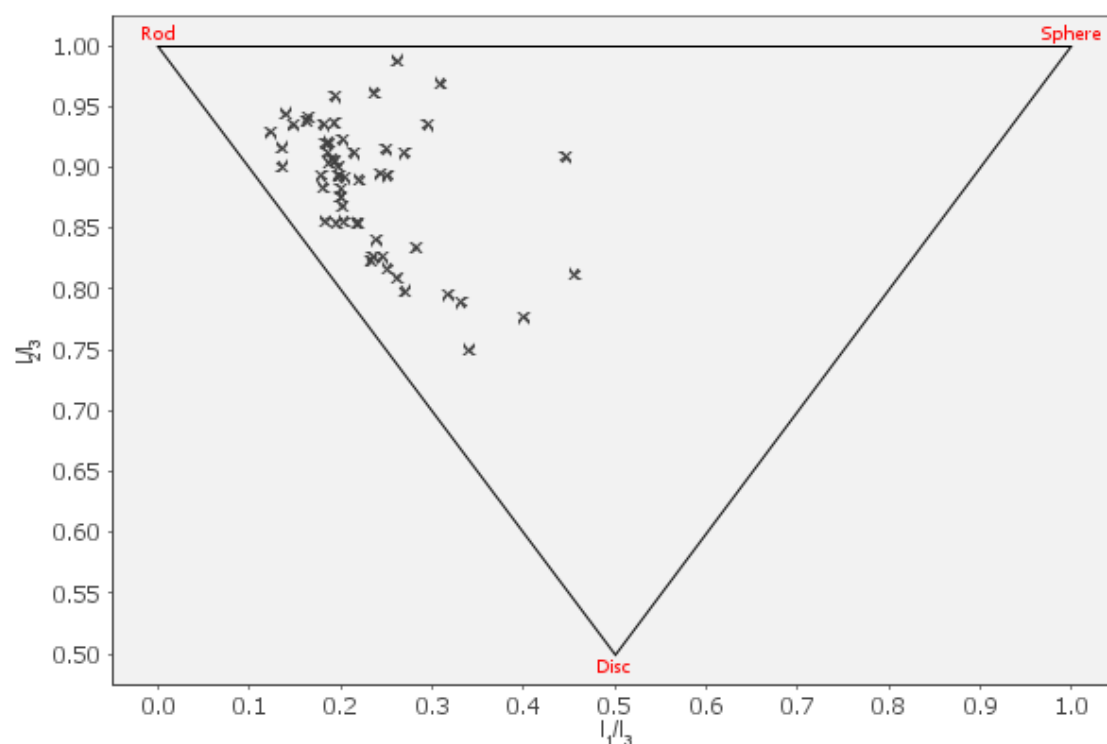


Figure 3.18. A selection of carboxylic acids was enumerated for use as building blocks in the creation of the 4,6-fused scaffold library, 55 carboxylic acids were selected for use in library synthesis and the resultant virtual compounds were visualised on a PMI plot, the virtual compounds display a high degree of three-dimensional diversity and have moved away from the rod-disk axis to populate under-exploited areas of chemical space.

Following the successful experimental validation, the 4,6 scaffold (**4b**) was prepared in accordance with the methodology discussed in Chapter Two. Library synthesis was divided into two sets owing to the differing methods of preparation, Set One involved 48 individual reactions whereby the 4,6-bicyclic scaffold was reacted with the pre-selected sulfonyl

chlorides, acid chlorides and isocyanates to access the diversified compound in a parallel fashion. The enumerated library explores a good range of chemical space, compounds possess a high degree of three-dimensionality causing them to move away from the rod-disc axis when visualised on a PMI plot (**Figure 3.19**).

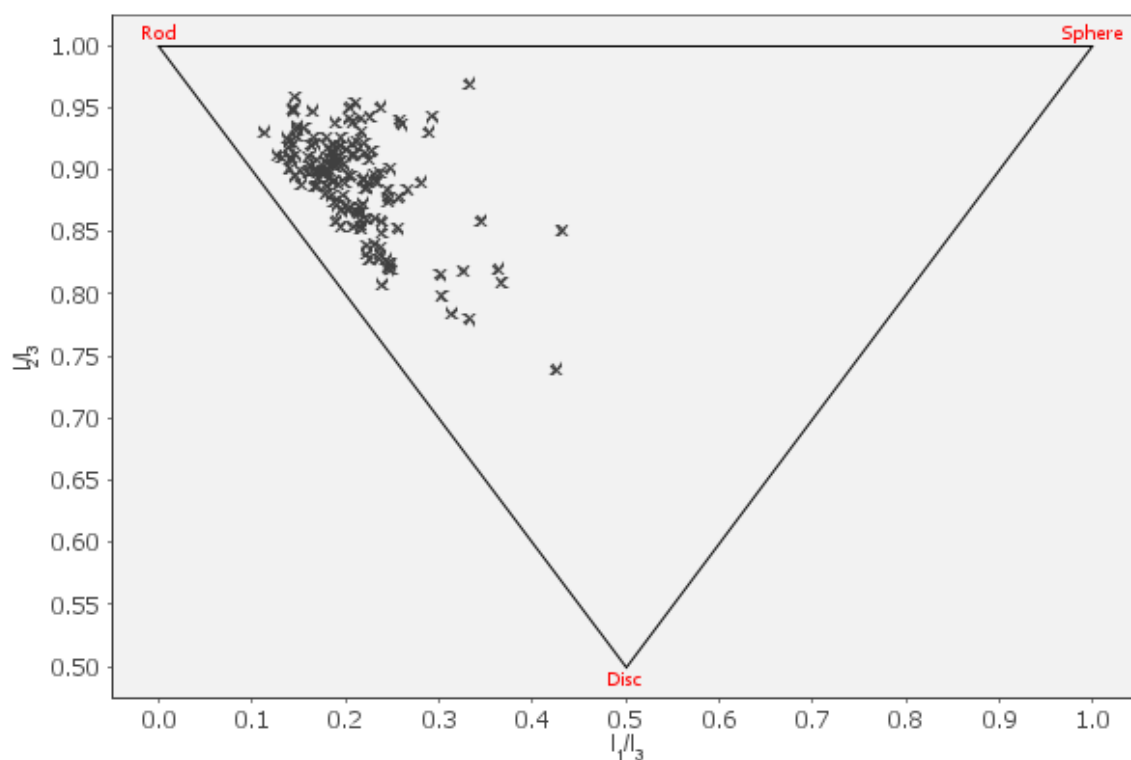


Figure 3.19. The final enumerated 4,6-fused scaffold library was visualised on a ternary PMI plot, the compound collection does not sit directly on the rod-disc axis and instead has moved towards the centre of the plot indicating a high degree of structural diversity and three-dimensionality allowing for the population of underutilised areas of chemical space.

Decoration of the scaffold (**4b**) with carboxylic acids, Set Two, involved 55 reactions conducted in parallel. The reaction vessels were sealed and were agitated overnight at room temperature using an orbital shaker (**Figure 3.20.**) which eliminates the need for magnetic stir bars allowing for faster reaction reformatting and purification. Reaction progression was periodically monitored using UPLC with 96-well plates. After 16 hours, the reactions were analysed and those which showed no conversion to the desired compound were discarded and

the remaining compounds were prepared for preparative purification by removal of DCM with centrifugal evaporation and were redissolved in DMF for purification.



Figure 3.20 . Library synthesis reactions were conducted in parallel and were agitated using an orbital shaker to ensure consistent stirring overnight.

3.3.4. 4,6-Fused Scaffold: Summary of Synthetic Results

95 compounds were successfully isolated after mass-directed preparative HPLC purification in low to moderate yields of between 15% and 50%. Using DataWarrior, the library was visualised as a three-dimensional scatter plot. Molecular weight was plotted against polar surface area and the calculated LogP values which demonstrated, using the descriptors, that the members of the library demonstrate molecular diversity, as per the goals of this project (**Figure 3.21**).

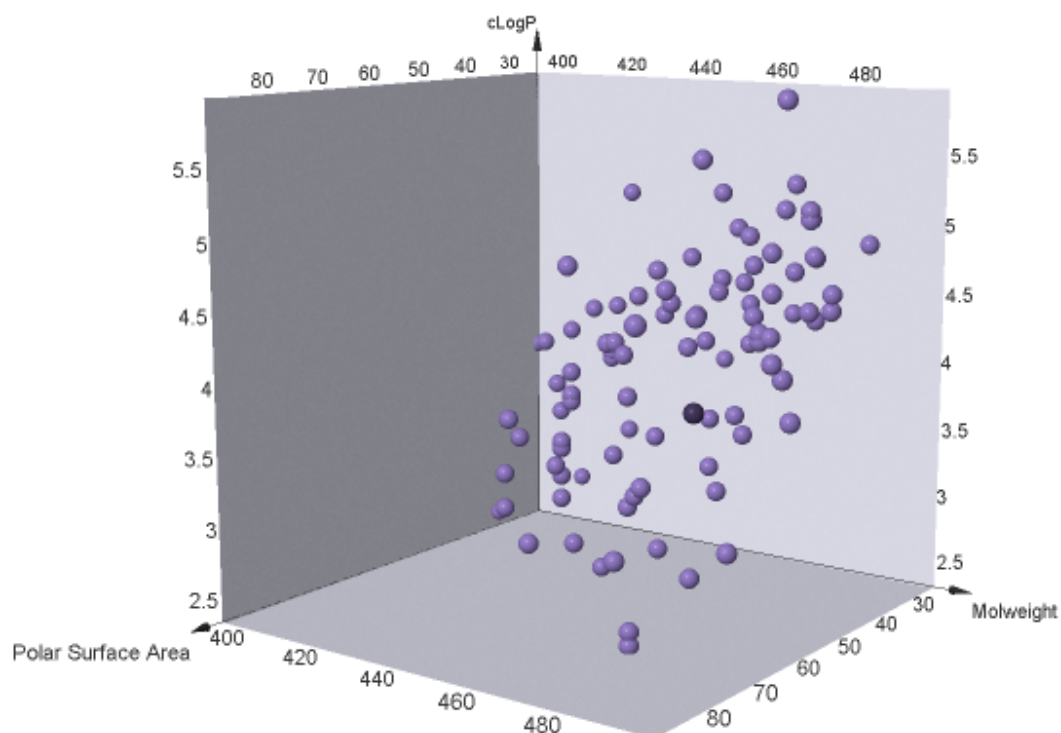


Figure 3.21. The members of the 4,6-fused scaffold library were plotted in three-dimensional space comparing their molecular weight, calculated logP and polar surface area values, the compounds have been designed to be inherently drug-like in terms of their molecular properties and are spread over a wide range of chemical space.

Additionally, principal component analysis (PCA) was carried out on the final library to gain an insight into the level of diversity within the library itself since diversity is a property based upon the relative similarity of compounds in each set rather than an absolute value.²¹⁷ The decorated 4,6-fused structures within this set occupy a relatively varied area of chemical space (Figure 3.22).

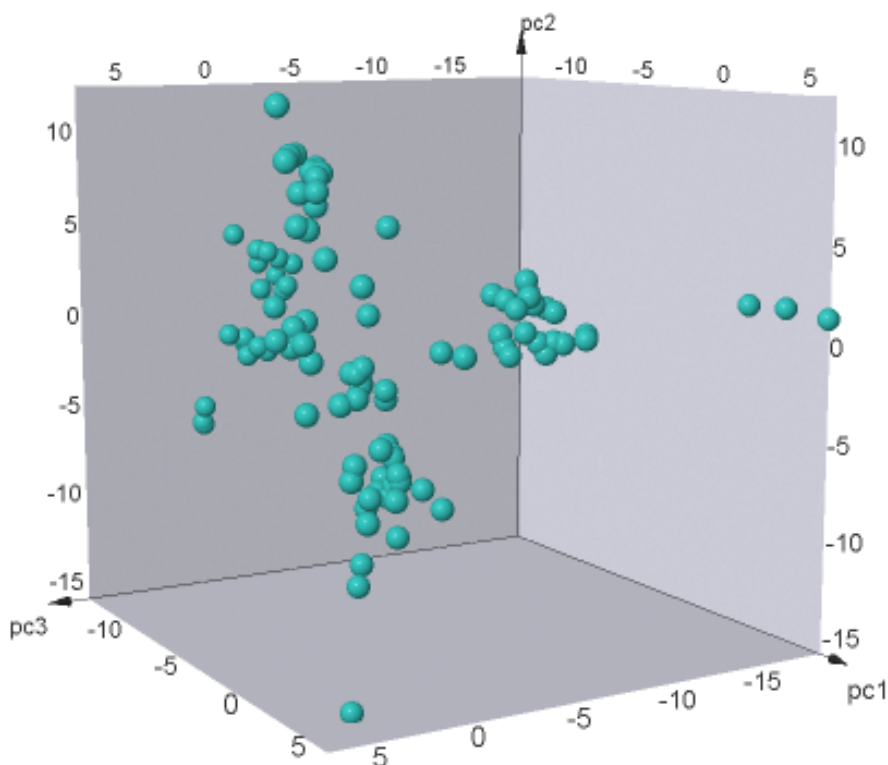


Figure 3.22. Principal component analysis was used to visualise the compound diversity within the library set. The “SkeletonSphere” molecular descriptor was calculated for each compound which was subsequently plotted on a three-dimensional plot. The final library set populates a diverse area of chemical space and displays a large degree of structural diversity.

Finally, PCA was carried out with the collected library and a collection of pharmaceutical agents which are currently available, to examine the diversity of this set compared to compounds which possess similar molecular properties. The ChEMBL database was filtered using the same parameters used during the enumeration of virtual libraries ($MW \leq 500$ Da, $HBD \leq 10$, $HBD \leq 5$ and $LogP \leq 5$), to create a set of 569 compounds which have been approved by the Food and Drug Administration (FDA).²¹⁸ Using DataWarrior, the SkeletonSphere molecular descriptor was applied to both the 4,6 library and the ChEMBL-derived set which was then used to create a three-dimensional plot (**Figure 3.23**). The 4,6-

decorated scaffold (red spheres) occupy a completely different area of chemical space when compared with the ChEMBL drug compounds despite having similar molecular properties.

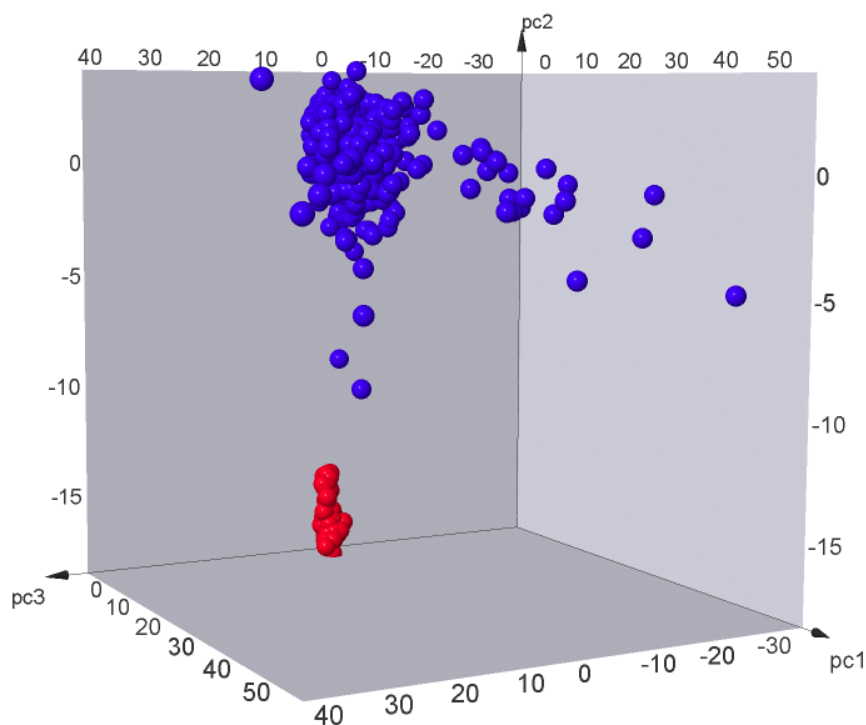
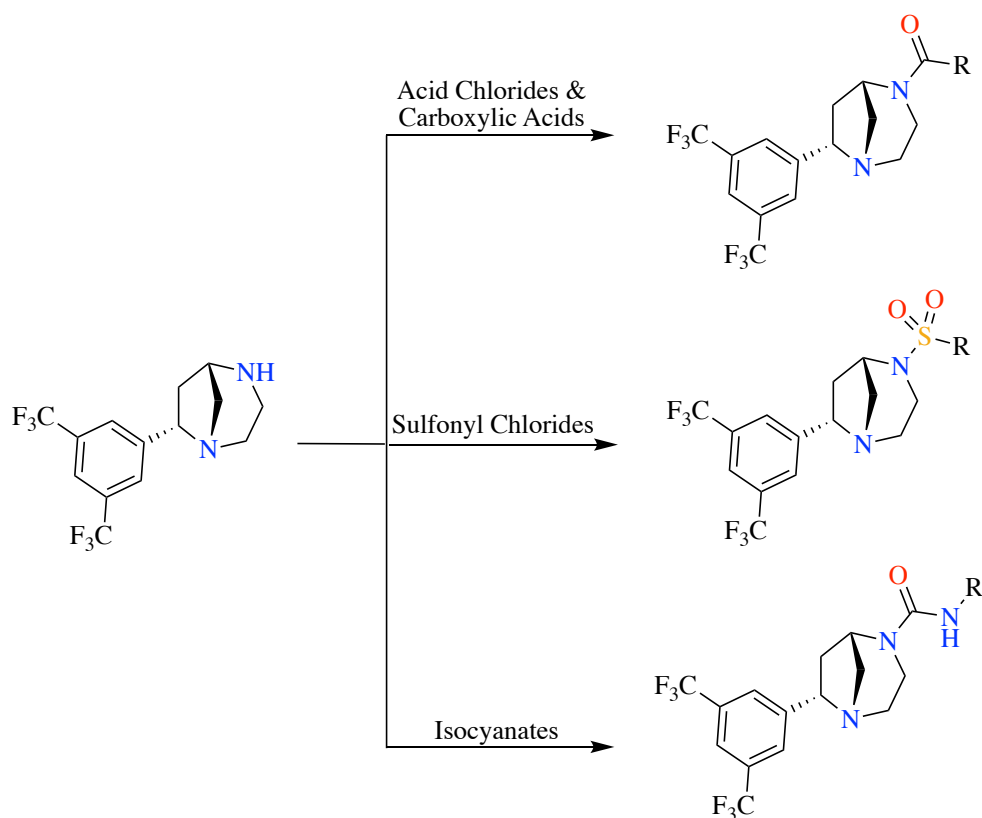


Figure 3.23. The 4,6-scaffold library (red spheres) underwent PC analysis and was plotted in space with a selection of marketed pharmaceutical compounds (blue spheres) with similar associated molecular properties. The novel 4,6-library compounds occupy a different area of chemical space compared to currently marketed drugs fulfilling the aims of this project.

3.3.5. 5,6-Bridged Scaffold: KNIME Pathway

Owing to the fortuitous discovery of the alternative 5,6-bicyclic scaffold, it was decided to synthesise a library to cover a greater area of chemical space and to study the difference in library compounds between both scaffolds. Acid chlorides/carboxylic acids, sulfonyl chlorides and isocyanates were chosen to decorate the 5,6-bridged scaffold (**Scheme 3.7**).



Scheme 3.7. A schematic demonstrating the decoration of the 5,6-bridged scaffold with acid chlorides, carboxylic acids, isocyanates and sulfonyl chlorides to create a diverse compound library

The workflow developed for the enumeration of the 4,6-scaffold was again employed for the decoration of the 5,6-pyrrolidine derived scaffold. To alleviate the issues caused in the previous library synthesis, SD files were created of all the acid chlorides, sulfonyl chlorides, isocyanates, and carboxylic acids available at that time, and were uploaded to an “SDF reader” node. The contents of the SD files were converted to their corresponding canonical SMILES strings to allow them to be processed by RDKit nodes at a later point. The 5,6-scaffold was added to the workflow using an additional reader node. Using “MarvinSketch” to generate a reaction query which was then connected to an “RDKit Two Component Reaction” node along with the reactants and scaffold-containing nodes, the node was executed to generate a collection of 286 compounds.

The logP values and additional molecular properties of the virtual library were calculated using the “XLogP” and "Molecular Properties” nodes, both developed by CDK.²⁰⁹ Again, the Lipinski guidelines were used to form the parameters used to refine the collection, reducing the number of compounds in the collection to 139.

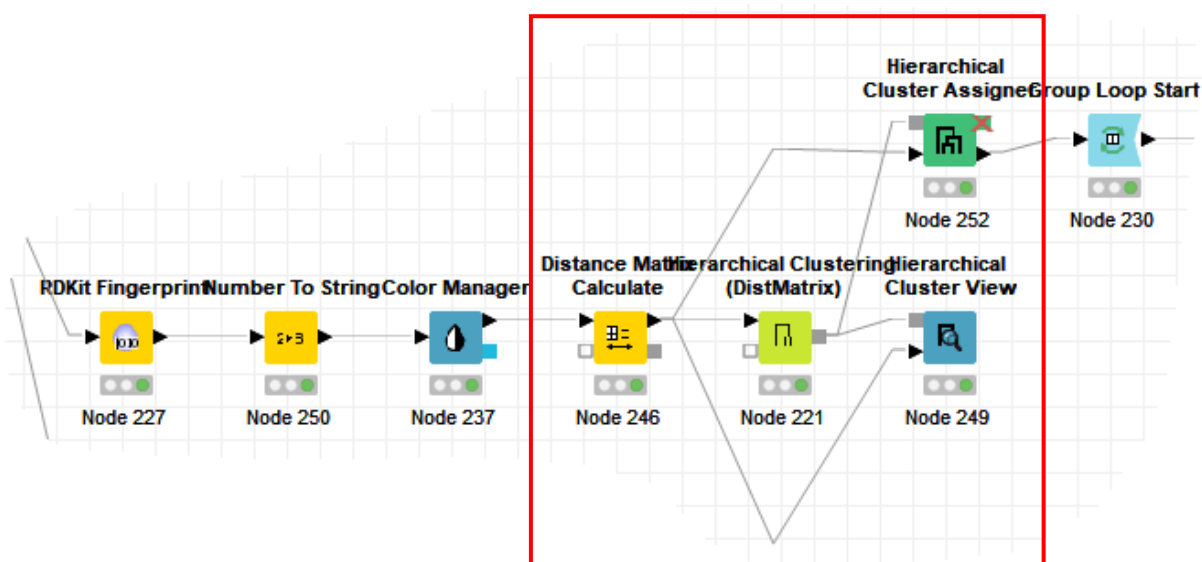


Figure 3.24. The virtual compound set was then clustered together using an agglomerative method of hierarchical clustering method. Ten cluster groups were created and linearly sampled to create a virtual library of 120 compounds displaying a high degree of diversity.

A molecular fingerprint was generated for each remaining virtual compound, using the Morgan fingerprint,²¹¹ allowing for rapid similarity comparisons to be carried out during the clustering step. The compound collection was then clustered using a hierarchical, agglomerative clustering which generated a ten cluster groups, which was each sampled in a linear fashion (**Figure 3.24**). After clustering, 120 virtual compounds were selected and were prepared for visualisation. The geometry of each molecule was optimised and energy in terms of kcal/mol calculated. The energy calculation was based on a particular force field, MMFF94 which was

developed by Merck.²¹⁶ The PMI-derived properties for each molecule were then calculated and the compound collection was then visualised on a triangular PMI scatter plot.

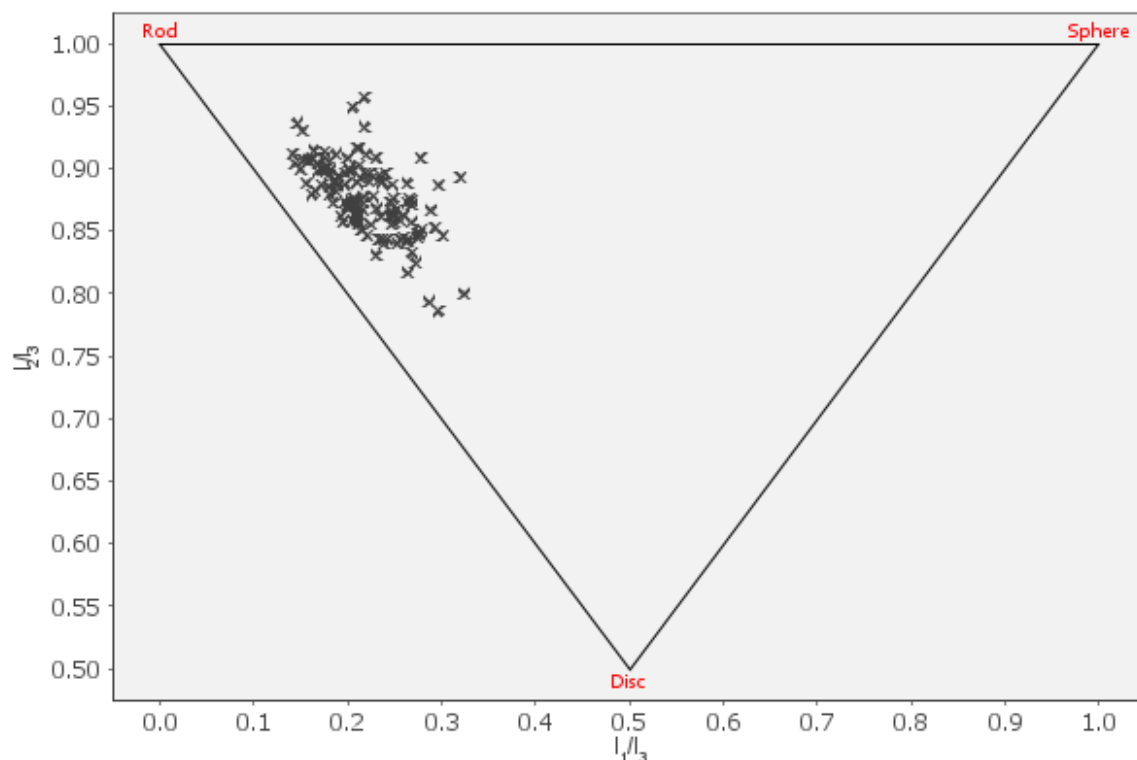
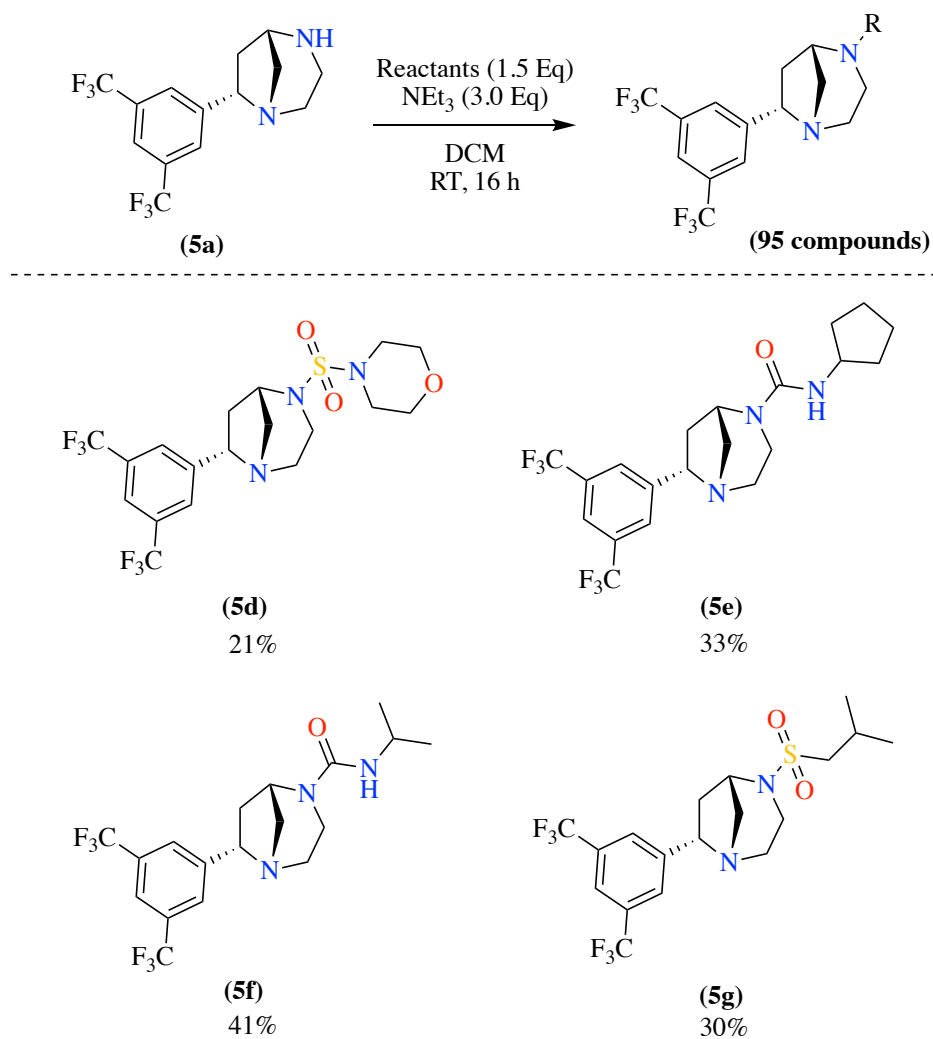


Figure 3.25. The enumerated 5,6-fused scaffold library was visualised with a PMI plot, the library selection does not sit directly on the rod-disk axis and had moved towards the centre of the plot indicating that library members possess a high degree of both three-dimensionality and structural diversity.

The three-dimensionality of the library compounds is evident when the compounds are plotted on a PMI plot (**Figure 3.25**). The library set has moved towards the centre of scatter plot away from the rod-disk axis. This increased dimensionality makes the novel compounds included in this library set notably different from the majority of pharmaceutical drugs currently available, the bulk of which predominately sit along the rod-disk axis when plotted in terms of their respective PMI-properties.¹⁰⁸

3.3.6. 5,6-Bridged Scaffold: Library Synthesis

A series of validation reactions were performed in preparation for library synthesis, a solution of scaffold (**5a**) was prepared in DCM (30 mg/mL) and portioned between four reaction vessels, which contained the corresponding reactant and three equivalents of triethylamine. The reaction mixtures were stirred at room temperature and conversion to the desired products was monitored using LCMS and UPLC. The reactions proceeded well with the desired product being the major component in each reaction after 16 hours. The reaction solvent was removed using a centrifugal evaporator and the samples were prepared for purification with HPLC and were collected in good yields with a purity of greater than 95% (**Scheme 3.8**).



Scheme 3.8. A small scale validation reaction was conducted to establish suitable reaction conditions for the decoration of the 5,6-bridged scaffold (SC-6- CF_3 -NH).

Following the successful synthesis and isolation of the decorated compounds at the validation stage, scaffold **(5a)** was prepared as discussed in Chapter Two. The library preparation procedure was divided into two sets depending on the reactants. Set One refers to reactions with acid chlorides, sulfonyl chlorides and isocyanates and Set Two refers to amide bond formation with carboxylic acids. Set One required the reaction of a collection of 50 acid chlorides, isocyanates, and sulfonyl chlorides with the 5,6-bicyclic scaffold, these reactants were measured and added to labelled vials followed by a solution of the scaffold **(5a)** in DCM.

Set Two involved the reaction of 24 carboxylic acids with 5,6-bicyclic scaffold via an amidation reaction. The reactions were sealed and agitated at room temperature overnight using an orbital shaker. Reaction progress was monitored with UPLC on 96 well plates, after 16 hours any reactions not showing the desired product by UPLC was discarded and the remaining reactions were prepared for purification through removal of the reaction solvent and resuspension of the remaining solid or oil in DMF prior to purification with preparative HPLC.

3.3.7. 5,6-Bridged Scaffold: Summary of Synthetic Results

Following purification, the samples were collected, reformatted from DMF, and analysed, in total 79 compounds were isolated in moderate yields, between 20-45% with a high level of purity (>90%). Using DataWarrior, the library of decorated scaffolds was plotted on a three-dimensional plot comparing the molecular weight, polar surface area and calculated LogP values of the set. Owing to the enumeration process, the synthesised compounds all fall within “lead-like space” but are relatively well spread throughout this area of chemical space (**Figure 3.26**).

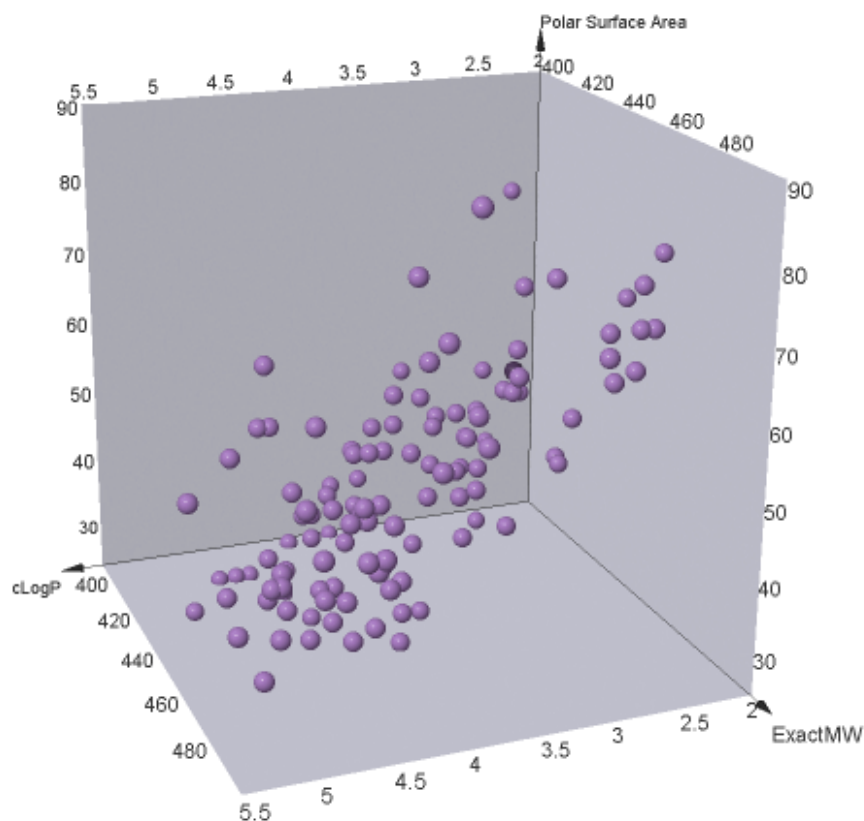


***Figure 3.26.** The members of the 5,6-bridged scaffold library were plotted in three-dimensional space comparing their molecular weight, calculated logP and polar surface area values, the compounds are well spread through chemical space and are inherently drug-like.*

In order to facilitate PCA of the final library set, the molecular descriptor “SkeletonSphere” was calculated to examine the diversity within the library. As can be seen in (**Figure 3.27**), the library members are well distributed throughout the relative area of chemical space that is populated.

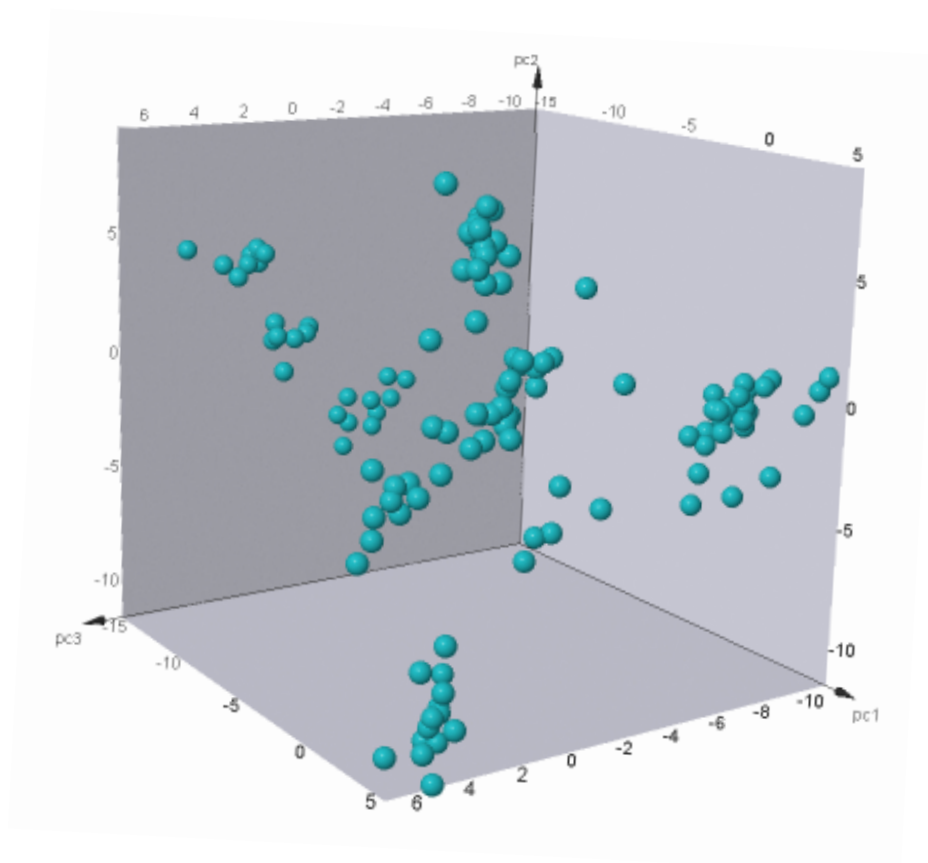


***Figure 27.** In order to visualise the level of diversity within the set a PC study was conducted, the “SkeletonSphere” molecular descriptor was calculated for each member of the compound library which were then plotted in space relative to eachother. The compound collection displays a wide range of structural diversity and populates a range of chemical space.*

As with the 4,6-library, the 5,6-decorated scaffolds also underwent an additional PCA study with the filtered set of pharmaceutical compounds downloaded from the ChEMBL database, 596 compounds in total. The marketed pharmaceuticals (blue spheres) occupy a distinct area of chemical space when compared to the novel 5,6-bridged final compounds (pink spheres), proving that this library set presents an opportunity for under-explored areas of chemical space to be reached (**Figure 3.28**).

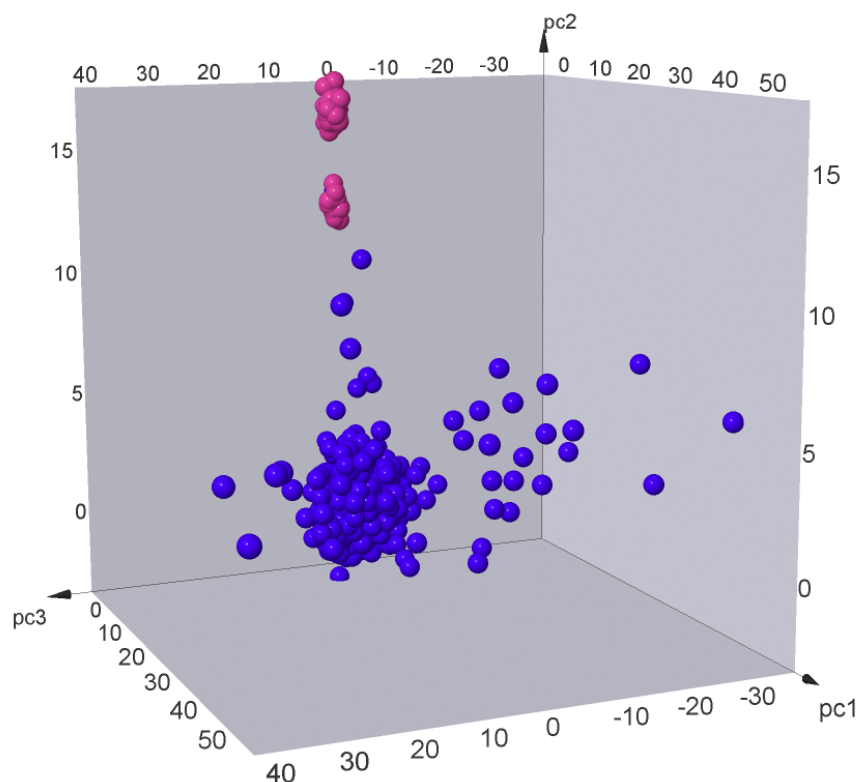


Figure 3.28. The 5,6-bridged scaffold library (pink spheres) underwent PC analysis and was plotted in space with a selection of marketed pharmaceutical compounds (blue spheres), the novel 5,6-bridged library compounds occupy a different area of chemical space to the marketed drug compounds.

3.4. Biological Evaluation of Library Compounds

3.4.1. hERG inhibition

Following the identification of lead compounds, they must then be evaluated using their drug-likeness parameters and cardiotoxicity. Cardiotoxicity and an interference with normal cardiac physiology is commonly cited as a reason for withdrawing many lead compounds from both early- and late-stage clinical trials.²¹⁹ Cardiotoxicity is commonly associated with hERG (human ether-à-go-go related gene) potassium (K^+) ion channel, which occurs in cardiac myocytes, a cell type found in the heart.²²⁰ The hERG ion channel is responsible for shaping

the rapidly activating component of the cardiac delayed rectifier potassium current (I_{Kr}), which plays a crucial role in the repolarisation of the cardiac action potential (**Figure 3.29**).²²¹

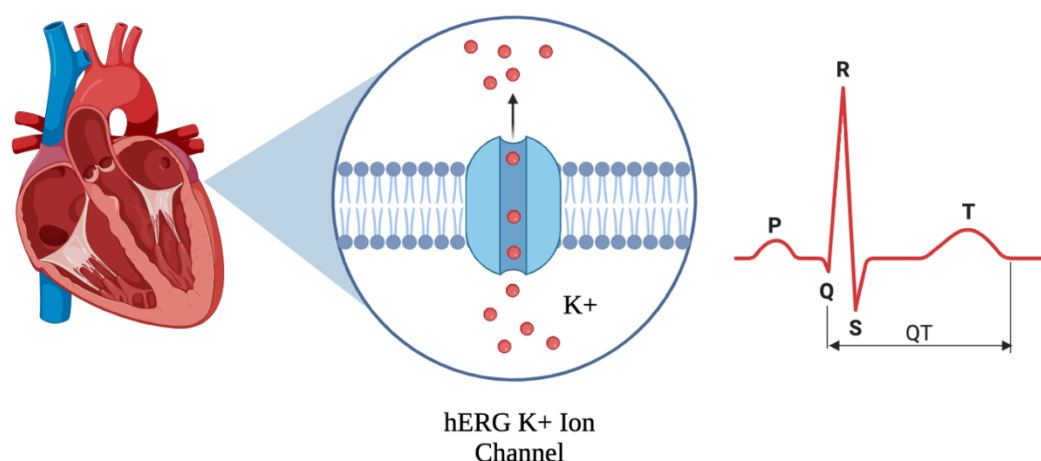


Figure 3.29. Cardiotoxicity is commonly cited as a reason for withdrawing lead compounds from early-stage clinical trials.

The hERG ion channel is responsible for shaping the rapidly activating component of the cardiac delayed rectifier potassium current (I_{Kr}), which plays a crucial role in the repolarisation of the cardiac action potential. Dysfunction of the potassium ion channel may cause a delayed repolarisation of the cardiac action potential, resulting in a prolonged QT interval. Created using BioRender.com.²²²

Dysfunction of K^+ ion channel can result in long QT syndrome (LQTS) or cardiac arrhythmia, which is caused by a delayed repolarisation of the cardiac action potential, resulting in an elongated QT interval.^{223, 224} The QT interval is a measure of time between the Q wave and the T wave of the heart's inherent electrical cycle, as measured on an electrocardiogram (ECG).²²⁵ Prolongation of the QT interval is associated with Torsades de Pointes (TdP), which can lead to sudden cardiac death through the development of an abnormal heart rhythm.²²⁶ Inhibition of the hERG ion channel and subsequent induction of LQTS is commonly attributed to drug interaction and occurs through several mechanisms. Interaction of a drug with a structurally unique receptor domain within the ion channel results in reduced permeation of potassium

through the channel causing a total block of hERG channel or an interference with the associated I_{K_r} current.²²⁷ Drug interaction can also cause reduction in the I_{K_r} through disorganisation of cell trafficking to the cell surface, causing fewer mature K^+ ion channels to be present on the cell surface.²²⁸

The importance of early measurement of hERG-related toxicity is driven by the inherent promiscuity of the protein.²²⁹ The channel can bind to a diverse range of compounds, with the majority of drug-like molecules displaying some degree of hERG inhibition,²³⁰ for example antibiotics,²³¹ anti-fungals,²³² anti-cancer agents,²³³ anti-psychotics,²³⁴ and anti-arrhythmic drugs,²³⁵ all of which have been shown to strongly block or induce disordered membrane trafficking of hERG ion channels. Several models for the *in silico* prediction of hERG toxicity have been developed to assist in compound selection during early-stage drug discovery,²³⁶ and a number of physiochemical properties have been linked to possible hERG inhibition, namely lipophilicity, the number of basic nitrogen atoms and number of rotatable bonds present within a given compound.^{237, 238} Generally, compounds with a high logP value, basic nitrogen atoms and a low level of structural rigidity are more likely to induce inhibition of the hERG channel.²³⁷

Seven compounds from the final 4,6-fused and 5,6-bridged library collection (**Figure 3.30**) were selected and evaluated in terms of their hERG inhibition using an *in vitro* patch-clamp assay. The patch-clamp technique is commonly used to study ionic currents in living cells or patches of the cell membrane.²³⁹ Testing was performed on the IonWorks Quattro automated patch-clamp at ambient room temperature. Compounds were tested at a single test concentration of 30 μ M with an incubation time of approximately three minutes. Individual data points are plotted as black circles and mean inhibition as a red bar. In this assay, <30%

inhibition was considered inactive and >50% inhibition was considered active and may be biologically significant.

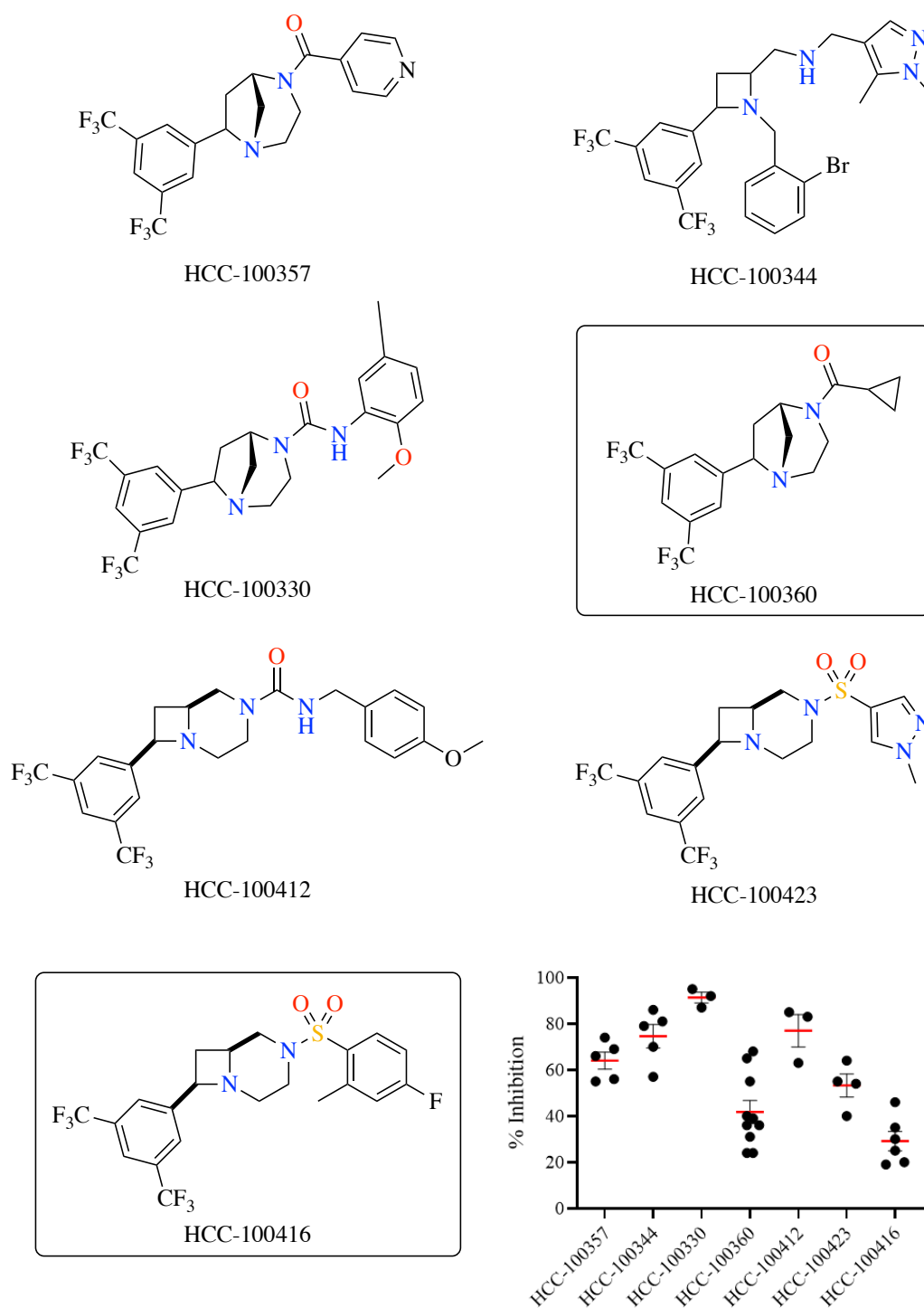


Figure 3.30. Seven compounds from the final compound libraries were submitted for preliminary hERG ion channel inhibition screening, the majority of compounds showed relatively high inhibition rates of >50% which may be biologically significant in terms of cardiotoxicity. Two compounds, HCC-100360 and HCC-100416, displayed inhibition rates of less than 50%.

Compounds HCC-100360 and HCC-100416 appear to have the lowest mean % hERG inhibition values of the data set, at 39% and 30% respectively. From this it can be assumed that these compounds do not inhibit the hERG ion channel to a biologically significant level. Compound HCC-100423 has a % inhibition value of 53% and may show a biologically significant level of inhibition in terms of cardiotoxicity. The remaining compounds in the data set all display a % inhibition of greater than 60%, which may be of biological significance in terms of ion channel inhibition. Although there is a greater chance of compounds which display a high % inhibition in initial screening assays inducing undesirable outcomes regarding cardiotoxicity, this is ultimately determined by the final therapeutic dose. This patch clamp assay was carried out at a concentration of 30 μ M, which would be considered a high concentration with regards to pharmaceutical compounds which allows for detailed data to be collated and considered in terms of safety when considering the primary efficacy towards the target molecule. hERG activity at a concentration of less than 10 μ M is generally acceptable, ideally compounds would have an IC₅₀ (half-maximal inhibitory concentration) value for drug activation between 30- to 100-fold lower than the IC₅₀ value calculated for hERG activation.

3.4.2. Anti-Tuberculosis Activity

A series of compounds were also used in early-stage biological testing to screen their cytotoxic activity towards *M. tuberculosis* using *A. baumannii*, *M. smegmatis* and *M. bovis* BCG (bacillus Calmette-Guérin) as representative analogues in an endpoint resazurin assay. The resazurin assay offers a simple, rapid, and sensitive measure for the viability of mammalian and bacterial cells.²⁴⁰ Living cells are metabolically active and reduce the non-fluorescent dye resazurin to

the strongly fluorescent product resorufin using mitochondrial reductase enzymes (**Figure 3.31**).²⁴¹ Samples are exposed to ultraviolet light ($\lambda = 560$ nm) and the fluorescence output recorded; this output is directly proportional to the number of viable cells in a given sample over a wide range of concentrations.²⁴²

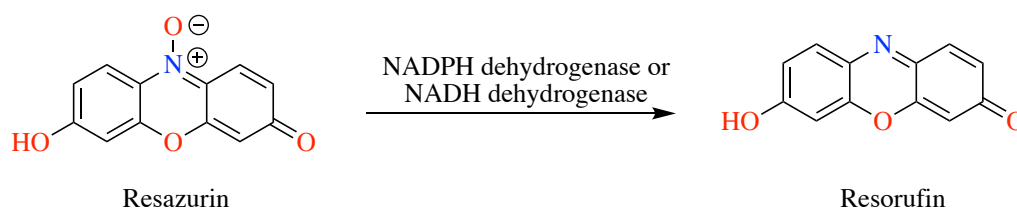


Figure 3.31. The resazurin assay is used to measure the viability of bacteria, living cells are metabolically active and reduce the non-fluorescent resazurin dye to the highly fluorescent resorufin product in an NADPH dependent reduction process.

Alongside the resazurin assay, optical density (OD) measurements were used to determine cell growth.²⁴³ *Staphylococcus aureus*, *pseudomonas aeruginosa* and *klebsiella pneumoniae* were grown in liquid broth, using OD measurements with 600 nm light an appropriate concentration of live cells (OD₆₀₀ = 0.05) and were incubated with the novel library compounds at 37 °C overnight. The % inhibition of cell growth was then measured against a positive control, namely rifampicin or kanamycin to determine the effect of the novel compounds on cellular metabolism, this was extrapolated from OD₆₀₀ absorption measurements.

Using the CDD Vault software,^{244, 245} the results of both the resazurin assays and OD₆₀₀ measurements were correlated. A combined total of 105 compounds were tested from the 4,6 and 5,6-bicyclic compound libraries and we plotted against the % inhibition of bacterial growth in both the resazurin assay and using the OD₆₀₀ measurements (**Figure 3.32**). The resultant scatter plot was then filtered, removing data points which related to negative inhibition values,

giving a collection of 42 bicyclic compounds which displayed inhibition of bacterial growth in both the resazurin assay and through optical density measurements.

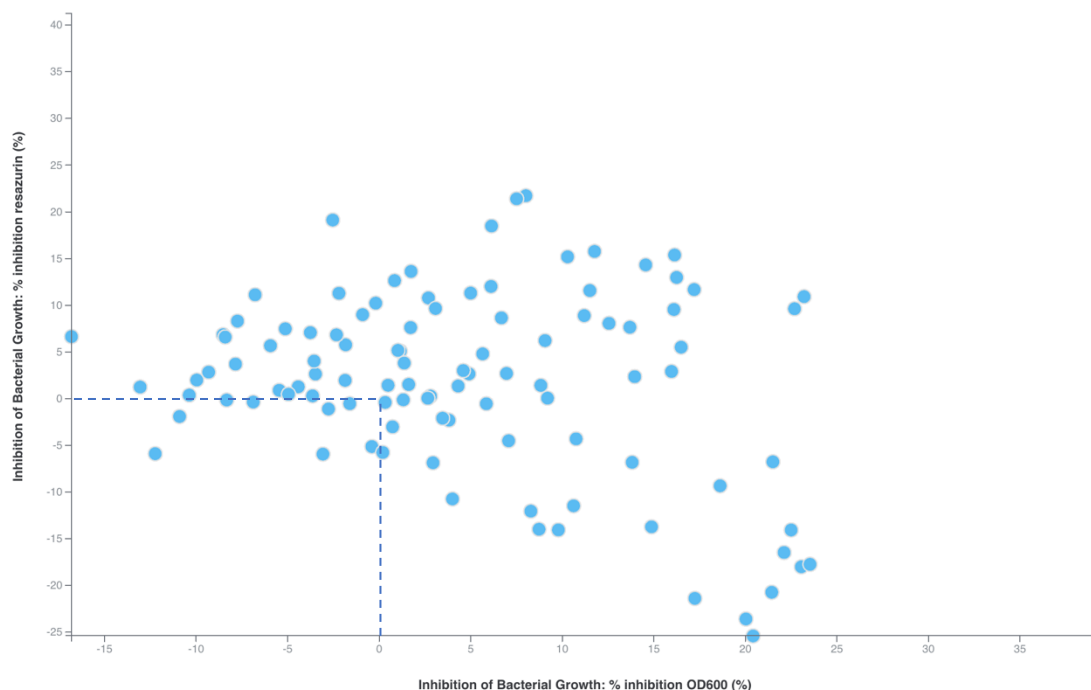


Figure 3.32. 105 compounds from the 4,6-fused and 5,6-bridged scaffold sets were submitted for biological testing to investigate their ability to inhibit bacterial growth.

As seen in **Figure 3.33**, the remaining compounds show a % inhibition value of 24% or less, however, 26 compounds display a % inhibition of 10% or greater in both the OD600 measurements and the resazurin assay suggesting that these compounds may possess some biological significance in terms of bacterial cytotoxicity and should be further investigated to established IC_{50} and minimum inhibitory concentration (MIC) values.

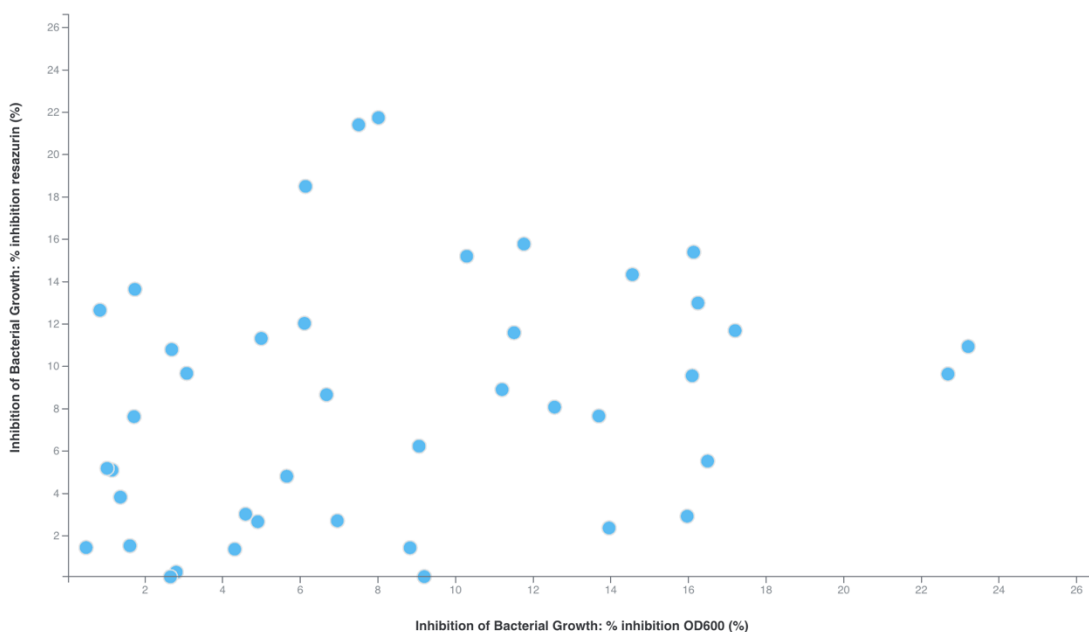


Figure 3.33. 42 of the 105 compounds tested displayed inhibition in both the resazurin assay and the OD600 bacterial growth measurement, the inhibition of bacterial growth suggests that these compounds are potential leads and should be submitted for further biological studies.

In addition to bicyclic library compounds, several azetidine-containing compounds, produced throughout the duration of the project, were also tested using OD600 and resazurin assays. These compounds performed well in both assays, most notably HCC-100333 and HCC-100344, both of which displayed considerable inhibition. HCC-100333 showed a 41% inhibition of growth in the resazurin assay along with 21% inhibition based on OD600 measurements (**Figure 3.34**). In the resazurin endpoint assay, HCC-100344 inhibited 38% of bacterial, it performed equally well in the OD600 tests, inhibiting bacterial growth by 39%. These results suggest that both compounds should be submitted for further study to establish IC_{50} and MIC_{99} values to establish their viability as targets towards anti-tuberculosis activity.

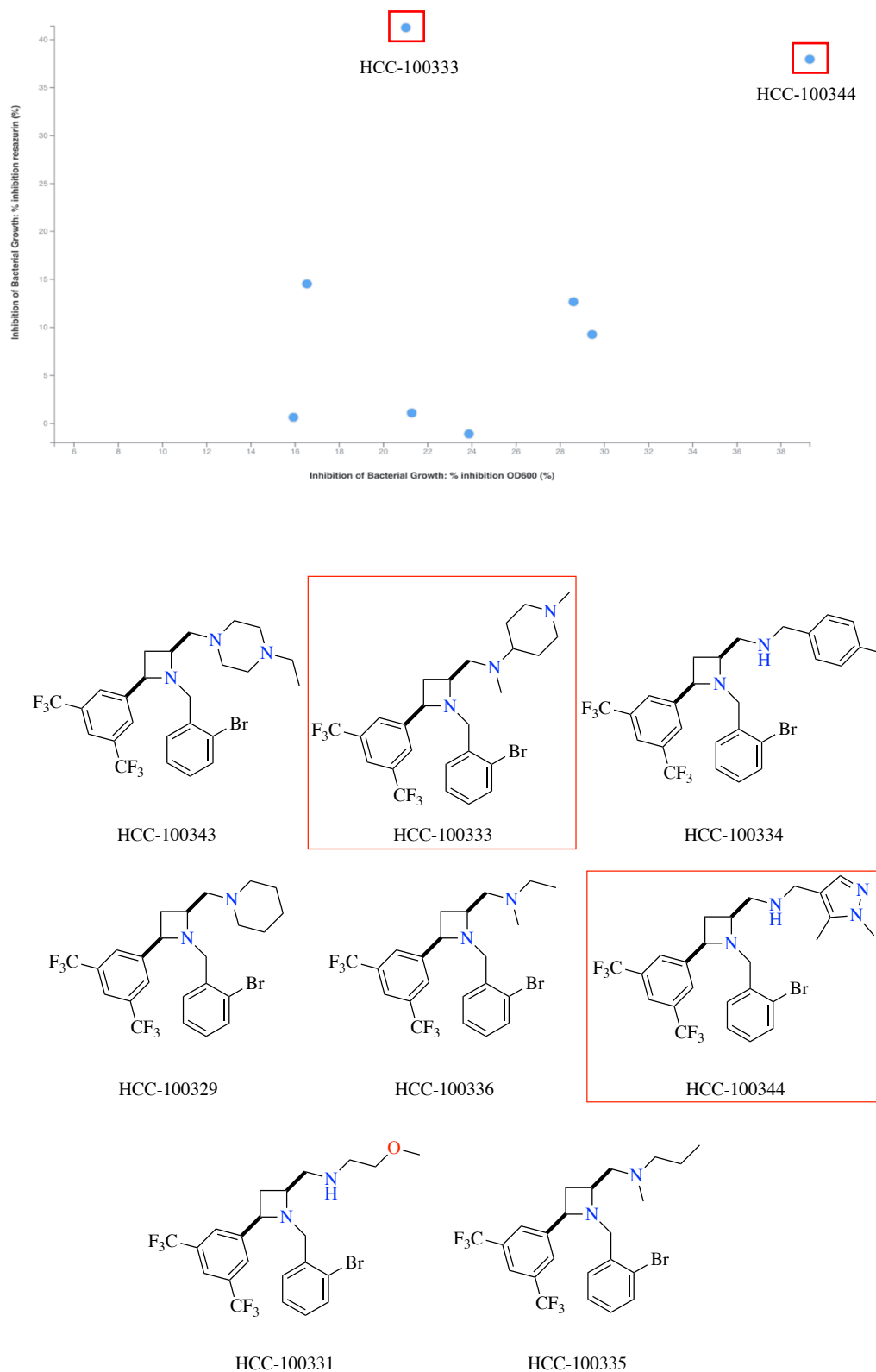


Figure 3.34. A series of amino-azetidines were submitted for preliminary biological testing to investigate their ability to inhibit bacterial growth. Seven compounds displayed inhibition in both the resazurin assay as well as the OD600 bacterial growth measurements with two compounds, HCC-100333 and HCC-100344, displaying particularly high inhibition in both assays. These compounds should be submitted for more detailed biological testing and optimisation studies.

3.5 Summary of Results

A series of compound libraries were designed, with the aid of computational software, and were subsequently synthesised in a parallel fashion. KNIME was used to create workflows informing the final compound selection, SD files containing the undecorated scaffolds and all the possible reactants were introduced to the workflow. In silico reactions were then performed to virtually create large groups of compounds which were then filtered according to a series of pre-defined parameters. The Ro5 guidelines previously determined by Lipinski were used to reduce the number of compounds in the set by removing compounds with a molecular weight of greater than 500 Da, with a cLogP greater than 5, and more than 10 HBD and more than 5 HBA. The resultant set of compounds was then clustered using a hierarchical agglomerative clustering methodology, allowing for the creation of a set of compounds which explores the widest area of chemical space possible. The clustered set was sampled to create a representative set which was then pushed forward for physical library synthesis.

Novel scaffolds were prepared on a multigram scale and reagents were added so as to facilitate library generation in a parallel fashion. Library reactions were monitored using UPLC and were subsequently purified using preparative HPLC resulting in over 100 novel compounds being synthesised. The final library compounds were visualised and compared to pharmaceutical compounds with similar molecular properties which are currently being marketed and were visualised alongside these FDA approved compounds using principal component analysis. This visual analysis shows that the novel compound collections synthesised occupy a different area of chemical space than marketed drugs currently available, successfully fulfilling the overarching aim of this project.

A selection of compounds was evaluated through early-stage biological testing, a hERG inhibition assay was used to identify potential issues with cardiotoxicity. Resazurin assays and OD600 measurements were used to evaluate the effectiveness of these compounds at inhibiting bacterial growth. These assays identified several compounds which may be of biological significance in terms of bacterial cytotoxicity and should be submitted for additional studies.

Chapter 4: Conclusion and Future Work

4.1. Conclusion

Over the course of this project, an innovative method for the design, computational assessment, and selection of novel compounds to populate underexplored and underutilised areas of chemical space has been developed and subsequently utilised to create libraries of novel bicyclic, heterocycle-containing compounds with a high degree of three dimensionality and drug-like properties (**Figure 4.1**).

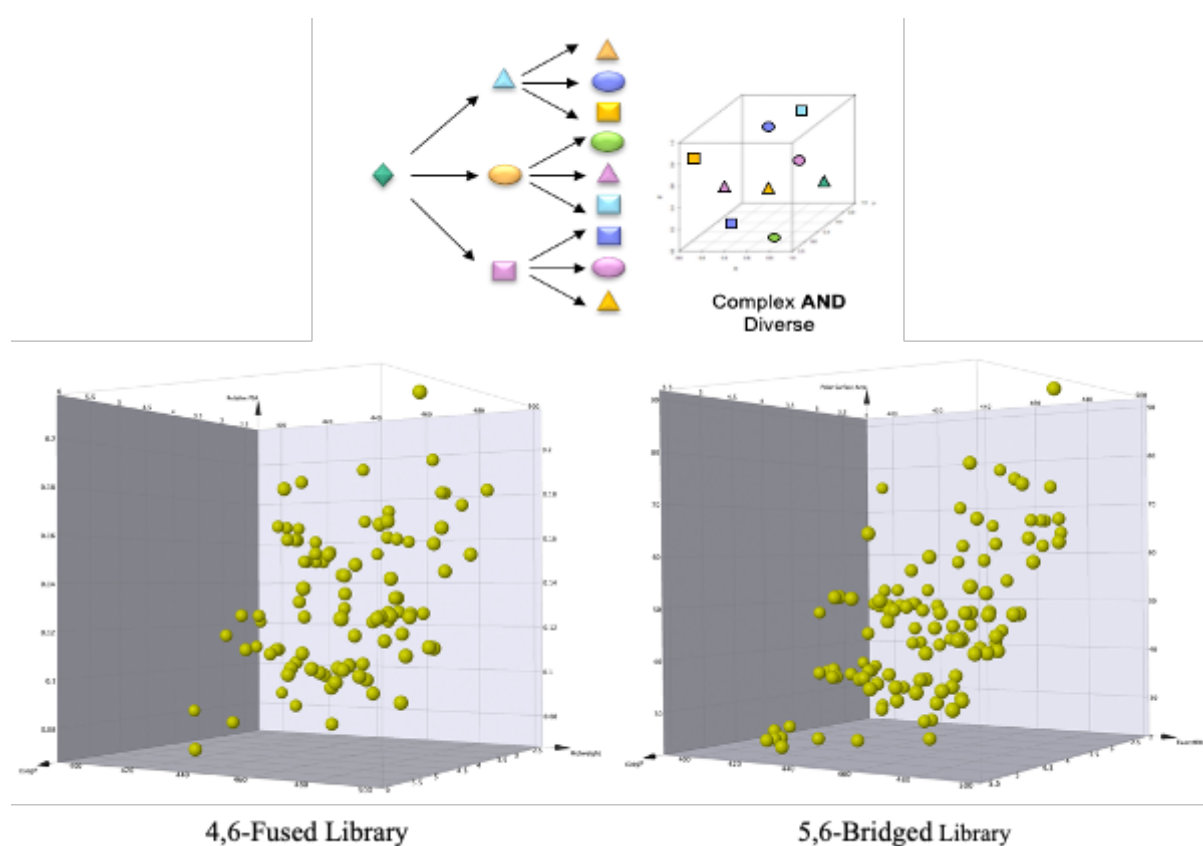


Figure 4.1. Two novel scaffold moieties, the 4,6-fused and the 5,6-bridged scaffold, have been synthesised and have been decorated to create two diverse compound libraries which are structurally complex and stereochemically diverse to populate underexplored areas of chemical space. The novel compound libraries have been designed to be inherently drug-like with a high degree of three-dimensionality.

Previous work carried out within the JSF group, centred around the development of a robust methodology for the creation of diastereoselective, 2,4-*cis*-azetidines, primarily with a benzylic group decorating the 1-position. The work carried out within in this project allowed for the scope of this work to be expanded further, enabling alkyl alcohol chains to be incorporated in place of the benzylic group, allowing for new chemistries to be explored at this position. Amino azetidines were prepared on a multigram scale in a high yield, while maintaining the previously observed diastereoselectivity.

An overarching aim of this project was to utilise the previously developed method for *cis*-azetidine synthesis for the development of a synthetic pathway towards novel, heterocycle-containing scaffolds with a bicyclic core. Several possible routes and synthetic methodologies were trialled as a means to achieving this aim. Reactions such as Buchwald-Hartwig C-N aminations and metathesis, which are classically favoured in industrial settings due to their robustness and high functional group tolerance were initially proposed as potential routes towards three-dimensional scaffolds. However, these methods proven to be significantly affected by steric and electronic effects making them unsuitable for scaffold development. The introduction of an alkyl alcohol chain on the 1-position of the azetidine ring allowed new chemistry to be employed at this position, Fukuyama-Mitsunobu reactions and Appel-type chemistry provided the key elements for cyclisation to occur in a concerted manner. This discovery allowed the generation of a novel 4,6-fused scaffold core in four steps, with the serendipitous discovery of the corresponding 5,6-bridged scaffold, formed from the five-membered iodo-pyrrolidine (**Figure 4.2**). These compounds were produced on a multigram scale and were easily purified using normal phase flash chromatography. Both compounds have a point of diversification and there is also potential for the groups on the aromatic ring to be varied to allow for the creation of additional scaffolds. Both the 4,6-fused (4b) and the 5,6-

bridged scaffold (5a) allow a wide range of chemical space to be accessed but the 5,6-bridged example is thought to be the most promising from a drug discovery perspective as it has a more three-dimensional configuration than the azetidine-derived alternative.

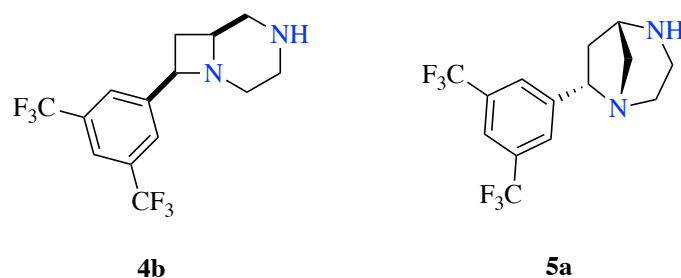


Figure 4.2. Two novel, bicyclic, N-heterocycle-containing scaffolds were synthesised for the creation of diverse compound libraries. The 4,6-fused scaffold (4b) was derived from a 2,4-azetidine ring system and the 5,6-bridged system (5a) was derived from a 2,4-pyrrolidine ring.

Following the successful synthesis of these novel scaffolds, open-source data analytics software was employed for the evaluation and enumeration of potential library compounds. KNIME was used to carry out *in silico* reactions between simple building blocks to create a virtual representation of the bicyclic 4,6-fused and 5,6-bridged scaffolds which were then computationally decorated with suitable reagents. This resulted in large sets of virtual compounds, which were then filtered based on a predetermined set of parameters in order to create smaller compound sets which possess drug-like properties in terms of molecular weight, hydrogen bond donors and acceptors and LogP value. The remaining compounds were then clustered, using a hierarchical, agglomerative clustering method, to sort compounds into groups based on their distances from each other in space. These cluster groups were sampled so as to simultaneously reduce the size of the compound library, while also ensuring that a wide range of chemical space is being covered by the representative set.

Compound libraries were synthesised to industry standard in a parallel fashion, these libraries were composed of 34 amino azetidines, 79 decorated 4,6-scaffolds and 95 decorated 5,6-scaffolds, resulting in a total of 208 novel compounds covering under exploited regions of chemical space. Although this figure may seem insignificant when compared to libraries which have been generated in a more combinatorial or high-throughput manner, which may contain upwards of 200,000 individual compounds, however, these libraries were not designed with the purpose of finding a hit towards a predefined target. Instead, the libraries designed and constructed within this project were created to be synthetically enabled, so as to allow for further elaboration, as required, in the future.

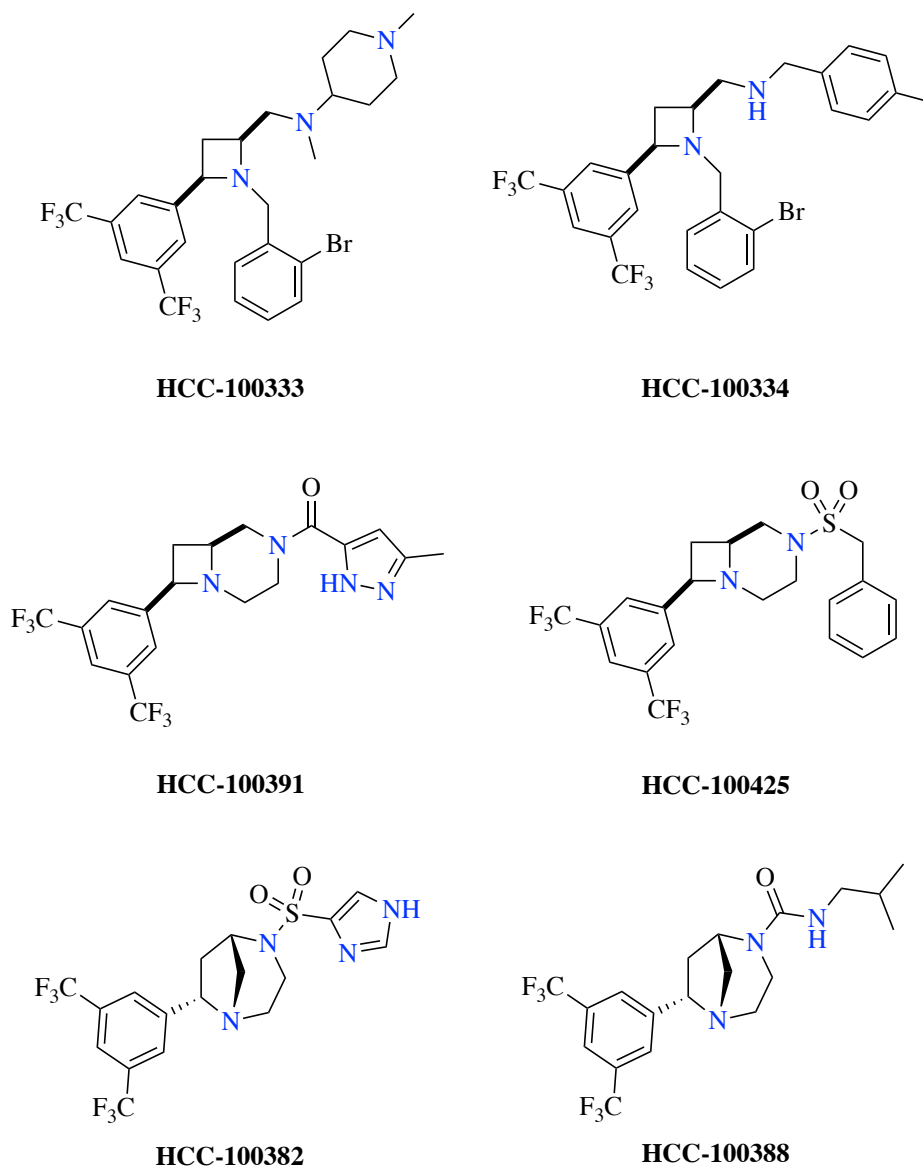


Figure 4.3. A selection of compounds which have been identified as good inhibitors of bacterial growth through early-stage biological screening from the amino-azetidine, 4,6-fused and 5,6-bridged library sets.

A selection of compounds from the final library sets were selected for early-stage biological testing to identify any potential lead compounds. Library compounds were used in phenotypic assays, namely the resazurin assay and OD₆₀₀ analysis, to determine their effectiveness with regards to the inhibition of bacterial growth, several compounds were identified as good inhibitors which warrants further, more detailed investigation (**Figure 4.3**). Both the IC₅₀ and MIC₉₉ values should be calculated, following on from these compounds can be tested in more

target-based assays, where the measured effect of the compound is directly dependant on a known target or biological pathway. Owing to these results further development of the library compounds may be necessary before progressing to more detailed toxicology and animal studies. Previous work within the JSF group has yielded decorated azetidines which possess anti-tuberculosis activity,²⁴⁶ preliminary studies on the compounds produced in this project yield similarly promising results. Several compounds have also been screened in primary screens against vancomycin-resistant bacteria, the results of these studies show favourable activity towards inhibition of gram-positive bacteria. Compounds generated as part of this project have been specifically designed to incorporate “drug-like” molecular properties, and thus are less lipophilic than previous hits which may allow for additional modes of action to be investigated.



Figure 4.4. A project increases in commercial value as it progresses through the drug discovery pipeline, this project has transversed early-stage drug discovery through the creation and decoration of the 4,6-fused and 5,6-bridged scaffold moieties. Libraries compounds have been submitted for biological testing and several possible hits have been identified and progressed for further testing and structural optimisation. Adapted from Sharma and co-workers.²⁴⁷

Commercial value is added to a project as lead compounds move along the drug discovery pipeline and progress from development to preclinical and clinical trials.²⁴⁸ With this in mind it can be said that the work conducted to develop bicyclic scaffold cores for drug discovery has increased in value throughout the course of this project (**Figure 4.4**). Through the synthesis and decoration of the isolated scaffolds a diverse collection of compounds has been generated to explore a wide range of under-utilised chemical space. These compounds have been subjected early-stage biological testing against tuberculosis models and vancomycin-resistant bacteria, both of which have shown promising preliminary results suggesting that the compounds synthesised as part of this work may continue to move along the drug discovery pipeline, subject to their success in later stage evaluation.

Previous work in the JSF group developed a methodology towards the iodine-mediated stereoselective synthesis of 2,4-*cis*-azetidine and 2,4-*cis*-pyrrolidine ring systems. Throughout this project, the scope of this work has been expanded to introduce a series of new substituents at the 1-position of the azetidine and pyrrolidine ring, allowing for new chemistry to be explored and subsequently exploited for the creation of novel, bicyclic, *N*-heterocyclic scaffold cores. The resultant scaffold cores were diversified through reaction with a series of building blocks in a DOS-orientated fashion to create novel compound libraries which display a high level of structural diversity and three-dimensionality (**Figure 4.5**). Additionally, compound libraries have been designed to possess inherently drug-like properties and have been submitted for early-stage biological screening to identify potential lead compounds.

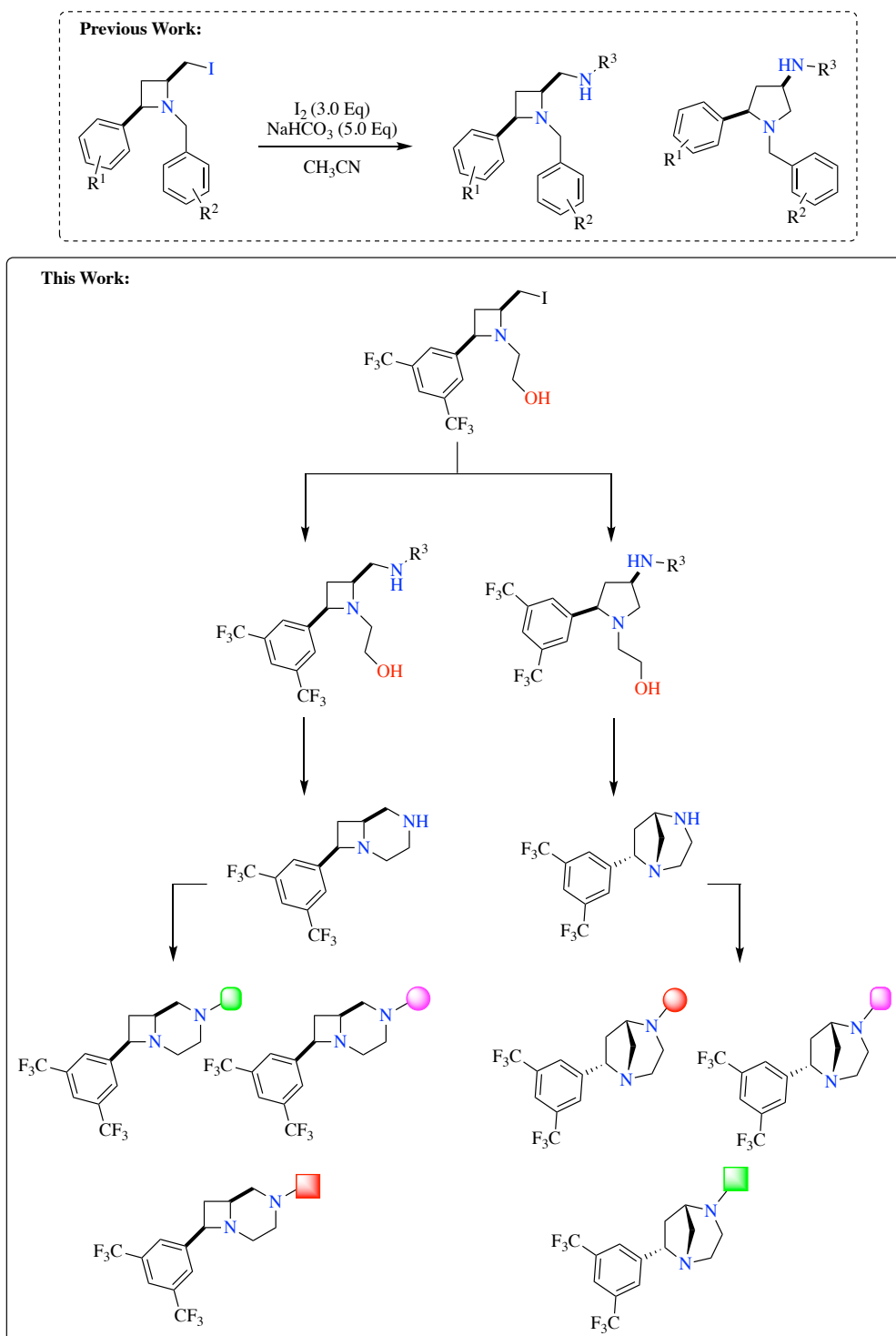


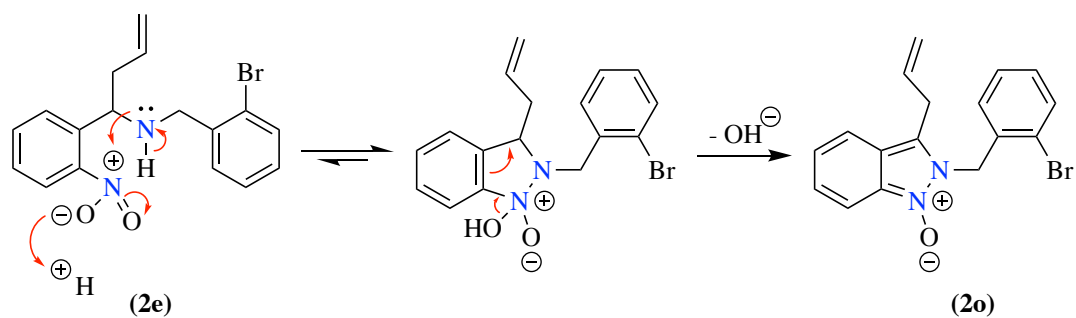
Figure 4.5. Previous work in the JSF group developed a methodology towards the iodine-mediated stereoselective synthesis of 2,4-cis-azetidine and 2,4-cis-pyrrolidine ring systems. Throughout this project, the scope of this work has been expanded to introduce new substituents at the 1-position of the azetidine and pyrrolidine which were then subsequently exploited for the creation of novel scaffolds. The newly developed scaffolds were decorated using a series of building blocks to create diverse compound libraries which possessed a high degree of structural diversity and three-dimensionality to populate underexplored areas of chemical space.

4.2. Future Perspectives

The work discussed in this thesis has laid the groundwork for the development of new lead compounds which explore under-populated areas of chemical space. However, there are several areas which can be elaborated on in order to expand and improve the scope of this work.

4.2.1. Exploration of Alternative Scaffold Cores

During the development of the 4,6-fused and 5,6-bridged scaffolds used in this project, it was found that the iodine-mediated cyclisation of (**2e**), resulted in an unexpected major product (66%) in place of the iodo-azetidine intermediate. It has been proposed that when the aromatic ring is decorated with a nitro group in the 2-position, it is subject to nucleophilic attack by the lone pair present on the secondary amine. This nucleophilic attack and subsequent electronic rearrangement results in the formation of a stable bicyclic indazole-type intermediate. This unexpected product was not explored as part of this work, and the indazole core is relatively planar it does possess multiple points which would be suitable for orthogonal diversification, with the additional possibility to perform an intramolecular Heck reaction to create a novel multicyclic structure with a high degree of unsaturation. As such, some further evaluation in terms of its' potential as a drug scaffold may be of interest.



Scheme 4.1. The discovery of an unexpected side product could be utilised as a new starting point for library generation as the novel indazole-type compound possesses several points for orthogonal diversification.

4.2.2. Potential for Scaffold Variation

At present, only 1,2,4-*cis*-azetidines have been successfully synthesised by the iodine-mediated ring closure method developed within the JSF group. With this in mind, further work to explore the analogues of these compounds, namely 1,2,4-*trans*-azetidines and 1,2,3-substituted-azetidines, both as single ring systems but also through transformation to their corresponding bicyclic scaffold moieties. By creating three-dimensional, bicyclic scaffolds from such analogues, *via* the method established within this project, additional areas of chemical space may be explored and thus exploited through hit-to-lead development protocols, allowing for the creation of the next generation of pharmaceutical agents, which possess a high degree of three-dimensionality when compared to those currently available.

4.2.3. Alternative Cyclisation Procedures

Presently, the cyclisation of homoallylic amines to the corresponding azetidine or pyrrolidine ring system is mediated using molecular iodine. Despite this method being chemically robust, iodine is not environmentally benign. As such, the exploration of alternative methods of cyclisation to minimise the cumulative environmental toxicity may be of interest. Preliminary

results within the JSF group suggest that electrochemistry allows for the cyclisation of homoallylic amines to pyrrolidine rings in the absence of iodine. These results suggest that azetidine rings could be produced *via* the same method.

4.2.4. Potential for Alternative Applications

The scaffolds developed throughout the duration of this project were designed primarily for use in drug discovery. However, it is proposed that the scope of project could be further expanded by considering the alternative applications for which these scaffolds may be suitable. The 4,6-fused and the 5,6-bridged scaffolds systems both possess a tertiary amine, with a predicted pKa value of 9.3 and 8.6 respectively.²⁴⁹ The pKa of DABCO (1,4-diazabicyclo[2.2.2]octane), which bears a degree of structural similarity to the scaffold moieties, is 8.8. DABCO is commonly employed as a tertiary amine organocatalyst in Bayliss-Hillman reactions and in the synthesis of polyurethane polymers. With this in mind, further studies conducted on the 4,6-fused and 5,6-bridged systems may provide insight into the possible uses for these scaffolds outside of traditional drug discovery.

Chapter 5: Experimental

5.1. General Information

Reagents were purchased from commercial suppliers (Acros Organics, Combi-Blocksm Fisher Scientific, VWR International) and were used without further purification. Anhydrous solvents were prepared using a solvent purification system which is monitored by Karl-Fischer titration to monitor water levels. Distilled solvents were stored in sealed round bottom flasks over 4 Å molecular sieves. Reactions carried out under anhydrous conditions were performed in an argon atmosphere using glassware dried in a 200 °C oven, hot glassware was allowed to cool under reduced pressure prior to use; liquids were added through a rubber septa. Reactions which required heating were submerged in preheated paraffin oil baths or heated using an aluminium mantle with an external temperature control probe. Reactions which required cooling (0 °C) were submerged in an ice/water bath. Room temperature refers to the ambient temperature at the time at which the reaction was carried out. Reactions were monitored using thin-layer chromatography using Merck silica gel 60 F₂₅₄ (aluminium- or glass-supported) plates, which were visualised using UV light (254 nm) and/or the standard visualising agents: permanganate/Δ, vanillin/Δ, anisaldehyde/Δ, ninhydrin/Δ or iodine vapour. Flash chromatography was carried out on Sigma Aldrich silica gel (60 Å, 230–400 mesh, 40–63 μm), Interchim prepacked spherical silica columns (60 Å, 30 μm) or Büchi Flashpure silica columns (irregular, 40 μm) and were carried out manually or using CombiFlash® Rf 200i with UV detection or BUCHI® Reveleris X2 using UV and ELSD detection. ¹H-NMR and ¹³C-NMR experiments were recorded using Bruker Neo-400 (¹H = 400 MHz, ¹³C = 101 MHz), AVIII300 (¹H = 300 MHz), Bruker Avance or Bruker Avance II-Ultrashield 400 (¹H = 400 MHz, ¹³C = 101 MHz) spectrometers at 295-300 K. ¹³C NMR spectra were recorded using the UDEFT, JMOD or APT pulse sequence from the Bruker standard pulse program library. 2D NMR spectra were recorded using the Bruker standard pulse program library. Chemical shifts (δ) are reported in parts per million (ppm), referenced to a residual solvent peak and coupling

constants (*J*) are given in Hertz (Hz). Multiplicities are reported as: b (broad), s (singlet), d (doublet), t (triplet), q (quartet) and m (multiplet), or some combination thereof. Infrared spectra were recorded neat on an Agilent Cary 630 FTIR (ZnSe) with Diamond ATR and wavelengths (ν) are reported in cm^{-1} . Mass spectra were obtained using Waters GCT Premier (EI), Waters LCT (ES) or Waters Synapt (ES) spectrometers. LCMS analysis was performed using Agilent 1260 Bin. with G1312B pump:

- SC_BASE: DAD: Agilent G1315C, 210, 220 and 220-320 nm, PDA: 210-320 nm, MSD MSD: Agilent LC/MSD G6130B ESI, pos/neg 100-1000; column: Waters XSelect™ CSH C18, 30x2.1 mm, 3.5 μm , Temp: 25 °C, Flow: 1 mL/min, Gradient: $t_0 = 5\%$ B, $t_{1.6 \text{ min}} = 98\%$ B, $t_3 \text{ min} = 98\%$ B, Posttime: 1.3 min, Eluent A: 10 mM ammoniumbicarbonate in water (pH=9.5), Eluent B: acetonitrile; $R_t = x.yy \text{ min}$, $M+H = xxx, xx\%$ product.
- SC_ACID: DAD: Agilent G1315D, 210, 220 and 220-320 nm, PDA: 210-320 nm, MSD: Agilent LC/MSD G6130B ESI, pos/neg 100-1000, ELSD Alltech 3300 gas flow 1.5 ml/min, gas temp: 40 °C; column: Waters XSelect™ CSH C18, 30x2.1 mm, 3.5 μm , Temp: 40 °C, Flow: 1 mL/min, Gradient: $t_0 = 5\%$ B, $t_{1.6 \text{ min}} = 98\%$ B, $t_3 \text{ min} = 98\%$ B, Posttime: 1.3 min, Eluent A: 0.1% formic acid in water, Eluent B: 0.1% formic acid in acetonitrile: $R_t = x.yy \text{ min}$, $M+H = xxx, xx\%$ product.

UPLC analysis was performed using Waters IClass; Bin. with UPIBSM pump:

- UPLC_SC_ACID: PDA: UPPDATC, 210-320 nm, MS: QDA ESI, pos/neg 100-800; column: Waters XSelect CSH C18, 50x2.1 mm, 2.5 μm , Temp: 40 °C, Flow: 0.6 mL/min, Gradient: $t_0 = 5\%$ B, $t_{1.3 \text{ min}} = 98\%$ B, $t_{1.7 \text{ min}} = 98\%$ B, Posttime: 0.3 min, Eluent A: 0.1% formic acid in water, Eluent B: 0.1% formic acid in acetonitrile: $R_t = x.yy \text{ min}$, $M+H = xxx, xx\%$ product.

- UPLC_SC_BASE: PDA: UPPDATC, 210-320 nm, SQD: MS: QDA ESI, pos/neg 100-800; column: Waters XSelect CSH C18, 50x2.1 mm, 2.5 μ m, Temp: 25°C, Flow: 0.6 mL/min, Gradient: t₀ = 5% B, t_{1.3min} = 98% B, t_{1.7min} = 98% B, Posttime: 0.3 min, Eluent A: 10mM ammonium bicarbonate in water (pH=9.5), Eluent B: acetonitrile: Rt = x.yy min, M+H = xxx, xx% product.
- UPLC_AN_ACID: PDA: UPPDATC, 210-320 nm, MS: QDA ESI, pos/neg 100-800; column: Waters XSelect CSH C18, 50x2.1 mm, 2.5 μ m, Temp: 40 °C, Flow: 0.6 mL/min, Gradient: t₀ = 5% B, t_{2.0min} = 98% B, t_{2.7min} = 98% B, Posttime: 0.3 min, Eluent A: 0.1% formic acid in water, Eluent B: 0.1% formic acid in acetonitrile: Rt = x.yy min, M+H = xxx, xx% product.
- UPLC_AN_BASE: PDA: UPPDATC, 210-320 nm, MS: QDA ESI, pos/neg 100-800; column: Waters XSelect CSH C18, 50x2.1 mm, 2.5 μ m, Temp: 25 °C, Flow: 0.6 mL/min, Gradient: t₀ = 5% B, t_{2.0min} = 98% B, t_{2.7min} = 98% B, Posttime: 0.3 min, Eluent A: 10mM ammonium bicarbonate in water (pH=9.5), Eluent B: acetonitrile: Rt = x.yy min, M+H = xxx, xx% product.

Preparative HPLC purification was carried out using Waters Modular Preparative HPLC System with Waters XSelect (C18, 100x30 mm, 10 μ m) column and ACQ-SQD2 mass spectrometry instrument:

- Acid: flow: 55 ml/min prep pump; column temp: RT; eluent A: 0.1% formic acid in water; eluent B: 100% acetonitrile, necessary gradient was determined from initial LCMS analysis; detection: DAD (220-320 nm); detection: MSD (ESI pos/neg) mass range: 100 – 800; fraction collection based on MS and DAD
- Base (Ammonium Bicarbonate): flow: 55 ml/min prep pump; column temp: RT; eluent A: 10mM ammonium bicarbonate in water pH=9.5, eluent B: 100% acetonitrile; necessary gradient was determined from initial LCMS analysis; detection: DAD (220-

320 nm); detection: MSD (ESI pos/neg) mass range: 100 – 800; fraction collection based on MS and DAD.

- Base (Ammonia): flow: 55 ml/min prep pump; column temp: RT; eluent A: 100mM ammonia in water, eluent B: 100% acetonitrile; necessary gradient was determined from initial LCMS analysis; detection: DAD (220-320 nm); detection: MSD (ESI pos/neg) mass range: 100 – 800; fraction collection based on MS and DAD

High-Resolution Mass Spectrometry (HRMS) was carried out using the LC-MS Q Exactive Focus high resolution mass spectrometer (Thermo Scientific). Before starting the analyses, the mass spectrometer is calibrated by infusion of a standard mixture using the syringe pump at 5 µl/min:

- Positive ion mode: Pierce calibration solution containing *N*-butylamine, caffeine, MRFA and Ultramark 1621 (Thermo Fisher Scientific product nr. 88323).
- Negative ion mode: Pierce calibration solution containing sodium dodecyl sulfate, sodium taurocholate, and Ultramark 1621 (Thermo Fisher Scientific product nr 88324).

Compound Analysis: A solution of the sample in acetonitrile with a concentration of 10 µg/ml is prepared. 1 µl sample is injected and analysed using the HRMS method. The data are acquired under full MS mode (resolution 70000 FWHM at 200 Da) over the mass range m/z of 150 – 2000. Standard ESI conditions compatible with the flow rate are applied: spray voltage 3.5 kV, auxiliary gas heater temperature 463 °C, capillary temperature 280 °C, sheath gas 58, auxiliary gas 16, sweep gas 3, S-lens RF level 50. Mass resolution is set at 70000 (< 3 ppm mass accuracy). If needed, these conditions were optimized. Data are evaluated using Xcalibur Qual Browser version 4.2.47 (Thermo Fisher).

5.2. General Procedures

5.2.1. General Procedure A: Imine Synthesis

To a stirred solution of aldehyde (1.1 Eq) in ethanol (0.3 M) at room temperature, amine (1.0 Eq) was added as a single portion. The reaction mixture was heated to reflux for 1.5 hours, solvent was removed *in vacuo*. The crude product was used in the next step without additional purification

5.2.2. General Procedure B: Homoallylic Amine Synthesis

Allyl bromide (3.0 Eq) was added to a stirred suspension of zinc powder (3.2 Eq) in tetrahydrofuran (0.3 M) at room temperature. Reaction mixture was stirred at room temperature for 2 hours to form allylzinc bromide *in situ*. Imine (1.0 Eq) was then added in a controlled manner to the reaction mixture, which was stirred at room temperature for 14 hours. The reaction mixture was quenched with a saturated solution of sodium bicarbonate, the liquid was then decanted off and the remaining precipitate was washed with ethyl acetate. The resultant solution was partitioned between water and was washed with ethyl acetate and washed with water and brine and dried over anhydrous magnesium sulfate. The solution was then filtered, and volatile components were removed *in vacuo*. The resultant material was then purified by column chromatography using Combiflash Rf200i or Revlaris system.

5.2.3. General Procedure C: Amino-azetidine Synthesis

To a solution of homoallylic amine (1.0 Eq) in acetonitrile (0.3 M), sodium bicarbonate (5.0 Eq) and iodine beads (3.0 Eq) were added. The reaction mixture was stirred at room

temperature for 16 hours. Formation of iodoazetidine intermediate was confirmed using LCMS. The result iodoazetidine was dissolved in dichloromethane (0.3 M) and stirred with an amine (2.5 Eq) and triethylamine (3.0 Eq) at room temperature for 16 hours. Formation of the desired product was confirmed using TLC analysis, volatile components of the reaction mixture were removed *in vacuo* and material was then purified by column chromatography using Combiflash Rf 200i or Revlaris system.

5.2.4. General Procedure D: *rac*-(6,8-*cis*)-8-phenyl-1,4-diazabicyclo[4.2.0]octane Synthesis (4,6-Fused Scaffold)

To a solution of homoallylic amine (1.0 Eq) in acetonitrile (0.3 M), sodium bicarbonate (5.0 Eq) and iodine beads (3.0 Eq) were added. The reaction mixture was stirred at room temperature for 16 hours. Formation of iodoazetidine intermediate was confirmed using LCMS. Reaction mixture was quenched with sodium thiosulphate solution, extracted with ethyl acetate, and washed with water and brine. Volatile components were removed *in vacuo* using a cool water bath (18-22 °C). Resultant material was then dissolved in *N,N*-dimethylformamide and was stirred with sodium azide (1.2 Eq) at room temperature for 16 hours at room temperature. Formation of azido-azetidine was confirmed using LCMS, the reaction mixture was extracted with ethyl acetate, and washed with water and brine. Organic fractions were then combined and dried over anhydrous magnesium sulfate, volatiles were removed *in vacuo*. The resultant material was then dissolved in tetrahydrofuran and stirred with triphenylphosphine (2.6 Eq) at room temperature for 2 hours, water (20.0 Eq) was then added as a single portion and the reaction mixture was stirred overnight. Reaction mixture was acidified to pH 2 using HCl aq. solution (1.0 M) and extracted with ethyl acetate, aqueous layer was collected and basified to pH 10 using NaOH solution (1.0 M) and was extracted with ethyl acetate and washed with water and brine. Organic fraction was dried over anhydrous

magnesium sulfate and volatile components were removed *in vacuo*. Material was then purified using flash column chromatography

5.2.5. General Procedure E: *rac*-(1,5-*cis*,1,7-*trans*)-7-phenyl-1,4-diazabicyclo[3.2.1]octane Synthesis (5,6-Bridged Scaffold)

To a solution of homoallylic amine (6.29 g, 25.5 mmol, 1.0 Eq) in acetonitrile (60 mL, 0.3 M), sodium bicarbonate (6.52 g, 78 mmol, 5.0 Eq) and iodine beads (11.82 g, 46.6 mmol, 3.0 Eq) were added. The reaction mixture was stirred at 50 °C for 16 hours. Formation of iodopyrrolidine intermediate was confirmed using LCMS. Reaction mixture was quenched with sodium thiosulphate solution, extracted with ethyl acetate, and washed with water and brine. Volatile components were removed *in vacuo* using a cool water bath (18 – 22 °C). Resultant material was then dissolved in *N,N*-dimethylformamide and was stirred with sodium azide (600 mg, 9.62 mmol, 1.2 Eq) at room temperature for 16 hours at room temperature. Formation of azidopyrrolidine was confirmed using LCMS, the reaction mixture was extracted with ethyl acetate, and washed with water and brine. Organic fractions were then combined and dried over anhydrous magnesium sulfate, volatiles were removed *in vacuo*. The resultant material was then dissolved in tetrahydrofuran and stirred with triphenylphosphine (4.2 g, 15.8 mmol, 2.6 Eq) at room temperature for 2 hours, water (2.2 mL, 122 mmol, 20.0 Eq) was then added as a single portion and the reaction mixture was stirred overnight. Reaction mixture was acidified to pH 2 using 1.0 M HCl solution and extracted with ethyl acetate, aqueous layer was collected and basified to pH 10 using 1.0M NaOH solution and was extracted with ethyl acetate and washed with water and brine. Organic fraction was dried over anhydrous magnesium sulfate and volatile components were removed *in vacuo*. Material was then purified using flash column chromatography.

5.2.6. General Procedure F: Azetidine Library Synthesis

To a solution of homoallylic amine (6.29 g, 25.5 mmol, 1.0 Eq) in acetonitrile (60 mL, 0.3M), sodium bicarbonate (6.52 g, 78 mmol, 5.0 Eq) and iodine beads (11.82 g, 46.6 mmol, 3.0 Eq) were added. The reaction mixture was stirred at room temperature for 16 hours. Formation of the iodoazetidine intermediate was confirmed using LCMS, reaction mixture was quenched with sodium thiosulfate, extracted with ethyl acetate, and washed with water and brine. Volatiles were removed *in vacuo*, resultant material was redissolved in dichloromethane (30mg/1ml) and portioned between reaction vessels containing the amine reactants (3.0 Eq) and triethylamine (0.05 mL, 0.185 mmol, 3.0 Eq). Reaction mixtures were stirred at room temperature using an orbital shaker for 24 hours. Reaction completion was determined using UPLC analysis. Dichloromethane was removed from the reaction vessels using centrifugal evaporation. Resultant materials were then redissolved in DMF (1 mL/vial) and purified using waters preparative HPLC.

5.2.7. General Procedure G: 4,6 Library Synthesis

To a solution of homoallylic amine (2.4 g, 5.9 mmol, 1.0 Eq) in acetonitrile (20 mL, 0.3 M), sodium bicarbonate (2.47 g, 29.5 mmol, 5.0 Eq) and iodine beads (4.49 g, 17.7 mmol, 3.0 Eq) were added. The reaction mixture was stirred at room temperature for 16 hours. Formation of iodoazetidine intermediate was confirmed using LCMS. Reaction mixture was quenched with sodium thiosulphate solution, extracted with ethyl acetate, and washed with water and brine. Volatile components were removed *in vacuo* using a cool water bath (18-22 °C). Resultant material was then dissolved in *N,N*-dimethylformamide and was stirred with sodium azide (440 mg, 6.76 mmol, 1.2 Eq) at room temperature for 16 hours at room temperature. Formation of azido-azetidine was confirmed using LCMS, the reaction mixture was extracted with ethyl

acetate, and washed with water and brine. Organic fractions were then combined and dried over anhydrous magnesium sulfate, volatiles were removed *in vacuo*. The resultant material was then dissolved in tetrahydrofuran and stirred with triphenylphosphine (3.15g, 12.0 mmol, 2.6 Eq) at room temperature for 2 hours, water (1.6 mL, 92.0 mmol, 20.0 Eq) was then added as a single portion and the reaction mixture was stirred overnight. Reaction mixture was acidified to pH 2 using 1.0 M HCl solution and extracted with ethyl acetate, aqueous layer was collected and basified to pH 10 using 1.0 M NaOH solution and was extracted with ethyl acetate and washed with water and brine. Organic fraction was dried over anhydrous magnesium sulfate and volatile components were removed *in vacuo*. Material was then purified using flash column chromatography giving the free amine scaffold (**4b**) which was subsequently decorated:

Protocol for isocyanates, sulfonyl chlorides and acyl chlorides:

Reactants (2.5 Eq) were measured into labelled reaction vials. A solution of the 4,6-fused scaffold (**4b**) was prepared in dichloromethane (30 mg/1 mL) and portioned into the reaction vials (1 mL/vial), triethylamine (3.0 Eq) was then added to each reaction. Reaction mixtures were stirred at room temperature using an orbital shaker for 24 hours. Reaction completion was determined using UPLC analysis. Dichloromethane was removed from the reaction vessels using centrifugal evaporation. Resultant materials were then redissolved in DMF (1 mL/vial) and purified using waters preparative HPLC.

Protocol for Carboxylic Acids:

Reactants (1.0 Eq) were measured into labelled reaction vials. A solution of HOAt (1.3 mg, 9.25 μ mol, 0.1 Eq), EDCI.HCl (19.51 mg, 0.102 mmol, 1.1 Eq) and triethylamine (0.015 mL, 0.111 mmol, 1.2 Eq) was prepared in dichloromethane (0.5 mL/reaction) and was added to the reaction vials. (**4b**) was dissolved in dichloromethane (30 mg/0.5 mL, 1.0 Eq) and was added

to the reaction vials (1 mL, total reaction volume). Reaction mixtures were stirred at room temperature for 24 hours using an orbital shaker. Reaction completion was confirmed using UPLC analysis. Dichloromethane was removed from the reaction mixtures using a centrifugal evaporator. Resultant material was redissolved in DMF and purified using preparative HPLC.

5.2.8. General Procedure H: 5,6 Library Synthesis

To a solution of homoallylic amine (2.39 g, 5.9 mmol, 1.0 Eq) in acetonitrile (20 mL, 0.3M), sodium bicarbonate (2.47 g, 29.5 mmol, 5.0 Eq) and iodine beads (4.49 g, 17.69 mmol, 3.0 Eq) were added. The reaction mixture was stirred at 50 °C for 16 hours. Formation of iodopyrrolidine intermediate was confirmed using LCMS. Reaction mixture was quenched with sodium thiosulphate solution, extracted with ethyl acetate, and washed with water and brine. Volatile components were removed *in vacuo* using a cool water bath (18 – 22 °C). Resultant material was then dissolved in *N,N*-dimethylformamide and was stirred with sodium azide (440 mg, 6.76 mmol, 1.2 Eq) at room temperature for 16 hours at room temperature. Formation of azido-pyrrolidine was confirmed using LCMS, the reaction mixture was extracted with ethyl acetate, and washed with water and brine. Organic fractions were then combined and dried over anhydrous magnesium sulfate, volatiles were removed *in vacuo*. The resultant material was then dissolved in tetrahydrofuran and stirred with triphenylphosphine (3.15 g, 12.0 mmol, 2.6 Eq) at room temperature for 2 hours, water (1.6 mL, 92.0 mmol, 20.0 Eq) was then added as a single portion and the reaction mixture was stirred overnight. Reaction mixture was acidified to pH 2 using 1.0M HCl solution and extracted with ethyl acetate, aqueous layer was collected and basified to pH 10 using 1.0 M NaOH solution and was extracted with ethyl acetate and washed with water and brine. Organic fraction was dried over anhydrous magnesium sulfate and volatile components were removed *in vacuo*. Material was then purified

using flash column chromatography to give the free amine scaffold (**5a**) which was subsequently decorated:

Protocol for isocyanates, sulfonyl chlorides and acyl chlorides:

Reactants (2.5 Eq) were measured into labelled reaction vials. A solution of (**5a**) was prepared in dichloromethane (30 mg/1mL) and portioned into the reaction vials (1 mL/vial), triethylamine (3.0 Eq) was then added to each reaction. Reaction mixtures were stirred at room temperature using an orbital shaker for 24 hours. Reaction completion was determined using UPLC analysis. Dichloromethane was removed from the reaction vessels using centrifugal evaporator. Resultant materials were then redissolved in DMF (1 mL/vial) and purified using preparative HPLC.

Protocol for Carboxylic Acids:

Reactants (1.0 Eq) were measured into labelled reaction vials. A solution of HOAt (1.3 mg, 9.25 μ mol, 0.1 Eq), EDCI.HCl (19.51 mg, 0.102 mmol, 1.1 Eq) and triethylamine (0.015 mL, 0.111 mmol, 1.2 Eq) was prepared in dichloromethane (0.5 mL/reaction) and was added to the reaction vials. (**5a**) was dissolved in dichloromethane (30 mg/0.5 mL, 1.0 Eq) and was added to the reaction vials (1 mL, total reaction volume). Reaction mixtures were stirred at room temperature for 24 hours using an orbital shaker. Reaction completion was confirmed using UPLC analysis. Dichloromethane was removed from the reaction mixtures using centrifugal evaporation. Resultant material was redissolved in DMF and purified using preparative HPLC.

5.2.9. General Procedure I: Inhibition of Bacterial Growth

An assay plate is created containing 5 µl of each drug at 800 µM in 80% DMSO. These will be diluted 40x by addition of cells, leaving a final DMSO concentration of 2% and drug concentrations of 20 µM. Bacterial strains are cultured until they reach mid-log growth (OD600 - 05). They are diluted to OD600 = 0.05 for addition into the assay plate. Then 195 µL of diluted culture is added into the assay plate. The plate is then incubated for 24-hours at 37 °C. For ESKAPE pathogens^{5,250} the OD600 is used a measure to determine growth/inhibition. For Mycobacteria, resazurin is added to the cells, re-incubated for 3 or 24 hours and then the fluorescence (ex-544, em-590), is used to determine inhibition.

Readout Definitions:

Name	Data Type	Unit	Description
Fluorescence		(RFU)	
% inhibition resazurin	Number	%	Normalised against positive and negative controls
OD600		(ABS)	
% inhibition OD600	Number	%	Normalised against positive and negative controls

⁵ ESKAPE pathogens (*Enterococcus faecium*, *Staphylococcus aureus*, *Klebsiella pneumoniae*, *Acinetobacter baumannii*, *Pseudomonas aeruginosa*, and *Enterobacter* species) are the leading cause of nosocomial infections throughout the world and are high priority pathogens for the identification of new inhibitors.

Control Layouts

☐ Positive control (hit)☐ Negative control☐ Reference molecule

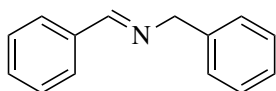
▼ Protocol Default 96-well Control Layout

	01	02	03	04	05	06	07	08	09	10	11	12
A	<input type="checkbox"/>											<input type="checkbox"/>
B	<input type="checkbox"/>											<input type="checkbox"/>
C	<input type="checkbox"/>											<input type="checkbox"/>
D	<input type="checkbox"/>											<input type="checkbox"/>
E	<input type="checkbox"/>											<input type="checkbox"/>
F	<input type="checkbox"/>											<input type="checkbox"/>
G	<input type="checkbox"/>											<input type="checkbox"/>
H	<input type="checkbox"/>											<input type="checkbox"/>

5.3.Characterisation Data

5.3.1. Imines

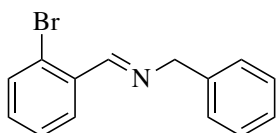
5.3.1.1. (*E*)-*N*-benzyl-1-phenylmethanimine (**1a**)



Prepared using *General Procedure A*: Benzylamine (0.12 mL, 1.1 mmol, 1.1 Eq), benzaldehyde (0.1 mL, 1.0 mmol, 1.0 Eq) and ethanol (10 mL). Yellow oil, >99%, 540 mg. Data in agreement with the reported literature values.²⁵¹

¹H NMR (300 MHz, Chloroform-*d*) δ 8.39 (t, *J* 1.4 Hz, 1H, *CHN*), 7.82 – 7.73 (m, 2H, *PhH*), 7.44 – 7.25 (m, 8H, *PhH*), 4.82 (d, *J* 1.4 Hz, 2H, *PhCH₂*). **¹³C NMR** (101 MHz, Chloroform-*d*) δ 162.1 (CH, *CH=N*), 139.3 (C, Ar), 136.2 (C, Ar), 130.8 (CH, Ar), 128.6 (CH, Ar), 128.5 (CH, Ar), 128.3 (CH, Ar), 128.0 (CH, Ar), 127.0 (CH, Ar), 65.1 (CH₂, *NCH₂*). **MS** TOF EI+ (*m/z*): 196.98 [*M*+H]⁺. **FTIR** ν_{max} 3225, 1631.

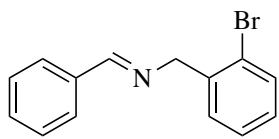
5.3.1.2. (*E*)-*N*-benzyl-1-(2-bromophenyl)methanimine (**1b**)



Prepared using *General Procedure A*: 2-Bromobenzaldehyde (1.1 mL, 9.2 mmol, 1.0 equiv.) and benzylamine (1.1 mL, 10.0 mmol, 1.1 Equiv) and ethanol (10 mL). Amber oil, >99%, 2.1 g. Data in agreement with the reported literature values.²⁵²

¹H NMR (300 MHz, Chloroform-*d*) δ 8.75 (d, *J* 1.6 Hz, 1H, *CHN*), 8.07 (dt, *J* 7.7, 1.7 Hz, 1H, *PhH*), 7.53 (dd, *J* = 7.9, 1.4 Hz, 1H, *PhH*), 7.40 – 7.17 (m, 8H, *PhH*), 4.84 (d, *J* 1.5 Hz, 2H, *PhCH₂*). **¹³C NMR** (101 MHz, chloroform-*d*) δ 160.8, 138.9, 134.5, 133.0, 130.8, 128.9, 128.6, 128.0, 127.6, 127.1, 125.1, 65.2. **MS** TOF EI+ (*m.z*): 274.11 [*M*]⁺. **FTIR** ν_{max} 1634.

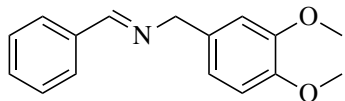
5.3.1.3. (E)-N-(2-bromobenzyl)-1-phenylmethanimine (**1c**)



Prepared using *General Procedure A*: Benzaldehyde (3.6 mmol, 1.0 equiv.), bromobenzylamine (4.3 mmol, 1.1 equiv.), and ethanol (10 mL). Amber oil, >99%, 1.1 g. Data in agreement with the reported literature values.²⁵²

¹H NMR (300 MHz, Chloroform-*d*) δ 8.43 (t, *J* 1.5 Hz, 1H, *CHN*), 7.84 – 7.79 (m, 2H, *PhH*), 7.61 – 7.56 (m, 1H, *PhH*), 7.48 – 7.41 (m, 4H, *PhH*), 7.31 (td, *J* 7.5, 1.3 Hz, 1H, *PhH*), 7.14 (td, *J* = 7.6, 1.8 Hz, 1H, *PhH*), 4.90 (s, 2H, *PhCH*₂). **¹³C NMR** (101 MHz, chloroform-*d*) δ 162.3, 139.2, 136.5, 132.9, 132.4, 131.3, 130.2, 129.1, 128.9, 128.7, 127.9, 123.9, 64.7. **MS** TOF EI+ (*m/z*): 274.11 [*M*]. **FTIR** ν_{max} 1644.

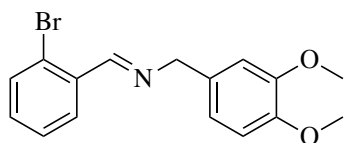
5.3.1.4. (E)-N-(3,4-dimethoxybenzyl)-1-phenylmethanimine (**1d**)



Prepared using *General Procedure A*: Benzaldehyde (1.0 mL, 9.8 mmol, 1.0 Eq), 3,4-dimethoxybenzylamine (1.7 mL, 11 mmol, 1.1 Eq) in ethanol (10 mL). Yellow oil, >99%, 2.8g. Data in agreement with the reported literature values.²⁵³

¹H NMR (400 MHz, Chloroform-*d*) δ 8.38 (t, *J* 1.4 Hz, 1H, *CHN*), 7.81 – 7.74 (m, 2H, *PhH*), 7.46 – 7.37 (m, 3H, *PhH*), 6.89 – 6.81 (m, 3H, *PhH*), 4.76 (dd, *J* 1.4, 0.7 Hz, 2H, *PhCH*₂), 3.88 (s, 3H, OCH₃), 3.87 (s, 3H, OCH₃). **¹³C NMR** (101 MHz, Chloroform-*d*) δ 161.8, 130.8, 128.6, 128.3, 120.2, 111.42, 111.3, 64.6, 55.9, 55.89. **MS** TOF EI+ (*m/z*): 336.12 [*M*+H]⁺. **FTIR** ν_{max} 1610, 1127.

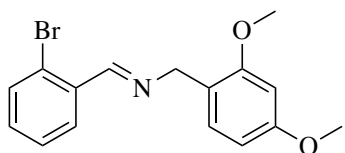
5.3.1.5. (*E*)-1-(2-bromophenyl)-*N*-(3,4-dimethoxybenzyl)methanimine (**1e**)



Prepared using *General Procedure A*: 2-Bromobenzaldehyde (7.4 mmol, 1.0 Eq), 3,4-dimethoxybenzylamine (8.1 mmol, 1.1 equiv.) and EtOH (10mL), Golden yellow oil, >99%, 2.5g.

¹H NMR (300 MHz, Chloroform-*d*) δ 8.75 (s, 1H, *PhH*), 8.05 (dd, *J* 7.7, 2.0 Hz, 1H, *PhH*), 7.60 – 7.54 (m, 1H, *PhH*), 7.37 – 7.27 (m, 2H, *PhCH=N*), 6.91 – 6.84 (s, 2H, *PhCH₂N*), 4.80 (s, 3H, OCH₃), 3.89 (s, 3H, OCH₃), 3.87 (s, 3H, OCH₃). **¹³C NMR** (101 MHz, Chloroform-*d*) δ 160.9, 132.9, 131.6, 130.2, 128.9, 127.5, 104.1, 98.5, 59.3, 55.4. **MS** TOF EI+ (*m/z*): 336.12 [M+H]⁺. **FTIR** ν_{max} 1610, 1206, 753.

5.3.1.6. (*E*)-1-(2-bromophenyl)-*N*-(2,4-dimethoxybenzyl)methanimine (**1f**)

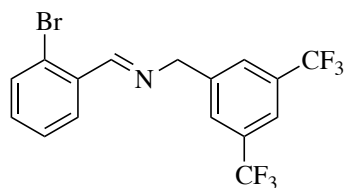


Prepared using *General Procedure A*: 2-Bromobenzaldehyde (0.87 mL, 7.4 mmol, 1.0 Eq), 2,4-dimethoxybenzylamine (1.2 mL, 8.1 mmol, 1.1 equiv.) in 10 mL of EtOH. Golden yellow

oil, >99%, 2.4g. Data in agreement with the reported literature values.²⁵⁴

¹H NMR (400 MHz, Chloroform-*d*) δ 8.72 (s, 1H, *CHN*), 8.04 (dd, *J* 7.8, 1.5 Hz, 1H, *PhH*), 7.55 (dd, *J* 7.8, 1.5 Hz, 1H, *PhH*), 7.32 (tdd, *J* 7.8, 1.3, 0.7 Hz, 1H, *PhH*), 7.27 – 7.19 (m, 2H, *PhH*), 6.51 – 6.46 (m, 2H, *PhH*), 4.80 (d, *J* 1.4 Hz, 2H, *PhCH₂*), 3.83 (s, 3H, OCH₃), 3.81 (s, 3H, OCH₃). **¹³C NMR** (101 MHz, Chloroform-*d*) δ 160.9, 132.9, 131.6, 130.2, 128.9, 127.5, 104.1, 98.5, 59.3, 55.4. **MS** TOF EI+ (*m/z*): 334.22 [M]⁺. **FTIR** ν_{max} 1610, 1286, 1262.

5.3.1.7. (*E*)-*N*-(3,5-bis(trifluoromethyl)benzyl)-1-(2-bromophenyl)methanimine (**1g**)

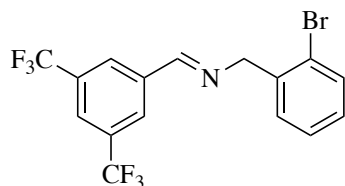


Prepared using *General Procedure A*: 2-Bromobenzaldehyde (0.28 mL, 2.4 mmol, 1.0 Eq), 3,5-bis(trifluoromethyl)benzylamine (0.65 g, 2.6 mmol, 1.1 equiv.)

in 10 mL of EtOH, heated to reflux for 1 h. The resultant product was analytically pure and was used without further purification. Opaque white oil, >99%, 1.4g.

¹H NMR (400 MHz, Chloroform-*d*) δ 8.85 (s, 1H, *CHN*), 8.09 (m, 1H, *PhH*), 7.85 (m, 2H, *PhH*), 7.80 (m, 1H, *PhH*), 7.63 – 7.58 (m, 1H, *PhH*), 7.41 – 7.28 (m, 2H, *PhH*), 4.96 (d, *J* 1.4 Hz, 2H, *PhCH₂*). **¹³C NMR** (101 MHz, Chloroform-*d*) δ 162.5, 141.8, 133.2, 132.4, 128.9, 128.0, 127.8, 63.8. **MS** TOF EI+ (*m/z*): 410.2 [*M*]⁺. **FTIR** *v*_{max} 1697, 681.

5.3.1.8. (*E*)-1-(3,5-bis(trifluoromethyl)phenyl)-*N*-(2-bromobenzyl)methanimine (**1h**)

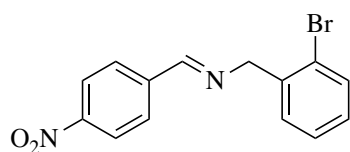


Prepared using *General Procedure A*: 3,5-Bis(trifluoromethyl)benzaldehyde (0.88 mL, 5.4 mmol, 1.0 Eq), 2-bromobenzylamine (1.0 g, 5.4 mmol, 1.1 equiv.) in 10

mL of EtOH. The resultant product was analytically pure and was used without further purification. Yellow oil, >99%, 2.2.g.

¹H NMR (400 MHz, Chloroform-*d*) δ 8.47 (s, 1H, *CHN*), 8.26 – 8.23 (m, 2H, *PhH*), 7.94 (m, 1H, *PhH*), 7.60 (dd, *J* 8.0, 1.2 Hz, 1H, *PhH*), 7.42 (m 1H, *PhH*), 7.34 (td, *J* 7.5, 1.3 Hz, 1H, *PhH*), 7.18 (m, 1H, *PhH*), 4.97 (d, *J* 1.6 Hz, 2H, *PhCH₂*). **¹³C NMR** (101 MHz, Chloroform-*d*) δ 159.5, 137.9, 137.5, 132.9, 130.2, 128.9, 127.8, 123.9 64.16. **MS** TOF EI+ (*m/z*): 410.1 [*M*]⁺. **FTIR** *v*_{max} 1638, 1276, 681

5.3.1.9. (*E*)-*N*-(2-bromobenzyl)-1-(4-nitrophenyl)methanimine (**1i**)

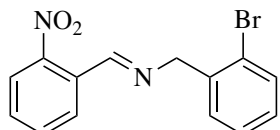


Prepared using *General Procedure A*: 4-Nitrobenzaldehyde (3.0 g, 19.8 mmol, 1.0 Eq), 2-Bromobenzylamine (2.74 mL, 21.8 mmol, 1.1 equiv.) in 25 mL of EtOH, heated to reflux for 30

min. The resultant solid was recrystallised from hot EtOH and was analytically pure and was used without further purification. White, needle-like crystals, 82%, 5.2 g.

¹H NMR (400 MHz, Chloroform-*d*) δ 8.49 (s, 1H, *CHN*), 8.31 – 7.94 (m, 2H, *PhH*), 7.60 (dd, *J* 8.0, 1.2 Hz, 1H, *PhH*), 7.42 (dd, *J* 7.6, 1.8 Hz, 1H, *PhH*), 7.33 (td, *J* 7.6, 1.4 Hz, 1H, *PhH*), 7.17 (td, *J* 7.6, 1.4 Hz, 1H, *PhH*), 4.98 – 4.94 (m, 2H, *PhCH*₂). **¹³C NMR** (101 MHz, Chloroform-*d*) δ 160.5, 147.5, 132.8, 130.0, 129.0, 128.9, 127.7, 123.9, 64.4. **MS** TOF EI+ (*m/z*): 318.9 [*M*]⁺

5.3.1.10. (*E*)-*N*-(2-bromobenzyl)-1-(2-nitrophenyl)methanimine (**1j**)

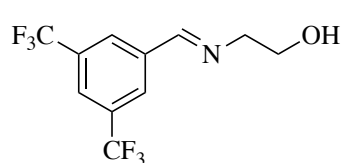


Prepared using *General Procedure A*: 2-Nitrobenzaldehyde (4.0 g, 26.5 mmol, 1.0 Eq), 2-Bromobenzylamine (3.70 mL, 29.4 mmol, 1.1

equiv.) in 15 mL of EtOH, heated to reflux for 30 min. The resultant solid was analytically pure and was used without further purification. Orange crystalline solid, >99%, 8.5 g. Data in agreement with the reported literature values.²⁵⁵

¹H NMR (400 MHz, Chloroform-*d*) δ 8.85 (d, *J* 1.6 Hz, 1H, *CHN*), 8.09 (ddd, *J* 35.2, 7.9, 1.4 Hz, 2H, *PhCH*₂), 7.71 – 7.66 (m, 1H, *PhCH*₂), 7.60 (dt, *J* 7.8, 1.2 Hz, 2H, *PhCH*₂), 7.43 (dd, *J* 7.6, 1.4 Hz, 1H, *PhCH*₂), 7.33 (td, *J* 7.6, 1.5 Hz, 1H, *PhCH*₂), 7.16 (td, *J* 7.7, 1.8 Hz, 1H, *PhCH*₂), 4.97 (d, *J* 1.6 Hz, 2H, *PhCH*₂). **¹³C NMR** (101 MHz, Chloroform-*d*) δ 160.4, 132.8, 129.9, 129.0, 128.9, 127.7, 123.9, 64.4. **MS** TOF EI+ (*m/z*): 319.0 [*M*]⁺

5.3.1.11. (*E*)-2-((3,5-bis(trifluoromethyl)benzylidene)amino)ethan-1-ol (**1k**)



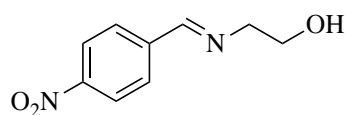
Prepared using *General Procedure A*: 3,5-Bis(trifluoromethyl)benzaldehyde (2.72 mL, 16.5 mmol, 1.0 Eq), ethanolamine (1.1 mL, 5.2mmol, 1.1 equiv.) in 50 mL of EtOH.

The resultant product was analytically pure and was used without further purification.

Colourless oil, >99%, 4.7.g.

¹H NMR (400 MHz, Chloroform-*d*) δ 7.81 (s, 2H), 7.78 (s, 1H), 5.70 (dddd, *J* 16.8, 10.5, 7.9, 6.3 Hz, 1H), 5.16 – 5.08 (m, 2H), 3.85 (dd, *J* 7.7, 5.9 Hz, 1H), 3.71 – 3.58 (m, 2H), 2.70 (ddd, *J* 12.3, 6.5, 3.7 Hz, 1H), 2.54 (ddd, *J* 12.3, 6.4, 3.9 Hz, 1H), 2.49 – 2.37 (m, 2H). **¹³C NMR** (101 MHz, Chloroform-*d*) δ 159.8, 128.1, 126.7, 124.1, 63.2, 62.1. **MS** TOF EI+ (*m/z*): 286.1 [M+H]⁺

5.3.1.12. (*E*)-2-((4-nitrobenzylidene)amino)ethan-1-ol (**1l**)

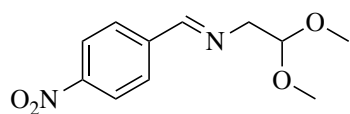


Prepared using *General Procedure A*: 4-Nitrobenzaldehyde (4.0 g, 26.5 mmol, 1.0 Eq), ethanolamine (1.8 mL, 29.1 mmol, 1.1

equiv.) in 50 mL of EtOH. The resultant product was analytically pure and was used without further purification. Pale yellow oil, >99%, 5.1g. Data in agreement with the reported literature values.²⁵⁶

¹H NMR (400 MHz, Chloroform-*d*) δ 8.45 (d, *J* 1.5 Hz, 1H, *CHN*), 8.31 – 8.26 (m, 2H, 3- & 5-*H* C₆H₄NO₂), 7.95 – 7.90 (m, 2H), 3.96 (t, *J* 4.7 Hz, 2H, NHCH₂CH₂), 3.91 – 3.81 (m, 2H NHCH₂CH₂), 1.57 (s, 1H, *CHNH*). **¹³C NMR** (101 MHz, Chloroform-*d*) δ 160.7, 128.9, 127.2, 123.9, 123.6, 63.4, 62.2. **MS** TOF EI+ (*m/z*): 195.1 [M+H]⁺

5.3.1.13. (*E*)-*N*-(2,2-dimethoxyethyl)-1-(4-nitrophenyl)methanimine (**1m**)

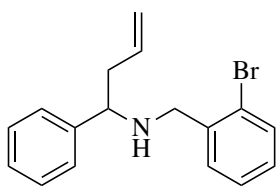


Prepared using *General Procedure A*: 4-Nitrobenzaldehyde (1.5 g, 9.9 mmol, 1.0 Eq), aminoacetaldehyde dimethyl acetal (1.2 mL, 10.9 mmol, 1.1 equiv.) in 25 mL of EtOH. The resultant product was analytically pure and was used without further purification. Pale yellow oil, >99%, 2.3g. Data in agreement with the reported literature values.²⁵⁷

¹H NMR (400 MHz, Chloroform-*d*) δ 8.37 (d, *J* 1.6 Hz, 1H, ArCHN), 8.31 – 8.23 (m, 2H, 3- & 5-*H* C₆H₄(NO₂)), 7.96 – 7.88 (m, 2H, 2- & 6-*H* C₆H₄(NO₂)), 4.70 (t, *J* 5.3 Hz, 1H, CH(CH₃)₂), 3.84 (dd, *J* 5.3, 1.4 Hz, 2H, NCH₂CH), 3.43 (s, 6H, OCH₃). **MS** TOF EI⁺ (*m/z*): 329.2.

5.3.2. Homoallylic Amines

5.3.2.1. *N*-(2-bromobenzyl)-1-phenylbut-3-en-1-amine (**2a**)

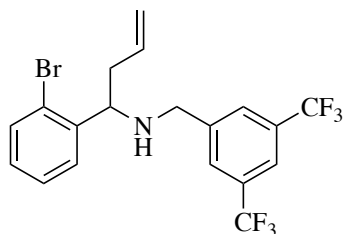


Prepared using *General Procedure B*: Imine **1c** (3.0g, 9.7 mmol, 1.0 Eq), zinc (dust, 2.5g, 39.0 mmol, 4.0 Eq), allyl bromide (2.5 mL, 29.0 mmol, 3.0 Eq) in THF (15 mL, 0.3 M). Colourless oil, 1.58g, 52%

¹H NMR (300 MHz, Chloroform-*d*) δ 7.53 (dt, *J* 7.9, 0.8 Hz, 1H, Ph*H*), 7.40 – 7.07 (m, 8H, Ph*H*), 5.77 – 5.62 (m, 1H, CH₂CHCH₂), 5.13 – 5.03 (m, 2H, CHCH₂), 3.74 (d, *J* 13.8 Hz, 1H), 3.65 (d, *J* 2.0 Hz, 1H), 2.48 – 2.31 (m, 2H, NHCH₂Ph), 2.07 (brs, 1H, NH). **¹³C NMR** (101 MHz, Chloroform-*d*) δ 144.1 (C, Ar), 139.8 (C, Ar), 135.8 (CH, CH₂CHCH₂), 133.3 (CH, Ar), 131.2 (CH, Ar), 129.0 (CH, Ar), 128.8 (CH, Ar), 127.8 (CH, Ar), 127.7 (CH, Ar), 127.6 (CH,

Ar), 124.5 (CH, Ar), 118.2 (CH₂, CH₂CH₂CH), 61.4 (CH, PhCHNH), 51.5 (CH₂, NHCH₂), 43.4 (CH₂, PhCHCH₂). **MS** TOF EI⁺ (*m/z*): 317.2 [M+H]⁺.

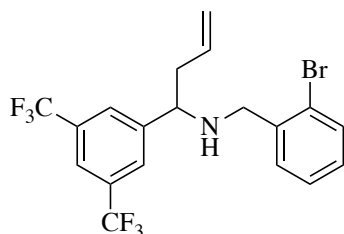
5.3.2.2. *N*-(3,5-bis(trifluoromethyl)benzyl)-1-(2-bromophenyl)but-3-en-1-amine (**2b**)



Prepared using *General Procedure B*: Imine **1g** (1.0 g, 2.4 mmol, 1.0 Eq), zinc (dust, 560 mg, 8.5 mmol, 3.5 Eq), allyl bromide (630 μ L, 7.3 mmol, 3.0 Eq) in THF (8 mL). Colourless oil, 930 mg, 85%.

¹H NMR (400 MHz, Chloroform-*d*) δ 7.73 (s, 3H, PhH), 7.54 (ddd, *J* 9.3, 7.9, 1.5 Hz, 2H, PhH), 7.33 (td, *J* 7.6, 1.3 Hz, 1H, PhH), 7.11 (ddd, *J* 8.0, 7.3, 1.8 Hz, 1H, PhH), 5.78 (m, 1H, CH₂CHCH₂), 5.16 – 5.09 (m, 2H, CHCH₂), 4.20 (dd, *J* 8.7, 4.6 Hz, 1H), 3.73 (d, *J* 2.9 Hz, 2H), 2.56 – 2.46 (m, 1H, CHCH₂CH), 2.34 – 2.24 (m, 1H, CHCH₂CH). **¹³C NMR** (101 MHz, Chloroform-*d*) δ 143.1, 141.7, 134.8, 133.0, 128.7, 128.1, 127.8, 124.1, 120.8, 118.3, 60.1, 50.8, 41.4. **MS** TOF EI⁺ (*m/z*): 452.2 [M]⁺. **FTIR** ν_{max} 1281, 1135.

5.3.2.3. 1-(3,5-bis(trifluoromethyl)phenyl)-*N*-(2-bromobenzyl)but-3-en-1-amine (**2c**)

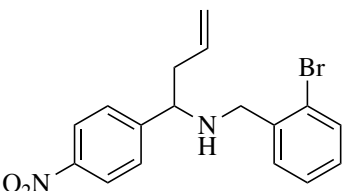


Prepared using *General Procedure B*: Imine **1h** (1.0g, 2.4 mmol, 3.0 Eq), zinc (dust, 550 mg, 8.5 mmol, 3.5 Eq), allyl bromide (630 μ L, 7.3 mmol, 3.0 Eq) in THF (anhydrous, 5 mL, 0.3M). Colourless oil, 830 mg, 83%

¹H NMR (400 MHz, Chloroform-*d*) δ 7.87 (s, 1H, PhH), 7.78 (s, 1H, PhH), 7.53 (dd, *J* 7.9, 1.3 Hz, 1H, PhH), 7.28 – 7.23 (m, 1H, PhH), 7.19 – 7.10 (m, 1H, PhH), 5.73 – 5.61 (m, 1H,

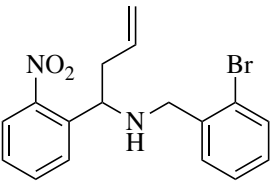
PhCHNH), 5.15 – 5.06 (m, 2H, NHCH₂Ph), 3.79 (dd, *J* 8.5, 5.2 Hz, 2H, NHCH₂Ph), 3.66 (dd, *J* 13.4, 2.8 Hz, 2H, CHCH₂CH), 1.87 (s, 1H, br s). ¹³C NMR (101 MHz, Chloroform-*d*) δ 133.9, 133.0, 132.9, 130.8, 130.7, 129.8, 127.7, 127.5, 119.0, 60.9, 51.8, 43.2. MS TOF EI+ (*m/z*): 452.0 [M]⁺. FTIR ν_{max} 1640, 1277, 682.

5.3.2.4. *N*-(2-bromobenzyl)-1-(4-nitrophenyl)but-3-en-1-amine (**2d**)

 Prepared using *General Procedure B*: Imine **1i** (4.0g, 12.5 mmol, 1.0 Eq), zinc (dust, 2.9g, 43.9 mmol, 3.5 Eq), allyl bromide (3.3 mL, 37.6 mmol, 3.0 Eq) in THF (anhydrous, 20 mL). White fluffy solid, 4.53g, 58%.

¹H NMR (400 MHz, Chloroform-*d*) δ 8.24 – 8.19 (m, 8H, PhN & PhBr), 5.72 – 5.61 (m, 1H, CH₂CHCH₂), 5.12 – 5.05 (m, 2H, CHCH₂), 3.77 (dd, *J* 8.1, 5.4 Hz, 2H, CHCH₂CH), 3.66 (dd, 2H, NHCH₂Ph). ¹³C NMR (101 MHz, Chloroform-*d*) δ 134.1, 133.0, 130.5, 128.9, 128.2, 127.4, 123.7, 118.7, 60.9, 51.7, 43.01. MS TOF EI+ (*m/z*): 361.0 [M]⁺

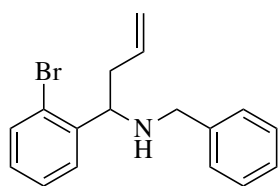
5.3.2.5. *N*-(2-bromobenzyl)-1-(2-nitrophenyl)but-3-en-1-amine (**2e**)

 Prepared using *General Procedure B*: Imine **1j** (1.5g, 4.7 mmol, 1.0 Eq), zinc (dust, 1.1g, 14.0 mmol, 3.5 Eq), allyl bromide (1.2 mL, 16.5 mmol, 3.0 Eq) in THF (anhydrous, 15 mL, 0.3M). Colourless oil, 240 mg, 14%.

¹H NMR (400 MHz, Chloroform-*d*) δ 7.97 (dd, *J* 7.9, 1.4 Hz, 1H, PhH), 7.81 (dd, *J* 8.1, 1.4 Hz, 1H, PhH), 7.65 – 7.59 (m, 1H, PhH), 7.51 (dd, *J* 7.9, 1.4 Hz, 1H, PhH), 7.39 (ddd, *J* 8.5,

7.4, 1.4 Hz, 1H, *PhH*), 7.22 (dd, $J = 7.5, 1.3$ Hz, 1H, *PhH*), 7.17 – 7.08 (m, 1H, *PhH*), 5.82 – 5.70 (m, 1H, CH_2CHCH_2), 5.15 – 5.08 (m, 2H, CHCH_2), 4.19 (dd, $J 8.9, 4.0$ Hz, 1H, CHCH_2CH), 3.61 (dd, $J 8.9, 4.0$ Hz, 1H, CHCH_2CH), 2.66 – 2.59 (m, 1H), 2.29 (dt, $J 14.0, 8.8$ Hz, 1H), 1.56 (br s, 1H, *NH*). ^{13}C NMR (101 MHz, Chloroform-*d*) δ 142.4 (ArC), 140.4 (ArC), 135.0 (ArC), 132.6 (CH_2CHCH_2), 128.7 (ArCH), 128.7 (ArCH), 128.6 (ArCH), 128.5 (ArCH), 128.4 (ArCH), 128.1 (ArCH), 128.1 (ArCH), 126.9 (ArCH), 117.9 (CHCH_2), 114.4 (ArC), 60.9 (CHCH_2CH), 51.4 (NHCH_2Ar), 43.1 (CH_2CHCH_2). MS TOF EI+ (m/z): 361.0 [M]⁺

5.3.2.6. *N*-benzyl-1-(2-bromophenyl)but-3-en-1-amine (**2f**)

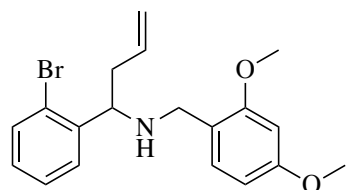


Prepared using *General Procedure B*: Imine **1b** (2.0g, 7.3 mmol, 1.0 Eq), zinc (dust, 2.9g, 29.2 mmol, 3.5 Eq), allyl bromide (1.9 mL, 22.0 mmol, 3.0 Eq) in THF (12.0 mL, 0.3 M). Yellow oil, 720 mg, 30%.

Data in agreement with the reported literature values.⁴⁴

^1H NMR (400 MHz, Chloroform-*d*) δ 7.54 – 7.51 (m, 1H, *PhH*), 7.40 – 7.32 (m, 4H, *PhH*), 7.30 – 7.22 (m, 3H, *PhH*), 7.14 – 7.08 (m, 1H, *PhH*), 5.75 – 5.64 (m, 1H, CH_2CHCH_2), 5.12 – 5.04 (m, 2H, CHCH_2), 3.76 – 3.69 (m, 1H, PhCHNH), 3.67 – 3.60 (m, 2H, NHCH_2Ph), 2.47 – 2.33 (m, 2H, CHCH_2), 1.79 (br s, 1H, *NH*). ^{13}C NMR (101 MHz, Chloroform-*d*) δ 143.6 (C, Ar), 139.3 (C, Ar), 135.4 (CH, CH_2CHCH_2), 132.9 (CH, Ar), 128.6 (CH, Ar), 128.4 (CH, Ar), 127.4 (CH, Ar), 127.3 (CH, Ar), 127.2 (CH, Ar), 117.9 (CH_2 , $\text{CH}_2\text{CH}_2\text{CH}$), 61.3 (CH, PhCHNH), 51.6 (CH_2 , NHCH_2Ph), 43.3 (CH_2CH_2). MS TOF EI+ (m/z): 317.2 [M+H]⁺

5.3.2.7. 1-(2-bromophenyl)-*N*-(2,4-dimethoxybenzyl)but-3-en-1-amine (**2g**)

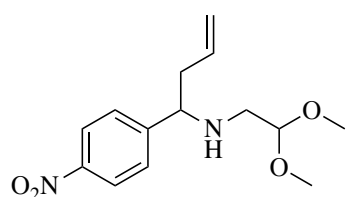


Prepared using *General Procedure B*: Imine **1f** (1.1g, 3.3 mmol, 1.0 Eq), zinc (dust, 750mg, 12.0 mmol, 3.5 Eq), allyl bromide (850 μ L, 9.9 mmol, 3.0 Eq) in THF (10 mL). Yellow oil, 850 mg,

88%.

¹H NMR (400 MHz, Chloroform-*d*) δ 7.68 (dd, *J* 7.8, 1.8 Hz, 1H, PhH), 7.53 (dd, *J* 7.9, 1.3 Hz, 1H, PhH), 7.37 – 7.30 (m, 1H, PhH), 7.10 (ddd, *J* 8.0, 7.3, 1.8 Hz, 1H, PhH), 6.99 (d, *J* 8.1 Hz, 1H, PhH), 6.45 – 6.36 (m, 2H, PhH), 5.72 (m, 1H, CH₂CHCH₂), 5.10 – 5.01 (m, 2H, CHCH₂), 4.16 – 4.09 (m, 1H, NHCH₂Ph), 3.80 (s, 3H, OCH₃), 3.78 (s, 3H, OCH₃), 3.62 (d, *J* 13.1 Hz, 1H, PhCHNH), 3.42 (d, *J* 13.1 Hz, 1H, NH). **¹³C NMR** (101 MHz, Chloroform-*d*) δ 160.4, 158.9, 143.2, 135.7, 133.2, 130.9, 129.0, 128.6, 127.9, 124.6, 121.3, 117.9, 104.1, 98.9, 59.6, 55.8, 55.6, 47.2, 41.8. **MS** TOF EI+: 376.26 [M⁺]. **FTIR** ν_{max} 2936, 1613, 1208.

5.3.2.8. *N*-(2,2-dimethoxyethyl)-1-(4-nitrophenyl)but-3-en-1-amine (**2h**)



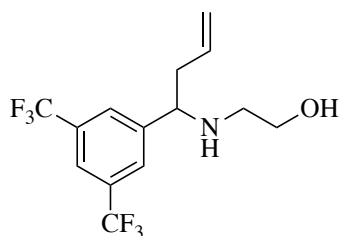
Prepared using *General Procedure B*: Imine **1m** (2.5 g, 10.5 mmol, 1.0 Eq), zinc (dust, 2.1 g, 31.5 mmol, 3.5 Eq), allyl bromide (2.7. mL, 31.5 mmol, 3.0 Eq) in THF (20 mL). Yellow

oil, 1.4g, 48%.

¹H NMR (400 MHz, Chloroform-*d*) δ 8.21 – 8.17 (m, 2H, 3- & 5-*H* C₆H₄(NO₂)), 7.52 – 7.49 (m, 2H, 2- & 6-*H* C₆H₄(NO₂)), 5.75 – 5.63 (m, 1H, CH₂CHCH₂), 5.13 – 5.04 (m, 2H, CH₂CHCH₂), 4.41 (dd, *J* 6.1, 4.7 Hz, 1H, CH(CH₃)₂), 3.77 (t, *J* 6.7 Hz, 1H, CHCH₂CH), 3.36 (s, 3H, CH₃), 3.31 (s, 3H, CH₃), 2.59 (dd, *J* 12.1, 6.1 Hz, 1H, NHCHHCH(OCH₃)₂), 2.48 (dd,

J 12.1, 6.1 Hz, 1H, NHCH \dot{H} CH(OCH $_3$) $_2$), 2.42 – 2.34 (m, 2H, CHCH $_2$ CH). ^{13}C NMR (101 MHz, Chloroform- d) δ 151.7 (1- C C $_6$ H $_4$ (NO $_2$)), 147.2 (4- C C $_6$ H $_4$ (NO $_2$)), 134.1 (CH $_2$ CHCH $_2$), 128.0 (2- & 6- C C $_6$ H $_4$ (NO $_2$)), 123.7 (3- & 5- C C $_6$ H $_4$ (NO $_2$)), 118.6 (CH $_2$ CHCH $_2$), 103.6 (CH(CH $_3$) $_2$), 62.2 (CHCH $_2$ CH), 53.9 (CH $_3$), 53.8 (CH $_3$), 49.0 (NHCH $_2$ CH(OCH $_3$) $_2$), 42.8 (CH $_2$ CHCH $_2$). MS TOF EI $^+$: 281.2 [M+H] $^+$.

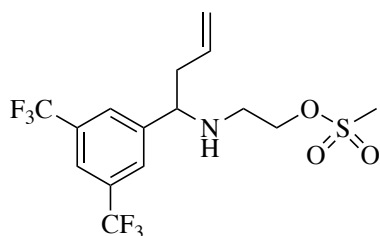
5.3.2.9. 2-((1-(3,5-bis(trifluoromethyl)phenyl)but-3-en-1-yl)amino)ethan-1-ol (**2i**)



Prepared using *General Procedure B*: Imine **1k** (8.25g, 28.9 mmol, 1.0 Eq), Zinc (dust, 6.05g, 93 mmol, 3.2 Eq) and allyl bromide (7.51 mL, 87 mmol, 3.0 Eq) in THF (100ml). Colourless oil, 8.16 g, 86%.

^1H NMR (400 MHz, Chloroform- d) δ 7.82 (s, 2H, Ar 2- & 6- H C $_6$ H $_3$ (CF $_3$) $_2$), 7.78 (s, 1H, Ar 4- H C $_6$ H $_3$ (CF $_3$) $_2$), 5.76 – 5.64 (m, 1H, CH $_2$ CHCH $_2$), 5.15 – 5.08 (m, 2H, CH $_2$ CHCH $_2$), 3.87 (t, J 6.8 Hz, 1H, ArCCHNH), 3.69 (ddd, J 10.2, 6.4, 3.8 Hz, 1H, NHCH $_2$ CHHOH), 3.62 (ddd, J 10.2, 6.4, 3.9 Hz, 1H, NHCH $_2$ CHHOH), 2.71 (ddd, J 12.3, 6.4, 3.8 Hz, 1H, NHCH \dot{H} CH $_2$ OH), 2.56 (ddd, J 12.3, 6.4, 3.9 Hz, 1H, NHCH \dot{H} CH $_2$ OH), 2.49 – 2.43 (m, 2H), CHCH $_2$ CH, 2.40 (s, 1H, NH). ^{13}C NMR (101 MHz, Chloroform- d) δ 146.2 (+ , 1- C C $_6$ H $_3$ (CF $_3$) $_2$), 133.6 (- , CH $_2$ CHCH $_2$), 131.8 (+ , q, J 33.4 Hz, C(CF $_3$) $_2$), 127.5 (- , 2- & 6-CH C $_6$ H $_3$ (CF $_3$) $_2$), 123.4 (+ , q, J 272.3 Hz, C(CF $_3$) $_2$), 121.4 (- , 4-CH C $_6$ H $_3$ (CF $_3$) $_2$), 119.1 (+ , CH $_3$ CHCH $_2$), 61.9 (- , ArCCHNH), 61.3 (+ , NHCH $_2$ CH $_2$ OH), 49.2 (+ , NHCH $_2$ CH $_2$ OH), 42.5 (+ , CHCH $_2$ CH). MS TOF EI $^+$ (m/z): 328.1 [M+H] $^+$

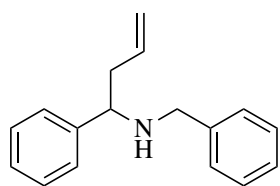
5.3.2.10. 2-((1-(3,5-bis(trifluoromethyl)phenyl)but-3-en-1-yl)amino)ethyl methanesulfonate
(**2j**)



A solution of Homoallylic amine **2i** (5.81g, 17.75 mmol, 1.0 Eq) was prepared in DCM (100 mL, 0.18 M) and was cooled to 0°C using an icebath. MsCl (1.52g, 19.53 mmol, 1.1 Eq), and TEA (3.71 mL, 26.6 mmol, 1.5 Eq) were added as a single portion, the reaction mixture was stirred at 0°C for 30 mins. The reaction was quenched with water (30 mL) and was extracted with DCM (3 x 30 mL), organic fractions were dried over Na₂SO₄, volatile components were removed in vacuo giving (**2i-i**) as a yellow oil, 7.2 g, 98%.

¹H NMR (400 MHz, Chloroform-*d*) δ 7.82 (s, 2H, Ar 2- & 6-*H* C₆H₃(CF₃)₂), 7.77 (s, 1H, Ar 4-*H* C₆H₃(CF₃)₂), 5.76 – 5.64 (m, 1H, CH₂CHCH₂), 5.17 – 5.07 (m, 2H, CH₂CHCH₂), 4.30 (ddd, *J* 9.8, 6.1, 3.6 Hz, 1H, NHCH₂CHHO), 4.21 (ddd, *J* 9.8, 6.1, 3.6 Hz, 1H, NHCH₂CHHO), 3.84 (dd, *J* 8.1, 5.4 Hz, 1H, ArCHNH), 3.03 (s, 3H, CH₃), 2.86 (ddd, *J* 13.5, 7.0, 3.6 Hz, 1H, NHCHHCH₂O), 2.69 (ddd, *J* 13.5, 7.0, 3.6 Hz, 1H, NHCHHCH₂O), 2.47 – 2.29 (m, 2H, CHCH₂CH), 1.90 (s, 1H, NH). **¹³C NMR** (101 MHz, Chloroform-*d*) δ 133.3 (1-*C* C₆H₃(CF₃)₂), 132.0 (CH₂CHCH₂), 131.7 (3- & 5-*C* C₆H₃(CF₃)₂), 127.7 (2- & 6-*C* C₆H₃(CF₃)₂), 121.6 (4-*C* C₆H₃(CF₃)₂), 119.4 (CH₂CHCH₂), 61.5 (NHCH₂CH₂), 46.0 (ArCHNH), 39.4 (NHCH₂CH₂), 37.5 (CHCH₂CH), 8.6 (CH₃). **MS** TOF EI⁺: 406.1 [M+H]⁺. **FTIR** ν_{max} 1263, 730.

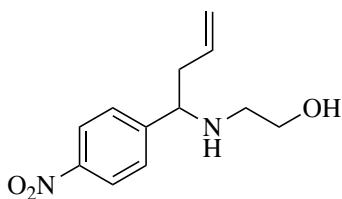
5.3.2.11. *N*-benzyl-1-phenylbut-3-en-1-amine (**2k**)



Prepared using *General Procedure B*: Imine **1a** (0.87 g, 3.4 mmol, 1.0 Eq), zinc (dust, 0.78g, 12.0 mmol, 3.5 Eq) and allyl bromide (0.88 mL, 10.0 mmol, 3.0 Eq) in THF (9 mL). Pale yellow oil, 370 mg, 44%. Data in agreement with the reported literature values.²⁵⁸

¹H NMR (300 MHz, Chloroform-*d*) δ 7.38 – 7.21 (m, 9H, PhH), 5.80 – 5.63 (m, 1H, CH₂CHCH₂), 5.10 – 4.98 (m, 2H, CHCH₂), 3.73 – 3.65 (m, 1H, PhCHNH), 3.52 (d, *J* 13.3 Hz, 2H, NHCH₂Ph), 1.81 (s, 1H, NH). **¹³C NMR** (75 MHz, Chloroform-*d*) δ 135.5, 128.4, 128.3, 128.1, 127.3, 127.1, 126.8, 118.8, 117.6, 61.6, 51.4, 43.2, 30.9. **FTIR** ν_{max} 1610, 1587.

5.3.2.12. 2-((1-(4-nitrophenyl)but-3-en-1-yl)amino)ethan-1-ol (**2l**)

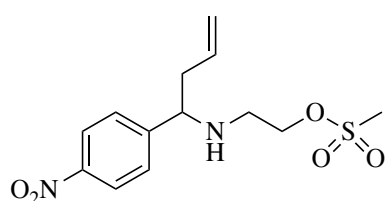


Prepared using *General Procedure B*: Imine **1l** (4.50g, 23.2 mmol, 1.0 Eq), zinc (dust, 4.85g, 74.2 mmol, 3.2 Eq) and allyl bromide (6.02 mL, 69.5 mmol, 3.0 Eq) in THF (100 mL). Pale yellow oil, 5.48g, 88%.

¹H NMR (400MHz, Chloroform-*d*) δ 8.22 – 8.17 (m, 2H, 3- & 5-*H* C₆H₄NO₂), 7.54 – 7.46 (m, 2H, 2- & 6-*H* C₆H₄NO₂), 5.76 – 5.64 (m, 1H, CH₂CHCH₂), 5.13 – 5.07 (m, 2H, CH₂CHCH₂), 3.85 – 3.79 (m, 1H, ArCHNH), 3.65 (ddd, *J* 10.7, 6.5, 3.8 Hz, 1H, NHCH₂CHH), 3.57 (ddd, *J* 10.7, 6.5, 3.8 Hz, 1H, NHCH₂CHH), 2.68 (ddd, *J* 12.3, 6.3, 3.8 Hz, 1H, NHCHHCH₂), 2.54 (ddd, *J* 12.3, 6.3, 3.8 Hz, 1H, NHCHHCH₂), 2.48 – 2.35 (m, 2H, CH₂CHCH₂). **¹³C NMR** (101 MHz, Chloroform-*d*) δ 151.6 (1-*C* C₆H₄NO₂), 147.2 (4-*C* C₆H₄NO₂), 134.1 (CH₂CHCH₂),

127.9 (3- & 5-*C* C₆H₄NO₂), 123.8 (2- & 6-*H* C₆H₄NO₂), 118.7 (CH₂CHCH₂), 62.0 (NHCH₂CH₂), 61.5 (ArCHNH), 49.2 (NHCH₂CH₂), 42.8 (CH₂CHCH₂). **MS** TOF EI⁺ (*m/z*): 237.1 [M+H].

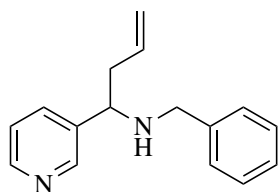
5.3.2.13. 2-((1-(4-nitrophenyl)but-3-en-1-yl)amino)ethyl methanesulfonate (**2m**)



A solution of Homoallylic amine **2l** (2.05g, 8.68 mmol, 1.0 Eq) was prepared in DCM (50 mL, 0.17M) and was cooled to 0°C using an icebath. MsCl (744 µL, 9.54 mmol, 1.1 Eq), and TEA (3.63 mL, 26.0 mmol, 3.0 Eq) were added as a single portion, the reaction mixture was stirred at 0°C for 30 mins. The reaction was quenched with water (20 mL) and was extracted with DCM (3 x 20 mL), organic fractions were dried over Na₂SO₄, volatile components were removed in vacuo giving (**2m**) as a yellow oil, 2.89g, >99%.

¹H NMR (400 MHz, Chloroform-*d*) δ 8.21 – 8.16 (m, 2H, 3- & 5-*H* C₆H₄NO₂), 7.53 – 7.48 (m, 2H, 2- & 6-*H* C₆H₄NO₂), 5.75 – 5.62 (m, 1H, CH₂CHCH₂), 5.14 – 5.04 (m, 2H, CH₂CHCH₂), 4.32 – 4.25 (ddd, *J* 10.5, 7.1, 3.8 Hz, 1H, NHCH₂CHH), 4.21 (ddd, *J* 10.5, 7.1, 3.8 Hz, 1H, NHCH₂CHH), 3.85 – 3.82 (m, 1H, ArCHNH), 3.03 (s, 3H, CH₃), 2.84 (ddd, *J* 13.6, 7.1, 3.8 Hz, 1H, NHCH₂CH₂O), 2.70 (ddd, *J* 13.6, 7.1, 3.8 Hz, 1H, NHCH₂CH₂O), 2.45 – 2.33 (m, 2H, CH₂CHCH₂). **¹³C NMR** (101 MHz, Chloroform-*d*) δ 150.9 (4-*C* C₆H₄NO₂), 147.3 (1-*C* C₆H₄NO₂), 133.8 (CH₂CHCH₂), 128.1 (2- & 6-*C* C₆H₄NO₂), 123.8 (3- & 5-*C* C₆H₄NO₂), 118.9 (CH₂CHCH₂), 61.5 (NHCH₂CH₂O), 53.4 (ArCHNH), 46.1 (NHCH₂CH₂O), 39.4 (CH₂CHCH₂), 37.5 (CH₃). **MS** TOF EI⁺: 315.0 [M+H]⁺. **FTIR** ν_{max} 3418, 1520, 1345, 1155, 857.

5.3.2.14. *N*-benzyl-1-(pyridin-3-yl)but-3-en-1-amine (**2n**)

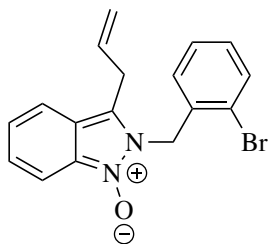


Prepared using General Procedure B: Imine (6.0 g, 30.6 mmol, 1.0 Eq), zinc (dust, 6.4g, 98.0 mmol, 3.2 Eq), allyl bromide (7.9 mL, 92.0 mmol, 3.0 Eq) in THF (anhydrous, 250 mL, 0.3M). Brown oil, 6.9g,

95%. Data in agreement with the reported literature values.²⁵⁹

¹H NMR (400 MHz, Chloroform-*d*) δ 8.57 (d, *J* 2.2 Hz, 1H, 2-CH C₅H₄N), 8.52 (dd, *J* 4.8, 1.7 Hz, 1H, 4-CH C₅H₄N), 7.74 (dt, *J* 8.0, 2.0 Hz, 1H, 2-CH C₅H₄N), 7.34 – 7.21 (m, 6H, 5-CH C₅H₄N, 2-, 3-, 4-, 5- & 6-CH C₆H₅), 5.75 – 5.63 (m, 1H, CH₂CHCH₂), 5.11 – 5.04 (m, 2H, CHCH₂), 3.74 (t, *J* 6.1 Hz, 1H, (C₆H₄N)CHNH), 3.61 (dd, *J* 53.6, 12.5 Hz, 2H, CHCH₂CH), 2.46 – 2.36 (m, 2H, NHCH₂(C₆H₅)), 1.76 (s, 1H, NH). **¹³C NMR** (101 MHz, Chloroform-*d*) δ 149.6 (- , 2-CH C₆H₄N), 148.7 (- , 4-CH C₆H₄N), 140.1 (+ , 1-C C₆H₅), 139.1 (+ , 1-C C₆H₄N), 134.8 (- , 6-CH C₆H₄N), 134.6 (- , 5-CH C₆H₄N), 128.4 (- , 3- & 5-CH C₆H₅), 128.1 (- , 2- & 6-CH C₆H₅), 127.1 (- , 4-CH C₆H₅), 123.5 (- , CH₂CHCH₂), 118.4 (+ , CH₂CHCH₂), 59.2 (- , (C₅H₄N)CHNH), 51.5 (+ , NHCH₂(C₆H₅)), 42.9 (+ , CHCH₂CH). **MS** TOF EI+ (*m/z*): 239.2 [M+H]⁺.

5.3.2.15. 3-allyl-2-(2-bromobenzyl)-2*H*-indazole 1-oxide (**2o**)

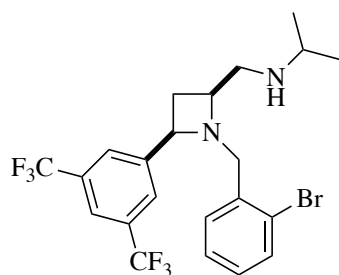


Prepared using General Procedure B: Imine **1j** (5.0 g, 15.7 mmol, 1.0 Eq), zinc (dust, 3.6 g, 54.8 mmol, 3.5 Eq), allyl bromide (4.1 mL, 47.0 mmol, 3.0 Eq) in THF (anhydrous, 20 mL, 0.3M). Orange crystalline solid, 5.1g, 93%.

¹H NMR (400 MHz, Chloroform-*d*) δ 7.74 (d, *J* 8.9 Hz, 1H, ArCH), 7.59 (dd, *J* 7.4, 1.9 Hz, 1H, ArCH), 7.56 – 7.52 (m, 1H, ArCH), 7.32 – 7.27 (m, 1H, , ArCH), 7.20 – 7.12 (m, 2H, ArCH), 7.09 (dd, *J* 8.7, 6.5 Hz, 1H), 6.69 (dd, *J* 7.1, 2.2 Hz, 1H, , ArCH), 5.83 (s, 2H, CH₂(C₆H₄Br)), 5.82 – 5.72 (m, 1H, CH₂CHCH₂), 5.12 – 4.99 (m, 2H, CH₂CHCH₂), 3.63 (dt, *J* 6.0, 1.7 Hz, 2H, CH₂CHCH₂). **¹³C NMR** (101 MHz, Chloroform-*d*) δ 132.8 (ArCH), 132.3 (CH₂CHCH₂), 129.5 (CCH₂CH), 128.2 (ArCH), 128.0 (ArCH), 126.9 (ArCH), 123.4 (ArCH), 119.4 (ArCH), 117.9 (CH₂CHCH₂), 113.2 (ArCH), 46.2 (CH₂(C₆H₄Br)), 29.1 (CH₂CHCH₂). **MS TOF EI+**: 343.1 [M⁺].

5.3.3. Amino-Azetidines

5.3.3.1. *rac*-*N*-(2,4-*cis*)-4-(3,5-bis(trifluoromethyl)phenyl)-1-(2-bromobenzyl)azetidin-2-yl)methyl)propan-2-amine (**3a**)

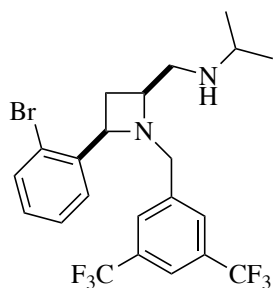


Prepared using *General Method C*: Homoallylic Amine **2c** (567 mg, 1.3 mmol, 1.0 Eq), Iodine (960 mg, 3.8 mmol, 3.0 Eq), NaHCO₃ (530 mg, 6.3 mmol, 5.0 Eq) in CH₃CN (5 mL), following isolation the iodo-azetidine intermediate was stirred with *N*-isopropyl amine (neat, 5 mL). Brown oil, 586 mg, 78%.

¹H NMR (400 MHz, Chloroform-*d*) δ 7.78 (s, 2H, Ar 2- & 6-*H* C₆H₃(CF₃)₂), 7.71 – 7.67 (m, 2H, ArH 4-*H* C₆H₃(CF₃)₂, ArH C₆H₄Br), 7.42 (dd, *J* 8.0, 1.2 Hz, 1H, Ar C₆H₄Br), 7.29 (td, *J* 7.6, 1.4 Hz, 1H, Ar C₆H₄Br), 7.06 (td, *J* 7.6, 1.4 Hz, 1H, Ar C₆H₄Br), 4.42 (app t, *J* 8.2 Hz, 1H, ArCCHCH₂), 3.91 (d, *J* 12.2 Hz, 1H NCHHArC), 3.71 (d, *J* 12.2 Hz, 1H, NCHHArC), 3.46 – 3.37 (m, 1H, NHCH(CH₃)₂), 2.72 (dt, *J* 10.5, 7.6 Hz, 1H, CHCH₂HNH), 2.66 – 2.56 (m, 2H, CH₂CHCH₂NH, CH₂CHCH₂HNH), 2.50 (dd, *J* 11.9, 5.8 Hz, 1H, CH₂CHCH₂HNH), 1.78 (dt, *J* 10.5, 8.5 Hz, 1H, CHCH₂HNH), 0.98 (d, *J* 6.3 Hz, 3H, NHCH(CH₃)₂), 0.92 (d, *J* 6.3 Hz, 3H, NHCH(CH₃)₂). **¹³C NMR** (101 MHz, Chloroform-*d*) δ 141.6 (+, ArCCH), 141.4 (+, ArCCH₂), 132.3 (-, ArCH), 131.4 (q, *J* 33.3 Hz, ArC(CF₃)₂), 129.1 (-, ArC 2- & 6-*H* C₆H₃(CF₃)₂), 128.5 (-, ArCH), 128.1 (-, ArCH), 127.5 (-, ArCH), 124.6 (+, ArC(CF₃)), 122.0 (+, ArCBr), 121.9 (+, ArC(CF₃)), 121.1 (-, ArC 4-*H* C₆H₃(CF₃)₂), 64.8 (-, ArCCHCH₂), 63.3 (-, NHCH(CH₃)₂), 61.2 (+, NCH₂ArC₆H₃(CF₃)₂), 52.1 (+, CHCH₂NH), 49.1 (-, CH₂CHCH₂), 30.9 (+, CHCH₂CH), 22.6 (-, CH(CH₃)₂), 22.2 (-, CH(CH₃)₂). **¹⁹F NMR** (377 MHz, Chloroform-*d*) δ -62.86 (C(CF₃)). **MS** TOF EI+ (*m/z*): 509.76 [M]⁺. **FTIR**

ν_{max} 1253, 1189, 1174. **HRMS** (m/z): calcd. for $\text{C}_{22}\text{H}_{23}\text{BrF}_6\text{N}_2$ $[\text{M}+\text{NH}_4]^+$, 525.09707, found, 525.0969.

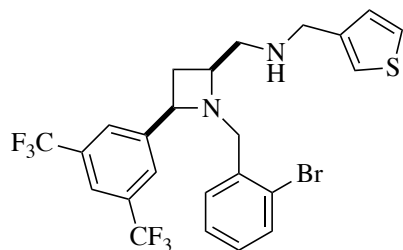
5.3.3.2. *rac-N*-(2,4-*cis*)-1-(3,5-bis(trifluoromethyl)benzyl)-4-(2-bromophenyl)azetidin-2-yl)methyl)propan-2-amine (**3b**)



Prepared using *General Method C*: Homoallylic Amine **2c** (470 mg, 1.0 mmol, 1.0 Eq), Iodine (790 mg, 3.1 mmol, 3.0 Eq), NaHCO_3 (440 mg, 5.2 mmol, 5.0 Eq) in CH_3CN (5 mL), following isolation the iodoazetidine intermediate was stirred with *N*-isopropyl amine (neat, 5 mL). Brown oil, 550 mg, 95%.

^1H NMR (400 MHz, Chloroform- d) δ 7.79 (s, 2H, Ar 2- & 6- H $\text{C}_6\text{H}_3(\text{CF}_3)_2$), 7.72 – 7.68 (m, 2H, Ar 4- H $\text{C}_6\text{H}_3(\text{CF}_3)_2$, Ar $\text{C}_6\text{H}_4\text{Br}$), 7.42 (dd, J 8.0, 1.2 Hz, 1H, Ar $\text{C}_6\text{H}_4\text{Br}$), 7.31 – 7.27 (m, 1H, Ar $\text{C}_6\text{H}_4\text{Br}$), 7.06 (td, J 7.6, 1.8 Hz, 1H, Ar $\text{C}_6\text{H}_4\text{Br}$), 4.42 (app t, J 8.2 Hz, 1H, ArCCHCH_2), 3.94 (d, J 13.3 Hz, 1H, NCHHArC) 3.74 (d, J 13.3 Hz, 1H, NCHHArC), 3.46 – 3.38 (m, 1H, $\text{CH}(\text{CH}_3)$), 2.72 (dt, J 10.5, 7.6 Hz, 1H, CHCHHCH), 2.66 – 2.59 (m, 2H, CHCHHCH), 2.51 (dd, J 11.9, 5.8 Hz, 2H, CHCHHCH), 1.78 (dt, J 10.5, 8.5 Hz, 1H, CHCHHCH), 0.98 (d, J 6.3 Hz, 3H, $\text{CH}(\text{CH}_3)$), 0.93 (d, J 6.3 Hz, 3H, $\text{CH}(\text{CH}_3)$). **^{13}C NMR** (101 MHz, Chloroform- d) δ 141.6 (+, ArCCH), 141.4 (+, ArCCH), 132.3 (-, ArCH), 131.6 (+, $\text{ArC}(\text{CF}_3)_2$), 131.2 (+, $\text{ArC}(\text{CF}_3)_2$), 129.1 (-, ArC 2- or 6- H $\text{C}_6\text{H}_3(\text{CF}_3)_2$), 128.5 (-, ArCH), 128.1 (-, ArCH), 127.5 (-, ArCH), 124.6, (+, $\text{ArC}(\text{CF}_3)_2$), 122.0 (+, ArCBr), 121.1 (-, ArC 4- H $\text{C}_6\text{H}_3(\text{CF}_3)_2$), 64.7 (-, ArCCHCH_2), 63.3 (-, $\text{CH}(\text{CH}_3)_2$), 61.2 (+, NCH_2ArC), 52.1 (+, $\text{CHCH}_2\text{CH}(\text{CH}_3)_2$), 49.1 (-, CH_2CHCH_2), 30.9 (+, ArCCHCH_2), 22.7 (-, $\text{CH}(\text{CH}_3)_2$), 22.3 (-, $\text{CH}(\text{CH}_3)_2$). **MS** TOF EI^+ : 509.76 $[\text{M}]^+$ **FTIR** ν_{max} 2992, 1185, 1134.

5.3.3.3. *rac-N-(2,4-cis)-4-(3,5-bis(trifluoromethyl)phenyl)-1-(2-bromobenzyl)azetidin-2-yl)-N-(thiophen-3-ylmethyl)methanamine (3c)*

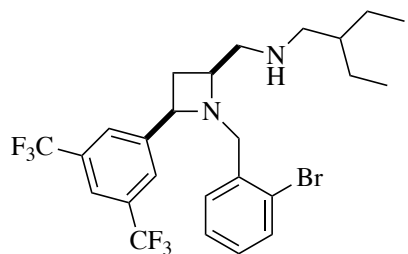


Prepared using *General Procedure C* in a parallel fashion:

Iodo-azetidine starting material (45 mg, 0.08 mmol, 1.0 Eq),
thiophen-3-ylmethanamine (23 mg, 0.2 mmol, 2.5 Eq),
triethylamine (0.24 mmol, 3.0 Eq). Brown oil, 18 mg, 40%.

¹H NMR (400 MHz, Chloroform-d) δ 8.52 – 8.49 (m, 2H, 2- & 4-*H* C₄H₃S), 7.76 (s, 2H, Ar 2- & 6-*H* C₆H₃(CF₃)₂), 7.66 (dt, *J* 7.8, 2.0 Hz, 1H, 3-*H* C₄H₃S), 7.62 (s, 1H, 4-*H* C₆H₃(CF₃)₂), 7.40 (dd, *J* 7.9, 1.3 Hz, 1H, 3-*H* C₆H₄Br), 7.17 (dd, *J* 7.9, 1.3 Hz, 1H, 6-*H* C₆H₄Br), 7.05 (td, *J* 7.8, 1.3 Hz, 1H, 5-*H* C₆H₄Br), 6.97 (td, *J* 7.8, 1.4 Hz, 1H, 4-*H* C₆H₄Br), 4.16 (t, *J* 8.1 Hz, 1H, ArCCHCH₂), 3.89 (d, *J* 12.2 Hz, 1H, NCHH(C₆H₄Br)), 3.78 – 3.67 (m, 3H, NCHH(C₆H₄Br), NHCH₂(C₄H₃S)), 3.50 (tt, *J* 8.1, 4.0 Hz, 1H, CH₂CHCH₂), 2.61 – 2.52 (m, 2H, CHCH₂NH), 2.52 – 2.46 (m, 1H, CHCH₂NH), 2.05 (dt, *J* 10.3, 8.4 Hz, 1H, CHCH₂NH), 1.78 (s, 1H, NH). **¹³C NMR** (101 MHz, Chloroform-d) δ 149.6 (1-C C₆H₃(CF₃)₂), 148.4 (1-C C₆H₄Br), 146.0 (1-C C₄H₃S), 136.5 (5-CH C₄H₃S), 135.5 (3-CH C₄H₃S), 133.1 (3-CH C₆H₄Br), 131.7 (6-CH C₆H₄Br), 131.1 (q, *J* 33.1 Hz, C(CF₃)₂), 129.2 (4-CH C₆H₄Br), 127.1 (5-CH C₆H₄Br), 126.8 (2- & 6-CH C₆H₃(CF₃)₂), 124.8 (2-C C₆H₄Br), 123.4 (2-CH C₄H₃S), 120.7 (4-CH C₆H₃(CF₃)₂), 64.6 (ArCCHCH₂), 61.9 (CH₂CHCH₂), 60.9 (NCH₂(C₆H₄Br)), 52.4 (CHCH₂NH), 51.5 (NHCH₂(C₄H₃S)), 30.7 (CHCH₂CH). **MS** ToF EI⁺ (*m/z*): 563.1.

5.3.3.4. *rac*-*N*-(2,4-*cis*)-4-(3,5-bis(trifluoromethyl)phenyl)-1-(2-bromobenzyl)azetidin-2-yl)methyl)pentan-3-amine (**3d**)



Prepared using *General Procedure C* in a parallel fashion:

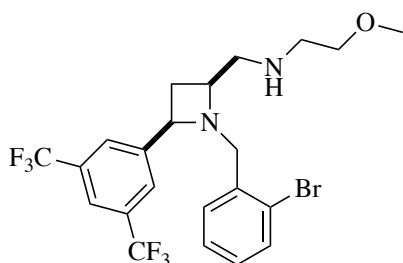
Iodo-azetidine starting material (45 mg, 0.08 mmol, 1.0 Eq),

2-ethylbutan-1-amine (20mg, 0.2 mmol, 2.5 Eq),

triethylamine (0.24 mmol, 3.0 Eq). Brown oil, 18 mg, 40%

¹H NMR (400 MHz, Chloroform-*d*) δ 7.77 (s, 2H, Ar 2- & 6-*H* C₆H₃(CF₃)₂), 7.61 (s, 1H, Ar 4-*H* C₆H₃(CF₃)₂), 7.41 (dd, *J* 8.0, 1.3 Hz, 1H, 3-*H* C₆H₄Br), 7.20 (dd, *J* 7.5, 1.8 Hz, 1H, 6-*H* C₆H₄Br), 7.06 (td, *J* 7.5, 1.8 Hz, 1H, 5-*H* C₆H₄Br), 6.97 (td, *J* 7.5, 1.8 Hz, 1H, 4-*H* C₆H₄Br), 4.15 (app t, *J* 8.2 Hz, 1H, ArCCHCH₂), 3.91 (d, *J* 12.5 Hz, 1H, NCHH(C₆H₄Br)), 3.71 (d, *J* 12.5 Hz, 1H, NCHH(C₆H₄Br)), 3.49 (tt, *J* 8.3, 4.1 Hz, 1H, CH₂CHCH₂), 2.62 – 2.52 (m, 2H, CHCH₂NH), 2.52 – 2.46 (m, 1H, CHCHHCH), 2.45 – 2.36 (m, 2H, NHCH₂CH), 2.03 (dt, *J* 10.4, 8.5 Hz, 1H, CHCHHCH), 1.63 (s, 1H, NH), 1.39 – 1.27 (m, 5H, CH(CH₂CH₃)₂, CH(CH₂CH₃)₂), 0.87 (td, *J* 7.2, 2.7 Hz, 6H, CH(CH₂CH₃)₂). **¹³C NMR** (101 MHz, Chloroform-*d*) δ 146.2 (1-*C* C₆H₃(CF₃)₂), 136.7 (1-*C* C₆H₄Br), 132.9 (3-CH C₆H₄Br), 131.6 (6-CH C₆H₄Br), 131.0 (q, *J* 32 Hz, C(CF₃)₂), 129.1 (5-CH C₆H₄Br), 127.1 (4-CH C₆H₄Br), 126.8 (2- & 6-CH C₆H₃(CF₃)₂), 124.8 (2-*C* C₆H₄Br), 120.4 (4-CH C₆H₃(CF₃)₂), 64.6 (ArCCHCH₂), 62.4 (CH₂CHCH₂), 60.9 (NCH₂(C₆H₄Br)), 53.5 (CHCH₂NH), 53.2 (NHCH₂CH), 41.1 (CH(CH₂CH₃)₂), 30.9 (CHCH₂CH), 24.1 (CH(CH₂CH₃)₂), 23.9 (CH(CH₂CH₃)₂), 11.1 (CH(CH₂CH₃)₂), 10.9 (CH(CH₂CH₃)₂). **FTIR** (ν_{\max} , neat): 2832, 1513, 1278, 1170, 1133. **MS** ToF EI+ (*m/z*): 551.1 [M⁺]. **HRMS** (ESI) *m/z* calcd for C₂₅H₂₉BrF₆N₂ [M+H]⁺ 551.14911, found 551.1481.

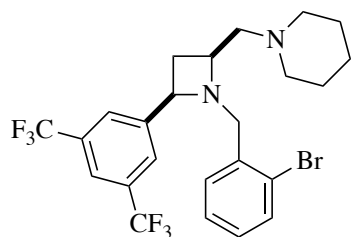
5.3.3.5. *rac*-*N*-(2,4-*cis*)-4-(3,5-bis(trifluoromethyl)phenyl)-1-(2-bromobenzyl)azetidin-2-yl)methyl)-2-methoxyethan-1-amine (**3e**)



Prepared using *General Procedure C* in a parallel fashion: Iodo-azetidine starting material (45 mg, 0.08 mmol, 1.0 Eq), 2-methoxyethan-1-amine (15, mg, 0.2 mmol, 2.5 Eq), triethylamine (0.24 mmol, 3.0 Eq). Brown oil, 10 mg, 23%.

¹H NMR (400 MHz, Chloroform-*d*) δ 7.75 (s, 2H, Ar 2- & 6-*H* C₆H₃(CF₃)₂), 7.60 (s, 1H, Ar 4-*H* C₆H₃(CF₃)₂), 7.41 (dd, *J* 7.9, 1.3 Hz, 1H), 7.27 – 7.17 (m, 3H), 7.06 (td, *J* 7.8, 1.3 Hz, 1H), 6.97 (td, *J* 7.8, 1.8 Hz, 1H), 4.16 (app t, *J* 8.1 Hz, 1H, ArCCHCH₂), 3.92 (d, *J* 12.1 Hz, 1H, NCHH(C₆H₄Br)), 3.72 (d, *J* 12.1 Hz, 1H, NCHH(C₆H₄Br)), 3.51 – 3.47 (m, 3H, CH₂CHCH₂, CH₂CH₂O), 3.37 (s, 3H, OCH₃), 2.76 – 2.72 (m, 2H, NHCH₂CH₂), 2.72 – 2.58 (m, 2H, CHCH₂NH), 2.53 (dt, *J* 10.4, 7.8 Hz, 1H, CHCHHCH), 1.96 (dt, *J* 10.4, 7.8 Hz, 1H, CHCHHCH). **¹³C NMR** (101 MHz, Chloroform-*d*) δ 132.9 (3-CH C₆H₄Br), 131.7 (6-CH C₆H₄Br), 129.0 (5-CH C₆H₄Br), 127.1 (4-CH C₆H₄Br), 126.8 (2- & 6-CH C₆H₃(CF₃)₂), 124.8 (2-C C₆H₄Br), 120.6 (4-CH C₆H₃(CF₃)₂), 71.9 (NHCH₂CH₂O), 64.7 (CHCH₂CH), 61.9 (CHCH₂CH), 60.8 (OCH₃), 58.9 (NCH₂ArC), 53.4 (CHCH₂NH), 49.8 (NHCH₂CH₂O), 31.4 (CH₂CHCH₂). **MS** ToF EI+ (*m/z*): 525.1 [M⁺]. **HRMS** (ESI) *m/z* calcd for C₂₂H₂₃BrF₆N₂O [M+H]⁺ 525.09707, found 525.09695.

5.3.3.6. *rac-N-(2,4-cis)-4-(3,5-bis(trifluoromethyl)phenyl)-1-(2-bromobenzyl)azetidin-2-yl)methyl)piperidine (3f)*

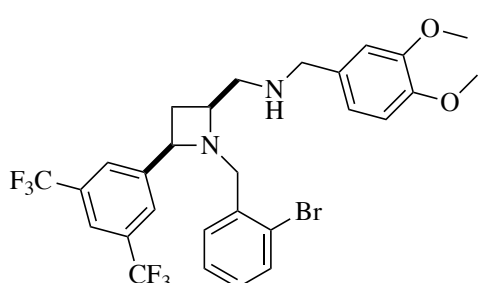


Prepared using *General Procedure C* in a parallel fashion: Iodoazetidine starting material (45 mg, 0.08 mmol, 1.0 Eq), piperidine (17 mg, 0.2 mmol, 2.5 Eq), triethylamine (0.24 mmol, 3.0 Eq). Brown oil, 26 mg, 60%.

¹H NMR (400 MHz, Chloroform-*d*) δ 7.71 (s, 2H, Ar 2- & 6-*H* C₆H₃(CF₃)₂), 7.58 (s, 1H, 4-*H* C₆H₃(CF₃)₂), 7.37 (dd, *J* 8.0, 1.3 Hz, 1H, Ar 3-*H* C₆H₄Br), 7.21 (dd, *J* 7.6, 1.8 Hz, 1H, Ar 5-*H* C₆H₄Br), 7.03 (td, *J* 7.5, 1.3 Hz, 1H, Ar 4-*H* C₆H₄Br), 6.93 (td, *J* 7.6, 1.8 Hz, 1H, Ar 6-*H* C₆H₄Br), 4.17 (app t, *J* 8.0 Hz, 1H, ArCCHCH₂), 3.93 (d, *J* 12.2 Hz, 1H, NCHH(C₆H₄Br)), 3.73 (d, *J* 12.2 Hz, 1H, NCHH(C₆H₄Br)), 3.55 – 3.47 (m, 1H, CH₂CHCH₂), 2.65 (dt, *J* 10.4, 7.3 Hz, 1H, CHCHHCH), 2.58 (dd, *J* 13.0, 3.7 Hz, 1H, CHCHHN(CH₂)₂), 2.47 – 2.36 (m, 5H, CHCHHN(CH₂)₂, N(CH₂CH₂)₂), 1.74 (dt, *J* 10.4, 7.3 Hz, 1H, CHCHHCH), 1.63 – 1.55 (m, 4H, N(CH₂CH₂)₂), 1.46 – 1.39 (m, 2H, N(CH₂CH₂)₂CH₂). **¹³C NMR** (101 MHz, Chloroform-*d*) δ 146.2 (+ , 1-C C₆H₃(CF₃)₂), 136.6 (+ , 1-C C₆H₄Br), 132.8 (- , 3-CH C₆H₄Br), 131.9 (- , 6-CH C₆H₄Br), 130.9 (+ , q, *J* 33.1 Hz, 3- & 5-C(CF₃)₂), 128.9 (- , 5-CH C₆H₄Br), 126.9 (- , 4-CH C₆H₄Br), 126.7 (- , 2- & 6-CH C₆H₃(CF₃)₂), 124.7 (+ , 2-C C₆H₄Br), 120.5 (- , 4-CH C₆H₃(CF₃)₂), 65.3 (- , ArCCHCH₂), 64.5 (+ , CHCH₂N), 60.9 (- , CH₂CHCH₂), 60.6 (+ , NCH₂(C₆H₄Br)), 55.2 (+ , N(CH₂CH₂)₂), 35.4 (+ , CHCH₂CH), 25.7 (+ , N(CH₂CH₂)₂), 24.0 (+ , N(CH₂CH₂)₂CH₂). **FTIR** (ν_{\max} , neat): 2937, 1278, 1174, 1133. **MS** ToF EI+ (*m/z*): 535.1 [M+]. **HRMS** (ESI) *m/z* calcd for C₂₄H₂₅BrF₆N₂ [M+H]⁺ 535.11781, found 535.11765.

5.3.4. CF₃ Amino-Azetidine Library

5.3.4.1. *rac*-*N*-(2,4-*cis*)-4-(3,5-bis(trifluoromethyl)phenyl)-1-(2-bromobenzyl)azetidin-2-yl)-*N*-(3,4-dimethoxybenzyl)methanamine (**3g**)

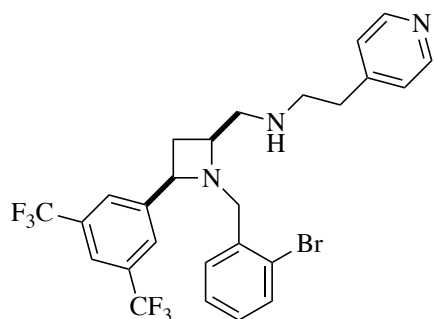


Prepared using *General Procedure F* in a parallel fashion: Iodo-azetidine starting material (45 mg, 0.08 mmol, 1.0 Eq), (3,4-dimethoxyphenyl)methanamine (33 mg, 0.2 mmol, 2.5 Eq), triethylamine (0.24 mmol, 3.0 Eq).

Colourless oil, 8 mg, 16%.

¹H NMR (400 MHz, Chloroform-*d*) δ 7.74 (s, 2H, Ar 2- & 6-*H* C₆H₃(CF₃)₂), 7.60 (s, 1H, Ar 4-*H* C₆H₃(CF₃)₂), 7.39 (dd, *J* 7.8, 1.3 Hz, 1H, 3-*H* C₆H₄Br), 7.16 (dd, *J* 7.5, 1.8 Hz, 1H, 6-*H* C₆H₄Br), 7.03 (td, *J* 7.5, 1.5 Hz, 1H, 5-*H* C₆H₄Br), 6.95 (td, *J* 7.5, 1.5 Hz, 1H, 4-*H* C₆H₄Br), 6.86 (s, 1H, 5-*H* C₆H₃(OCH₃)₂), 6.83 (d, *J* 1.7 Hz, 2H, 2- & 6-*H* C₆H₃(OCH₃)₂), 4.16 (app t, *J* 8.2 Hz, 1H, ArCCHCH₂), 3.94 – 3.86 (m, 8H, NCH₂(C₆H₄Br), O(CH₃)₂), 3.72 – 3.67 (m, 2H, NHCH₂(C₆H₃(OCH₃)₂), 3.50 (tt, *J* = 8.3, 4.3 Hz, 1H, CH₂CHCH₂), 2.69 – 2.57 (m, 2H, CHCH₂NH), 2.52 (dt, *J* 10.5, 8.6 Hz, 1H, CHCH₂CH), 2.07 (s, 1H, NH), 2.00 (dt, *J* 10.5, 8.6 Hz, 1H, CHCH₂CH). **¹³C NMR** (101 MHz, Chloroform-*d*) δ 133.0 (–, 3-CH C₆H₄Br), 131.7 (–, 6-CH C₆H₄Br), 129.2 (–, 4-CH C₆H₄Br), 127.1 (–, 5-CH C₆H₄Br), 126.7 (–, 2- & 6-CH C₆H₃(CF₃)₂), 120.7 (–, 4-CH C₆H₃(CF₃)₂), 120.2 (–, 5-CH C₆H₃(OCH₃)₂), 111.3 (–, 2-CH C₆H₃(OCH₃)₂), 110.9 (–, 6-CH C₆H₃(OCH₃)₂), 64.7 (–, ArCCHCH₂), 61.9 (–, CH₂CHCH₂), 61.0 (+, NCH₂(C₆H₄Br)), 55.9 (–, (OCH₃)₂), 55.8 (–, (OCH₃)₂), 53.8 (+, CHCH₂NH), 52.5 (+, NHCH(C₆H₃(OCH₃)₂), 31.1 (+, CHCH₂CH). **MS** ToF EI+ (*m/z*): 617.1 [M+]. **HRMS** (ESI) *m/z* calcd for C₂₈H₂₇BrF₆N₂O₂ [M+H]⁺ 617.12329, found 617.12298.

5.3.4.2. *rac-N-(2,4-cis)-4-(3,5-bis(trifluoromethyl)phenyl)-1-(2-(2-bromobenzyl)azetidin-2-yl)methyl)-2-(pyridin-4-yl)ethan-1-amine (3h)*

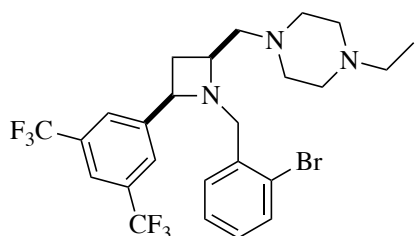


Prepared using *General Procedure F* in a parallel fashion:

Iodo-azetidine starting material (45 mg, 0.08 mmol, 1.0 Eq), 2-(pyridin-4-yl)ethan-1-amine (24mg, 0.2 mmol, 2.5 Eq), triethylamine (0.24 mmol, 3.0 Eq) Colourless oil, 15 mg, 33%.

¹H NMR (400 MHz, Chloroform-d) δ 8.53 – 8.49 (m, 2H, 3- & 5-*H* C₅H₄N), 7.75 (s, 2H, 2- & 6-*H* C₆H₃(CF₃)₂), 7.63 (s, 1H, 4-*H* C₆H₃(CF₃)₂), 7.41 (dd, *J* 7.9, 1.4 Hz, 1H, 3-*H* C₆H₄Br), 7.16 – 7.11 (m, 3H, 6-*H* C₆H₄Br, 2- & 6-*H* C₅H₄N), 7.05 (td, *J* 7.9, 1.4 Hz, 1H, 4-*H* C₆H₄Br), 6.98 (td, *J* 7.6, 1.8 Hz, 1H, 5-*H* C₆H₄Br), 4.15 (app t, *J* 8.1 Hz, 1H, ArCCHCH₂), 3.88 (d, *J* 12.5 Hz, 1H, NCHH(C₆H₄Br)), 3.68 (d, *J* 12.5 Hz, 1H, NCHH(C₆H₄Br)), 3.47 (tt, *J* 8.3, 4.1 Hz, 1H, CH₂CHCH₂), 2.85 – 2.74 (m, 4H, NHCH₂CH₂, NHCH₂CH₂), 2.63 (dd, *J* 12.2, 3.6 Hz, 1H, CHCHHNNH), 2.56 – 2.44 (m, 2H CHCHHNNH, CHCHHCH), 1.99 (dt, *J* 10.4, 8.5 Hz, 1H, CHCHHCH), 1.93 (s, 1H, NH). **¹³C NMR** (101 MHz, Chloroform-d) δ 149.7 (-, 2- & 6-CH C₆H₄N), 145.8 (+ , 1-C C₆H₄N), 141.8 (+ , 1-C C₆H₃(CF₃)₂), 140.7 (+ , 1-C C₆H₄Br) 136.5 (+ , 2-C C₆H₄Br), 133.0 (-, 3-CH C₆H₄Br), 131.7 (-, 6-CH C₆H₄Br), 129.2 (-, 5-CH C₆H₄Br), 127.1 (-, 4-CH C₆H₄Br), 126.8 (-, 2- & 6-CH C₆H₃(CF₃)₂), 124.2 (-, 3- & 5-CH C₆H₄N), 120.7 (-, 4-CH C₆H₃(CF₃)₂), 64.7 (-, ArCCHCH₂), 61.8 (-, CH₂CHCH₂), 60.9 (+ , NCH₂(C₆H₄Br)), 52.9 (+ , CHCH₂NH), 50.6 (+ , NHCH₂CH₂), 35.9 (+ , NHCH₂CH₂), 30.9 (+ , CHCH₂CH). **FTIR** (ν_{\max} , neat): 2825, 1278, 1170, 1133. **MS** ToF EI+ (*m/z*): 572.1 [M+]. **HRMS** (ESI) *m/z* calcd for C₂₆H₂₄BrF₆N₃ [M+H]⁺ 572.11306, found 572.11288.

5.3.4.3. *rac-N-(2,4-cis)-4-(3,5-bis(trifluoromethyl)phenyl)-1-(2-bromobenzyl)azetidin-2-yl)methyl)-4-ethylpiperazine (3i)*



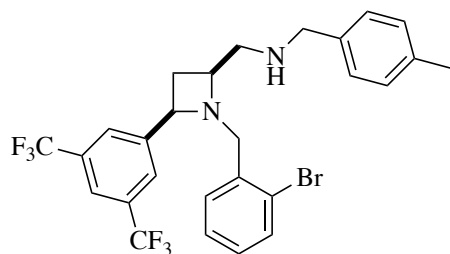
Prepared using *General Procedure F* in a parallel fashion:

Iodo-azetidine starting material (45 mg, 0.08 mmol, 1.0 Eq), 1-ethylpiperazine (23 mg, 0.2 mmol, 2.5 Eq), triethylamine (0.24 mmol, 3.0 Eq). Colourless oil, 13 mg, 29%.

¹H NMR (400 MHz, Chloroform-d) δ 7.73 (s, 2H, Ar 2- & 6-CH C₆H₃(CF₃)₂), 7.60 (s, 1H, Ar 4-CH C₆H₃(CF₃)₂), 7.39 (dd, *J* 7.9, 1.8 Hz, 1H, Ar 3-CH C₆H₄Br), 7.21 (dd, *J* 7.9, 1.8 Hz, 1H, Ar 6-CH C₆H₄Br), 7.04 (td, *J* 7.9, 1.7 Hz, 1H, Ar 5-CH C₆H₄Br), 6.95 (td, *J* 7.9, 1.8 Hz, 1H, Ar 4-CH C₆H₄Br), 4.16 (app t, *J* 8.1 Hz, 1H, ArCHCHCH₂), 3.86 (d, *J* 10.9 Hz, 1H, NCHH(C₆H₄Br)), 3.66 (d, *J* 10.9 Hz, 1H, NCHH(C₆H₄Br)), 3.45 (tt, *J* 7.2, 4.0 Hz, 1H, CH₂CHCH₂), 2.64 – 2.41 (m, 13H, CHCH₂N, N(CH₂CH₂)N, N(CH₂CH₂)N, NCH₂CH₃, CHCHHCH), 1.77 (dt, *J* 10.4, 8.5 Hz, 1H, CHCHHCH), 1.11 (t, *J* 7.2 Hz, 3H, NCH₂CH₃).

¹³C NMR (101 MHz, Chloroform-d) δ 146.1 (+, 1-C C₆H₃(CF₃)₂), 136.6 (+, 1-C C₆H₄Br), 132.8 (-, 3-CH C₆H₄Br), 131.8 (-, 6-CH C₆H₄Br), 130.9 (+, q, *J* 34.5 Hz, C(CF₃)₂), 128.9 (-, 5-CH C₆H₄Br), 126.9 (-, 4-CH C₆H₄Br), 126.7 (-, 2- & 6-CH C₆H₃(CF₃)₂), 124.8 (+, 2-C C₆H₄Br), 120.6 (-, 4-CH C₆H₃(CF₃)₂), 65.1 (-, ArCCHCH₂), 63.4 (+, CHCH₂N), 60.9 (-, CH₂CHCH₂), 60.7 (+, NCH₂(C₆H₄Br)), 53.44(+, N(CH₂CH₂)N), 52.4 (+, N(CH₂CH₂)N), 52.2 (+, NCH₂CH₃), 34.4 (+, CHCH₂CH), 11.5 (-, NCH₂CH₃). **FTIR** (ν_{\max} , neat): 2810, 1375, 1278, 1133. **MS** ToF EI+ (*m/z*): 564.1 [M+]. **HRMS** (ESI) *m/z* calcd for C₂₅H₂₈BrF₆N₃ [M+H]⁺ 564.14436, found 564.14410.

5.3.4.4. *rac*-*N*-(2,4-*cis*)-4-(3,5-bis(trifluoromethyl)phenyl)-1-(2-bromobenzyl)azetidin-2-yl)-*N*-(4-methylbenzyl)methanamine (**3j**)

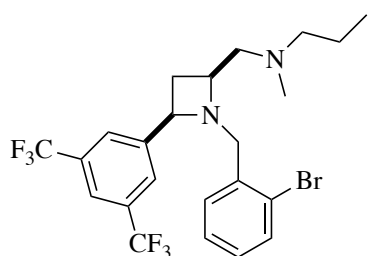


Prepared using *General Procedure F* in a parallel fashion: Iodo-azetidine starting material (45 mg, 0.08 mmol, 1.0 Eq), *p*-tolylmethanamine (24 mg, 0.2 mmol, 2.5 Eq), triethylamine (0.24 mmol, 3.0 Eq). Colourless

oil, 13 mg, 26%.

¹H NMR (400 MHz, Chloroform-*d*) δ 7.74 (s, 2H, Ar 2- & 6-*H* C₆H₃(CF₃)₂), 7.60 (s, 1H, 4-*H* C₆H₃(CF₃)₂), 7.39 (dd, *J* 7.9, 1.3 Hz, 1H, Ar 3-*H* C₆H₄Br), 7.20 – 7.11 (m, 5H, Ar 5-*H* C₆H₄Br, Ar 2-, 3-, 5- & 6-*H* (C₆H₄)CH₃), 7.03 (td, *J* 7.6, 1.6 Hz, 1H, Ar 4-*H* C₆H₄Br), 6.95 (td, *J* 7.6, 1.6 Hz, 1H, Ar 6-*H* C₆H₄Br), 4.16 (app t, *J* 8.2 Hz, 1H, ArCCHCH₂), 3.87 (d, *J* 13.3 Hz, 1H, NCHHArC), 3.67 (d, *J* 13.3 Hz, 1H, NCHHArC), 3.71 (s, 2H, NHCH₂(C₆H₄Br)), 3.49 (tt, *J* 8.5, 4.3 Hz, 1H, CH₂CHCH₂), 2.63 (qd, *J* 12.3, 4.4 Hz, 2H, CHCH₂NHCH₂), 2.51 (dt, *J* 10.3, 7.6 Hz, 1H, CHCH₂CH), 2.35 (s, 3H, (C₆H₄)CH₃), 2.05 – 1.96 (m, 2H, CHCH₂CH, CH₂NHCH₂). **¹³C NMR** (101 MHz, Chloroform-*d*) δ 146.0 (+, 1-C C₆H₃(CF₃)₂), 136.9 (+, 1-C C₆H₄Br), 136.5 (+, 1-C C₆H₄(CH₃)), 132.9 (-, 3-CH C₆H₄Br), 131.7 (-, 4-CH C₆H₄Br), 130.9 (+, q, *J* 32.9 Hz, 3- & 5-C(CF₃)₂), 129.1 (-, 2-, 3-, 5- & 6-CH (C₆H₄)CH₃), 127.9 (-, 6-CH C₆H₄Br), 127.1 (-, 5-CH C₆H₄Br), 126.7 (-, 2- & 6-CH C₆H₃(CF₃)₂), 124.8 (+, (CH)₂CHCH₃), 120.7 (-, 4-CH C₆H₃(CF₃)₂), 64.7 (-, ArCCHCH₂), 61.9 (-, CH₂CHCH₂), 60.9 (+, NCH₂(C₆H₄Br)), 53.8 (+, CHCH₂NH), 52.6 (+, CH₂NHCH₂), 31.0 (+, CHCH₂CH), 21.1 (-, (C₆H₄)CH₃). **FTIR** (ν_{\max} , neat): 2825, 1278, 1170, 1133. **MS** ToF EI+ (*m/z*): 571.1 [M⁺]. **HRMS** (ESI) *m/z* calcd for C₂₇H₂₅BrF₆N₂ [M+H]⁺ 571.11781, found 571.11717.

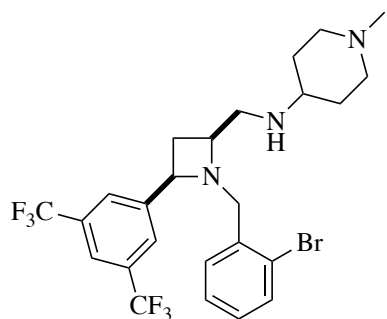
5.3.4.5. *rac-N-(2,4-cis)-4-(3,5-bis(trifluoromethyl)phenyl)-1-(2-bromobenzyl)azetidin-2-yl)methyl)-N-methylpropan-1-amine (3k)*



Prepared using *General Procedure F* in a parallel fashion: Iodoazetidine starting material (45 mg, 0.08 mmol, 1.0 Eq), *N*-methylpropan-1-amine (15 mg, 0.2 mmol, 2.5 Eq), triethylamine (0.24 mmol, 3.0 Eq). Colourless oil, 6 mg, 15%.

¹H NMR (400 MHz, Chloroform-*d*) δ 7.74 (s, 2H, Ar 2- & 6-*H* C₆H₃(CF₃)₂), 7.60 (s, 1H, Ar 4-*H* C₆H₃(CF₃)₂), 7.40 (dd, *J* 7.6, 1.3 Hz, 1H, Ar 3-*H* C₆H₄Br), 7.22 (dd, *J* 7.6, 1.8 Hz, 1H, Ar 5-*H* C₆H₄Br), 7.05 (td, *J* 7.6, 1.3 Hz, 1H, Ar 4-*H* C₆H₄Br), 6.96 (td, *J* 7.6, 1.8 Hz, 1H, Ar 6-*H* C₆H₄Br), 4.16 (app t, *J* 8.1 Hz, 1H, ArCCHCH₂), 3.93 (d, *J* 12.3 Hz, 1H, NCHHArC), 3.73 (d, *J* 12.3 Hz, 1H, NCHHArC), 3.42 (qd, *J* 8.0, 3.7 Hz, 1H, CH₂CHCH₂), 2.66 (dt, *J* 10.4, 7.3 Hz, 1H, CHCHHCH), 2.52 – 2.36 (m, 2H, CHCH₂N(CH₃)CH₂), 2.31 – 2.22 (m, 2H, N(CH₃)CH₂CH₂), 2.20 (s, 3H, N(CH₂)₂CH₃), 1.72 (dt, *J* 10.4, 7.3 Hz, 1H, CHCHHCH), 1.49 – 1.37 (m, 2H, CH₂CH₂CH₃), 0.87 (t, *J* 7.4 Hz, 3H, CH₂CH₃). **¹³C NMR** (101 MHz, Chloroform-*d*) δ 146.2 (+, 1-C C₆H₃(CF₃)₂), 136.7 (+, 1-C C₆H₄Br), 132.8 (-, 3-CH C₆H₄Br), 131.9 (-, 4-CH C₆H₄Br), 128.9 (-, 6-CH C₆H₄Br), 126.9 (-, 5-CH C₆H₄Br), 126.8 (-, 2- & 6-CH C₆H₃(CF₃)₂), 124.8 (+, 2-C C₆H₄Br), 120.6 (-, 4-CH C₆H₃(CF₃)₂), 65.1 (-, ArCCHCH₂), 63.1 (+, CHCH₂N(CH₃)), 61.4 (-, CH₂CHCH₂N), 60.63 (+, NCH₂(C₆H₄Br)), 60.61 (+, N(CH₃)CH₂CH₂), 43.3 (-, N(CH₃)CH₂), 35.0 (+, NCH₂CH₂CH₃), 20.4 (+, CHCH₂CH), 11.8 (-, CH₂CH₂CH₃). **FTIR** (ν_{max} , neat): 2963.2, 2799.2, 1379.1, 1278.5, 1177.8, 1136.8 **MS** ToF EI+ (*m/z*): 523.0 [M+]⁺ (⁷⁹Br) & 525.0 [M+2]⁺ (⁸¹Br). **HRMS** (ESI) *m/z* calcd for C₂₃H₂₅BrF₆N₂S [M+H+CH₃OH]⁺ 555.08988, found 555.08983.

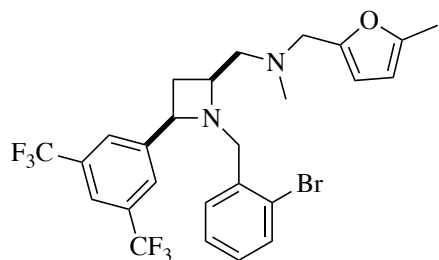
5.3.4.6. *rac*-*N*-(2,4-*cis*)-4-(3,5-bis(trifluoromethyl)phenyl)-1-(2-bromobenzyl)azetidin-2-yl)methyl)-1-methylpiperidin-4-amine (**3l**)



Prepared using *General Procedure F* in a parallel fashion:
Iodo-azetidine starting material (45 mg, 0.08 mmol, 1.0 Eq),
1-methylpiperidin-4-amine (23 mg, 0.2 mmol, 2.5 Eq),
triethylamine (0.24 mmol, 3.0 Eq). Colourless oil, 11 mg,
24%.

¹H NMR (400 MHz, Chloroform-*d*) δ 7.80 (s, 2H, Ar 2- & 6-*H* C₆H₃(CF₃)₂), 7.63 (s, 1H, Ar 4-*H* C₆H₃(CF₃)₂), 7.44 (dd, *J* 8.0, 1.4 Hz, 1H, Ar 3-*H* C₆H₄Br), 7.21 (dd, *J* 7.5, 1.9 Hz, 1H, Ar 5-*H* C₆H₄Br), 7.09 (td, *J* 7.5, 1.9 Hz, 1H, Ar 4-*H* C₆H₄Br), 7.00 (td, *J* 7.5, 1.9 Hz, 1H, Ar 6-*H* C₆H₄Br), 4.16 (app t, *J* 8.1 Hz, 1H, ArCCHCH₂), 3.91 (d, *J* 11.8 Hz, 1H, NCHHArC), 3.71 (d, *J* 11.8 Hz, 1H, NCHHArC), 3.53 – 3.46 (m, 1H, CH₂CHCH₂), 2.88 (dd, *J* 11.4, 6.0 Hz, 3H, N(CH₂CH₂)₂N), 2.59 – 2.47 (m, 3H, CHCHHCH, CHCH₂N), 2.35 (s, 3H, NCH₃), 2.01 (dt, *J* 10.4, 8.3 Hz, 1H, CHCHHCH), 1.91 – 1.78 (m, 2H, N(CH₂CHH)₂N), 1.49 – 1.37 (m, 2H, N(CH₂CHH)₂N). **¹³C NMR** (101 MHz, Chloroform-*d*) δ 146.1 (+, 1-C C₆H₃(CF₃)₂), 136.6 (+, 1-C C₆H₄Br), 133.1 (-, 3-CH C₆H₄Br), 131.7 (-, 4-CH C₆H₄Br), 131.0 (+, q, *J* 34.8 Hz, 3- & 5-C C₆H₃(CF₃)₂), 129.2 (-, 6-CH C₆H₄Br), 127.1 (-, 5-CH C₆H₄Br), 126.8 (-, 2- & 6-CH C₆H₃(CF₃)₂), 124.8 (+, C(CF₃)₂), 120.7 (-, 4-CH C₆H₃(CF₃)₂), 64.5 (-, ArCCHCH₂), 62.1 (-, CH₂CHCH₂), 60.9 (+, CHCH₂N), 50.0 (+, C(CH₂CH₂)₂N), 45.4 (-, NCH₃), 31.8 (+, CHCH₂CH), 30.8 (+, C(CH₂CH₂)₂N). **FTIR** (ν_{\max} , neat): 2940.9, 2788.0, 1595.3, 1371.7, 1258.7, 1170.4, 1133.1 **MS** ToF EI+ (*m/z*): 564.1 [M]⁺ + (⁷⁹Br) & 566.0 [M+2]⁺ (⁸¹Br). **HRMS** (ESI) *m/z* calcd for C₂₅H₂₈BrF₆N₃ [M+H]⁺ 564.14436, found 564.14397 (-0.68 ppm error)

5.3.4.7. *rac-N-(2,4-cis)-4-(3,5-bis(trifluoromethyl)phenyl)-1-(2-bromobenzyl)azetidin-2-yl)-N-methyl-N-((5-methylfuran-2-yl)methyl)methanamine (3m)*



Prepared using *General Procedure F* in a parallel fashion:

Iodo-azetidine starting material (45 mg, 0.08 mmol, 1.0 Eq), *N*-methyl-1-(5-methylfuran-2-yl)methanamine (25 mg, 0.2 mmol, 2.5 Eq), triethylamine (0.24 mmol, 3.0 Eq).

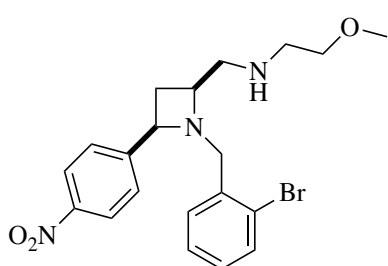
Colourless oil, 18 mg, 39%.

¹H NMR (400 MHz, Chloroform-*d*) δ 7.71 (d, *J* 1.6 Hz, 2H, 2- & 6-*H* C₆H₃(CF₃)₂), 7.59 (s, 1H, 4-*H* C₆H₃(CF₃)₂), 7.38 (dd, *J* 7.6, 1.8 Hz, 1H, Ar 3-*H* C₆H₄Br), 7.19 (dd, *J* 7.6, 1.8 Hz, 1H, 5-*H* C₆H₄Br), 7.03 (td, *J* 7.6, 1.8 Hz, 1H, 4-*H* C₆H₄Br), 6.94 (td, *J* 7.6, 1.8 Hz, 1H, 6-*H* C₆H₄Br), 6.04 (d, *J* 3.0 Hz, 1H, 5-*H* C₄H₂O), 5.88 (dd, *J* 3.0, 1.1 Hz, 1H, 4-*H* C₄H₂O), 4.16 (app t, *J* 8.1 Hz, 1H, ArCCHCH₂), 3.92 (d, *J* 12.4 Hz, 1H, NCHHArC), 3.72 (d, *J* 12.4 Hz, 1H, NCHHArC), 3.53 – 3.42 (m, 3H, CH₂CHCH₂, NCH₂(C₄H₂O)), 2.69 – 2.56 (m, 2H, CHCHHN(CH₃)CH₂, CHCHHCH), 2.47 (dd, *J* 12.9, 8.1 Hz, 1H, CHCHHN(CH₃)CH₂), 2.26 (s, 3H, N(CH₂)CH₃), 2.25 (s, 3H, 3-CH₃ C₄H₂O), 1.71 (dt, *J* 10.4, 8.4 Hz, 1H, CHCHHCH).

¹³C NMR (101 MHz, Chloroform-*d*) δ 146.2 (+, 3-C C₄H₂O), 136.6 (+, 1-C C₄H₂O), 132.8 (-, 3-CH C₆H₅Br), 131.8 (-, 6-CH C₆H₅Br), 131.1 (+, 1-C C₆H₃(CF₃)₂), 128.9 (-, 4-CH C₆H₅Br), 127.5 (+, 1-C C₆H₅Br), 126.9 (5-CH C₆H₅Br), 126.8 (-, 2- & 6-CH C₆H₃(CF₃)₂), 124.8 (+, 2-C C₆H₄Br), 120.6 (-, 4-CH C₆H₃(CF₃)₂), 109.6 (-, 5-CH C₄H₂O), 105.9 (4-CH C₄H₂O), 65.0 (-, ArCCHCH₂), 61.9 (+, CHCH₂N(CH₃)CH₂), 61.1 (-, CH₂CHCH₂N), 60.5 (+, N(CH₃)CH₂(C₄H₂O)), 54.6 (+, NCH₂(C₆H₄Br)), 43.1 (-, N(CH₂)₂CH₃), 34.8 (+, CHCH₂CH), 13.6 (-, (C₄H₂O)CH₃). **MS** TOF EI+ (*m/z*): 575.1 [M]⁺. **HRMS** (*m/z*): calcd. for C₂₆H₂₅BrF₆N₂O [M+H]⁺, 575.11272, found, 575.11232.

5.3.5. NO₂ Amino-Azetidine Set

5.3.5.1. *rac*-*N*-(2,4-*cis*)-1-(2-bromobenzyl)-4-(4-nitrophenyl)azetidin-2-yl)methyl)-2-methoxyethan-1-amine (**3n**)



Prepared using *General Procedure F* in a parallel fashion:

Iodo-azetidine starting material (25 mg, 0.056 mmol, 1.0

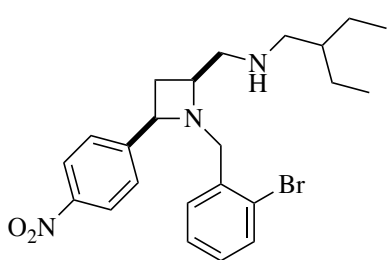
Eq), 2-methoxyethan-1-amine (6 mg, 0.08 mmol, 1.5 Eq),

triethylamine (24 μ L, 0.17 mmol, 3.0 Eq). Brown oil, 5 mg,

21%

¹H NMR (400 MHz, Chloroform-*d*) δ 8.05 (d, *J* 8.4 Hz, 2H, 3- & 5-*H* C₆H₄NO₂), 7.47 (d, *J* 9.1 Hz, 2H, 2- & 6-*H* C₆H₄NO₂), 7.20 – 7.06 (m, 3H, 3-, 5- & 6-*H* C₆H₄Br), 7.01 (td, *J* 7.6, 1.8 Hz, 1H, 4-*H* C₆H₄Br), 4.17 (dd, *J* 16.43, 8.27 Hz, 1H, CHCH₂CH), 3.93 (d, *J* 12.7 Hz, 1H, NCHHAr), 3.79 – 3.72 (m, 2H, NCHHAr, CHCH₂CH), 3.47 (t, *J* 5.3 Hz, 2H, NHCH₂CH₂), 3.37 (s, 3H, CH₃), 2.73 (t, *J* 5.3 Hz, 2H, CHCH₂NH), 2.53 (dt, *J* 10.3, 7.2 Hz, 1H, CHCHHCH), 2.41 – 2.33 (m, 2H, NHCH₂CH₂), 1.92 (dt, *J* 10.3, 7.2 Hz, 1H, CHCHHCH). **¹³C NMR** (101 MHz, Chloroform-*d*) δ 151.6 (4-*C* C₆H₄NO₂), 134.1 (3-*C* C₆H₄Br), 132.9 (6-*C* C₆H₄Br), 130.5 (4-*C* C₆H₄Br), 128.9 (5-*C* C₆H₄Br), 128.2 (2- & 6-*C* C₆H₄NO₂), 123.8 (3- & 5-*C* C₆H₄NO₂), 123.3 (2-*C* C₆H₄Br), 65.1 (NHCH₂CH₂), 60.9 (ArCHCH₂), 60.8 (CHCH₂CH), 58.9 (CH₃), 51.65 (NCH₂Ar), 49.7 (CHCH₂NH), 43.1 (NHCH₂CH₂), 31.5 (CHCH₂CH). **MS** TOF EI⁺ (*m/z*): 434.1 [M]⁺.

5.3.5.2. *rac-N-(2,4-cis)-1-(2-bromobenzyl)-4-(4-nitrophenyl)azetidin-2-yl)methyl)-2-ethylbutan-1-amine (30)*



Prepared using *General Procedure F* in a parallel fashion:

Iodo-azetidine intermediate (25 mg, 0.056 mmol, 1.0 Eq)

intermediate was dissolved in DCM (1.0 mL) and stirred with

2-ethylbutylamine (8.5 mg, 0.08 mmol, 1.5 Eq) and

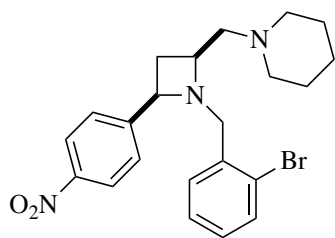
triethylamine (24 μ L, 0.17 mmol, 3.0 Eq). Brown Oil, 10.5 mg, 32%.

^1H NMR (400 MHz, Chloroform-*d*) δ 8.11 (d, *J* 7.8 Hz, 2H, 3- & 5-*H* C₆H₄NO₂), 7.49 (d, *J* 9.0 Hz, 2H, 2- & 6-*H* C₆H₄NO₂), 7.29 – 7.23 (m, 2H, 3- & 5-*H* C₆H₄Br), 7.18 (td, *J* 7.6, 1.5 Hz, 1H, 6-*H* C₆H₄Br), 7.09 (td, *J* 7.6, 1.5 Hz, 1H, 3-*H* C₆H₄Br), 4.23 (dd, *J* 8.2 Hz, 1H, ArCHCH₂), 3.95 (d, *J* 12.1 Hz, 1H, NCHHAr), 3.75 (d, *J* 12.1 Hz, 1H, NCHHAr), 3.07 – 3.00 (m, 1H, CHCH₂CH), 2.69 (dd, *J* 12.0, 6.1 Hz, 1H, CHCHH₂NH), 2.63 – 2.52 (m, 2H, CHCHH₂NH, CHCHH₂CH), 2.47 (dd, *J* 12.4, 5.3 Hz, 1H, CHHCH(CH₂CH₃)₂), 2.34 (dd, *J* 12.4, 5.3 Hz, 1H, CHHCH(CH₂CH₃)₂), 2.14 (dt, *J* 11.2, 8.7 Hz, 1H, CHCHH₂CH), 1.56 – 1.52 (m, 1H, CH(CH₂CH₃)₂), 1.40 – 1.29 (m, 4H, CH(CH₂CH₃)₂), 0.91 – 0.83 (m, 6H, CH(CH₂CH₃)₂).

^{13}C NMR (101 MHz, Chloroform-*d*) δ 149.6 (4-*C* C₆H₄NO₂), 136.3 (3-*C* C₆H₄Br), 133.2 (2- & 6-*C* C₆H₄NO₂), 131.8 (5-*C* C₆H₄Br), 129.6 (4-*C* C₆H₄Br), 127.3 (3- & 5-*C* C₆H₄NO₂), 123.6 (6-*C* C₆H₄Br), 65.0 (ArCHCH₂CH), 60.7 (CHCH₂CH), 59.9 (NCH₂Ar), 52.0 (CHCH₂NH), 38.8 (NHCH₂CH), 30.7 (CH(CH₂CH₃)₂), 23.5 (CHCH₂CH), 10.6 (CH(CH₂CH₃)₂), 10.5 (CH(CH₂CH₃)₂).

MS TOF EI⁺ (*m/z*): 460.1 [M]⁺. **HRMS** (*m/z*): calcd. for C₂₃H₃₀BrN₃O₂ [M+H]⁺, 460.15942, found, 460.1588

5.3.5.3. *rac-N-(2,4-cis)-1-(2-bromobenzyl)-4-(4-nitrophenyl)azetidin-2-yl)methyl)piperidine (3p)*

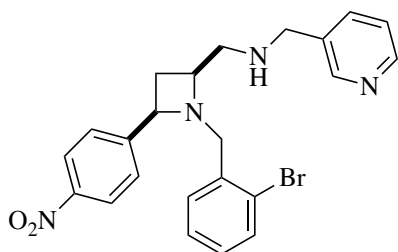


Prepared using *General Procedure F* in a parallel fashion: Iodoazetidine intermediate (25 mg, 0.056 mmol, 1.0 Eq) intermediate was dissolved in DCM (1.0 mL) and stirred with piperidine (8.5 μ L, 0.08 mmol, 1.5 Eq) and triethylamine (24

μ L, 0.17 mmol, 3.0 Eq). Brown Oil, 11.1 mg, 30%.

^1H NMR (400 MHz, Chloroform-*d*) δ 8.06 – 7.98 (m, 2H, 3- & 5-*H* C₆H₄NO₂), 7.46 – 7.41 (m, 2H, , 2- & 6-*H* C₆H₄NO₂), 7.31 – 7.22 (m, 2H, 3- & 5-*H* C₆H₄Br), 7.07 (td, *J* 7.6, 1.5 Hz, 1H, 6-*H* C₆H₄Br), 6.98 (td, *J* 7.6, 1.5 Hz, 1H, 3-*H* C₆H₄Br), 4.18 (dd, *J* 8.1 Hz, 1H, ArCHCH₂), 3.98 (d, *J* 12.8 Hz, 1H, NCHHAr), 3.71 (d, *J* 12.8 Hz, 1H, NCHHAr), 3.51 (m, 1H, CHCH₂CH), 2.65 (dt, *J* 10.4, 8.5 Hz, 1H, CHCH₂CH), 2.57 (dd, *J* 12.9, 3.6 Hz, 1H, CHCH₂CH), 2.47 – 2.33 (m, 5H, CHCH₂CH, N(CH₂CH₂)₂CH₂), 1.73 (dt, *J* 10.4, 8.5 Hz, 1H, CHCH₂CH), 1.62 – 1.54 (m, 4H, N(CH₂CH₂)₂CH₂), 1.47 – 1.36 (m, 2H, N(CH₂CH₂)₂CH₂). **^{13}C NMR** (101 MHz, Chloroform-*d*) δ 151.2 (1-*C* C₆H₄NO₂), 146.8 (4-*C* C₆H₄NO₂), 136.9 (1-*C* C₆H₄Br), 132.7 (3-*C* C₆H₄Br), 131.8 (6-*C* C₆H₄Br), 128.9 (4-*C* C₆H₄Br), 128.2 (5-*C* C₆H₄Br), 127.2 (2- & 6-*C* C₆H₄NO₂), 123.7 (2-*C* C₆H₄Br), 123.2 (3- & 5-*C* C₆H₄NO₂), 65.6 (CHCH₂CH), 64.7 (CHCH₂N), 60.6 (CHCH₂CH), 55.1 (N(CH₂CH₂)₂CH₂), 51.6 (NCH₂Ar), 35.5 (CHCH₂CH), 25.6 (N(CH₂CH₂)₂CH₂), 23.9 (N(CH₂CH₂)₂CH₂). **MS** TOF EI+ (*m/z*): 444.1 [M]⁺. **HRMS** (*m/z*): calcd. for C₂₂H₂₆BrN₃O₂ [M+H]⁺, 444.12812, found, 444.1274

5.3.5.4. *rac-N-(2,4-cis)-1-(2-bromobenzyl)-4-(4-nitrophenyl)azetidin-2-yl)-N-(pyridin-3-ylmethyl)methanamine (3q)*



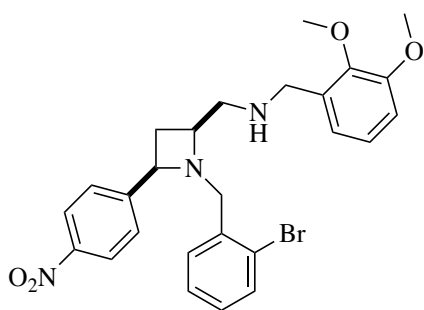
Prepared using *General Procedure F* in a parallel fashion:

Iodo-azetidine (25 mg, 0.056 mmol, 1.0 Eq) intermediate was dissolved in DCM (1.0 mL) and stirred with 3-methylpyridine (7.8 μ L, 0.08 mmol, 1.5 Eq) and

triethylamine (24 μ L, 0.17 mmol, 3.0 Eq). Brown Oil, 14.4 mg, 39%.

^1H NMR (400 MHz, Chloroform-*d*) δ 8.51 – 8.48 (m, 2H, 2- & 4-*H* C₆H₄N), 8.09 – 8.04 (m, 2H, 3- & 5-*H* C₆H₄NO₂), 7.61 (dt, *J* 7.7, 2.0 Hz, 1H, 6-*H* C₆H₄N), 7.50 – 7.46 (m, 2H, 2- & 6-*H* C₆H₄NO₂), 7.50 – 7.46 (1H, 5-*H* C₆H₄N), 7.26 – 7.20 (m, 2H, 3- & 5-*H* C₆H₄Br), 7.08 (td, *J* 7.6, 1.5 Hz, 1H, 6-*H* C₆H₄Br), 7.00 (td, *J* 7.6, 1.5 Hz, 1H, 4-*H* C₆H₄Br), 4.16 (app t, *J* 8.2 Hz, 1H, CHCH₂CH), 3.88 (d, *J* 12.4 Hz, 1H, NCHHAr), 3.77 – 3.64 (m, 3H, NCHHAr, NHCH₂Ar), 3.52 – 3.45 (m, 1H, CHCH₂CH), 2.58 – 2.45 (m, 3H, CHCHHCH. CHCH₂NH), 2.03 (dt, *J* 10.3, 8.6 Hz, 1H, CHCHHCH). **MS** TOF EI⁺ (*m/z*): 467.1 [M]⁺. **HRMS** (*m/z*): calcd. for C₂₃H₂₃BrN₄O₂ [M+H]⁺, 467.10772, found, 467.1070.

5.3.5.5. *rac*-*N*-(2,4-*cis*)-1-(2-bromobenzyl)-4-(4-nitrophenyl)azetidin-2-yl)-*N*-(2,3-dimethoxybenzyl)methanamine (**3r**)



Prepared using *General Procedure F* in a parallel fashion:

Iodo-azetidine intermediate (25 mg, 0.056 mmol, 1.0 Eq)

intermediate was dissolved in DCM (1.0 mL) and stirred

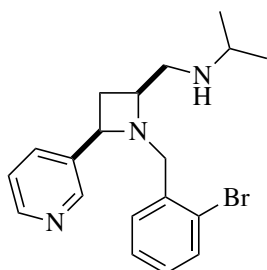
with 2,4-dimethoxybenzylamine 12.0 μ L, 0.08 mmol, 1.5

Eq) and triethylamine (24 μ L, 0.17 mmol, 3.0 Eq). Brown

Oil, 6.1 mg, 15%.

^1H NMR (400 MHz, Chloroform-*d*) δ 8.07 – 8.03 (m, 2H, , 3- & 5-*H* C₆H₄NO₂), 7.46 – 7.42 (m, 2H, 2- & 6-*H* C₆H₄NO₂), 7.40 (dd, *J* 7.6, 1.6 Hz, 1H, 3-*H* C₆H₄Br), 7.17 (dd, *J* 7.6, 1.6 Hz, 1H, 5-*H* C₆H₄Br), 7.13 (d, *J* 8.1 Hz, 1H, 6-*H* C₆H₃(OCH₃)₂), 7.06 (td, *J* 7.6, 1.6 Hz, 1H, 6-*H* C₆H₄Br), 6.98 (td, *J* 7.6, 1.6 Hz, 1H, 4-*H* C₆H₄Br), 6.48 – 6.42 (m, 2H, 4- & 5-*H* C₆H₃(OCH₃)₂), 4.17 (dd, *J* 8.2 Hz, 1H, CHCH₂CH), 3.86 (d, *J* 13.2Hz, 1H, NCHHAr), 3.83 (s, 3H, OCH₃), 3.82 (s, 3H, OCH₃), 3.81 – 3.68 (m, 3H, NCHHAr, NHCH₂(C₆H₃(OCH₃)₂)), 3.57 – 3.49 (m, 1H, CHCH₂CH), 2.81 (dd, *J* 12.5, 4.4 Hz, 1H, CHCHH₂NH), 2.66 (dd, *J* 12.5, 4.4 Hz, 1H, CHCHH₂NH), 2.53 (dt, *J* 10.7, 8.1 Hz, 1H, CHCHHCH), 2.00 (dt, *J* 10.7, 8.1 Hz, 1H, CHCHHCH). **MS** TOF EI⁺ (*m/z*): 526.1 [M]⁺. **HRMS** (*m/z*): calcd. for C₂₆H₂₈BrN₃O₄ [M+H]⁺, 567.43100, found, 526.1327.

5.3.5.6. *rac-N-(2,4-cis)-1-(2-bromobenzyl)-4-(pyridin-3-yl)azetidin-2-yl)methyl)propan-2-amine (3s)*



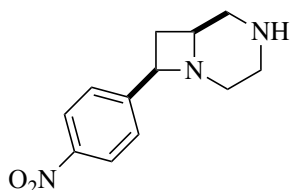
Prepared using *General Procedure F* in a parallel fashion: Iodoazetidine intermediate (25 mg, 0.056 mmol, 1.0 Eq) intermediate was dissolved in DCM (1.0 mL) and stirred with *N*-isopropylamine (45 μ L, 0.17 mmol, 1.5 Eq) and triethylamine (24 μ L, 0.17 mmol, 3.0 Eq).

Brown Oil, 6.2 mg, 21%

^1H NMR (400 MHz, Chloroform- d) δ 8.53 (d, J 2.3 Hz, 1H, 2- H C₅H₄N), 8.40 (dd, J 4.8, 1.7 Hz, 1H, 4- H C₅H₄N), 7.75 (dt, J 7.8, 2.0 Hz, 1H, 6- H C₅H₄N), 7.45 (dd, J 8.0, 1.3 Hz, 1H, 3- H C₆H₄Br), 7.28 (dd, J 7.6, 1.8 Hz, 1H, 5- H C₅H₄N), 7.18 – 7.14 (m, 1H, 5- H C₆H₄Br), 7.11 (td, J 7.6, 1.8 Hz, 1H, 6- H C₆H₄Br), 7.01 (td, J 7.6, 1.8 Hz, 1H, 4- H C₆H₄Br), 4.07 (app t, J 8.1 Hz, 1H, ArCCHCH₂), 3.88 (d, J 12.5 Hz, 1H, NCHHArC), 3.68 (d, J 12.5 Hz, 1H, NCHHArC), 3.47 – 3.40 (m, 1H, NHCH(CH₃)), 2.63 – 2.40 (m, 5H, CHCH₂CH(CH₃), CH₂CHCH₂, CHCHHCH), 1.99 (dt, J 10.4, 8.6 Hz, 1H, CHCHHCH), 1.00 (d, J 6.2 Hz, 3H, CH(CH₃)), 0.94 (d, J 6.2 Hz, 3H, CH(CH₃)). **^{13}C NMR** (101 MHz, Chloroform- d) δ 148.6 (-, ArCHNArCH), 148.5 (-, ArCHNArCH), 138.5 (+ , ArC C₅H₄N), 137.2 (+ , ArC C₆H₄Br), 134.6 (-, ArCH C₅H₄N), 132.8 (-, ArCH C₆H₄Br), 131.6 (-, ArCH C₆H₄Br), 128.9 (-, ArCH C₆H₄Br), 127.1 (-, ArCH C₆H₄Br), 124.6 (+ , ArCBr C₆H₄Br), 123.2 (-, ArCH C₅H₄N), 63.4 (-, ArCCHCH₂), 62.6 (-, CH(CH₃)₂), 60.9 (+ , NCH₂ArC), 51.5 (+ , CHCH₂NH), 49.2 (-, CH₂CHCH₂), 31.1 (+ , CHCH₂CH), 23.2 (-, CH(CH₃)), 22.6 (-, CH(CH₃)). **MS** TOF EI⁺ (m/z): 373.1 [M]⁺.

5.3.6. 4,6-Fused Bicyclic Scaffolds

5.3.6.1. *rac*-(6,8-*cis*)-(4-nitrophenyl)-1,4-diazabicyclo[4.2.0]octane (**4a**)



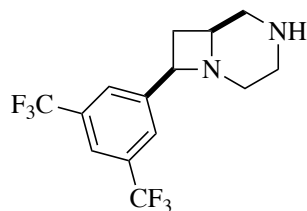
Prepared using *General Procedure D*: Azido-Azetidine intermediate (2.7 g, 6.1 mmol, 1.0 Eq), triphenylphosphine (4.6 g, 15.8 mmol, 2.5 Eq) and water (2.2 mL, 122.0 mmol, 20.0 Eq) in THF (25 mL, 0.24M).

Colourless oil, 1.9 g, 72%

¹H NMR (400 MHz, Chloroform-*d*) δ 8.18 (d, *J* 8.5 Hz, 2H, 3- & 5-CH C₆H₄NO₂), 7.55 (d, *J* 8.5 Hz, 2H, 2- & 6-CH C₆H₄NO₂), 4.31 (dd, *J* 8.0, 5.6 Hz, 1H, ArCCHCH₂), 3.10 – 2.99 (m, 4H, CHCH₂NH, CHCH₂NH, NCHHCH₂N), 2.93 – 2.86 (m, 1H, NCHHCH₂N), 2.81 – 2.79 (m, 1H, NCH₂CHHN), 2.78 (s, 1H, NH), 2.56 (dd, *J* 10.1, 3.5 Hz, 1H, NCH₂CHHN), 2.48 (dt, *J* 9.3, 5.9 Hz, 1H, CHCHHCH), 2.09 (q, *J* 8.7 Hz, 1H, CHCHHCH). **¹³C NMR** (101 MHz, Chloroform-*d*) δ 149.1 (+ , 1-C C₆H₄NO₂), 147.3 (+ , 4-C C₆H₄NO₂), 127.3 (- , 2- & 6-CH C₆H₄NO₂), 123.7 (- , 3- & 5-CH C₆H₄NO₂), 67.0 (- , ArCCHCH₂), 61.5 (- , CH₂CHCH₂), 51.3 (+ , NCH₂CH₂N), 49.5 (+ , NCH₂CH₂N), 45.1 (+ , CHCH₂NH), 37.2 (+ , CHCH₂CH). **FTIR** ν_{\max} 3276, 1274, 894. **MS** ToF EI⁺ (*m/z*): 234.1 [M+H]⁺. **HRMS** (ESI) *m/z* calcd for C₁₂H₁₅N₃O₂ [M+H]⁺ 234.12370, found 234.1237.

5.3.6.2. *rac*-(6,8-*cis*)-8-(3,5-bis(trifluoromethyl)phenyl)-1,4-diazabicyclo[4.2.0]octane

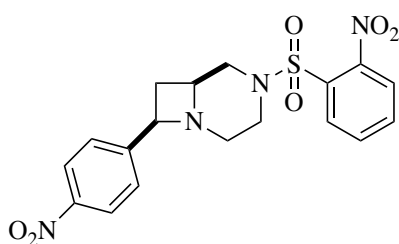
(4b)



Prepared using *General Procedure D*: Azido-Azetidine intermediate (10.6 g, 23.8 mmol, 1.0 Eq), triphenylphosphine (16.1g, 61.7 mmol, 2.5 Eq) and water (8.6 mL, 475 mmol, 20.0 Eq) in THF (120 mL, 0.24M). Colourless oil, 3.5g, 49%

¹H NMR (400 MHz, Chloroform-*d*) δ 7.90 (s, 2H, Ar), 7.75 (s, 1H, Ar), 4.01 (dd, *J* 8.2, 8.2 Hz, 1H, ArCHCH₂), 3.20 (ddd, *J* 12.7, 8.0, 4.8 Hz, 1H, ArCHCH₂CH), 2.86 (qd, *J* 13.2, 4.8 Hz, 2H, CHNCH₂CH₂), 2.80 – 2.73 (m, 1H, NCH₂CHHN), 2.65 – 2.48 (m, 4H, ArCHCHHCH, NCH₂CHHN, CHCH₂CHCH₂N), (dt, *J* 10.6, 8.4 Hz, 1H, ArCHCHHCH), 1.37 (s, 1H, NH). **¹³C NMR** (101 MHz, Chloroform-*d*) δ 126.7 (Ar), 121.2 (Ar), 65.1 (ArCH), 64.1 (ArCHCH₂CH), 61.4 (NCH₂CH₂NH), 46.3 (NCH₂CH₂NH), 40.3 (CHCH₂CH), 30.4 (ArCHCH₂CH). **FTIR** ν_{max} 3276, 2832, 894. **MS** ToF EI+ (*m/z*): 325.1 [M+H]⁺. **HRMS** (ESI) *m/z* calcd for C₁₄H₁₄F₆N₂ [M+H]⁺ 325.11339, found 325.1140.

5.3.6.3. *rac*-(6,8-*cis*)-8-(4-nitrophenyl)-4-((2-nitrophenyl)sulfonyl)-1,4-diazabicyclo[4.2.0]octane (**4c**)

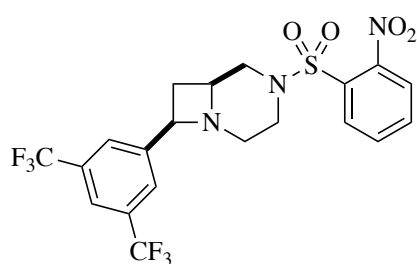


Protected azetidine (80 mg, 0.18 mmol 1.0 Eq) was dissolved in dichloromethane (1.7 mL, 0.04 M) and was subsequently cooled to 0 °C. Triethylamine (77 μ L, 0.55 mmol, 3.0 Eq) was added followed by the dropwise addition of methanesulfonyl chloride (1.2 μ L, 0.27 μ mol, 1.1 Eq). The reaction mixture was stirred for 30 min at 0 °C. and was quenched with water (4 mL), the aqueous layer was extracted with dichloromethane (3 x 10 mL). The combined organic fractions were dried over Na₂SO₄, filtered and concentrated *in vacuo* to provide the crude mesylated product. The resultant sulfonate was redissolved in *N,N*-dimethylformamide (1.7 mL, 0.044 M) and potassium carbonate (51 mg, 37 mmol, 2.0 Eq) was added as a single portion. The reaction mixture was heated to 65 °C for 1 h. The reaction mixture was cooled and extracted with ethyl acetate (3 x 10 mL) and washed with water (2 x 10 mL) and brine (4 x 10 mL). The combined organic fractions were dried over Na₂SO₄, and solvent was removed under reduced pressure and the resulting residue was purified using reverse-phase chromatography using CH₃CN/H₂O to provide pure product (**4a**) as a yellow oil, 13.4 mg, 18%.

¹H NMR (400 MHz, Chloroform-*d*) δ 8.18 – 8.13 (m, 2H, 3- & 5-*H* C₆H₄NO₂), 8.05 (dd, *J* 7.3, 1.9 Hz, 1H, 2-*H* SO₂(C₆H₄NO₂)), 7.80 – 7.70 (m, 2H, 4- & 5-*H* SO₂(C₆H₄NO₂)), 7.67 (dd, *J* 7.5, 1.7 Hz, 1H, 6-*H* SO₂(C₆H₄NO₂)), 7.53 – 7.48 (m, 2H, 2- & 6-*H* C₆H₄NO₂), 4.51 (dd, *J* 5.6, 2.9 Hz, 1H, *CHCH*₂*CH*), 4.33 – 4.28 (m, 1H, *CH*₂*CHCH*₂), 3.59 – 3.49 (m, 1H, *CHCHHN*), 3.31 – 3.18 (m, 2H, *CHCHHN*, *NCH*₂*CHHN*), 3.04 (dt, *J* 12.3, 2.1 Hz, 1H, *NCHHCH*₂*N*), 2.94 (t, *J* 10.2 Hz, 1H, *NCH*₂*CHHN*), 2.60 – 2.55 (m, 1H, *NCHHCH*₂*N*), 2.49 (td, *J* 14.2, 7.2 Hz, 1H, *CHCHHCH*), 2.01 (dt, *J* 14.3, 7.2 Hz, 1H, *CHCHHCH*). **¹³C NMR**

(101 MHz, Chloroform-*d*) δ 134.3, 131.1, 130.7, 124.4, 123.8, 123.8, 64.2, 58.7, 56.9, 52.9, 43.6, 40.9, 37.1. **MS** ToF EI+ (*m/z*): 419.0 [M+H]⁺.

5.3.6.4. *rac*-(6,8-*cis*)-8-(3,5-bis(trifluoromethyl)phenyl)-4-((2-nitrophenyl)sulfonyl)-1,4-diazabicyclo[4.2.0]octane (**4d**)



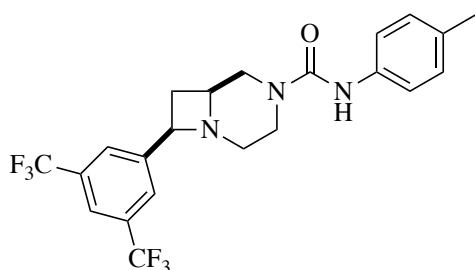
Protected azetidine (500 mg, 0.948 mmol 1.0 Eq) was dissolved in dichloromethane (10 mL) and was subsequently cooled to 0 °C. Triethylamine (396 μ L, 2.8 mmol, 3.0 Eq) was added followed by the dropwise addition of methanesulfonyl chloride (81 μ L, 1.1 mmol, 1.1 Eq). The reaction mixture was stirred for 30 min at 0 °C. and was quenched with water (8 mL), the aqueous layer was extracted with dichloromethane (3 x 15 mL). The combined organic fractions were dried over Na₂SO₄, filtered and concentrated *in vacuo* to provide the crude mesylated product. The resultant sulfonate was redissolved in *N,N*-dimethylformamide (10 mL) and potassium carbonate (262 mg, 1.9 mmol, 2.0 Eq) was added as a single portion. The reaction mixture was heated to 65 °C for 1 h. The reaction mixture was cooled and extracted with ethyl acetate (3 x 15 mL) and washed with water (2 x 15 mL) and brine (4 x 15 mL). The combined organic fractions were dried over Na₂SO₄, and solvent was removed under reduced pressure and the resulting residue was purified using reverse-phase chromatography using CH₃CN/H₂O to provide pure product (**SC-5-CF₃-1**) as a yellow oil, 382 mg, 87%.

¹H NMR (400 MHz, Chloroform-*d*) δ 8.02 – 7.98 (m, 1H, 3-*H* C₆H₄NO₂), 7.82 (s, 2H, 2- & 6-*H* C₆H₃(CF₃)₂), 7.77 (s, 1H, 4-*H* C₆H₃(CF₃)₂), 7.76 – 7.70 (m, 2H, 4- & 5-*H* C₆H₄NO₂), 7.67 – 7.63 (m, 1H, 6-*H* C₆H₄NO₂), 4.32 (dd, *J* 8.0, 5.4 Hz, 1H, CHCH₂CH), 3.97 – 3.89 (m, 1H, CHCHHN), 3.86 (td, *J* 12.3, 1.6 Hz, 1H, NCH₂CHHN), 3.17 (td, *J* 11.7, 3.5 Hz, 1H,

NCH_2CHHN), 3.11 – 3.03 (m, 2H, CH_2CHCH_2 , CHCHHN), 2.86 (td, J 10.4, 3.4 Hz, 1H, NCHHCH_2N), 2.61 (td, J 10.4, 3.4 Hz, 1H, NCHHCH_2N), 2.53 (dt, J 8.9, 5.2 Hz, 1H, CHCHHCH), 2.05 (q, J 8.9 Hz, 1H, CHCHHCH). ^{13}C NMR (101 MHz, Chloroform- d) δ 148.3 (2- C $\text{C}_6\text{H}_4\text{NO}_2$), 144.1 (1- C $\text{C}_6\text{H}_3(\text{CF}_3)_2$), 133.8 (6- C $\text{C}_6\text{H}_4\text{NO}_2$), 131.8 (1- C $\text{C}_6\text{H}_4\text{NO}_2$), 131.7 (q, J 32.2 Hz, 3- & 5- C $\text{C}_6\text{H}_3(\text{CF}_3)_2$), 131.7 (5- C $\text{C}_6\text{H}_4\text{NO}_2$), 130.9 (4- C $\text{C}_6\text{H}_4\text{NO}_2$), 126.8 (2- & 6- C $\text{C}_6\text{H}_3(\text{CF}_3)_2$), 124.2 (3- C $\text{C}_6\text{H}_4\text{NO}_2$), 123.3 (q, J 272.7 Hz, CF_3), 121.5 (4- C $\text{C}_6\text{H}_3(\text{CF}_3)_2$), 66.2 (CHCH_2CH), 59.7 (CHCH_2CH), 50.9 (CHCH_2N), 49.8 ($\text{NCH}_2\text{CH}_2\text{N}$), 46.1 ($\text{NCH}_2\text{CH}_2\text{N}$), 36.9 (CHCH_2CH). **MS** ToF EI+ (m/z): 510.0 $[\text{M}+\text{H}]^+$. **HRMS** (ESI) m/z calcd for $\text{C}_{20}\text{H}_{17}\text{F}_6\text{N}_3\text{O}_4\text{S}$ $[\text{M}+\text{H}]^+$ 510.09167, found 510.0907.

5.3.7. 4,6-Fused Scaffold Library

5.3.7.1. *rac*-(6,8-*cis*)-8-(3,5-bis(trifluoromethyl)phenyl)-*N*-(*p*-tolyl)-1,4-diazabicyclo[4.2.0]octane-4-carboxamide (**4e**)

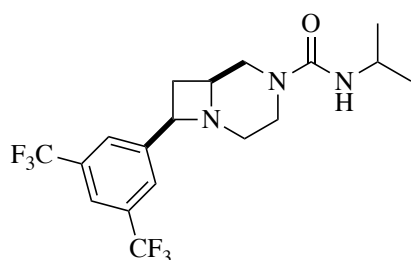


Prepared using *General Procedure G* in a parallel fashion: 4,6-fused scaffold (**4b**) (30 mg, 0.093 mmol, 1.0Eq), 1-isocyanato-4-methylbenzene (18.48 mg, 0.139 mmol, 1.5 Eq), triethylamine (38.7 μ L, 0.278

mmol, 3.0 Eq) in dichloromethane (1 mL, 0.093 M). Purified using preparative HPLC under basic conditions, 32 mg, 76%

¹H NMR (400 MHz, Chloroform-*d*) δ 7.85 (s, 2H, 2- & 6-*H* C₆H₃(CF₃)₂), 7.80 (s, 1H, 4-*H* C₆H₃(CF₃)₂), 7.25 – 7.20 (m, 2H, 3- & 5-*H* C₆H₄(CH₃)), 7.13 – 7.06 (m, 2H, 2- & 6-*H* C₆H₄(CH₃)), 6.25 (s, 1H, NH), 4.43 (dd, *J* 7.9, 5.7 Hz, 1H, CHCH₂CH), 4.07 (dd, *J* 8.5, 8.5 Hz, 1H, NCH₂CHHN), 3.96 (dt, *J* 12.4, 3.2 Hz, 1H, CHCHHN), 3.28 (td, *J* 12.4, 3.2 Hz, 1H, CHCHHN), 3.18 – 3.14 (m, 2H, NCH₂CHN, CH₂CHCH₂), 2.85 (dt, *J* 10.1, 3.5 Hz, 1H, NCHHCH₂N), 2.63 – 2.50 (m, 2H, NCHHCH₂N, CHCHHCH), 2.30 (s, 3H, CH₃), 2.23 – 2.12 (m, 1H, CHCHHCH). **¹³C NMR** (101 MHz, Chloroform-*d*) δ 155.4, 138.89, 138.8, 128.8, 127.2, 124.2, 120.8, 117.1, 65.8, 59.0, 48.5, 47.5, 43.7, 34.4, 21.5. **FTIR** ν_{max} 3004, 2840, 1617, 1036. **MS** ToF EI+ (*m/z*): 458.2. **HRMS** (ESI) *m/z* calcd for C₂₂H₂₁F₆N₃O [M+H]⁺ 458.16616, found 458.1656.

5.3.7.2. *rac*-(6,8-*cis*)-8-(3,5-bis(trifluoromethyl)phenyl)-*N*-isopropyl-1,4-diazabicyclo[4.2.0]octane-4-carboxamide (**4f**)



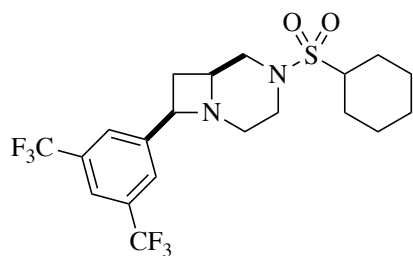
Prepared using *General Procedure G* in a parallel fashion:

4,6-fused scaffold (**4b**) (30 mg, 0.093 mmol, 1.0 Eq), 2-isocyanatopropane (11.81 mg, 0.139 mmol, 1.5 Eq), triethylamine (39 μ L, 0.278 mmol, 3.0 Eq) in

dichloromethane (1 mL, 0.093 M). Purified using preparative HPLC. Colourless solid, 20 mg, 53%.

¹H NMR (400 MHz, Chloroform-*d*) δ 7.83 (s, 2H, Ar), 7.79 (s, 1H, Ar), 4.40 (dd, *J* 7.9, 5.8 Hz, 1H, ArCHCH₂CH), 4.15 (d, *J* 7.8 Hz, 1H, NHCHCH₃), 3.98 (hept, *J* 7.3 Hz, 1H, NHCHCH₃), 3.91 (dd, *J* 10.8, 2.4 Hz, 1H, CHCH₂CHCHH), 3.78 (dt, *J* 12.3, 3.3 Hz, 1H, NCH₂CHHN), 3.19 – 2.98 (m, 3H, CHCH₂CHCH₂, CHCH₂CHCHH, NCH₂CHHN), 2.80 (dt, *J* 10.2, 3.5 Hz, 1H, NCHHCH₂N), 2.58 – 2.42 (m, 2H, NCHHCH₂N, ArCHCHHCH), 2.15 (q, *J* 8.6 Hz, 1H, ArCHCHHCH), 1.17 (s, 3H, CHCH₃), 1.15 (s, 3H, CHCH₃). **¹³C NMR** (101 MHz, Chloroform-*d*) δ 127.0 (Ar), 121.5 (Ar), 65.9 (ArCH), 59.3 (CHCH₂CHCH₂), 48.8 (NCH₂CH₂N), 47.6 (CH₂CHCH₂N), 43.4 (NCH₂CH₂N), 42.7 (CHCH₃), 35.3 (ArCHCH₂CH), 23.5 (CH₃). **FTIR** ν_{max} 2933, 894. **MS** ToF EI⁺ (*m/z*): 410.2. **HRMS** (ESI) *m/z* calcd for C₁₈H₂₁F₆N₃O [M+H]⁺ 410.16616, found 410.1651.

5.3.7.3. *rac*-(6,8-*cis*)-8-(3,5-bis(trifluoromethyl)phenyl)-4-(cyclohexylsulfonyl)-1,4-diazabicyclo[4.2.0]octane (**4g**)



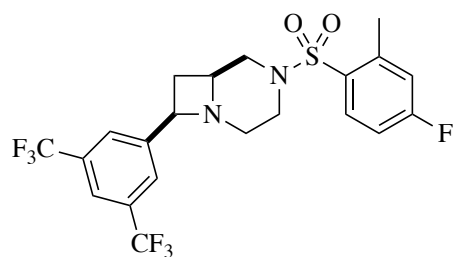
Prepared using *General Procedure G* in a parallel fashion:

4,6-fused scaffold (**4b**) (40 mg, 0.123 mmol, 1.0 Eq), cyclohexanesulfonyl chloride (27 μ L, 0.185 mmol, 1.5 Eq), triethylamine (52 μ L, 0.370 mmol, 3.0 Eq) in

dichloromethane (1 mL, 0.123 M). Purified using preparative HPLC. Colourless oil, 28 mg, 48%.

¹H NMR (400 MHz, Chloroform-*d*) δ 7.84 (s, 2H, Ar), 7.78 (s, 1H, Ar), 4.29 (dd, *J* 8.0, 5.5 Hz, 1H, CHCH₂CH), 3.87 (dd, *J* 10.9, 2.2 Hz, 1H, CH₂CHCHHN), 3.85 – 3.80 (m, 1H, NCH₂CHHN), 3.26 (ddd, *J* 12.3, 10.9, 3.4 Hz, 1H, NCH₂CHHN), 3.11 (q, *J* 10.3 Hz, 1H, CH₂CHCHHN), 3.04 (tdd, *J* 9.8, 5.2, 2.1 Hz, 1H, CH₂CHCH₂N), 2.91 (tt, *J* 12.0, 3.4 Hz, 1H, SCHCH₂), 2.81 (ddd, *J* 10.0, 3.4, 1.6 Hz, 1H, NCHHCH₂N), 2.56 (td, *J* 10.5, 3.2 Hz, 1H, NCHHCH₂N), 2.49 (dt, *J* 9.1, 5.4 Hz, 1H, ArCHCHHCH), 2.14 (dt, *J* 14.4, 3.3 Hz, 2H, SCHCHHCH₂), 2.04 (q, *J* 8.7 Hz, 1H, ArCHCHHCH), 1.90 (dt, *J* 12.4, 3.5 Hz, 2H, SCHCH₂CHHCH₂), 1.75 – 1.68 (m, 1H, CH₂CHHCH₂), 1.52 (qd, *J* 12.4, 3.5 Hz, 2H, SCHCHHCH₂), 1.35 – 1.17 (m, 3H, SCHCH₂CHHCH₂, CH₂CHHCH₂). **¹³C NMR** (101 MHz, Chloroform-*d*) δ 126.8 (Ar), 121.5 (Ar), 66.4 (ArCH), 61.8 (SCHCH₂), 60.5 (ArCHCH₂CH), 51.2 (CH₂CHCH₂), 50.6 (NCH₂CH₂N), 46.3 (NCH₂CH₂N), 37.1 (ArCHCH₂CH), 26.6 (SCHCH₂CH₂), 25.3 (SCHCH₂CH₂), 25.2 (CH₂CH₂CH₂). **FTIR** ν_{max} 3026, 1349 **MS** ToF EI⁺ (*m/z*): 471.2

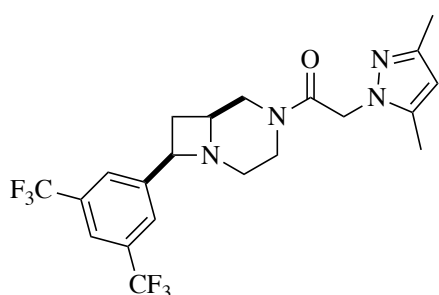
5.3.7.4. *rac*-(6,8-*cis*)-8-(3,5-bis(trifluoromethyl)phenyl)-4-((4-fluoro-2-methylphenyl)sulfonyl)-1,4-diazabicyclo[4.2.0]octane (**4h**)



Prepared using *General Procedure G* in a parallel fashion: 4,6-fused scaffold (**4b**) (30 mg, 0.093 mmol, 1.0 Eq), 4-fluoro-2-methylbenzenesulfonyl chloride (29 mg, 0.139 mmol, 1.5 Eq), triethylamine (38.7 μ L, 0.278 mmol, 3.0 Eq) in dichloromethane (1 mL, 0.093 M). Purified using preparative HPLC, 10 mg, 25%

^1H NMR (400 MHz, Chloroform-*d*) δ 8.00 (td, *J* 7.9, 7.5, 5.2 Hz, 1H, 6-*H* C₆H₃F(CH₃)), 7.88 (s, 2H, 2- & 6-*H* C₆H₃(CF₃)₂), 7.83 (s, 1H, 4-*H* C₆H₃(CF₃)₂), 7.05 – 6.91 (m, 2H, 3- & 5-*H* C₆H₃F(CH₃)), 4.05 (app t, *J* 8.2 Hz, 1H, CHCH₂CH), 3.39 (dd, *J* 12.1, 7.8 Hz, 1H, CHCHHN), 3.18 – 3.06 (m, 3H, CH₂CHCH₂, CHCHHN, NCH₂CHHN), 3.01 – 2.86 (m, 2H, NCH₂CHHN, NCHHCH₂N), 2.65 – 2.62 (m, 1H, NCHHCH₂N), 2.56 – 2.51 (m, 1H, CHCHHCH), 2.49 (s, 3H, CH₃), 1.87 (dt, *J* 10.9, 8.5 Hz, 1H, CHCHHCH). **^{13}C NMR** (101 MHz, Chloroform-*d*) δ 145.5 (1-*C* C₆H₃(CF₃)₂), 132.1 (2- & 6-*C* C₆H₃(CF₃)₂), 126.9 (6-*C* C₆H₃F(CH₃)), 121.9 (4-*C* C₆H₃(CF₃)₂), 119.3 (3-*C* C₆H₃F(CH₃)), 113.1 (5-*C* C₆H₃F(CH₃)), 65.3 (CHCH₂CH), 61.7 (CHCH₂CH), 57.2 (CHCH₂N), 46.5 (NCH₂CH₂N), 41.3 (NCH₂CH₂N), 29.9 (CHCH₂CH), 20.3 (CH₃). **FTIR** ν_{max} 3295, 1602, 1479, 1278, 1155. **MS** ToF EI+ (*m/z*): 497.1 [M+H]⁺. **HRMS** (ESI) *m/z* calcd for C₂₁H₁₉F₇N₂O₂S [M+H]⁺ 497.44382, found 497.1119.

5.3.7.5. *rac*-(6,8-*cis*)-8-(3,5-bis(trifluoromethyl)phenyl)-1,4-diazabicyclo[4.2.0]octan-4-yl)-2-(3,5-dimethyl-1*H*-pyrazol-1-yl)ethan-1-one (**4i**)



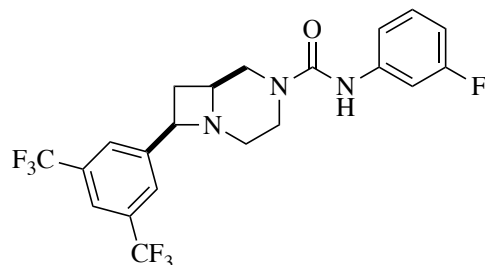
Prepared using *General Procedure G* in a parallel fashion:

4,6-fused scaffold (**4b**) (30 mg, 0.093 mmol, 1.0Eq), 2-(3,5-dimethyl-1*H*-pyrazol-1-yl)acetic acid (14 mg, 0.093 mmol, 1.0 Eq), EDC.HCl (16 mg, 0.1 mmol, 1.1.Eq), HOAt (1.2 mg, 0.0093 mmol, 0.1 Eq) triethylamine (16

μL, 0.11 mmol, 1.2 Eq) in dichloromethane (1 mL, 0.093 M). Purified using preparative HPLC, 11 mg, 31%.

¹H NMR (400 MHz, Chloroform-*d*) δ 7.80 (s, 2H, 2- & 6-*H* C₆H₃(CF₃)₂), 7.75 (s, 4-*H* C₆H₃(CF₃)₂), 5.86 (s, 1H, C₃HN₂(CH₃)₂), 4.67 (s, 2H, C=OCH₂N), 4.02 (app t, *J* 8.1 Hz, 1H, CHCH₂CH), 3.50 (dd, *J* 14.0, 6.3 Hz, 1H, CHCHHN), 3.35 – 3.27 (m, 1H, CH₂CHCH₂), 3.27 – 3.18 (m, 2H, CHCHHN, NCH₂CHHN), 2.94 (dt, *J* 13.5, 5.8 Hz, 1H, NCH₂CHHN), 2.69 – 2.64 (m, 1H, NCHHCH₂N), 2.56 – 2.47 (m, 2H, NCH₂CHHN, CHCHHCH), 2.19 (s, 3H, CH₃), 2.13 (s, 3H, CH₃), 1.65 (dt, *J* 10.7, 8.3 Hz, 1H, CHCHHCH). **¹³C NMR** (101 MHz, Chloroform-*d*) δ 168.4 (NC=O), 149.3 (3-*C* C₃HN₂(CH₃)₂), 149.0 (1-*C* C₆H₃(CF₃)₂), 146.0 (5-*C* C₃HN₂(CH₃)₂), 140.4 (2- & 6-*C* C₆H₃(CF₃)₂), 131.7 (q, *J* 33.1 Hz, 3- & 5-*C* C₆H₃(CF₃)₂), 126.6 (4-*C* C₆H₃(CF₃)₂), 105.9 (4-*C* C₃HN₂(CH₃)₂), 61.1 (CHCH₂CH), 56.9 (CHCH₂CH), 51.8 (NCH₂CH₂N), 51.6 (NCH₂CH₂N), 51.2 (CHCH₂N), 37.8 (C=OCH₂), 30.6 (CHCH₂CH), 13.5 (CH₃), 10.9 (CH₃). **FTIR** ν_{max} 3287, 1666, 1278. **MS** ToF EI+ (*m/z*): 461.1 [M+H]⁺. **HRMS** (ESI) *m/z* calcd for C₂₁H₂₂F₆N₄O [M+H]⁺ 461.17706, found 461.1758.

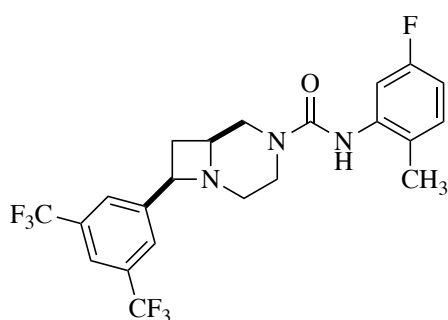
5.3.7.6. *rac*-(6,8-*cis*)-8-(3,5-bis(trifluoromethyl)phenyl)-*N*-(3-fluorophenyl)-1,4-diazabicyclo[4.2.0]octane-4-carboxamide (**4j**)



Prepared using *General Procedure G* in a parallel fashion: 4,6-fused scaffold (**4b**) (30 mg, 0.093 mmol, 1.0 Eq), 1-fluoro-3-isocyanatobenzene (19 mg, 0.139 mmol, 1.5 Eq), triethylamine (38.7 μ L, 0.278 mmol, 3.0 Eq) in dichloromethane (1 mL, 0.093 M). Purified using preparative HPLC, 9.9 mg, 26%

¹H NMR (400 MHz, Chloroform-*d*) δ 7.86 (s, 2H, 2- & 6-*H* C₆H₃(CF₃)₂), 7.82 (s, 1H, 4-*H* C₆H₃(CF₃)₂), 7.31 – 7.19 (m, 2H, 2- & 5-*H* C₆H₄F), 7.00 (dd, *J* 8.0, 2.0 Hz, 1H, 6-*H* C₆H₄F), 6.78 – 6.69 (m, 1H, 4-*H* C₆H₄F), 6.44 (s, 1H, NH), 4.55 (app. s, 1H,), 4.09 – 4.03 (m, 1H, CHCHHN), 3.94 (dt, *J* 12.3, 4.0 Hz, 1H, NCH₂CHHN), 3.37 – 3.20 (m, 3H, CH₂CHCH₂, NCH₂CHHN, CHCHHN), 2.87 (dt, *J* 10.5, 3.6 Hz, 1H, NCHHCN₂N), 2.63 – 2.57 (m, 2H, NCHHCN₂N, CHCHHCH), 2.25 (q, *J* 9.2 Hz, 1H, CHCHHCH). **¹³C NMR** (101 MHz, Chloroform-*d*) δ 168.4 (5-*C* C₆H₄F), 167.7 (C=ON), 149.3 (1-*C* C₆H₃(CF₃)₂), 149.0 (1-*C* C₆H₄F), 146.0 (*C* C₆H₄F), 140.6 (*C* C₆H₄F), 140.4 (*C* C₆H₄F), 126.6 (2- & 6-*C* C₆H₃(CF₃)₂), 121.5 (4-*C* C₆H₃(CF₃)₂), 105.9 (5-*C* C₆H₄F), 65.2 (CHCH₂CH), 61.1 (CHCH₂CH), 51.7 (NCH₂CH₂N), 51.5 (CHCH₂N), 51.2 (NCH₂CH₂N), 30.6 (CHCH₂CH). **FTIR** ν_{max} 3309, 1640, 1282, 1133. **MS** ToF EI+ (*m/z*): 462.3 [M+H]⁺. **HRMS** (ESI) *m/z* calcd for C₂₁H₁₈F₇N₃O [M+H]⁺ 462.14109, found 462.1400.

5.3.7.7. *rac*-(6,8-*cis*)-8-(3,5-bis(trifluoromethyl)phenyl)-*N*-(5-fluoro-2-methylphenyl)-1,4-diazabicyclo[4.2.0]octane-4-carboxamide (**4k**)

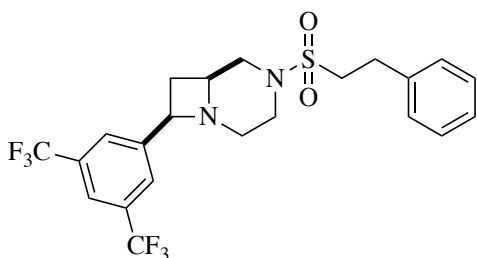


Prepared using *General Procedure G* in a parallel fashion: 4,6-fused scaffold (**4b**) (30 mg, 0.093 mmol, 1.0 Eq), 4-fluoro-2-isocyanato-1-methylbenzene (21 mg, 0.139 mmol, 1.5 Eq), triethylamine (38.7 μ L, 0.278 mmol, 3.0 Eq) in dichloromethane (1 mL, 0.093 M).

Purified using preparative HPLC, 10.5 mg, 28%.

¹H NMR (400 MHz, Chloroform-*d*) δ 7.87 (s, 2H, 2- & 6-*H* C₆H₃(CF₃)₂), 7.82 (s, 1H, 4-*H* C₆H₃(CF₃)₂), 7.58 (dd, *J* 11.0, 2.7 Hz, 1H, 6-*H* C₆H₃F(CH₃)), 7.09 (dt, *J* 8.6, 6.4 Hz, 1H, 3-*H* C₆H₃F(CH₃)), 6.70 (td, *J* 8.2, 2.7 Hz, 1H, 4-*H* C₆H₃F(CH₃)), 6.17 (d, *J* 3.4 Hz, 1H, *NH*), 4.71 (app. t, *J* 8.2 Hz, 1H, *CHCH*₂*CH*), 4.09 – 4.03 (m, 1H, *CHCHHN*), 3.99 – 3.91 (m, 1H, *NCH*₂*CHHN*), 3.40 – 3.21 (m, 3H, *CHCHHN*, *NCH*₂*CHHN*, *CH*₂*CHCH*₂), 2.89 (dt, *J* 10.4, 3.6 Hz, 1H, *NCHHCH*₂*N*), 2.62 (ddd, *J* 12.0, 7.6, 4.3 Hz, 2H, *NCHHCH*₂*N*, *CHCHHCH*), 2.33 – 2.22 (m, 1H, *CHCHHCH*), 2.20 (s, 3H, *CH*₃). **¹³C NMR** (101 MHz, Chloroform-*d*) δ 162.5 (NC=ONH), 155.0 (3-CF C₆H₃F(CH₃)), 130.9 (1-C C₆H₃(CF₃)₂), 130.9 (1-C C₆H₃F(CH₃)), 127.1 (2- & 6-C C₆H₃(CF₃)₂), 121.9 (4-C C₆H₃(CF₃)₂), 110.3 (6-C C₆H₃F(CH₃)), 109.1 (4-C C₆H₃F(CH₃)), 58.9 (*CHCH*₂*CH*) 52.86 (*CH*₂*CHCH*₂), 48.8 (*NCH*₂*CH*₂*N*), 43.4 (*NCH*₂*CH*₂*N*), 31.5 (*CHCH*₂*CH*), 17.1 (*CH*₃). **FTIR** ν_{max} 3295, 1640, 1278, 1133. **MS** ToF EI+ (*m/z*): 467.2 [M+H]⁺. **HRMS** (ESI) *m/z* calcd for C₂₂H₂₀F₇N₃O [M+H]⁺ 476.15674, found 476.1557.

5.3.7.8. *rac*-(6,8-*cis*)-8-(3,5-bis(trifluoromethyl)phenyl)-4-(phenethylsulfonyl)-1,4-diazabicyclo[4.2.0]octane (**4l**)

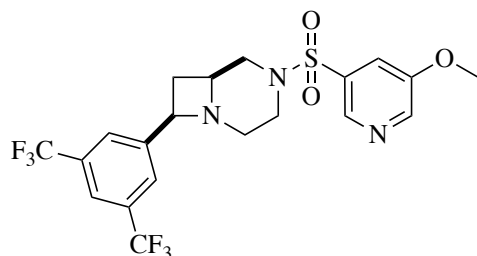


Prepared using *General Procedure G* in a parallel fashion: 4,6-fused scaffold (**4b**) (30 mg, 0.093 mmol, 1.0 Eq), 2-phenylethane-1-sulfonyl chloride (28 mg, 0.139 mmol, 1.5 Eq), triethylamine (38.7 μ L, 0.278

mmol, 3.0 Eq) in dichloromethane (1 mL, 0.093 M). Purified using preparative HPLC, 7 mg, 18%.

^1H NMR (400 MHz, Chloroform-*d*) δ 7.83 (s, 2H, Ar), 7.78 (s, 1H, Ar), 7.38 – 7.31 (m, 2H, Ar), 7.30 – 7.22 (m, 3H, Ar), 4.30 (dd, *J* 8.0, 5.5 Hz, 1H, ArCHCH₂), 3.86 (d, *J* 9.4 Hz, 1H, CH₂CHCHHN), 3.84 – 3.80 (m, 1H, NCH₂CHHN), 3.26 – 3.11 (m, 5H, NCH₂CHHN, SCHHCH₂C, SCH₂CHHC), 3.08 – 2.96 (m, 2H, CHCH₂CHCH₂, CH₂CHCHH), 2.85 (dq, *J* 10.2, 2.4 Hz, 1H, NCHHCH₂N), 2.58 (td, *J* 10.1, 2.4 Hz, 1H, NCHHCH₂N), 2.51 (dt, *J* 9.1, 5.3 Hz, 1H, ArCHCHHCH), 2.04 (q, *J* 9.1 Hz, 1H, ArCHCHHCH). **^{13}C NMR** (101 MHz, Chloroform-*d*) δ 128.9 (Ar), 128.4 (Ar), 127.0 (Ar), 126.6 (Ar), 121.6 (Ar), 66.3 (ArCH), 59.9 (CH₂CH₂Ar), 51.6 (CH₂CHCH₂), 50.6 (CHCH₂N), 50.0 (NCH₂CH₂N), 45.7 (NCH₂CH₂N), 36.9 (ArCHCH₂CH), 29.5 (CH₂CH₂Ar). FTIR ν_{max} 2832, 1338, 1278, 1133. **MS** ToF EI+ (*m/z*): 493.2 [M+H]⁺. **HRMS** (ESI) *m/z* calcd for C₂₂H₂₂F₆N₂O₂S [M+H]⁺ 493.13789, found 493.1368.

5.3.7.9. *rac*-(6,8-*cis*)-8-(3,5-bis(trifluoromethyl)phenyl)-4-((5-methoxypyridin-3-yl)sulfonyl)-1,4-diazabicyclo[4.2.0]octane (**4m**)

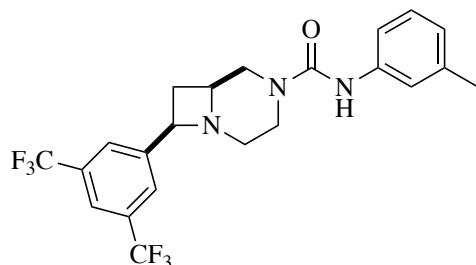


Prepared using *General Procedure G* in a parallel fashion: 4,6-fused scaffold (**4b**) (30 mg, 0.093 mmol, 1.0 Eq), 5-methoxypyridine-3-sulfonyl chloride (29 mg, 0.139 mmol, 1.5 Eq), triethylamine (38.7 μ L,

0.278 mmol, 3.0 Eq) in dichloromethane (1 mL, 0.093 M). Purified using preparative HPLC, 9 mg, 23%

¹H NMR (400 MHz, Chloroform-*d*) δ 8.60 (d, *J* 1.8 Hz, 1H, Ar), 8.54 (d, *J* 1.8 Hz, 1H, Ar), 7.76 (s, 3H, Ar), 7.51 (dd, *J* 2.9, 1.8 Hz, 1H, Ar), 4.28 (dd, *J* 8.0, 5.4 Hz, 1H, ArCHCH₂), 3.95 (s, 3H, OCH₃), 3.91 (dd, *J* 10.0, 2.7 Hz, 1H, CH₂CHCHHN), 3.87 – 3.82 (m, 1H, NCHHCH₂N), 3.08 (dd, *J* 10.0, 2.7 Hz, 1H, CH₂CHCHHN), 2.88 – 2.82 (m, 1H, NCHHCH₂N), 2.79 (td, *J* 11.0, 3.5 Hz, 1H, NCH₂CHHN), 2.70 – 2.62 (t, *J* 2.7 Hz, 1H, CH₂CHCH₂), 2.66 – 2.59 (m, 1H, NCH₂CHHN), 2.50 (dt, *J* 9.1, 5.5 Hz, 1H, ArCHCHHCH), 2.00 (q, *J* 9.1 Hz, 1H, ArCHCHHCH). **¹³C NMR** (101 MHz, Chloroform-*d*) δ 155.7 (ArCOCH₃), 143.9 (ArCCH), 142.2 (ArC), 139.9 (ArC), 134.0 (ArC), 131.9 (ArC), 131.6 (ArC), 126.8 (ArC), 118.3 (ArC), 66.3 (ArCCH), 59.3 (CHCH₂CH), 56.1 (NCH₂CH₂N), 50.7 (CH₂CHCH₂), 49.6 (NCH₂CH₂N), 45.9 (CHCH₂CH), 36.8 (ArCOCH₃). **FTIR** (ν_{max} , neat): 2948.3, 2855.1, 1338.1, 1274.7, 1166.7, 1125.7 **MS** ToF EI+ (*m/z*): 496.1 [M+H]⁺ **HRMS** (ESI) *m/z* calcd for C₂₀H₁₉F₆N₃O₃S [M+H]⁺ 496.11241, found 496.1111.

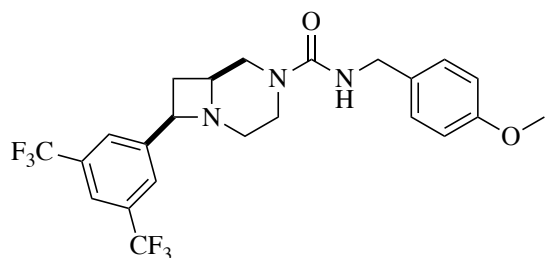
5.3.7.10. *rac*-(6,8-*cis*)-8-(3,5-bis(trifluoromethyl)phenyl)-*N*-(*m*-tolyl)-1,4-diazabicyclo[4.2.0]octane-4-carboxamide (**4n**)



Prepared using *General Procedure G* in a parallel fashion: 4,6-fused scaffold (**4b**) (30 mg, 0.093 mmol, 1.0Eq), 1-isocyanato-3-methylbenzene (19 mg, 0.139 mmol, 1.5 Eq), triethylamine (38.7 μ L, 0.278 mmol, 3.0 Eq) in dichloromethane (1 mL, 0.093 M). Purified using preparative HPLC, 9 mg, 24%.

¹H NMR (400 MHz, Chloroform-*d*) δ 7.86 (s, 2H, Ar 2- & 6-*H* C₆H₃(CF₃)₂), 7.81 (s, 1H, Ar 4-*H* C₆H₃(CF₃)₂), 7.22 (d, *J* 2.0 Hz, 1H, Ar 2-*H* C₆H₄(CH₃)), 7.17 (t, *J* 7.7 Hz, 1H, Ar 6-*H* C₆H₄(CH₃)), 7.12 – 7.08 (m, 1H, Ar 5-*H* C₆H₄(CH₃)), 6.87 (d, *J* 7.7 Hz, 1H, Ar 4-*H* C₆H₄(CH₃)), 6.29 (s, 1H, NH), 4.52 (appt s, 1H, ArCHCH₂), 4.06 (dd, *J* 10.7, 2.0 Hz, 1H, NCH₂CHHN), 3.94 (dt, *J* 12.4, 3.5 Hz, 1H, CHCHHN), 3.34 – 3.17 (m, 3H, CH₂CHCH₂, CHCHHN, NCH₂CHHN), 2.88 – 2.83 (m, 1H, NCHHCH₂N), 2.62 – 2.55 (m, 2H, NCHHCH₂N, CHCHHCH), 2.32 (s, 3H, CH₃), 2.23 (q, *J* 8.7 Hz, 1H, CHCHHCH). **¹³C NMR** (101 MHz, Chloroform-*d*) δ 155.4 (C=O), 138.9 (1-C C₆H₃(CF₃)₂), 138.6 (CCH₃), 128.8 (2-CH C₆H₄(CH₃)), 127.2 (2- & 6-CH C₆H₃(CF₃)₂), 124.2 (4-CH C₆H₄(CH₃)), 121.8 (4-CH C₆H₃(CF₃)₂), 120.8 (5-CH C₆H₄(CH₃)), 117.1 (6-CH C₆H₄(CH₃)), 65.7 (ArCHCH₂), 59.1 (CH₂CHCH₂), 48.3 (NCH₂CH₂N), 47.7 (NCH₂CH₂N), 43.7 (CHCH₂N), 35.3 (CHCH₂CH), 21.5 (CH₃). **FTIR** (ν_{max} , neat): 3309, 1640, 1442, 1282, 1133. **MS** ToF EI+ (*m/z*): 458.2 [M+H]⁺. **HRMS** (ESI) *m/z* calcd for C₂₂H₂₁F₆N₃O [M+H]⁺ 458.16616, found 458.1655.

5.3.7.11. *rac*-(6,8-*cis*)-8-(3,5-bis(trifluoromethyl)phenyl)-*N*-(4-methoxybenzyl)-1,4-diazabicyclo[4.2.0]octane-4-carboxamide (**4o**)



Prepared using *General Procedure G* in a parallel fashion: 4,6-fused scaffold (**4b**) (30 mg, 0.093 mmol, 1.0 Eq), 1-(isocyanatomethyl)-4-methoxybenzene (23 mg, 0.139 mmol, 1.5

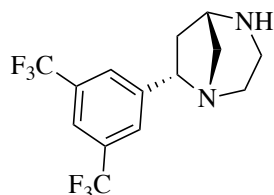
Eq), triethylamine (38.7 μ L, 0.278 mmol, 3.0 Eq) in dichloromethane (1 mL, 0.093 M). Purified using preparative HPLC, 8 mg, 22%

¹H NMR (400 MHz, Chloroform-*d*) δ 7.84 (s, 2H, Ar 2- & 6-CH C₆H₃(CF₃)₂), 7.80 (s, 1H, Ar 4-CH C₆H₃(CF₃)₂), 7.24 (dd, *J* 8.2, Hz, 2H, 2- & 6-CH C₆H₄(OCH₃)), 6.87 (d, *J* 8.2 Hz, 2H, 3- & 5-CH C₆H₄(OCH₃)), 4.59 (dd, *J* 5.3, 5.3 Hz, 1H, ArCHCH₂), 4.50 (s, 1H, NH), 4.37 (d, *J* 5.3 Hz, 2H, NHCH₂(C₆H₄(OCH₃))), 3.94 (dd, *J* 11.5, 3.0 Hz, 1H, NCH₂CHHN), 3.80 (s, 3H, OCH₃), 3.79 – 3.73 (m, 1H, CHCHHN), 3.23 – 3.10 (m, 3H, CH₂CHCH₂, NCH₂CHHN, CHCHHN), 2.80 (dt, *J* 10.3, 3.6 Hz, 1H, NCHHCH₂N), 2.59 – 2.49 (m, 2H, NCHHCH₂N, CHCHHCH), 2.21 (q, *J* 9.4 Hz, 1H, CHCHHCH). **¹³C NMR** (101 MHz, Chloroform-*d*) δ 158.9 (COCH₃), 157.7 (C=O), 131.9 (1-C C₆H₃(CF₃)₂), 131.3 (1-C C₆H₄(OCH₃)), 129.2 (2- & 6-CH C₆H₄(OCH₃)), 127.2 (2- & 6-CH C₆H₃(CF₃)₂), 121.7 (4-CH C₆H₃(CF₃)₂), 114.1 (3- & 5-CH C₆H₄(OCH₃)), 65.7 (ArCHCH₂), 59.1 (CH₂CHCH₂), 55.3 (OCH₃), 44.7 (NCH₂CH₂N), 43.3 (NCH₂CH₂N), 42.0 (NHCH₂(C₆H₄(OCH₃))), 25.8 (CHCH₂CH). **FTIR** (ν_{max} , neat): 2918.5, 2840.2, 1617.87, 1539.4, 1278.5, 1170.4, 1129.4 **MS** ToF EI+ (*m/z*): 488.2 [M+H]⁺. **HRMS** (ESI) *m/z* calcd for C₂₃H₂₃F₆N₃O₂ [M+H]⁺ 488.17672, found 488.1759.

5.3.8. 5,6-Bridged Bicyclic Scaffolds

5.3.8.1. *rac*-(1,5-*cis*,1,7-*trans*)-7-(3,5-bis(trifluoromethyl)phenyl)-1,4-

diazabicyclo[3.2.1]octane (**5a**)

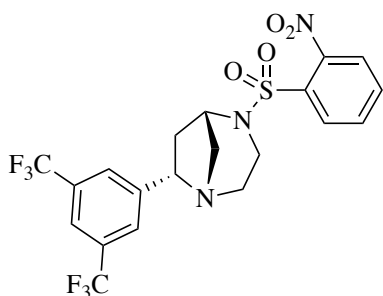


Prepared using *General Procedure D*: Azido-pyrrolidine intermediate (1.48 g, 3.32 mmol, 1.0 Eq), triphenylphosphine (2.26 g, 8.62 mmol, 2.6 Eq), water (1.20 mL, 66.3 mmol, 20.0 Eq) in THF (15 mL, 0.22 M).

Purified using flash chromatography (0 – 8% MeOH:DCM with 1% ammonia). Pale yellow oil, 777mg, 72%.

¹H NMR (400 MHz, Chloroform-*d*) δ 7.85 (d, *J* 1.7 Hz, 2H, Ph*H*), 7.76 (s, 1H, Ph*H*), 4.25 (dd, *J* 7.9, 5.4 Hz, 1H, PhCHNCH₂), 3.07 (ddd, *J* 12.6, 10.6, 3.6 Hz, 1H, PhCHCH₂CH₂CHHN), 3.00 – 2.94 (m, 3H, NCH₂CHHNHCH₂), 2.94 – 2.86 (m, 1H, NCH₂CHHN), 2.77 (ddd, *J* 9.8, 3.8, 1.7 Hz, 1H, NCHHCH₂N), 2.52 – 2.44 (m, 2H, CHHCHNCHH), 2.09 – 2.02 (m, 2H, CHHCHNCH₂). **¹³C NMR** (101 MHz, Chloroform-*d*) δ 127.3 (Ar), 121.6 (Ar), 67.5 (ArCHN), 62.9 (CH₂CHNH), 52.5 (CHNCH₂CH₂), 50.2 (CHNCH₂CH₂), 45.9 (CHCH₂N), 38.3 (ArCHCH₂CHCH₂N). **FTIR** (ν_{max} , neat): 2944, 1379, 1274, 1121. **MS** ToF EI+ (*m/z*): 325.2 **HRMS** (ESI) *m/z* calcd for C₁₄H₁₄F₆N₂ [M+H]⁺ 325.11339, found 325.1137.

5.3.8.2. *rac*-(1,5-*cis*,1,7-*trans*)-7-(3,5-bis(trifluoromethyl)phenyl)-4-((2-nitrophenyl)sulfonyl)-1,4-diazabicyclo[3.2.1]octane (**5b**)

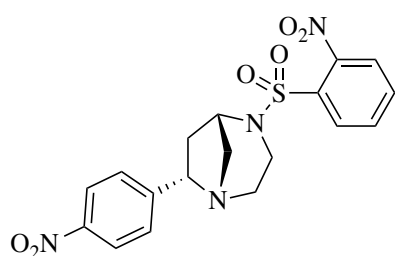


Protected amino-azetidine (570 mg, 1.1 mmol 1.0 Eq) was dissolved in dichloromethane (12 mL) and was subsequently cooled to 0 °C. Triethylamine (452 μL , 3.2 mmol, 3.0 Eq) was added followed by the dropwise addition of methanesulfonyl chloride (93 μL , 1.2 mmol, 1.1 Eq). The reaction mixture was stirred for 30 min at 0 °C. and was quenched with water (15 mL), the aqueous layer was extracted with dichloromethane (3 x 15 mL). The combined organic fractions were dried over Na_2SO_4 , filtered and concentrated *in vacuo* to provide the crude mesylated product. The resultant sulfonate was redissolved in *N,N*-dimethylformamide (12.0 mL) and potassium carbonate (299 mg, 2.2 mmol, 2.0 Eq) was added as a single portion. The reaction mixture was heated to 65 °C for 1 h. The reaction mixture was cooled and extracted with ethyl acetate (3 x 15 mL) and washed with water (2 x 15 mL) and brine (4 x 15 mL). The combined organic fractions were dried over Na_2SO_4 , and solvent was removed under reduced pressure and the resulting residue was purified using reverse-phase chromatography using $\text{CH}_3\text{CN}/\text{H}_2\text{O}$ to provide pure product (**5b**) as a yellow oil, 479 mg, 87%.

^1H NMR (400 MHz, Chloroform-*d*) δ 8.04 – 7.98 (m, 1H, Ar), 7.81 (s, 2H, Ar), 7.77 (s, 1H, Ar), 7.73 (ddd, J 6.9, 4.2, 1.9 Hz, 2H, Ar), 7.67 – 7.64 (m, 1H, Ar), 4.30 (dd, J 8.0, 5.4 Hz, 1H, ArCHN), 3.91 (dd, J = 8.4, 8.4 Hz, 1H, NCHHCH₂N), 3.88 – 3.83 (m, 1H, CH₂CHCHHN), 3.17 (td, J 11.7, 3.5 Hz, 1H, NCHHCH₂N), 3.11 – 3.02 (m, 2H, CH₂CHCHHN), 2.86 (td, J 10.6, 3.2 Hz, 1H, NCH₂CHHN), 2.61 (td, J 10.6, 3.2 Hz, 1H, NCH₂CHHN), 2.52 (dt, J 8.8, 5.2 Hz, 1H, ArCHCHHCH), 2.09 – 2.02 (m, 1H, ArCHCHHCH). **^{13}C NMR** (101 MHz,

Chloroform-*d*) δ 133.7 (Ar), 131.6 (Ar), 130.9 (Ar), 126.8 (Ar), 124.2 (Ar), 121.9 (Ar), 66.3 (ArCHCH₂), 59.7 (CH₂CHCH₂N), 50.9 (CH₂CHCH₂N), 49.9 (NCH₂CH₂N), 46.0 (NCH₂CH₂N), 36.9 (ArCHCH₂CH). **MS** ToF EI+ (*m/z*): 510.0 **HRMS** (ESI) *m/z* calcd for C₂₀H₁₇F₆N₃O₄S [M+H]⁺ 510.09167, found 510.0907.

5.3.8.3. *rac*-(1,5-*cis*,1,7-*trans*)-7-(4-nitrophenyl)-4-((2-nitrophenyl)sulfonyl)-1,4-diazabicyclo[3.2.1]octane (**5c**)



N-(((2*S*,4*R*)-1-(2-hydroxyethyl)-4-(4-nitrophenyl)azetidine-2-yl)methyl)-2-nitrobenzenesulfonamide (380 mg, 0.871 mmol, 1.0 Eq) was dissolved in dichloromethane (10.0 mL, 0.04 M) and was subsequently cooled to 0 °C. Triethylamine

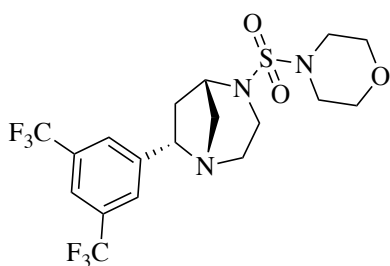
(0.36 mL, 2.61 mmol, 3.0 Eq) was added followed by the dropwise addition of methanesulfonyl chloride (75 µL, 0.958 mmol, 1.1 Eq). The reaction mixture was stirred for 30 min at 0 °C. and was quenched with water (10 mL), the aqueous layer was extracted with dichloromethane (3 x 10 mL). The combined organic fractions were dried over Na₂SO₄, filtered and concentrated *in vacuo* to provide the crude mesylated product. The resultant sulfonate was redissolved in *N,N*-dimethylformamide (10.0mL, 0.044 M) and potassium carbonate (241 mg, 1.741 mmol, 2.0 Eq)) was added as a single portion. The reaction mixture was heated to 65 °C for 1 h. The reaction mixture was cooled and extracted with ethyl acetate (3 x 10 mL) and washed with water (2 x 10 mL) and brine (4 x 10 mL). The combined organic fractions were dried over Na₂SO₄, and solvent was removed under reduced pressure and the resulting residue was purified using reverse-phase chromatography using CH₃CN/H₂O to provide pure product (**5c**) as a yellow oil, 100 mg, 27%.

¹H NMR (400 MHz, Chloroform-*d*) δ 8.16 (d, *J* 8.15, 2H, Ar), 8.05 (dd, *J* 7.3, 1.9 Hz, 1H, Ar), 7.75 (td, *J* 7.3, 1.9 Hz, 2H, Ar), 7.67 (dd, *J* 7.3, 1.9 Hz, 1H, Ar), 7.51 (d, *J* 8.5 Hz, 2H, Ar), 4.51 (dd, *J* 5.6, 2.9 Hz, 1H, ArCHCH₂), 4.33 – 4.27 (m, 1H, NCH₂CHHN), 3.59 – 3.50 (m, 1H, NCH₂CHHN), 3.31 – 3.18 (m, 2H, CHNCH₂CH), 3.04 (dt, *J* 12.2, 2.1 Hz, 1H, CHCHCHN), 2.97 – 2.89 (m, 1H, NCHHCH₂N), 2.58 (dd, *J* 12.4, 3.0 Hz, 1H, NCHHCH₂N), 2.49 (dt, *J* 14.3, 5.4 Hz, 1H, ArCHHCH), 2.01 (dt, *J* 14.3, 5.4 Hz, 1H, ArCHHCH). ¹³C NMR

(101 MHz, Chloroform-*d*) δ 131.3, 130.6, 125.8, 124.3, 123.9, 63.0, 58.8, 57.4, 52.7, 45.5, 38.3, 25.4. **MS** ToF EI+ (*m/z*): 419.0.

5.3.9. 5,6-Bridged Scaffold Library

5.3.9.1. *rac*-(1,5-*cis*,1,7-*trans*)-7-(3,5-bis(trifluoromethyl)phenyl)-1,4-diazabicyclo[3.2.1]octan-4-yl)sulfonyl)morpholine (**5d**)



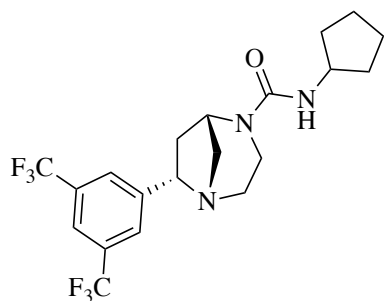
Prepared using *General Procedure H* in a parallel fashion:

5,6-Bridged Scaffold (**5a**) (30 mg, 0.093 mmol, 1.0 Eq), morpholine-4-sulfonyl chloride (26 mg, 0.139 mmol, 1.5 Eq), triethylamine (38.7 μ L, 0.278 mmol, 3.0 Eq) in

dichloromethane (1 mL, 0.093 M). Purified using preparative HPLC, 10 mg, 26%.

¹H NMR (400 MHz, Chloroform-*d*) δ 7.83 (s, 2H, 2- & 6-*H* C₆H₃(CF₃)₂), 7.78 (s, 1H, 4-*H* C₆H₃(CF₃)₂), 4.29 (dd, *J* 8.0, 5.4 Hz, 1H, ArCHCH₂CH), 3.84 – 3.76 (m, 2H, NCHHCH₂N, CH₂CHCHHN), 3.76 – 3.72 (m, 4H, NCH₂CH₂O), 3.29 – 3.24 (m, 1H, NCHHCH₂N), 3.24 – 3.20 (m, 4H, NCH₂CH₂O), 3.11 (appt t, *J* 10.3 Hz, 1H, CHCH₂CHCH₂), 3.07 – 2.99 (m, 1H, CH₂CHCHHN), 2.82 (td, *J* 11.0, 3.5, Hz, 1H, NCH₂CHHN), 2.56 (td, *J* 11.0, 3.5 Hz, 1H, NCH₂CHHN), 2.50 (td, *J* 9.9, 4.6 Hz, 1H, ArCHCHHCH), 2.05 (q, *J* 8.8 Hz, 1H, ArCHCHHCH). **¹³C NMR** (101 MHz, Chloroform-*d*) δ 144.1 (1-*C* C₆H₃(CF₃)₂), 131.7 (q, *J* 33.5 Hz, 3- & 5-*C* C₆H₃(CF₃)₂), 126.8 (2- & 6-*C* C₆H₃(CF₃)₂), 123.3 (q, *J* 33.5 Hz, 273.3 Hz, CF₃) 121.6 (4-*C* C₆H₃(CF₃)₂), 66.4 (CHCH₂CH), 66.3 (N(CH₂CH₂)O), 59.9 (CH₂CHCH₂), 51.5 (CHCH₂N), 49.9 (NCH₂CH₂N), 46.6 (NCH₂CH₂N), 46.5 (N(CH₂CH₂)O), 36.9 (CHCH₂CH). **FTIR** (ν_{\max} , neat): 2858, 1342, 913. **MS** ToF EI+ (*m/z*): 474.2. **HRMS** (ESI) *m/z* calcd for C₁₈H₂₁F₆N₃O₃S [M+H]⁺ 474.12806, found 474.1274.

5.3.9.2. *rac*-(1,5-*cis*,1,7-*trans*)-7-(3,5-bis(trifluoromethyl)phenyl)-*N*-cyclopentyl-1,4-diazabicyclo[3.2.1]octane-4-carboxamide (**5e**)

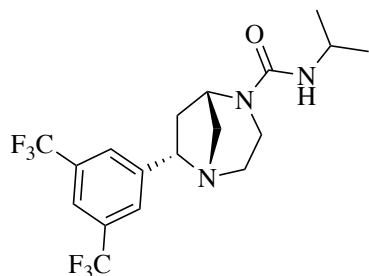


Prepared using *General Procedure H* in a parallel fashion: 5,6-Bridged Scaffold (**5a**) (30 mg, 0.093 mmol, 1.0 Eq), isocyanatocyclopentane (15 mg, 0.139 mmol, 1.5 Eq), triethylamine (38.7 μ L, 0.278 mmol, 3.0 Eq) in dichloromethane (1 mL, 0.093 M). Purified using preparative

HPLC, 12 mg, 33%.

¹H NMR (400 MHz, Chloroform-*d*) δ 7.83 (s, 2H, 2- & 6-*H* C₆H₃(CF₃)₂), 7.78 (s, 1H, 4-*H* C₆H₃(CF₃)₂), 4.40 (dd, *J* 8.0, 5.8 Hz, 1H, ArCHCH₂), 4.27 (d, *J* 6.8 Hz, 1H, NH), 4.11 (h, *J* 6.9 Hz, 1H, NHCHCH₂), 3.91 (dd, *J* 10.8, 2.3 Hz, 1H, CH₂CHCHHN), 3.79 (dt, *J* 12.4, 3.3 Hz, 1H, NCHHCH₂N), 3.17 – 3.00 (m, 3H, NCHHCH₂N, CH₂CHCH₂N, CH₂CHCHHN), 2.79 (dt, *J* 10.2, 3.5 Hz, 1H, NCH₂CHHN), 2.60 – 2.44 (m, 2H, NCH₂CHHN, ArCHCHHCH), 2.15 (q, *J* 8.6 Hz, 1H, ArCHCHHCH), 2.07 – 1.93 (m, 2H, CHCH₂CHHCHHCH₂), 1.74 – 1.51 (m, 4H, CH₂CH₂CH₂CH₂), 1.41 – 1.28 (m, 2H, CHCH₂CHHCHHCH₂). **¹³C NMR** (101 MHz, Chloroform-*d*) δ 157.72 (NC=ON), 143.9 (1-*C* C₆H₃(CF₃)₂), 131.7 (q, *J* 33.2 Hz, 3- & 5-*C* C₆H₃(CF₃)₂), 127.0 (2- & 6-*C* C₆H₃(CF₃)₂), 121.5 (4-*C* C₆H₃(CF₃)₂), 65.9 (CHCH₂CH), 59.3 (CHCH₂CH), 52.7 (CH(CH₂CH₂)), 48.8 (NCH₂CH₂N), 47.6 (CHCH₂N), 43.4 (NCH₂CH₂N), 35.3 (CH(CH₂CH₂)), 33.6 (CH(CH₂CH₂)), 23.7 (CHCH₂CH). **FTIR** (ν_{\max} , neat): 2955, 1528, 902. **MS** ToF EI+ (*m/z*): 436.2. **HRMS** (ESI) *m/z* calcd for C₂₀H₂₃F₆N₃O [M+H]⁺ 436.18181, found 436.1813.

5.3.9.3. *rac*-(1,5-*cis*,1,7-*trans*)-7-(3,5-bis(trifluoromethyl)phenyl)-*N*-isopropyl-1,4-diazabicyclo[3.2.1]octane-4-carboxamide (**5f**)

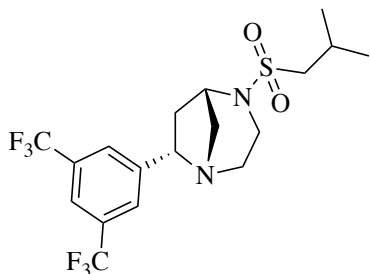


Prepared using *General Procedure H* in a parallel fashion: 5,6-Bridged Scaffold (**5a**) (30 mg, 0.093 mmol, 1.0 Eq), 2-isocyanatopropane (12 mg, 0.139 mmol, 1.5 Eq), triethylamine (38.7 μ L, 0.278 mmol, 3.0 Eq) in dichloromethane (1 mL, 0.093

M). Purified using preparative HPLC, 15mg, 41%.

¹H NMR (400 MHz, Chloroform-*d*) δ 7.83 (s, 2H, Ar), 7.78 (s, 1H, Ar), 4.41 (dd, *J* 8.0, 5.9 Hz, 1H, ArCHCH₂), 4.15 (d, *J* 7.3 Hz, 1H, NH), 3.98 (hept, *J* 6.7 Hz, 1H, NHCHCH₃), 3.91 (dd, *J* 11.0, 2.4 Hz, 1H, CH₂CHCHHN), 3.78 (dt, *J* 12.4, 3.3 Hz, 1H, NCHHCH₂N), 3.18 – 3.02 (m, 3H, CH₂CHCH₂N, CH₂CHCHHN, NCHHCH₂N), 2.80 (dt, *J* 10.1, 3.4 Hz, 1H, NCH₂CHHN), 2.57 – 2.46 (m, 2H, NCH₂CHHN, ArCHCHHCH), 2.16 (q, *J* 8.7 Hz, 1H, ArCHCHHCH), 1.17 (s, 3H, CHCH₃), 1.15 (s, 3H, CHCH₃). **¹³C NMR** (101 MHz, Chloroform-*d*) δ 157.3 (NC=ONH), 143.9 (ArCCHCH₂), 131.7 (q, *J* 33.0 Hz, 3- & 5-C C₆H₃(CF₃)₂), 127.0 (ArC), 124.7 (ArC), 121.9 (ArC), 121.5 (ArC), 65.9 (ArCCH), 59.3 (CHCH₂CH), 48.8 (NCH₂CH₂N), 47.6 (CH₂CHCH₂N), 43.4 (NCH₂CH₂N), 42.7 (NHCHCH₃), 35.3 (CHCH₂CH), 23.5 (CHCH₃). **FTIR** (ν_{max} , neat): 3339, 1528, 1021 **MS** ToF EI⁺ (*m/z*): 410.2 **HRMS** (ESI) *m/z* calcd C₁₈H₂₁F₆N₃O [M+H]⁺ 410.16616, found 410.1651.

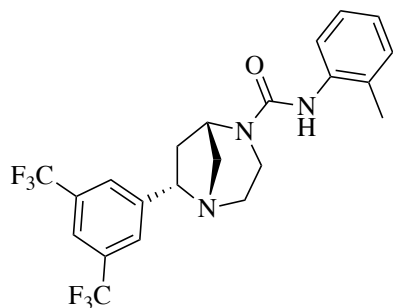
5.3.9.4. *rac*-(1,5-*cis*,1,7-*trans*)-7-(3,5-bis(trifluoromethyl)phenyl)-4-(isobutylsulfonyl)-1,4-diazabicyclo[3.2.1]octane (**5g**)



Prepared using *General Procedure H* in a parallel fashion: 5,6-Bridged Scaffold (**5a**) (30 mg, 0.093 mmol, 1.0 Eq), 2-methylpropane-1-sulfonyl chloride (22 mg, 0.139 mmol, 1.5 Eq), triethylamine (38.7 μ L, 0.278 mmol, 3.0 Eq) in dichloromethane (1 mL, 0.093 M). Purified using preparative HPLC, 11 mg, 30%.

^1H NMR (400 MHz, Chloroform-*d*) δ 7.84 (s, 2H, Ar), 7.78 (s, 1H, Ar), 4.31 (dd, *J* 7.9, 5.4 Hz, 1H), 3.84 (dd, *J* 10.2, 2.4 Hz, 1H, ArCHCH₂), 3.82 – 3.77 (m, 1H, CH₂CHCHHN), 3.13 (td, *J* 11.3, 3.4 Hz, 1H, NCHHCH₂N), 3.08 – 3.03 (m, 1H, CH₂CHCHHN), 2.97 (t, *J* 10.1 Hz, 1H, CH₂CHCH₂), 2.88 – 2.83 (m, 1H, NCH₂CHHN), 2.81 (dd, *J* 6.6, 1.9 Hz, 2H, SCH₂CHCH₃), 2.59 (td, *J* 10.5, 3.2 Hz, 1H, NCH₂CHHN), 2.51 (dt, *J* 9.2, 5.4 Hz, 1H, ArCHCHHCH), 2.30 (hept, *J* 6.7 Hz, 1H, CH₂CHCH₃), 2.05 (q, *J* 8.9 Hz, 1H, ArCHCHHCH), 1.14 (s, 3H, CHCH₃), 1.12 (s, 3H, CHCH₃). **^{13}C NMR** (101 MHz, Chloroform-*d*) δ 144.2 (ArCCHCH₂), 131.8 (q, *J* 34.8 Hz, 3- & 5-C C₆H₃(CF₃)₂), 126.8 (ArC), 124.7 (ArC), 121.56 (ArC), 66.3 (ArCCHCH₂), 59.9 (CHCH₂CHCH₂), 57.2 (SCH₂CHCH₃), 50.5 (NCH₂CH₂N), 50.0 (CH₂CHCH₂N), 45.6 (NCH₂CH₂N), 36.9 (ArCHCH₂CH), 24.6 (CH₂CHCH₃), 22.8 (CHCH₃), 22.7 (CHCH₃). **FTIR** (ν_{max} , neat): 2959, 1336, 984. **MS** ToF EI+ (*m/z*): 445.1 **HRMS** (ESI) *m/z* calcd C₁₈H₂₂F₆N₂O₂S [M+H]⁺ 445.13789, found 445.1374.

5.3.9.5. *rac*-(1,5-*cis*,1,7-*trans*)-7-(3,5-bis(trifluoromethyl)phenyl)-*N*-(*o*-tolyl)-1,4-diazabicyclo[3.2.1]octane-4-carboxamide (**5h**)

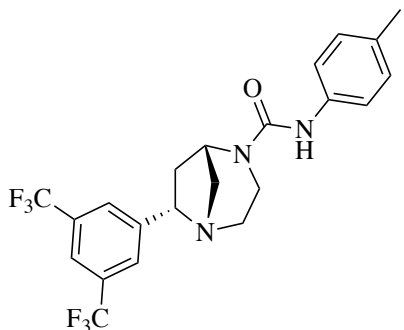


Prepared using *General Procedure H* in a parallel fashion: 5,6-Bridged Scaffold (**5a**) (30 mg, 0.093 mmol, 1.0 Eq), 1-isocyanato-2-methylbenzene (19 mg, 0.139 mmol, 1.5 Eq), triethylamine (38.7 μ L, 0.278 mmol, 3.0 Eq) in dichloromethane (1 mL, 0.093 M). Purified using preparative

HPLC, 11mg, 30%

^1H NMR (400 MHz, Chloroform-*d*) δ 8.07 (dd, *J* 7.8, 1.5 Hz, 1H, Ar), 7.92 (dd, *J* 7.8, 1.5 Hz, 1H Ar), 7.81 – 7.70 (m, 5H, Ar), 4.29 (dd, *J* 8.0, 5.5 Hz, 1H, ArCHCH₂), 4.00 (dd, *J* 10.6, 2.6 Hz, 1H, CH₂CHCHHN), 3.91 (ddt, *J* 12.1, 3.0, 1.4 Hz, 1H, NCHHCH₂N), 3.13 – 3.00 (m, 2H, CH₂CHCHHN, NCHHCH₂N), 2.95 (t, *J* 10.4 Hz, 1H, CH₂CHCH₂), 2.85 (td, *J* 10.2, 3.7, 1H, NCH₂CHHN), 2.62 (td, *J* 10.2, 3.7 Hz, 1H, NCH₂CHHN), 2.52 (dt, *J* 9.1, 5.4 Hz, 1H, ArCHCHHCH), 2.03 (q, *J* 8.0 Hz, 1H, ArCHCHHCH). **^{13}C NMR** (101 MHz, Chloroform-*d*) δ 144.0 (NC=ONH), 141.1 (ArCCH), 135.7 (ArC), 132.9 (ArC), 132.7 (ArC), 131.9 (ArCCF₃), 131.6 (CF₃), 130.3 (ArC), 126.7 (ArC), 121.6 (ArC), 116.3 (NHArC), 110.8 (ArCCH₃), 66.3 (ArCHCH₂), 59.6 (CH₂CHCH₂), 50.9 (CHCH₂N), 49.8 (NCH₂CH₂N), 45.9 (NCH₂CH₂N), 36.9 (ArCHCH₂CH). **FTIR** (ν_{max} , neat): 2836, 1453, 984. **MS** ToF EI+ (*m/z*): 490.3. **HRMS** (ESI) *m/z* calcd for C₂₁H₁₇F₆N₃O₂S [M+H]⁺ 490.10184, found 490.1010

5.3.9.6. *rac*-(1,5-*cis*,1,7-*trans*)-7-(3,5-bis(trifluoromethyl)phenyl)-*N*-(*p*-tolyl)-1,4-diazabicyclo[3.2.1]octane-4-carboxamide (**5i**)



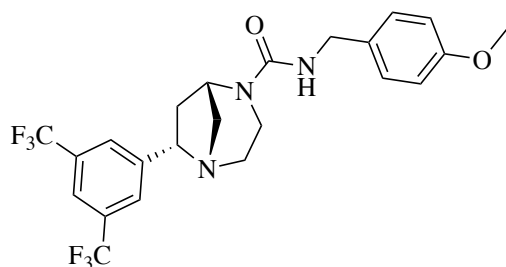
Prepared using *General Procedure H* in a parallel fashion:

5,6-Bridged Scaffold (**5a**) (30 mg, 0.093 mmol, 1.0 Eq), 1-isocyanato-4-methylbenzene (19 mg, 0.139 mmol, 1.5 Eq), triethylamine (38.7 μ L, 0.278 mmol, 3.0 Eq) in dichloromethane (1 mL, 0.093 M). Purified using preparative

HPLC, 15 mg, 41%.

¹H NMR (400 MHz, Chloroform-*d*) δ 7.85 (s, 2H, Ar), 7.80 (s, 1H, Ar), 7.24 – 7.21 (m, 2H, Ar), 7.12 – 7.07 (m, 2H, Ar), 6.26 (s, 1H, NH), 4.42 (dd, *J* 8.0, 5.8 Hz, 1H, ArCHCH₂), 4.06 (dd, *J* 9.8, 7.6 Hz, 1H, CH₂CHCHHN), 3.97 (dt, *J* 12.5, 3.2 Hz, 1H, NCHHCH₂N), 3.28 (dt, *J* 12.5, 3.2 Hz, 1H, NCHHCH₂N), 3.20 – 3.13 (m, 2H, CH₂CHCH₂N, CH₂CHCHHN), 2.85 (dt, *J* 10.2, 3.4 Hz, 1H, NCH₂CHHN), 2.60 – 2.52 (m, 2H, ArCHCHHCH, NCH₂CHHN), 2.30 (s, 3H, ArCH₃), 2.21 – 2.14 (m, 1H, ArCHCHHCH). **¹³C NMR** (101 MHz, Chloroform-*d*) δ 155.57 (NC=ONH), 143.8 (ArCCH), 136.3 (ArCCH₃), 132.9 (ArCCF₃), 131.7 (q, *J* 33.0 Hz, 3- & 5-C C₆H₃(CF₃)₂), 129.4 (ArC), 127.0 (ArC), 124.7 (NHArC), 121.4 (ArC), 120.4 (ArC), 66.0 (ArCHCH₂), 59.4 (CHCH₂CH), 48.9 (CH₂CHCH₂N), 48.2 (NCH₂CH₂N), 35.5 (NCH₂CH₂N), 20.7 (ArCH₃). **FTIR** (ν_{\max} , neat): 3309, 2862, 1129. **MS** ToF EI+ (*m/z*): 458.1 **HRMS** (ESI) *m/z* calcd for C₂₂H₂₁F₆N₃O [M+H]⁺ 458.16616, found 458.1656.

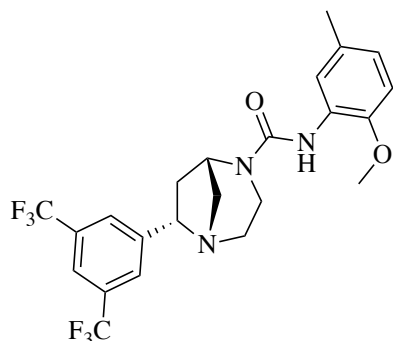
5.3.9.7. *rac*-(1,5-*cis*,1,7-*trans*)-7-(3,5-bis(trifluoromethyl)phenyl)-*N*-(4-methoxybenzyl)-1,4-diazabicyclo[3.2.1]octane-4-carboxamide (**5j**)



Prepared using *General Procedure H* in a parallel fashion: 5,6-Bridged Scaffold (**5a**) (30 mg, 0.093 mmol, 1.0 Eq), 1-(isocyanatomethyl)-4-methoxybenzene (23 mg, 0.139 mmol, 1.5 Eq), triethylamine (38.7 μ L, 0.278 mmol, 3.0 Eq) in dichloromethane (1 mL, 0.093 M). Purified using preparative HPLC, 12 mg, 32%.

^1H NMR (400 MHz, Chloroform-*d*) δ 7.83 (s, 2H, Ar), 7.78 (s, 1H, Ar), 7.26 – 7.22 (m, 2H, Ar), 6.89 – 6.85 (m, 2H, Ar), 4.60 (dd, *J* 5.2, 1.9 Hz, 1H, ArCHCH₂), 4.42 – 4.35 (m, 2H, CH₂CHCHHN, NCHHCN), 3.94 (d, *J* 8.9 Hz, 1H, NHCHHC), 3.80 (s, 3H, OCH₃), 3.17 (dt, *J* 12.5, 3.9 Hz, 1H, NCHHCN), 3.12 – 3.04 (m, 2H, CH₂CHCHHN, NCHHC), 2.80 (dt, *J* 10.1, 3.4 Hz, 1H, NCH₂CHHN), 2.58 – 2.44 (m, 2H, NCH₂CHHN, ArCHCHHC), 2.14 (dt, *J* 9.7, 8.3 Hz, 1H, ArCHCHHC), 1.68 (s, 1H, C=ONHC). **^{13}C NMR** (101 MHz, Chloroform-*d*) δ 158.9 (ArCOCH₃), 157.8 (NC=ONH), 143.8 (ArCCH), 131.4 (ArCCF₃), 129.2 (ArCH), 127.0 (ArCH), 121.5 (ArCH), 114.1 (ArCH), 65.9 (ArCCH), 59.3 (CH₂CHCH₂), 55.3 (NHCH₂C), 48.9 (CH₂CHCH₂N), 47.8 (NCH₂CH₂N), 44.7 (NCH₂CH₂N), 43.6 (ArCCHCH₂CH), 35.4 (OCH₃). **FTIR** (ν_{max} , neat): 3347, 2840, 1174. **MS** ToF EI+ (*m/z*): 488.2 **HRMS** (ESI) *m/z* calcd for C₂₃H₂₃F₆N₃O₂ [M+H]⁺ 488.17672, found 488.1762.

5.3.9.8. *rac*-(1,5-*cis*,1,7-*trans*)-7-(3,5-bis(trifluoromethyl)phenyl)-*N*-(2-methoxy-5-methylphenyl)-1,4-diazabicyclo[3.2.1]octane-4-carboxamide (**5k**)



Prepared using *General Procedure H* in a parallel fashion:

5,6-Bridged Scaffold (**5a**) (30 mg, 0.093 mmol, 1.0 Eq), 2-

isocyanato-1-methoxy-4-methylbenzene (23 mg, 0.139

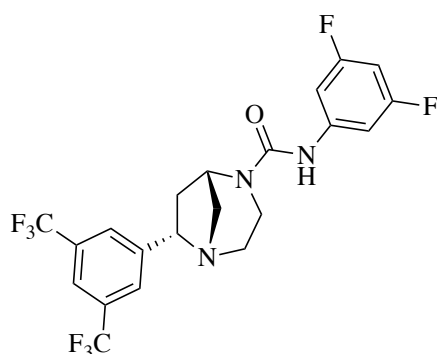
mmol, 1.5 Eq), triethylamine (38.7 μ L, 0.278 mmol, 3.0 Eq)

in dichloromethane (1 mL, 0.093 M). Purified using

preparative HPLC, 10mg, 26%.

¹H NMR (400 MHz, Chloroform-*d*) δ 7.98 (d, *J* 1.7 Hz, 1H, Ar), 7.86 (s, 2H, Ar), 7.80 (s, 1H, Ar), 7.03 (s, 1H, NH), 6.75 (d, *J* 2.4 Hz, 2H, Ar), 4.43 (dd, *J* 7.9, 5.8 Hz, 1H, ArCHCH₂), 4.08 (d, *J* 8.9 Hz, 1H, CH₂CHCHHN), 4.00 (dt, *J* 12.6, 3.4 Hz, 1H, NCHHCH₂N), 3.85 (s, 3H, ArOCH₃), 3.30 (dt, *J* 13.1, 3.8 Hz, 1H, NCHHCH₂N), 3.23 – 3.13 (m, 2H, CH₂CHCH₂, CH₂CHCHHN), 2.87 (dt, *J* 10.3, 3.4 Hz, 1H, NCH₂CHHN), 2.61 – 2.53 (m, 2H, NCH₂CHHN, ArCHCHHCH), 2.29 (s, 3H, ArCH₃), 2.19 (q, *J* 8.5 Hz, 1H, ArCHCHHCH). **¹³C NMR** (101 MHz, Chloroform-*d*) δ 155.1 (NC=ONH), 145.6 (ArCOCH₃), 143.8 (ArCCH₂), 130.7 (ArCCF₃), 128.4 (ArCCH₃), 127.1 (ArC), 124.7 (NHArC), 122.3 (ArC), 122.0 (ArC), 119.8 (ArC), 109.6 (ArC), 65.9 (ArCHCH₂), 59.4 (CH₂CHCH₂), 55.9 (ArOCH₃), 48.9 (NCH₂CH₂N), 48.0 (CHCH₂N), 43.8 (NCH₂CH₂N), 35.6 (ArCHCH₂CH), 21.1 (ArCH₃). **FTIR** (ν_{\max} , neat): 2948, 1032. **MS** ToF EI⁺ (*m/z*): 488.2 **HRMS** (ESI) *m/z* calcd for C₂₃H₂₃F₆N₃O₂ [M+H]⁺ 488.17672, found 488.1759.

5.3.9.9. *rac*-(1,5-*cis*,1,7-*trans*)-7-(3,5-bis(trifluoromethyl)phenyl)-*N*-(3,5-difluorophenyl)-1,4-diazabicyclo[3.2.1]octane-4-carboxamide (**5l**)



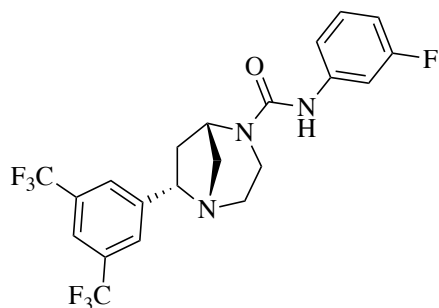
Prepared using *General Procedure H* in a parallel fashion:

5,6-Bridged Scaffold (**5a**) (30 mg, 0.093 mmol, 1.0 Eq), 1,3-difluoro-5-isocyanatobenzene (22 mg, 0.139 mmol, 1.5 Eq), triethylamine (38.7 μ L, 0.278 mmol, 3.0 Eq) in dichloromethane (1 mL, 0.093 M). Purified using

preparative HPLC, 13 mg, 34%.

¹H NMR (400 MHz, Chloroform-*d*) δ 7.85 (s, 2H, Ar), 7.80 (s, 1H, Ar), 7.04 – 6.92 (m, 2H, Ar), 6.51 – 6.45 (m, 1H, Ar), 6.44 (s, 1H, *NH*), 4.43 (dd, *J* 7.9, 5.8 Hz, 1H, ArCHCH₂), 4.05 (dd, *J* 10.9, 2.2 Hz, 1H, CH₂CHCHHN), 3.97 (dt, *J* 12.6, 3.3 Hz, 1H, NCHHCH₂N), 3.30 (dt, *J* 12.6, 3.3 Hz, 1H, CH₂CHCHHN), 3.23 – 3.16 (m, 1H, CH₂CHCH₂), 3.13 (dt, *J* 10.3, 3.4 Hz, 1H, NCHHCH₂N), 2.88 (dt, *J* 10.3, 3.4 Hz, 1H, NCH₂CHHN), 2.62 – 2.52 (m, 2H, NCH₂CHHN, ArCHCHHCH), 2.19 (q, *J* 8.6 Hz, 1H, ArCHCHHCH). **¹³C NMR** (101 MHz, Chloroform-*d*) δ 154.5 (NC=ONH), 143.6 (ArC), 131.9 (ArC), 131.7 (ArC), 127.0 (ArC), 124.7 (ArC), 121.9 (ArC), 121.6 (ArC), 102.6 (ArC), 102.3 (ArC), 66.0 (ArCHCH₂), 59.3 (CH₂CHCH₂N), 48.9 (NCH₂CH₂N), 48.2 (CH₂CHCH₂N), 43.9 (NCH₂CH₂N), 35.6 (ArCCHCH₂CH). **FTIR** (ν_{max} , neat): 3309. 998 **MS** ToF EI+ (*m/z*): 480.2 **HRMS** (ESI) *m/z* calcd for C₂₁H₁₇F₈N₃O [M+H]⁺ 480.13166, found 480.1309.

5.3.9.10. *rac*-(1,5-*cis*,1,7-*trans*)-7-(3,5-bis(trifluoromethyl)phenyl)-*N*-(3-fluorophenyl)-1,4-diazabicyclo[3.2.1]octane-4-carboxamide (**5m**)



Prepared using *General Procedure H* in a parallel fashion:

5,6-Bridged Scaffold (**5a**) (30 mg, 0.093 mmol, 1.0 Eq),

1-fluoro-3-isocyanatobenzene (19 mg, 0.139 mmol, 1.5

Eq), triethylamine (38.7 μ L, 0.278 mmol, 3.0 Eq) in

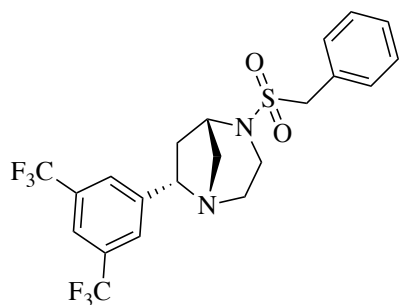
dichloromethane (1 mL, 0.093 M). Purified using

preparative HPLC, 9 mg, 24%.

¹H NMR (400 MHz, Chloroform-*d*) δ 7.86 (s, 2H, Ar), 7.80 (s, 1H, Ar), 7.31 (dt, *J* 11.2, 2.3 Hz, 1H, Ar), 7.22 (td, *J* 8.1, 6.4 Hz, 1H, Ar), 7.00 (dd, *J* 8.3, 2.0 Hz, 1H, Ar), 6.74 (td, *J* 8.3, 2.5 Hz, 1H, Ar), 6.39 (s, 1H, *NH*), 4.43 (dd, *J* 7.9, 5.8 Hz, 1H, ArCHCH₂), 4.06 (d, *J* 9.5 Hz, 1H, CH₂CHCHHN), 3.98 (dt, *J* 12.6, 3.3 Hz, 1H, NCHHCH₂N), 3.30 (dt, *J* 12.5, 3.6 Hz, 1H, NCHHCH₂N), 3.23 – 3.11 (m, 2H, CH₂CHCH₂N, CH₂CHCHHN), 2.87 (dt, *J* 10.2, 3.4 Hz, 1H, NCH₂CHHN), 2.63 – 2.51 (m, 2H, NCH₂CHHN, ArCHCHHCH), 2.18 (q, *J* 8.6 Hz, 1H, ArCHCHHCH). **¹³C NMR** (101 MHz, Chloroform-*d*) δ 154.9 (NC=ONH), 143.7 (ArCF), 140.6 (ArCCHCH₂), 131.9 (ArCCF₃), 129.9 (ArCCF₃), 127.0 (ArC), 121.9 (NHArC), 114.9 (ArC), 109.9 (ArC), 109.7 (ArC), 107.4 (ArC), 107.1 (ArC), 66.0 (ArCCHCH₂), 59.3 (CH₂CHCH₂N), 48.9 (NCH₂CH₂N), 48.2 (CHCH₂N), 43.9 (NCH₂CH₂N), 35.6 (CHCH₂CH).

FTIR (ν_{max} , neat): 3391, 1133. **MS** ToF EI⁺ (*m/z*): 461.1 **HRMS** (ESI) *m/z* calcd for C₂₁H₁₈F₇N₃O [M+H]⁺ 462.14109, found 462.1400.

5.3.9.11. *rac*-(1,5-*cis*,1,7-*trans*)-4-(benzylsulfonyl)-7-(3,5-bis(trifluoromethyl)phenyl)-1,4-diazabicyclo[3.2.1]octane (**5n**)



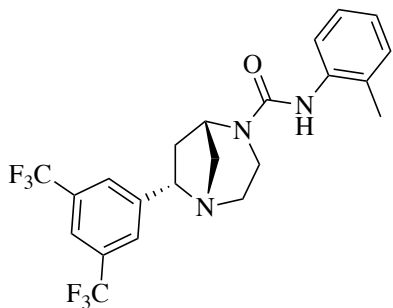
Prepared using *General Procedure H* in a parallel fashion:

5,6-Bridged Scaffold (**5a**) (30 mg, 0.093 mmol, 1.0 Eq), phenylmethanesulfonyl chloride (26 mg, 0.139 mmol, 1.5 Eq), triethylamine (38.7 μ L, 0.278 mmol, 3.0 Eq) in dichloromethane (1 mL, 0.093 M). Purified using preparative

HPLC, 8 mg, 21%.

¹H NMR (400 MHz, Chloroform-*d*) δ 7.79 (s, 2H, Ar), 7.77 (s, 1H, Ar), 7.44 – 7.40 (m, 5H, Ar), 4.26 – 4.21 (m, 3H, ArCHCH₂, SCH₂ArC), 3.68 (dd, *J* 11.1, 2.6 Hz, 1H, CH₂CHCHHN), 3.66 – 3.61 (m, 1H, NCHHCH₂N), 2.98 – 2.90 (m, 2H, NCHHCH₂N, CH₂CHCH₂N), 2.79 (dd, *J* 11.1, 2.6 Hz, 1H, CH₂CHCHHN), 2.75 – 2.68 (m, 1H, NCH₂CHHN), 2.49 – 2.40 (m, 2H, NCH₂CHHN, ArCHCHHCH), 1.97 (q, *J* 8.9 Hz, 1H, ArCHCHHCH). **¹³C NMR** (101 MHz, Chloroform-*d*) δ 144.2 (ArCCH), 131.9 (ArCCF₃), 131.6 (ArCCF₃), 130.7 (ArC), 128.8 (ArC), 126.8 (ArC), 124.7 (ArC), 121.9 (ArC), 121.6 (ArC), 66.3 (ArCCH), 60.1 (CHCH₂CHCH₂), 57.6 (SCH₂ArC), 50.9 (CH₂CHCH₂N), 50.2 (NCH₂CH₂N), 46.1 (NCH₂CH₂N), 36.8 ArCHCH₂CH). **FTIR** (ν_{max} , neat): 1278, 916 **MS** ToF EI+ (*m/z*): 479.1 **HRMS** (ESI) *m/z* calcd C₂₁H₂₀F₆N₂O₂S [M+H]⁺ 479.12224, found 479.1213.

5.3.9.12. *rac*-(1,5-*cis*,1,7-*trans*)-7-(3,5-bis(trifluoromethyl)phenyl)-*N*-(*o*-tolyl)-1,4-diazabicyclo[3.2.1]octane-4-carboxamide (**5o**)



Prepared using *General Procedure H* in a parallel fashion: 5,6-Bridged Scaffold (**5a**) (30 mg, 0.093 mmol, 1.0 Eq), 1-isocyanato-2-methylbenzene (19 mg, 0.139 mmol, 1.5 Eq), triethylamine (38.7 μ L, 0.278 mmol, 3.0 Eq) in dichloromethane (1 mL, 0.093 M). Purified using preparative

HPLC, 11 mg, 30%.

¹H NMR (400 MHz, Chloroform-*d*) δ 7.86 (s, 2H, Ar), 7.80 (s, 1H, Ar), 7.23 (d, *J* 1.9 Hz, 1H, Ar), 7.17 (t, *J* 7.4 Hz, 1H, Ar), 7.13 – 7.09 (m, 1H, Ar), 6.86 (d, *J* 7.4 Hz, 1H, Ar), 6.29 (s, 1H, NH), 4.42 (dd, *J* 7.9, 5.9 Hz, 1H, ArCHCH₂), 4.11 – 4.02 (m, 1H, CH₂CHCHHN), 3.97 (dt, *J* 12.6, 3.2 Hz, 1H, NCHHCH₂N), 3.28 (dt, *J* 12.6, 3.2 Hz, 1H, NCHHCH₂N), 3.21 – 3.11 (m, 2H, CH₂CHCH₂N, CH₂CHCHHN), 2.85 (dt, *J* 10.3, 3.4 Hz, 1H, NCH₂CHHN), 2.60 – 2.52 (m, 2H, NCH₂CHHN, ArCHCHHCH), 2.33 (s, 3H, ArCH₃), 2.18 (q, *J* 8.6 Hz, 1H, ArCHCHHCH). **¹³C NMR** (101 MHz, Chloroform-*d*) δ 155.4 (NC=ONH), 143.78 (ArCCH), 138.83 (NHArC), 131.77 (q, *J* 33.1 Hz, 3- & 5-*C* C₆H₃(CF₃)₂), 128.7 (ArC), 127.1 (ArC), 124.7 (ArCCH₃), 124.1 (ArC), 121.9 (ArC), 121.6 (ArC), 120.8 (ArC), 117.0 (ArC), 66.0 (ArCCHCH₂), 59.4 (CH₂CHCH₂N), 49.0 (NCH₂CH₂N), 48.2 (CH₂CHCH₂N), 43.9 (NCH₂CH₂N), 35.6 (CHCH₂CHCH₂), 21.5 (ArCCH₃). **FTIR** (ν_{max} , neat): 2948, 1535, 1032. **MS** ToF EI+ (*m/z*): 458.2 **HRMS** (ESI) *m/z* calcd C₂₂H₂₁F₆N₃O [M+H]⁺ 458.16616, found 458.1655.

5.3. X-Ray Crystallography

5.4.1. X-Ray Crystallography: General Information

A suitable crystal was selected and measured on an Agilent SuperNova diffractometer using an Atlas detector. The crystal was kept at 100.00(10) K during data collection. Using Olex2,²⁶⁰ the structure was solved with the ShelXT²⁶¹ structure solution program using Intrinsic Phasing and refined with the ShelXL²⁶² refinement package Least Squares minimisation.. All non-hydrogen atoms were refined with anisotropic displacement parameters. All hydrogen atoms were added at calculated positions and refined by use of a riding model with isotropic displacement parameters based on the equivalent isotropic displacement parameter (U_{eq}) of the parent atom. Crystallography data was processed and solved by Dr. Louise Male.

5.4.2. Crystal Data

$C_{18}H_{21}F_6N_3O$ ($M = 409.38$ g/mol): monoclinic, space group P21/c (no. 14), $a = 13.8215(8)$ Å, $b = 15.5380(10)$ Å, $c = 9.1588(5)$ Å, $\beta = 101.769(5)^\circ$, $V = 1925.6(2)$ Å³, $Z = 4$, $T = 100.01(10)$ K, $\mu(\text{Cu K}\alpha) = 1.131$ mm⁻¹, $D_{calc} = 1.412$ g/cm³, 35885 reflections measured ($8.666^\circ \leq 2\Theta \leq 148.056^\circ$), 3832 unique ($R_{int} = 0.0361$, $R_{sigma} = 0.0159$) which were used in all calculations. The final R_1 was 0.0506 ($I > 2\sigma(I)$) and wR_2 was 0.1387 (all data) (**Figure 5.1**).

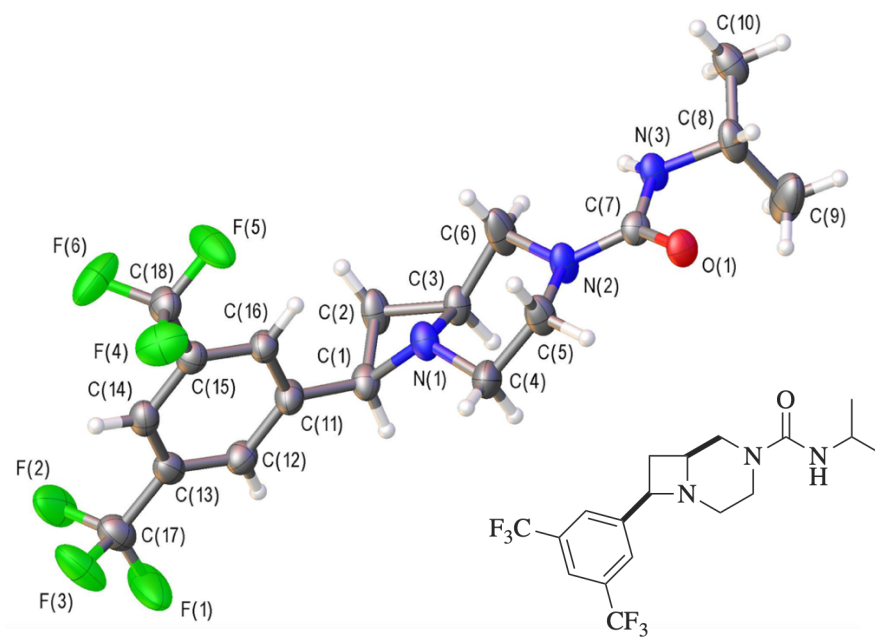


Figure 5.1. An x-ray crystal structure was obtained of **SC-5-CF₃-3** with ellipsoids drawn at the 50 % probability level, to further confirm the structure and stereochemistry of the 4,6-fused scaffold. The crystal structure was solved by Dr. Louise Male.

6. Bibliography

1. V. Mehra, I. Lumb, A. Anand and V. Kumar, *RSC Adv.*, 2017, **7**, 45763-45783.
2. D. R. Parmar, J. Y. Soni, R. Guduru, R. H. Rayani, R. V. Kusurkar and A. G. Vala, *Arch. Pharm.*, 2021, 1-33.
3. A. Brandi, S. Cicchi and F. M. Cordero, *Chem. Rev.*, 2008, **108**, 3988-4035.
4. T. Dudev and C. Lim, *J. Am. Chem. Soc.*, 1998, **120**, 4450-4458.
5. H. Mughal and M. Szostak, *Org. Biomol. Chem.*, 2021, **19**, 3274-3286.
6. S. Gabriel and J. Weiner, *Berichte der deutschen chemischen Gesellschaft*, 1888, **21**, 2669-2679.
7. O. V. Dorofeeva, V. S. Mastryukov, L. V. Vilkov and I. Hargittai, *J. Chem. Soc., Chem. Commun.*, 1973, 772a-772a.
8. J. Catalán, O. Mo and M. Yáñez, *J. Mol. Struct.*, 1978, **43**, 251-257.
9. T. Egawa and K. Kuchitsu, *J. Mol. Spectrosc.*, 1988, **128**, 469-477.
10. V. S. Mastryukov, O. V. Dorofeeva and L. V. Vilkov, *J. Mol. Struct.*, 1976, **34**, 99-112.
11. J. Yasamura, *J. Chem. Abstr.*, 1963, **59**, 2313.
12. D. H. Wadsworth, *J. Org. Chem.*, 1967, **32**, 1184-1187.
13. G. He, Y. Zhao, S. Zhang, C. Lu and G. Chen, *J. Am. Chem. Soc.*, 2012, **134**, 3-6.
14. J. Zhao, X.-J. Zhao, P. Cao, J.-K. Liu and B. Wu, *Org. Lett.*, 2017, **19**, 4880-4883.
15. B. Bhaskararao, S. Singh, M. Anand, P. Verma, P. Prakash, A. C. S. Malakar, H. F. Schaefer and R. B. Sunoj, *Chem Sci*, 2020, **11**, 208-216.
16. M. Nappi, C. He, W. G. Whitehurst, B. G. N. Chappell and M. J. Gaunt, *Angew. Chem. Int. Ed.*, 2018, **57**, 3178-3182.
17. K. L. Jensen, D. U. Nielsen and T. F. Jamison, *Chem. Eur. J.*, 2015, **21**, 7379-7383.
18. Y. Ju and R. S. Varma, *J. Org. Chem.*, 2006, **71**, 135-141.
19. M. C. Hillier and C.-y. Chen, *J. Org. Chem.*, 2006, **71**, 7885-7887.
20. R. A. Miller, F. Lang, B. Marcune, D. Zewge, Z. J. Song and S. Karady, *Synth. Commun.*, 2003, **33**, 3347-3353.
21. S. Kenis, M. D'hooghe, G. Verniest, T. A. Dang Thi, C. Pham The, T. Van Nguyen and N. De Kimpe, *J. Org. Chem.*, 2012, **77**, 5982-5992.
22. S. Mangelinckx, B. De Sterck, F. Colpaert, S. Catak, J. Jacobs, S. Rooryck, M. Waroquier, V. Van Speybroeck and N. De Kimpe, *J. Org. Chem.*, 2012, **77**, 3415-3425.
23. A. Žukauskaitė, S. Mangelinckx, V. Buinauskaitė, A. Šackus and N. De Kimpe, *Amino Acids*, 2011, **41**, 541-558.
24. M. S. Dowling, D. P. Fernando, J. Hou, B. Liu and A. C. Smith, *J. Org. Chem.*, 2016, **81**, 3031-3036.
25. T. J. Senter, M. C. O'Reilly, K. M. Chong, G. A. Sulikowski and C. W. Lindsley, *Tetrahedron Lett.*, 2015, **56**, 1276-1279.
26. F. Bellina, M. Biagetti, A. Carpita and R. Rossi, *Tetrahedron*, 2001, **57**, 2857-2870.
27. J. J. Chen, H. Y. Fang, C. Y. Duh and I. S. Chen, *Planta Med.*, 2005, **71**, 470-475.
28. A.-Y. Peng and Y.-X. Ding, *Tetrahedron*, 2005, **61**, 10303-10308.
29. B. Crone and S. F. Kirsch, *J. Org. Chem.*, 2007, **72**, 5435-5438.
30. M. J. Mphahlele, *Molecules*, 2009, **14**.

31. P. T. Parvatkar, P. S. Parameswaran and S. G. Tilve, *Chem. Eur. J.*, 2012, **18**, 5460-5489.
32. T. Aggarwal, S. Kumar and A. K. Verma, *Org. Biomol. Chem.*, 2016, **14**, 7639-7653.
33. N. Ajvazi and S. Stavber, *Compd.*, 2022, **2**.
34. E. Gabriele, F. V. Singh, D. M. Freudendahl and T. Wirth, *Tetrahedron*, 2012, **68**, 10573-10576.
35. K. Ramalinga, P. Vijayalakshmi and T. N. B. Kaimal, *Tetrahedron Lett.*, 2002, **43**, 879-882.
36. J. S. Yadav, B. V. Reddy, A. Reddy and A. V. Narsaiah, *Synthesis*, 2007, **20**, 3191-3194.
37. S. V. More, M. N. V. Sastry, C.-C. Wang and C.-F. Yao, *Tetrahedron Lett.*, 2005, **46**, 6345-6348.
38. N. Kerru, L. Gummididi, S. Maddila, K. K. Gangu and S. B. Jonnalagadda, *Molecules*, 2020, **25**, 1909.
39. M. S. Yusubov and V. V. Zhdankin, *Resource-Efficient Technologies*, 2015, **1**, 49-67.
40. S. G. Davies, R. L. Nicholson, P. D. Price, P. M. Roberts, A. J. Russell, E. D. Savory, A. D. Smith and J. E. Thomson, *Tetrahedron: Asymmetry*, 2009, **20**, 758-772.
41. X. Zhang, Y. Zhou, H. Wang, D. Guo, D. Ye, Y. Xu, H. Jiang and H. Liu, *Adv. Synth. Catal.*, 2011, **353**, 1429-1437.
42. M. Álvarez-Corral, M. Muñoz-Dorado and I. Rodríguez-García, *Chem. Rev.*, 2008, **108**, 3174-3198.
43. S. Knapp, K. E. Rodriques, A. T. Levorse and R. M. Ornaf, *Tetrahedron Lett.*, 1985, **26**, 1803-1806.
44. A. Feula, L. Male and J. S. Fossey, *Org. Lett.*, 2010, **12**, 5044-5047.
45. A. Feula, S. S. Dhillon, R. Byravan, M. Sangha, R. Ebanks, M. A. Hama Salih, N. Spencer, L. Male, I. Magyary, W.-P. Deng, F. Müller and J. S. Fossey, *Org. Biomol. Chem.*, 2013, **11**, 5083-5093.
46. L. Fowden, *Biochem. J.*, 1956, **64**, 323-332.
47. Y. Hamada and T. Shioiri, *J. Org. Chem.*, 1986, **51**, 5489-5490.
48. K. Isono, K. Asahi and S. Suzuki, *J. Am. Chem. Soc.*, 1969, **91**, 7490-7505.
49. Y.-T. Di, H.-P. He, Y.-S. Wang, L.-B. Li, Y. Lu, J.-B. Gong, X. Fang, N.-C. Kong, S.-L. Li, H.-J. Zhu and X.-J. Hao, *Org. Lett.*, 2007, **9**, 1355-1358.
50. N. Kern, M. Hoffmann, A. Blanc, J.-M. Weibel and P. Pale, *Org. Lett.*, 2013, **15**, 836-839.
51. C. Brotherton-Pleiss, P. Yue, Y. Zhu, K. Nakamura, W. Chen, W. Fu, C. Kubota, J. Chen, F. Alonso-Valenteen, S. Mikhael, L. Medina-Kauwe, M. A. Tius, F. Lopez-Tapia and J. Turkson, *J. Med. Chem.*, 2021, **64**, 695-710.
52. Q. Yan, Y. Wang, W. Zhang and Y. Li, *Mar. Drugs*, 2016, **14**, 85.
53. K. Kumura, Y. Wakiyama, K. Ueda, E. Umemura, T. Watanabe, E. Shitara, H. Fushimi, T. Yoshida and K. Ajito, *J. Antibiot.*, 2016, **69**, 440-445.
54. M. Noolvi, S. Agrawal, H. Patel, A. Badiger, M. Gaba and A. Zambre, *Arab. J. Chem.*, 2014, **7**, 219-226.

55. M. D. Black, R. J. Stevens, N. Rogacki, R. E. Featherstone, Y. Senyah, O. Giardino, B. Borowsky, J. Stemmelin, C. Cohen, P. Pichat, M. Arad, S. Barak, A. De Levie, I. Weiner, G. Griebel and G. B. Varty, *Psychopharmacology*, 2011, **215**, 149-163.
56. S. Crunkhorn, *Nat. Rev. Drug Discov.*, 2016, **15**, 750-750.
57. A. Johansson, C. Löfberg, M. Antonsson, S. von Unge, M. A. Hayes, R. Judkins, K. Ploj, L. Benthem, D. Lindén, P. Brodin, M. Wennerberg, M. Fredenwall, L. Li, J. Persson, R. Bergman, A. Pettersen, P. Gennemark and A. Hogner, *J. Med. Chem.*, 2016, **59**, 2497-2511.
58. S. J. Yang, J. Kim, S. E. Lee, J. Y. Ahn, S. Y. Choi and S. W. Cho, *BMB Rep*, 2017, **50**, 634-639.
59. H. Duan, M. Ning, X. Chen, Q. Zou, L. Zhang, Y. Feng, L. Zhang, Y. Leng and J. Shen, *J. Med. Chem.*, 2012, **55**, 10475-10489.
60. M. K. Mandal, S. Ghosh, H. R. Bhat, L. Naesens and U. P. Singh, *Bioorg. Chem.*, 2020, **104**, 104320.
61. N. Madhavi and B. L. Rani, *Int. J. Res. Dev. Pharm. Life. Sci.*, 2014, **2014**.
62. G. Cucchiaro, Y. Xiao, A. Gonzalez-Sulser and K. J. Kellar, *Anesthesiology*, 2008, **109**, 512-519.
63. L. Z. Huang, C. Campos, J. Ly, F. Ivy Carroll and M. Quik, *Neuropharmacology*, 2011, **60**, 861-868.
64. J. T. Lowe, M. D. Lee, L. B. Akella, E. Davoine, E. J. Donckele, L. Durak, J. R. Duvall, B. Gerard, E. B. Holson, A. Joliton, S. Kesavan, B. C. Lemercier, H. Liu, J.-C. Marié, C. A. Mulrooney, G. Muncipinto, M. Welzel-O'Shea, L. M. Panko, A. Rowley, B.-C. Suh, M. Thomas, F. F. Wagner, J. Wei, M. A. Foley and L. A. Marcaurelle, *J. Org. Chem.*, 2012, **77**, 7187-7211.
65. R. E. Pratley and A. Salsali, *Curr. Med. Res. Opin.*, 2007, **23**, 919-931.
66. D. P. Phillips, W. Gao, Y. Yang, G. Zhang, I. K. Lerario, T. L. Lau, J. Jiang, X. Wang, D. G. Nguyen, B. G. Bhat, C. Trotter, H. Sullivan, G. Welzel, J. Landry, Y. Chen, S. B. Joseph, C. Li, W. P. Gordon, W. Richmond, K. Johnson, A. Bretz, B. Bursulaya, S. Pan, P. McNamara and H. M. Seidel, *J. Med. Chem.*, 2014, **57**, 3263-3282.
67. T. A. Brandt, S. Caron, D. B. Damon, J. DiBrino, A. Ghosh, D. A. Griffith, S. Kedia, J. A. Ragan, P. R. Rose, B. C. Vanderplas and L. Wei, *Tetrahedron*, 2009, **65**, 3292-3304.
68. Adams, D. R.; Bentley, J.; Bodkin, C. D.; Cliffe, I. A.; Edward, J.; Davidson, P.; Mansell, H. L.; Monck, N. J.; Shepherd, R. G.; Shepherd, J. M. Azetidinecarboxamide derivatives for treating CNS disorders. US Patent 6,831,078 B1, Dec 14, 2004
69. M. Han, C. Song, N. Jeong and H.-G. Hahn, *ACS Med. Chem. Lett.*, 2014, **5**, 999-1004.
70. Brunette, S. R.; Abeywardane, A.; Burke, M. J.; Kapadia, S. R.; Kirrane, T. M.; Netherton, M. R.; Razavi, H.; Rodriguez, S.; Saha, A.; Sibley, R.; Keenan, L. L. S.; Takahashi, H.; Turner, M. R.; Wu, J. P.; Young, E. R. R.; Zhang, Q.; Zhang, Q.; Zindell, R. M. Benzodioxanes for inhibiting leukotriene production. International Patent 2013134226 A1, Sep 12, 2013

71. A. A. Kirichok, I. O. Shton, I. M. Pishel, S. A. Zozulya, P. O. Borysko, V. Kubyshkin, O. A. Zaporozhets, A. A. Tolmachev and P. K. Mykhailiuk, *Chem. Eur. J.*, 2018, **24**, 5444-5449.
72. F. Pammolli, L. Magazzini and M. Riccaboni, *Nat. Rev. Drug Discov.*, 2011, **10**, 428-438.
73. M. E. Bunnage, *Nat. Chem. Biol.*, 2011, **7**, 335-339.
74. I. Kola and J. Landis, *Nat. Rev. Drug Discov.*, 2004, **3**, 711-716.
75. J. A. DiMasi, *Clin. Pharmacol. Ther.*, 1995, **58**, 1-14.
76. J. W. Scannell and J. Bosley, *PLoS One*, 2016, **11**, e0147215.
77. J. P. Hughes, S. Rees, S. B. Kalindjian and K. L. Philpott, *Br. J. Pharmacol.*, 2011, **162**, 1239-1249.
78. D. Cook, D. Brown, R. Alexander, R. March, P. Morgan, G. Satterthwaite and M. N. Pangalos, *Nat. Rev. Drug Discov.*, 2014, **13**, 419-431.
79. V. Prachayasittikul, A. Worachartcheewan, W. Shoombuatong, N. Songtawe, S. Simeon, V. Prachayasittikul and C. Nantasenamat, *Curr. Top. Med. Chem.*, 2015, **15**, 1780-1800.
80. K. H. Bleicher, H.-J. Böhm, K. Müller and A. I. Alanine, *Nat. Rev. Drug Discov.*, 2003, **2**, 369-378.
81. G. A. Van Norman, *JACC Basic. Transl. Sci.*, 2019, **4**, 428-437.
82. S. Gopishetty, V. Kota and A. K. Guddati, *Am. J. Transl. Res.*, 2020, **12**, 5977-5983.
83. C. A. Umscheid, D. J. Margolis and C. E. Grossman, *Postgrad. Med.*, 2011, **123**, 194-204.
84. M. Hay, D. W. Thomas, J. L. Craighead, C. Economides and J. Rosenthal, *Nat. Biotechnol.*, 2014, **32**, 40-51.
85. P. M. Adcock, P. Pastor, F. Medley, J. E. Patterson and T. V. Murphy, *J. Infect. Des.*, 1998, **178**, 577-580.
86. S. Buffet-Bataillon, P. Tattevin, M. Bonnaure-Mallet and A. Jolivet-Gougeon, *Int. J. Antimicrob. Agents*, 2012, **39**, 381-389.
87. J. Bibette, *Proc. Natl. Acad. Sci.*, 2012, **109**, 649.
88. D. M. Volochnyuk, S. V. Ryabukhin, Y. S. Moroz, O. Savych, A. Chuprina, D. Horvath, Y. Zabolotna, A. Varnek and D. B. Judd, *Drug Discov. Today*, 2019, **24**, 390-402.
89. R. Liu, X. Li and K. S. Lam, *Curr. Opin. Chem. Biol.*, 2017, **38**, 117-126.
90. A. A. Hajare, S. S. Salunkhe, S. S. Mali, S. A. Gorde, S. J. Nadaf and S. A. Pishawikar, *Am. J. PharmTech. Res.*, 2014, **4**, 112-129.
91. C. A. Lipinski, F. Lombardo, B. W. Dominy and P. J. Feeney, *Adv. Drug. Deliv. Rev.*, 1997, **23**, 3-25.
92. P. Leeson, *Nature*, 2012, **481**, 455-456.
93. M. J. Waring, J. Arrowsmith, A. R. Leach, P. D. Leeson, S. Mandrell, R. M. Owen, G. Pairaudeau, W. D. Pennie, S. D. Pickett, J. Wang, O. Wallace and A. Weir, *Nat. Rev. Drug Discov.*, 2015, **14**, 475-486.
94. A. Bahmani, S. Saaidpour and A. Rostami, *Sci. Rep.*, 2017, **7**, 5760.
95. M. S. Alavijeh, M. Chishty, M. Z. Qaiser and A. M. Palmer, *NeuroRx*, 2005, **2**, 554-571.

96. P. D. Dobson and D. B. Kell, *Nat Rev Drug Discov*, 2008, **7**, 205-220.
97. P. Wils, A. Warnery, V. Phung-Ba, S. Legrain and D. Scherman, *J. Pharmacol. Exp. Ther.*, 1994, **269**, 654.
98. L. Z. Benet, C. M. Hosey, O. Ursu and T. I. Oprea, *Adv. Drug. Deliv. Rev.*, 2016, **101**, 89-98.
99. A. Nadin, C. Hattotuwigama and I. Churcher, *Angew. Chem. Int. Ed. Engl.*, 2012, **51**, 1114-1122.
100. S. J. Teague, A. M. Davis, P. D. Leeson and T. Oprea, *Angew. Chem. Int. Ed. Engl.*, 1999, **38**, 3743-3748.
101. D. J. Foley, R. G. Doveston, I. Churcher, A. Nelson and S. P. Marsden, *Chem. Commun.*, 2015, **51**, 11174-11177.
102. M. M. Hann and T. I. Oprea, *Curr. Opin. Chem. Biol.*, 2004, **8**, 255-263.
103. S. L. Kidd, T. J. Osberger, N. Mateu, H. F. Sore and D. R. Spring, *Front. Chem.*, 2018, **6**.
104. R. Doveston, S. Marsden and A. Nelson, *Drug Discov. Today*, 2014, **19**, 813-819.
105. A. Koutsoukas, S. Paricharak, W. R. J. D. Galloway, D. R. Spring, A. P. Ijzerman, R. C. Glen, D. Marcus and A. Bender, *J. Chem. Inf. Model.*, 2014, **54**, 230-242.
106. W. H. B. Sauer and M. K. Schwarz, *J. Chem. Inf. Comput. Sci.*, 2003, **43**, 987-1003.
107. N. C. Firth, N. Brown and J. Blagg, *J. Chem. Inf. Model.*, 2012, **52**, 2516-2525.
108. F. Lovering, J. Bikker and C. Humblet, *J. Med. Chem.*, 2009, **52**, 6752-6756.
109. M. Badertscher, K. Bischofberger, M. E. Munk and E. Pretsch, *J. Chem. Inf. Comput. Sci.*, 2001, **41**, 889-893.
110. J. Sadowski, J. Gasteiger and G. Klebe, *J. Chem. Inf. Comput. Sci.*, 1994, **34**, 1000-1008.
111. V. Schomaker, J. Waser, R. E. Marsh and G. Bergman, *Acta Crystallogr.*, 1959, **12**, 600-604.
112. I. Colomer, C. J. Empson, P. Craven, Z. Owen, R. G. Doveston, I. Churcher, S. P. Marsden and A. Nelson, *Chem. Commun.*, 2016, **52**, 7209-7212.
113. C. N. Morrison, K. E. Prosser, R. W. Stokes, A. Cordes, N. Metzler-Nolte and S. M. Cohen, *Chem Sci*, 2020, **11**, 1216-1225.
114. A. W. Hung, A. Ramek, Y. Wang, T. Kaya, J. A. Wilson, P. A. Clemons and D. W. Young, *Proc. Natl. Acad. Sci.*, 2011, **108**, 6799.
115. A. Giuliani, *Drug Discov. Today*, 2017, **22**, 1069-1076.
116. M. Ringnér, *Nat. Biotechnol.*, 2008, **26**, 303-304.
117. L. Bober, U. Judycka-Proma, M. Koba and T. Baczek, *J. Chromatogr. Sci.*, 2011, **49**, 758-763.
118. B. E. Evans, K. E. Rittle, M. G. Bock, R. M. DiPardo, R. M. Freidinger, W. L. Whitter, G. F. Lundell, D. F. Veber, P. S. Anderson, R. S. L. Chang, V. J. Lotti, D. J. Cerino, T. B. Chen, P. J. Kling, K. A. Kunkel, J. P. Springer and J. Hirshfield, *J. Med. Chem.*, 1988, **31**, 2235-2246.
119. M. E. Welsch, S. A. Snyder and B. R. Stockwell, *Curr. Opin. Chem. Biol.*, 2010, **14**, 347-361.
120. L. Yet, *Privileged Structures in Drug Discovery: Medicinal Chemistry and Synthesis*, John Wiley & Sons, 2018.

121. P. Schneider and G. Schneider, *Angew. Chem. Int. Ed.*, 2017, **56**, 7971-7974.
122. T. Shiro, T. Fukaya and M. Tobe, *Eur. J. Med. Chem.*, 2015, **97**, 397-408.
123. N. A. McGrath, M. Brichacek and J. T. Njardarson, *J. Chem. Educ.*, 2010, **87**, 1348-1349.
124. W. R. J. D. Galloway, A. Bender, M. Welch and D. R. Spring, *Chem. Commun.*, 2009, 2446-2462.
125. C. Lipinski and A. Hopkins, *Nature*, 2004, **432**, 855-861.
126. S. L. Schreiber, *Science*, 2000, **287**, 1964.
127. R. J. Spandl, A. Bender and D. R. Spring, *Org. Biomol. Chem.*, 2008, **6**, 1149-1158.
128. R. J. Spandl, M. Díaz-Gavilán, K. M. O'Connell, G. L. Thomas and D. R. Spring, *Chem. Rec.*, 2008, **8**, 129-142.
129. W. R. J. D. Galloway, A. Isidro-Llobet and D. R. Spring, *Nat. Commun.*, 2010, **1**, 80.
130. W. R. J. D. Galloway and D. R. Spring, *Expert. Opin. Drug. Discov.*, 2009, **4**, 467-472.
131. D. Burke Martin, M. Berger Eric and L. Schreiber Stuart, *Science*, 2003, **302**, 613-618.
132. D. Morton, S. Leach, C. Cordier, S. Warriner and A. Nelson, *Angew. Chem. Int. Ed.*, 2009, **48**, 104-109.
133. T. E. Nielsen and S. L. Schreiber, *Angew. Chem. Int. Ed.*, 2008, **47**, 48-56.
134. S.-W. Li and R. A. Batey, *Chem. Commun.*, 2004, 1382-1383.
135. D.-K. Wang, L.-X. Dai, X.-L. Hou and Y. Zhang, *Tetrahedron Lett.*, 1996, **37**, 4187-4188.
136. V. V. Kouznetsov, J. R. Castro, C. O. Puentes, E. E. Stashenko, J. R. Martinez, C. Ochoa, D. M. Pereira, J. J. Ruiz, C. F. Portillo, S. M. Serrano, A. G. Barrio, A. Bahsas and J. Amaro-Luis, *Arch. Pharm.*, 2005, **338**, 32-37.
137. M.-H. Lin, S.-F. Hung, L.-Z. Lin, W.-S. Tsai and T.-H. Chuang, *Org. Lett.*, 2011, **13**, 332-335.
138. Y. Yamamoto, T. Komatsu and K. Maruyama, *J. Org. Chem.*, 1985, **50**, 3115-3121.
139. M. Bao, H. Nakamura and Y. Yamamoto, *Tetrahedron Lett.*, 2000, **41**, 131-134.
140. X.-W. Sun, M. Liu, M.-H. Xu and G.-Q. Lin, *Org. Lett.*, 2008, **10**, 1259-1262.
141. Z.-L. Shen, H.-L. Cheong and T.-P. Loh, *Chem. Eur. J.*, 2008, **14**, 1875-1880.
142. B. Hatano, K. Nagahashi and T. Kijima, *J. Org. Chem.*, 2008, **73**, 9188-9191.
143. W. Lu and T. H. Chan, *J. Org. Chem.*, 2000, **65**, 8589-8594.
144. S. Yamamura, M. Toda and Y. Hirata, *Org. Synth.*, 1973, **53**, 86.
145. J. E. Baldwin, R. C. Thomas, L. I. Kruse and L. Silberman, *J. Org. Chem.*, 1977, **42**, 3846-3852.
146. J. E. Baldwin, *J. Chem. Soc., Chem. Commun.*, 1976, 734-736.
147. J. E. Baldwin and M. J. Lusch, *Tetrahedron*, 1982, **38**, 2939-2947.
148. J. E. Baldwin and L. I. Kruse, *J. Chem. Soc., Chem. Commun.*, 1977, 233-235.
149. F. Durrat, M. V. Sanchez, F. Couty, G. Evano and J. Marrot, *Eur. J. Org. Chem.*, 2008, **2008**, 3286-3297.
150. F. Couty, F. Durrat and D. Prim, *Tetrahedron Lett.*, 2003, **44**, 5209-5212.
151. W. Van Brabandt, R. Van Landeghem and N. De Kimpe, *Org. Lett.*, 2006, **8**, 1105-1108.
152. M. Heuckendorff, L. T. Poulsen and H. H. Jensen, *J Org Chem*, 2016, **81**, 4988-5006.

153. S. Rohrbach, A. J. Smith, J. H. Pang, D. L. Poole, T. Tuttle, S. Chiba and J. A. Murphy, *Angew. Chem. Int. Ed.*, 2019, **58**, 16368-16388.
154. Y. Kasai, K. Sato, S. Utsumi and S. Ichikawa, *Chembiochem*, 2018, **19**, 1866-1872.
155. J. T. Bowler, F. M. Wong, S. Gronert, J. R. Keeffe and W. Wu, *Org. Biomol. Chem.*, 2014, **12**, 6175-6180.
156. E. Banide, V. Lemau de Talancé, G. Schmidt, H. Lubin, S. Comesse, L. Dechoux, L. Hamon and C. Kadouri-Puchot, *Eur. J. Org. Chem.*, 2007, **2007**, 4517-4524.
157. R. Dorel, C. P. Grugel and A. M. Haydl, *Angew. Chem. Int. Ed.*, 2019, **58**, 17118-17129.
158. M. J. Bosiak, A. A. Zielińska, P. Trzaska, D. Kędziera and J. Adams, *J. Org. Chem.*, 2021, **86**, 17594-17605.
159. M. Mari, F. Bartoccini and G. Piersanti, *J. Org. Chem.*, 2013, **78**, 7727-7734.
160. A. G. K. Reddy and G. Satyanarayana, *Tetrahedron*, 2012, **68**, 8003-8010.
161. B. P. Fors, P. Krattiger, E. Strieter and S. L. Buchwald, *Org. Lett.*, 2008, **10**, 3505-3508.
162. P. Ruiz-Castillo and S. L. Buchwald, *Chem. Rev.*, 2016, **116**, 12564-12649.
163. D. S. Surry and S. L. Buchwald, *Angew. Chem. Int. Ed.*, 2008, **47**, 6338-6361.
164. T. S. Ratani, S. Bachman, G. C. Fu and J. C. Peters, *J. Am. Chem. Soc.*, 2015, **137**, 13902-13907.
165. S.-H. Kim, N. Bowden and R. H. Grubbs, *J. Am. Chem. Soc.*, 1994, **116**, 10801-10802.
166. S. Kotha and S. Pulletikurti, *RSC Adv.*, 2018, **8**, 14906-14915.
167. S. Kotha and A. Fatma, *ChemistrySelect*, 2021, **6**, 12018-12021.
168. M. Maraswami, J. Goh and T.-P. Loh, *Org. Lett.*, 2020, **22**, 9724-9728.
169. O. I. Afanasyev, E. Kuchuk, D. L. Usanov and D. Chusov, *Chem. Rev.*, 2019, **119**, 11857-11911.
170. A. Y. Sukhorukov, *Front. Chem.*, 2020, **8**.
171. K. Murugesan, T. Senthamarai, V. G. Chandrashekhar, K. Natte, P. C. J. Kamer, M. Beller and R. V. Jagadeesh, *Chem. Soc. Rev.*, 2020, **49**, 6273-6328.
172. F. Clemente, C. Matassini and F. Cardona, *Eur. J. Org. Chem.*, 2020, **2020**, 4447-4462.
173. D. B. G. Williams, A. Cullen, A. Fourie, H. Henning, M. Lawton, W. Mommsen, P. Nangu, J. Parker and A. Renison, *Green Chem.*, 2010, **12**, 1919-1921.
174. A. B. Smith, G. A. Sulikowski, M. M. Sulikowski and K. Fujimoto, *J. Am. Chem. Soc.*, 1992, **114**, 2567-2576.
175. H. Fujioka, N. Kotoku, Y. Nagatomi and Y. Kita, *Tetrahedron Lett.*, 2000, **41**, 1829-1832.
176. Z. Luo, Y. Pan, Z. Yao, J. Yang, X. Zhang, X. Liu, L. Xu and Q.-H. Fan, *Green Chem.*, 2021, **23**, 5205-5211.
177. T. Kan, H. Kobayashi and T. Fukuyama, *Synlett*, 2002, **5**, 697-699.
178. A. Fujiwara, T. Kan and T. Fukuyama, *Synlett*, 2000, **11**, 1667-1669.
179. C. W. Zapf, J. R. Del Valle and M. Goodman, *Biorg. Med. Chem. Lett.*, 2005, **15**, 4033-4036.
180. D. C. Batesky, M. J. Goldfogel and D. J. Weix, *J. Org. Chem.*, 2017, **82**, 9931-9936.
181. M. C. Etter and P. W. Baures, *J. Am. Chem. Soc.*, 1988, **110**, 639-640.
182. J. Dodge, A., J. Nissen, S. and M. Presnell, *Org. Synth.*, 1996, **73**, 110.

183. I. M. Downie, J. B. Holmes and J. B. Lee, *Chemistry & Industry* 1966, 900-901.
184. R. Appel, *Angew. Chem. Int. Ed.*, 1975, **14**, 801-811.
185. C. J. Smith, C. D. Smith, N. Nikbin, S. V. Ley and I. R. Baxendale, *Org. Biomol. Chem.*, 2011, **9**, 1927-1937.
186. B. Lecea, I. Arrastia, A. Arrieta, G. Roa, X. Lopez, M. I. Arriortua, J. M. Ugalde and F. P. Cossío, *J. Org. Chem.*, 1996, **61**, 3070-3079.
187. C. Guisado, J. E. Waterhouse, W. S. Price, M. R. Jorgensen and A. D. Miller, *Org. Biomol. Chem.*, 2005, **3**, 1049-1057.
188. R. De Marco, M. L. Di Gioia, A. Leggio, A. Liguori and M. C. Viscomi, *Eur. J. Org. Chem.*, 2009, **2009**, 3795-3800.
189. S. Brogi, T. C. Ramalho, K. Kuca, J. L. Medina-Franco and M. Valko, *Front. Chem.*, 2020, **8**.
190. M. R. Berthold, N. Cebron, F. Dill, T. R. Gabriel, T. Kötter, T. Meinl, P. Ohl, C. Sieb, K. Thiel and B. Wiswedel, Berlin, Heidelberg, 2008.
191. T. Sander, J. Freyss, M. von Korff and C. Rufener, *J. Chem. Inf. Model.*, 2015, **55**, 460-473.
192. RDKit: Open-Source Cheminformatics Software, <http://www.rdkit.org/>).
193. ChemAxon, <https://chemaxon.com/>).
194. Chemistry Development Kit, <https://cdk.github.io/>).
195. W. A. Warr, *J. Comput. Aided Mol. Des.*, 2012, **26**, 801-804.
196. L. Kaufman and P. J. Rousseeuw, *Finding Groups in Data: An Introduction to Cluster Analysis.*, Wiley, 1990.
197. V. Tomar, M. Mazumder, R. Chandra, J. Yang and M. K. Sakharkar, in *Encyclopedia of Bioinformatics and Computational Biology*, eds. S. Ranganathan, M. Gribskov, K. Nakai and C. Schönbach, Academic Press, Oxford, 2019, DOI: <https://doi.org/10.1016/B978-0-12-809633-8.20157-X>, pp. 741-760.
198. DataWarrior, <https://openmolecules.org/datawarrior/>).
199. H. Moriwaki, Y.-S. Tian, N. Kawashita and T. Takagi, *J. Cheminform.*, 2018, **10**, 4.
200. L. Xue and J. Bajorath, *Comb. Chem. High Throughput Screen.*, 2000, **3**, 363-372.
201. D. C. Kombo, K. Tallapragada, R. Jain, J. Chewing, A. A. Mazurov, J. D. Speake, T. A. Hauser and S. Toler, *J. Chem. Inf. Model.*, 2013, **53**, 327-342.
202. I. Muegge and P. Mukherjee, *Expert Opin. Drug Discov.*, 2016, **11**, 137-148.
203. R. Winter, F. Montanari, F. Noé and D.-A. Clevert, *Chem. Sci.*, 2019, **10**, 1692-1701.
204. S. Egieyeh, J. Syce, A. Christoffels and S. F. Malan, *Molecules*, 2016, **21**.
205. S. Putta, J. Eksterowicz, C. Lemmen and R. Stanton, *J. Chem. Inf. Comput. Sci.*, 2003, **43**, 1623-1635.
206. Selected Structure Sets, <https://www.sigmaaldrich.com/GB/en/technical-documents/technical-article/chemistry-and-synthesis/lead-discovery/selected-structure>).
207. R. Wang, L. Lai and S. Wang, *J. Comput. Aided Mol. Des.*, 2002, **16**, 11-26.
208. R. Wang, Y. Fu and L. Lai, *J. Chem. Inf. Comput. Sci.*, 1997, 615-621.
209. C. Steinbeck, Y. Han, S. Kuhn, O. Horlacher, E. Luttmann and E. Willighagen, *J. Chem. Inf. Comput. Sci.*, 2003, **43**, 493-500.

210. C. A. Lipinski, F. Lombardo, B. W. Dominy and P. J. Feeney, *Adv. Drug. Deliv. Rev.*, 2001, **46**, 3-26.
211. A. Capecchi, D. Probst and J.-L. Reymond, *J. Cheminform.*, 2020, **12**, 43.
212. H. L. Morgan, *J. Chem. Doc.*, 1965, **5**, 107-113.
213. D. Rogers and M. Hahn, *J. Chem. Inf. Model.*, 2010, **50**, 742-754.
214. D. Probst and J.-L. Reymond, *J. Cheminform.*, 2018, **10**, 66.
215. N. M. O'Boyle and R. A. Sayle, *J. Cheminform.*, 2016, **8**, 36.
216. T. A. Halgren, *J. Comput. Chem.*, 1996, **17**, 490-519.
217. J. J. Perez, *Chem. Soc. Rev.*, 2005, **34**, 143-152.
218. ChEMBL database, <https://www.ebi.ac.uk/chembl/>.
219. P. Ferdinandy, I. Baczkó, P. Bencsik, Z. Giricz, A. Görbe, P. Pacher, Z. V. Varga, A. Varró and R. Schulz, *Eur. Heart J.*, 2019, **40**, 1771-1777.
220. T. Żolek, M. Qile, P. Kaźmierczak, M. Bloothoof, M. A. G. van der Heyden and D. Maciejewska, *RSC Adv.*, 2019, **9**, 38355-38371.
221. M. K. B. Jonsson, M. A. G. van der Heyden and T. A. B. van Veen, *J. Mol. Cell. Cardiol.*, 2012, **53**, 369-374.
222. BioRender, <https://biorender.com/>.
223. D. M. Roden, *Circulation*, 2008, **118**, 981-982.
224. H. Morita, J. Wu and D. P. Zipes, *Lancet*, 2008, **372**, 750-763.
225. P. G. Postema and A. A. M. Wilde, *Curr. Cardiol. Rev.*, 2014, **10**, 287-294.
226. D. Pickham, E. Helfenbein, J. A. Shinn, G. Chan, M. Funk, A. Weinacker, J.-N. Liu and B. J. Drew, *Crit. Care Med.*, 2012, **40**.
227. M. C. Sanguinetti and J. S. Mitcheson, *Trends Pharmacol Sci*, 2005, **26**, 119-124.
228. L. L. Eckhardt, S. Rajamani and C. T. January, *Br J Pharmacol*, 2005, **145**, 3-4.
229. J. I. Vandenberg, B. D. Walker and T. J. Campbell, *Trends Pharmacol Sci*, 2001, **22**, 240-246.
230. B. D. Guth and G. Rast, *Br. J. Pharmacol.*, 2010, **159**, 22-24.
231. A. J. Alexandrou, R. S. Duncan, A. Sullivan, J. C. Hancox, D. J. Leishman, H. J. Witchel and J. L. Leaney, *Br. J. Pharmacol.*, 2006, **147**, 905-916.
232. K. Kikuchi, T. Nagatomo, H. Abe, K. Kawakami, H. J. Duff, J. C. Makielski, C. T. January and Y. Nakashima, *Br J Pharmacol*, 2005, **144**, 840-848.
233. V. M. Patil, A. Gaurav, P. Garg and N. Masand, *J. Egypt Natl. Canc. Inst.*, 2021, **33**, 33.
234. J. S. Silvestre and J. R. Prous, *Methods Find. Exp. Clin. Pharmacol.*, 2007, **29**, 457-465.
235. P. S. Spector, M. E. Curran, M. T. Keating and M. C. Sanguinetti, *Circ Res*, 1996, **78**, 499-503.
236. B. J. Ridder, D. J. Leishman, M. Bridgland-Taylor, M. Samieegohar, X. Han, W. W. Wu, A. Randolph, P. Tran, J. Sheng, T. Danker, A. Lindqvist, D. Konrad, S. Hebeisen, L. Polonchuk, E. Gissinger, M. Renganathan, B. Koci, H. Wei, J. Fan, P. Levesque, J. Kwagh, J. Imredy, J. Zhai, M. Rogers, E. Humphries, R. Kirby, S. Stoelzle-Feix, N. Brinkwirth, M. G. Rotordam, N. Becker, S. Friis, M. Rapedius, T. A. Goetze, T. Strassmaier, G. Okeyo, J. Kramer, Y. Kuryshev, C. Wu, H. Himmel, G. R. Mirams, D. G. Strauss, R. Bardenet and Z. Li, *Toxicol. Appl. Pharmacol.*, 2020, **394**, 114961.

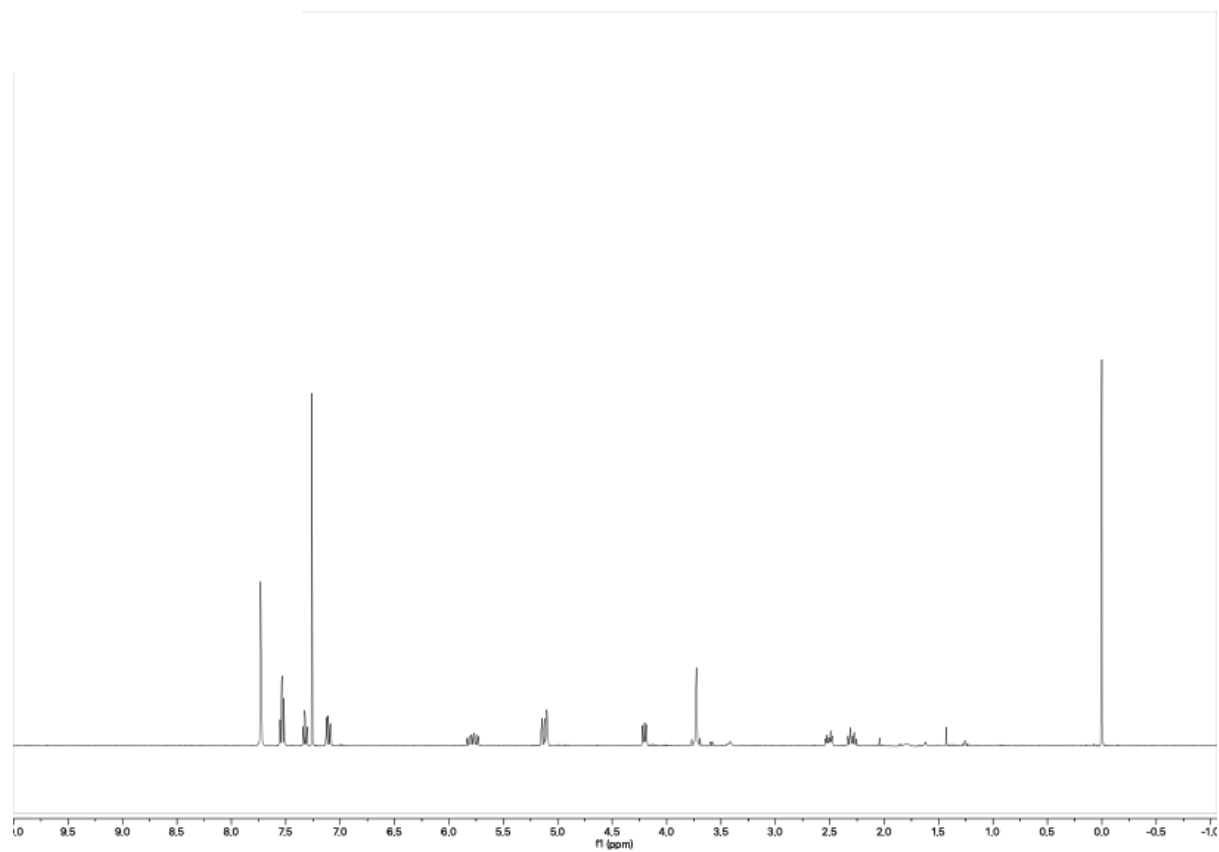
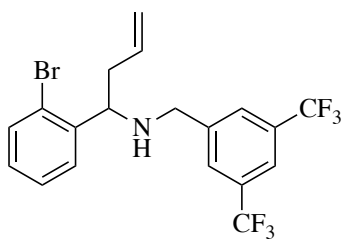
237. A. Garrido, A. Lepailleur, S. M. Mignani, P. Dallemagne and C. Rochais, *Eur. J. Med. Chem.*, 2020, **195**, 112290.
238. D. J. Leishman, M. M. Abernathy and E. B. Wang, *J. Pharmacol. Toxicol. Methods*, 2020, **105**, 106900.
239. T. Danker and C. Möller, *Front. Pharm.*, 2014, **5**.
240. J.-C. Palomino, A. Martin, M. Camacho, H. Guerra, J. Swings and F. Portaels, *Antimicrob. Agents Chemother.*, 2002, **46**, 2720-2722.
241. A. Walzl, C. Unger, N. Kramer, D. Unterleuthner, M. Scherzer, M. Hengstschläger, D. Schwanzer-Pfeiffer and H. Dolznig, *J. Biomol. Screen.*, 2014, **19**, 1047-1059.
242. E. Travnickova, P. Mikula, J. Oprsal, M. Bohacova, L. Kubac, D. Kimmer, J. Soukupova and M. Bittner, *AMB Express*, 2019, **9**, 183.
243. J. H. Parish, *Biochemistry of Bacterial Growth, 3rd Edition: Edited by J Mandelstam, K McQuillen and I Dawes. pp 449. Blackwell Scientific Publications. Oxford. ISBN 0-632-00323-5 and ISBN 0-632-00596-3*, 1985.
244. M. Hohman, K. Gregory, K. Chibale, P. J. Smith, S. Ekins and B. Bunin, *Drug Discov. Today*, 2009, **14**, 261-270.
245. CDD Vault (www.collaborativedrug.com).
246. A. Lanne, Y. Cui, E. Browne, P. G. E. Craven, N. J. Cundy, N. J. Coltman, K. Dale, A. Feula, J. Frampton, A. Goff, M. A. Hama Salih, X. Lang, X. Li, C. W. Moon, M. Morton, J. Pascoe, X. Peng, V. Portman, C. Press, T. Schulz-Utermoehl, M. Tortorella, Z. Tu, Z. E. Underwood, C. Wang, A. Yoshizawa, T. Zhang, S. J. Waddell, J. Bacon, C. Neagoie, J. S. Fossey and L. J. Alderwick, *bioRxiv*, 2020, DOI: 10.1101/2020.09.03.281170, 2020.2009.2003.281170.
247. D. A. Parasrampur, L. Z. Benet and A. Sharma, *AAPS. J.*, 2018, **20**, 1-16.
248. K. M. Bode-Greuel and K. J. Nickisch, *J. Commer. Biotechnol.*, 2008, **14**, 307-325.
249. X. Pan, H. Wang, C. Li, J. Z. H. Zhang and C. Ji, *J. Chem. Inf. Model.*, 2021, **61**, 3159-3165.
250. S. Santajit and N. Indrawattana, *Biomed Res Int*, 2016, **2016**, 2475067-2475067.
251. F. Schaufelberger, L. Hu and O. Ramström, *Chem. Eur. J.*, 2015, **21**, 9776-9783.
252. T. Nguyen, W. Chiu, X. Wang, M. O. Sattler and J. A. Love, *Org. Lett.*, 2016, **18**, 5492-5495.
253. K. Hattori and H. Yamamoto, *Tetrahedron*, 1993, **49**, 1749-1760.
254. S. M. Sheehan, J. J. Masters, M. R. Wiley, S. C. Young, J. W. Liebeschuetz, S. D. Jones, C. W. Murray, J. B. Franciskovich, D. B. Engel, W. W. Weber, J. Marimuthu, J. A. Kyle, J. K. Smallwood, M. W. Farmen and G. F. Smith, *Biorg. Med. Chem. Lett.*, 2003, **13**, 2255-2259.
255. J. L. Kenwright, W. R. J. D. Galloway, D. T. Blackwell, A. Isidro-Llobet, J. Hodgkinson, L. Wortmann, S. D. Bowden, M. Welch and D. R. Spring, *Chem. Eur. J.*, 2011, **17**, 2981-2986.
256. H. Paulsen, J.-C. Jacquinet and W. Rust, *Carbohydr. Res.*, 1982, **104**, 195-219.
257. L. I. Kruse, C. Kaiser, W. E. DeWolf, J. S. Frazee, S. T. Ross, J. Wawro, M. Wise, K. E. Flaim and J. L. Sawyer, *J. Med. Chem.*, 1987, **30**, 486-494.
258. Y. Nishida, M. Ueda, M. Hayashi, N. Takeda and O. Miyata, *Eur. J. Org. Chem.*, 2016, **2016**, 22-25.

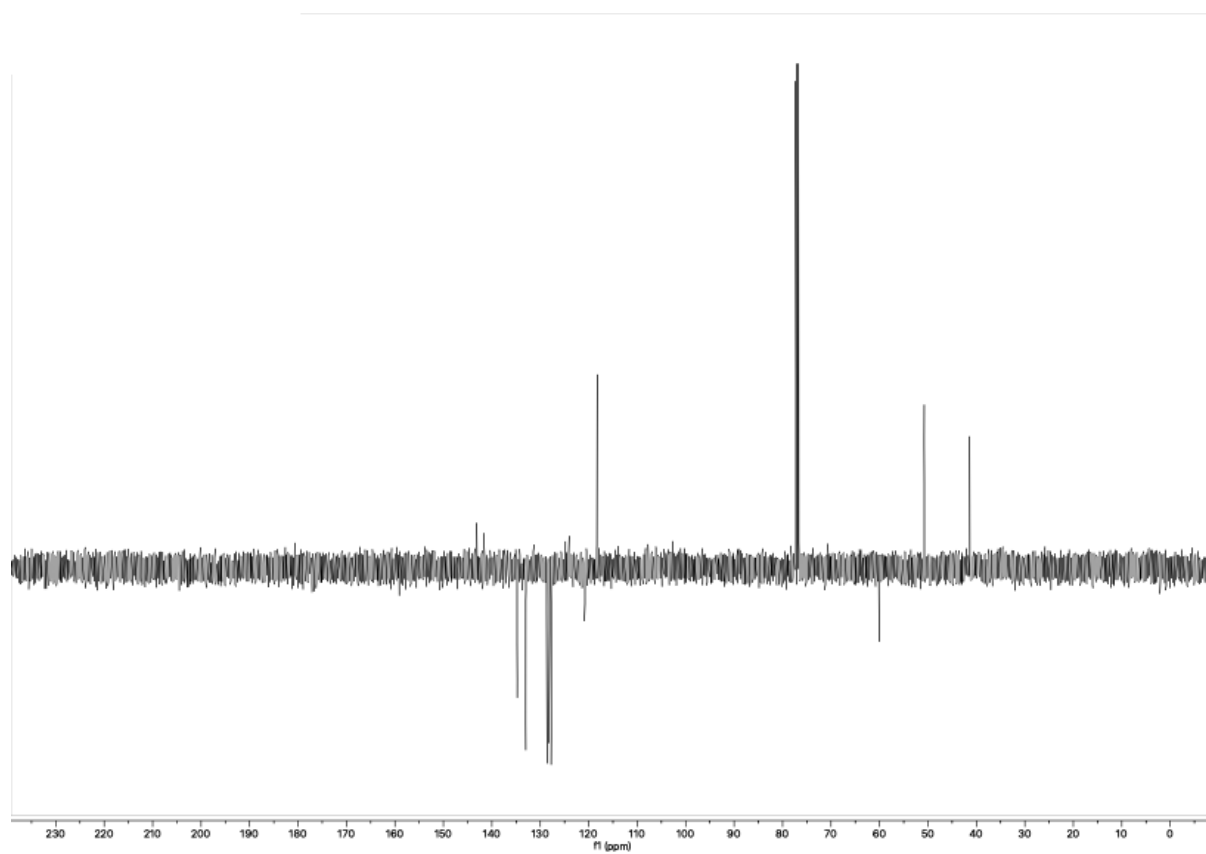
- 259. A. Varlamov, V. Kouznetsov, F. Zubkov, A. Chernyshev, O. Shurupova, L. Y. V. Mendez, A. P. Rodriguez, J. R. Castro and A. J. Rosas-Romero, *Synthesis*, 2002, **2002**, 0771-0783.
- 260. O. V. Dolomanov, L. J. Bourhis, R. J. Gildea, J. A. K. Howard and H. Puschmann, *J. Appl. Crystallogr.*, 2009, **42**, 339-341.
- 261. G. M. Sheldrick, *Acta Crystallogr. Sect. A: Found. Crystallogr.*, 2015, **71**, 3-8.
- 262. G. M. Sheldrick, *Acta Crystallogr. Sect. C: Cryst. Struct. Commun.*, 2015, **71**, 3-8.

7. Supplementary Information

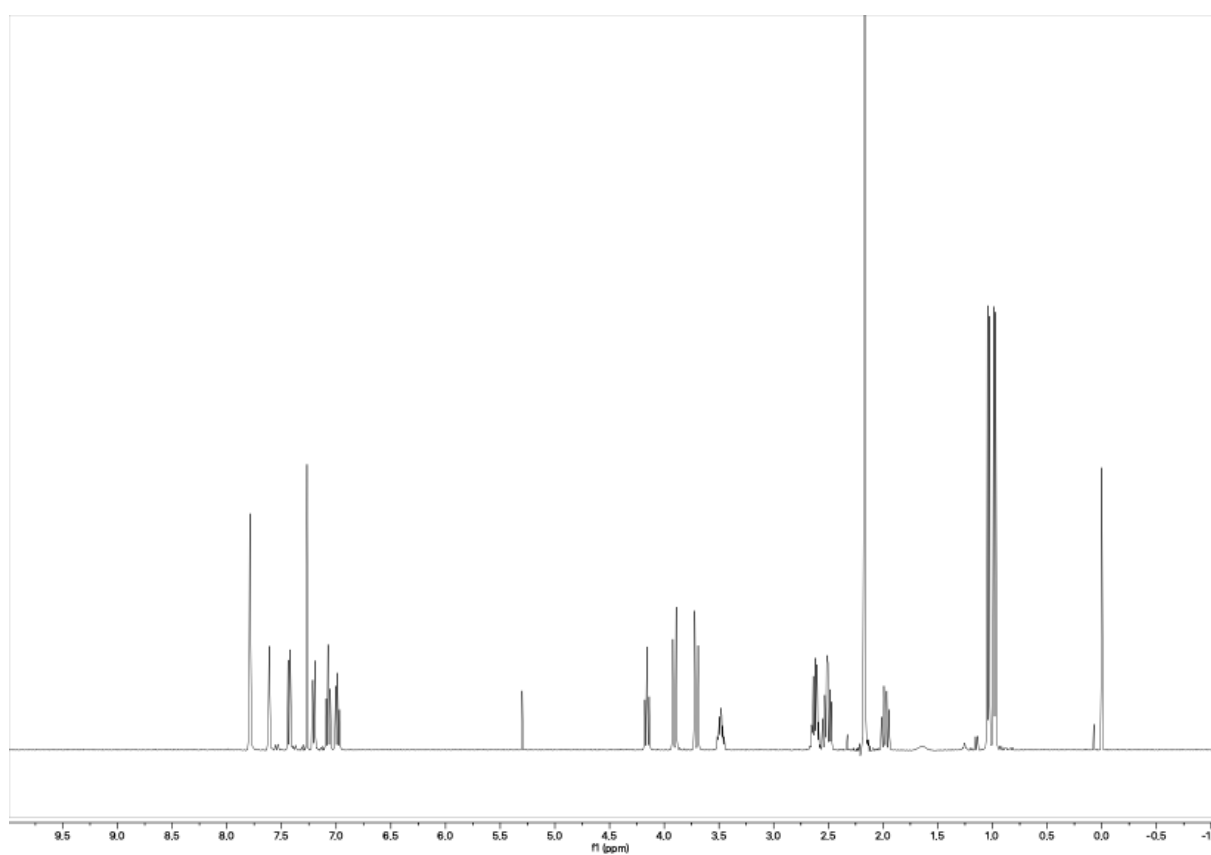
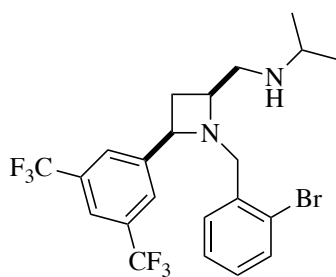
7.1. Representative NMR Spectra

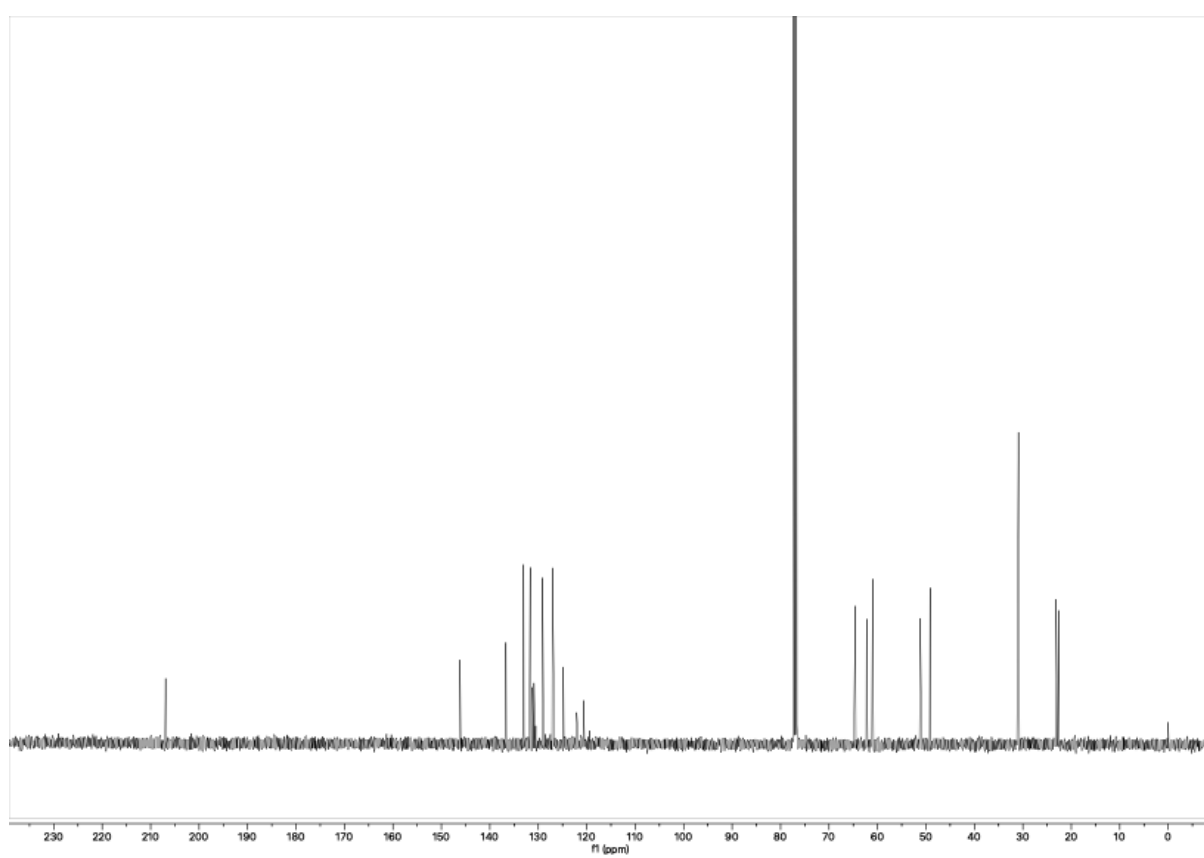
7.1.1. Representative NMR of Homoallylic Amine (Bis-Aryl)



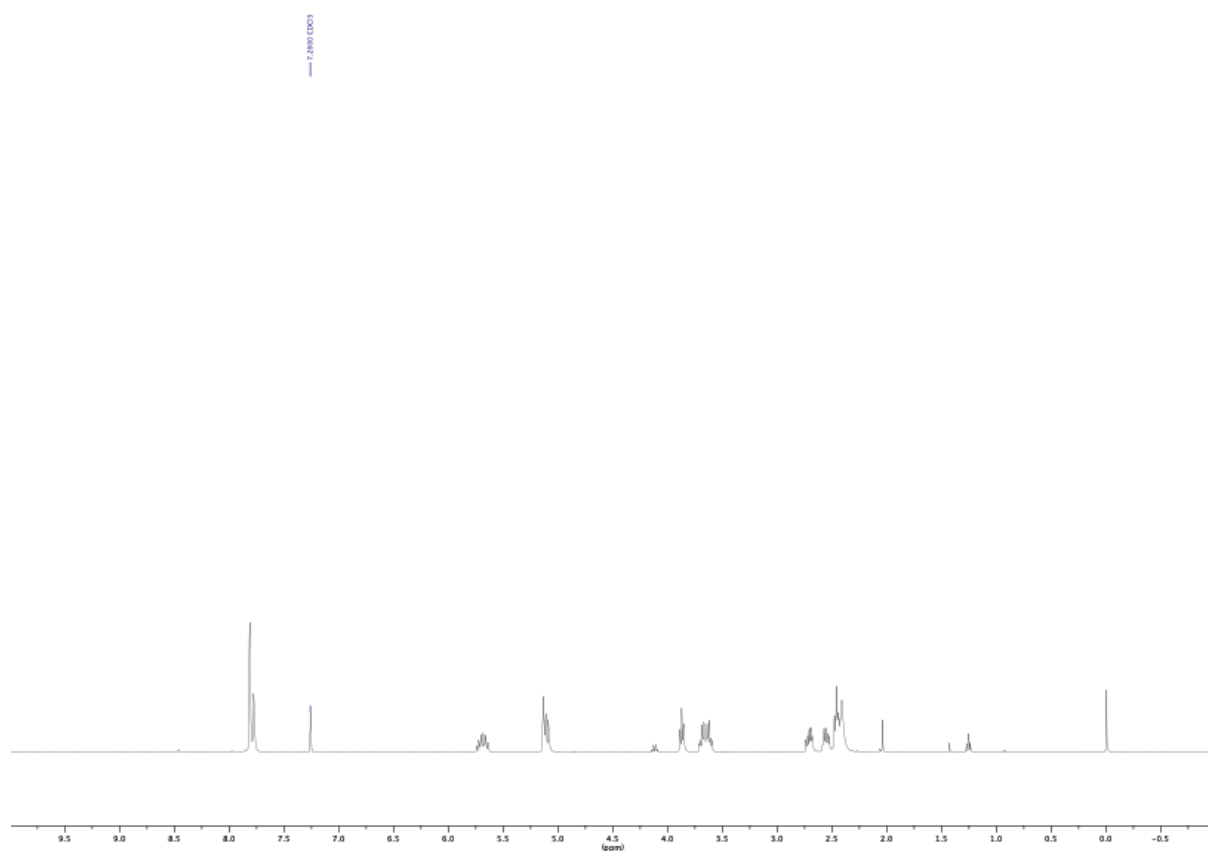
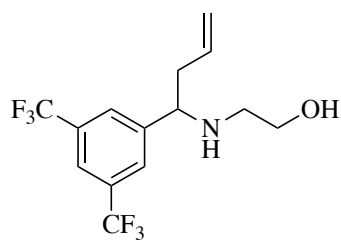


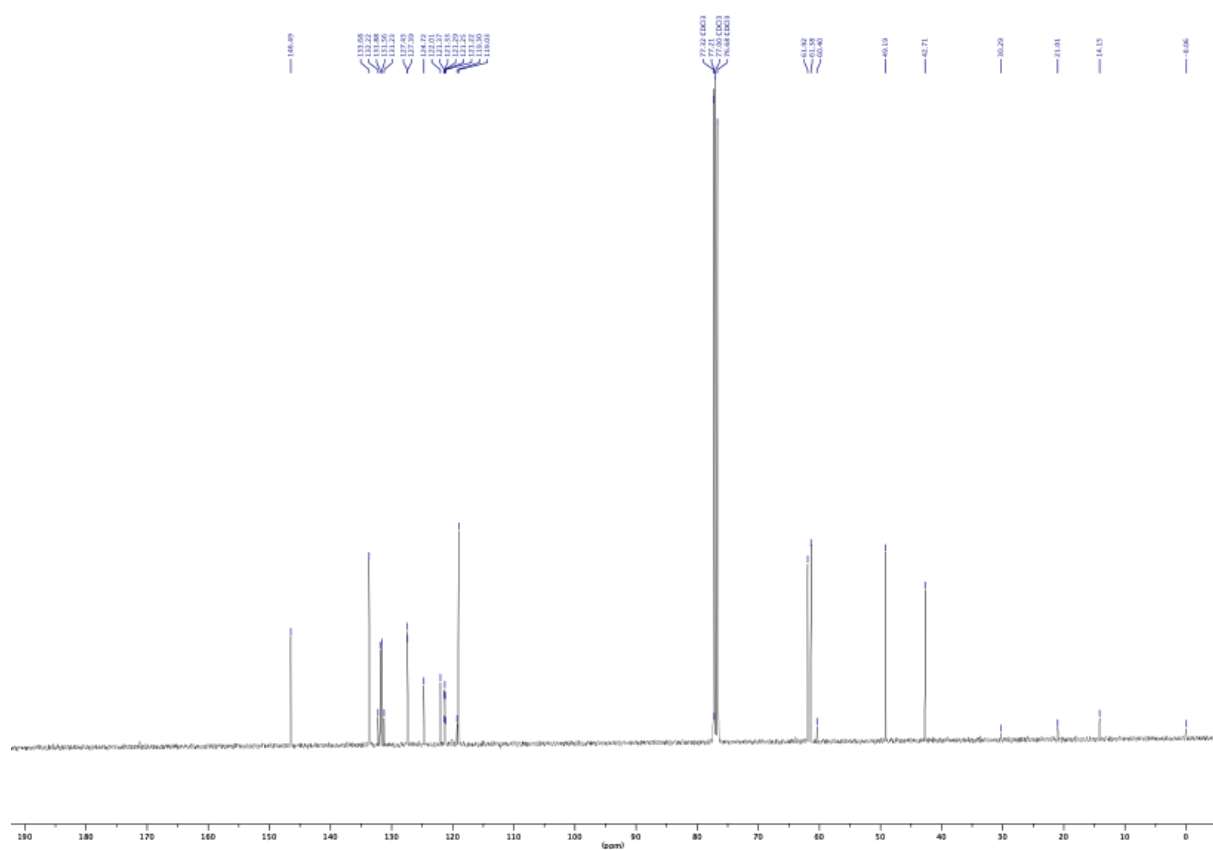
7.1.2. Representative NMR of Amino-Azetidine



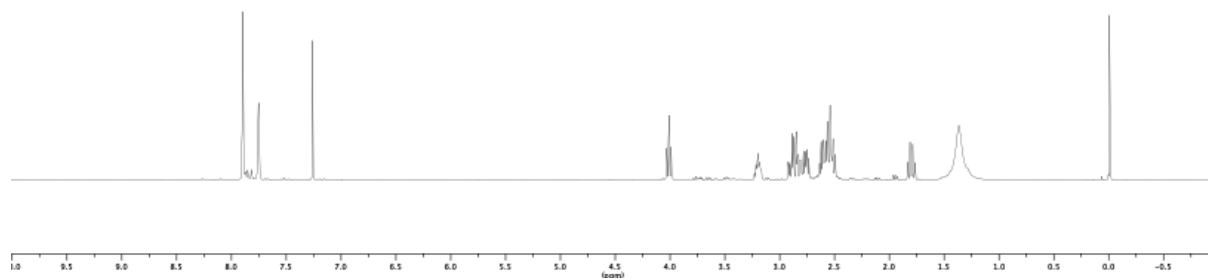
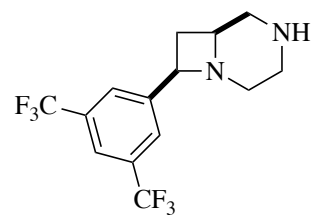


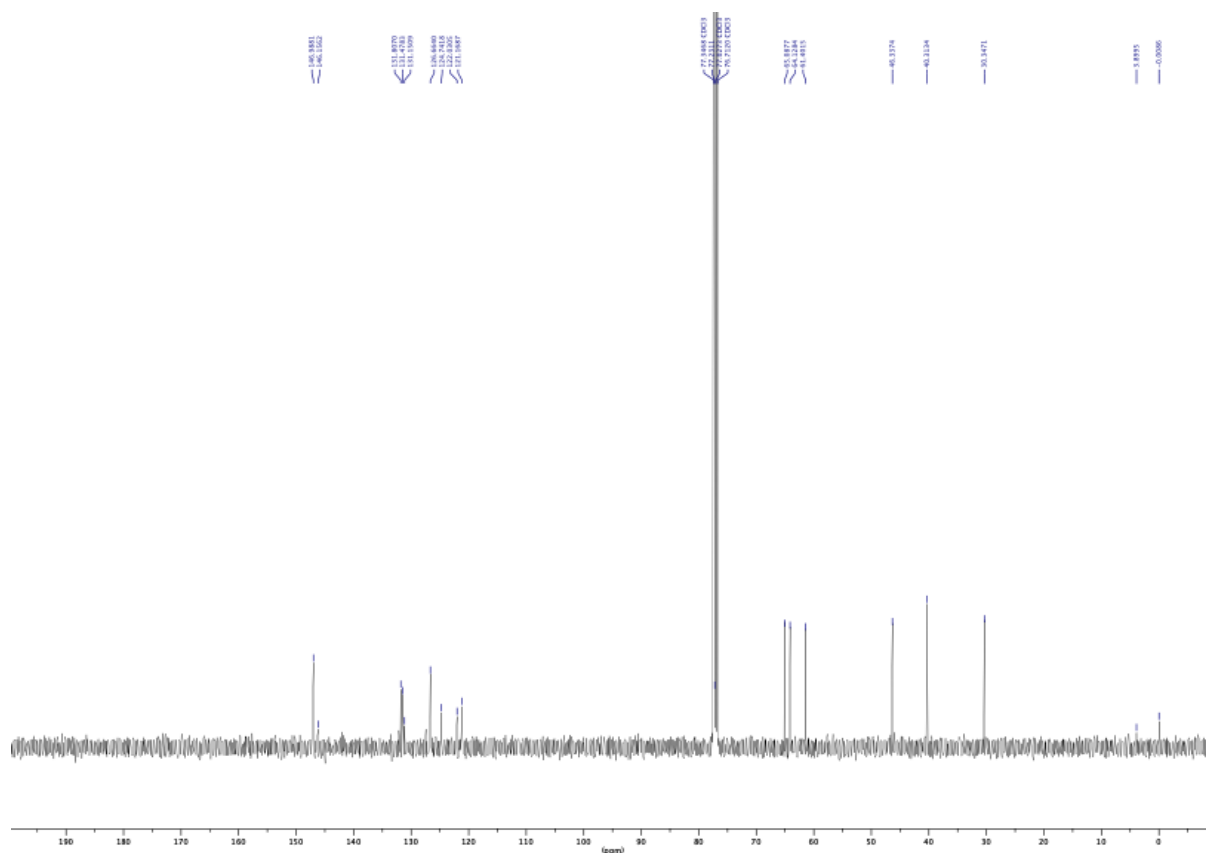
7.1.3. Representative NMR of Homoallylic Amine (Amino Ethanol)



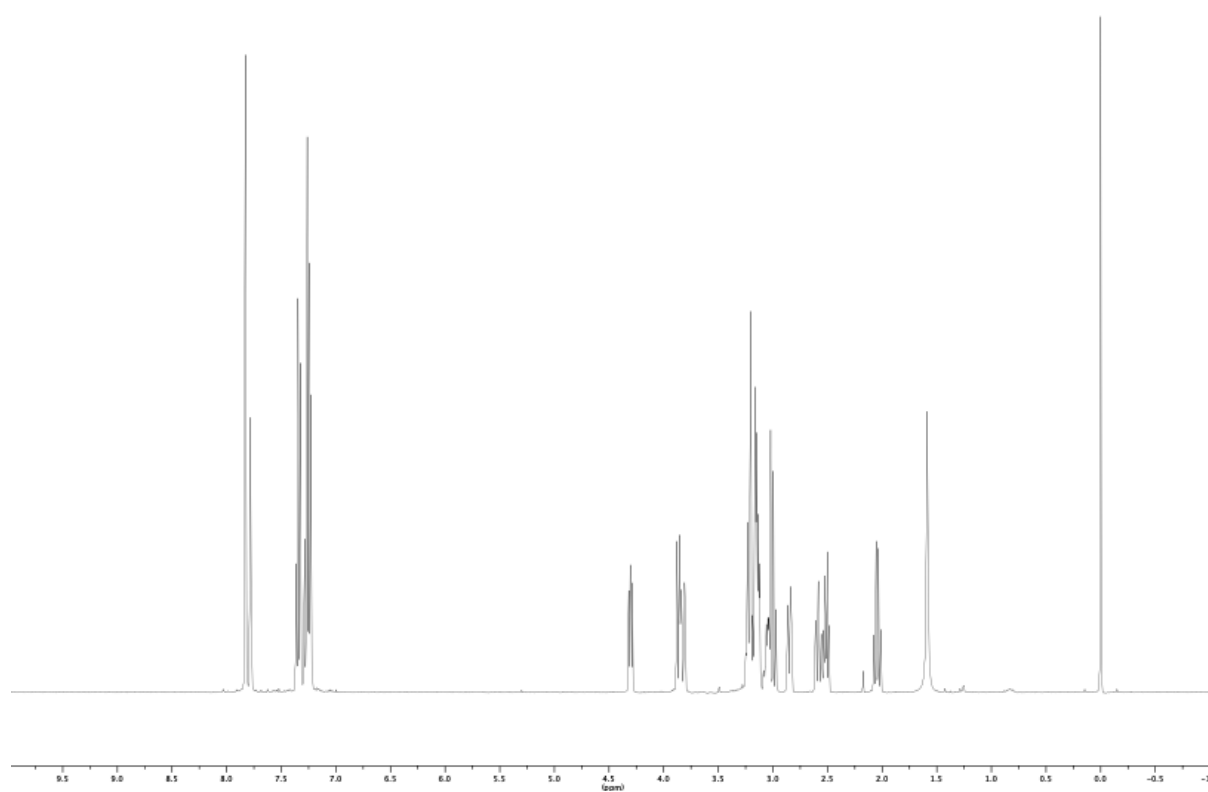
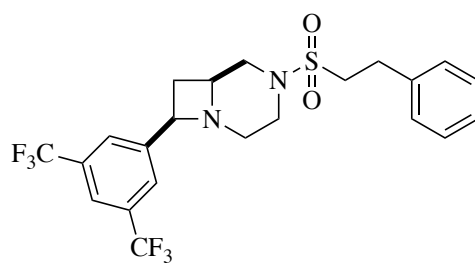


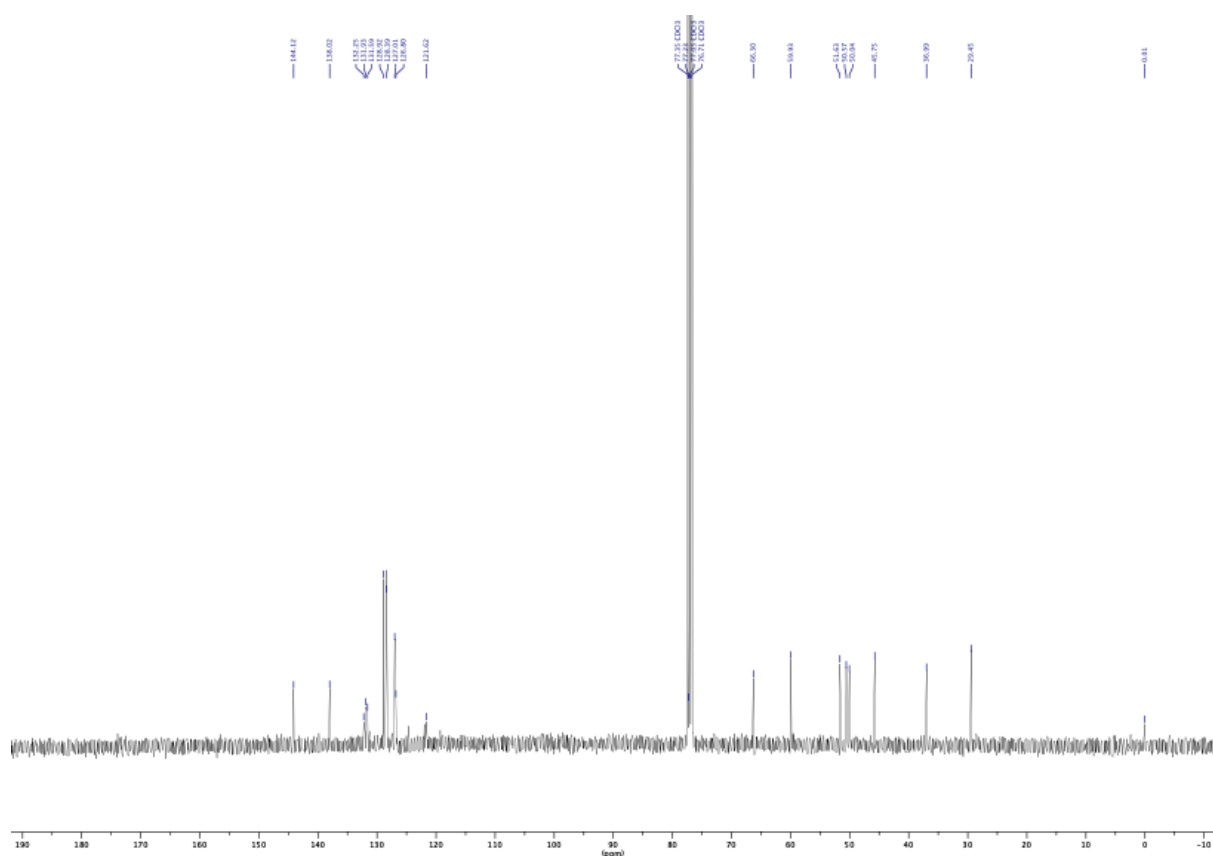
7.1.4. Representative NMR Spectra for 4,6-Fused Scaffold



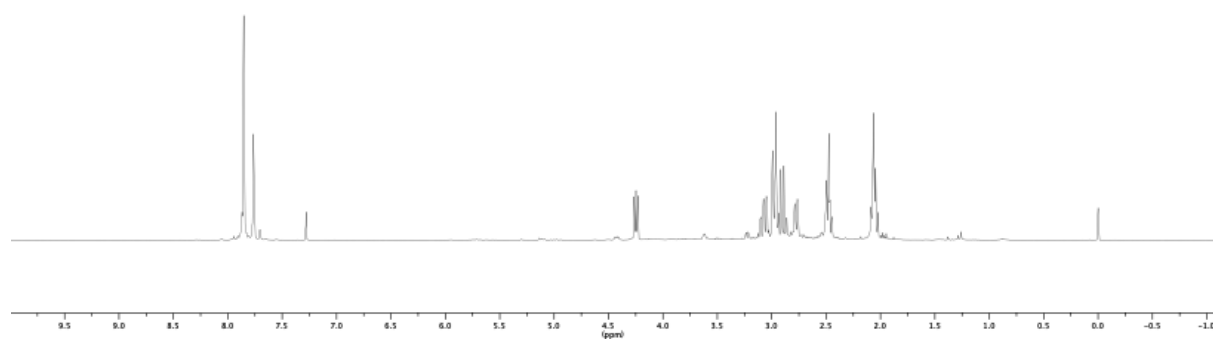
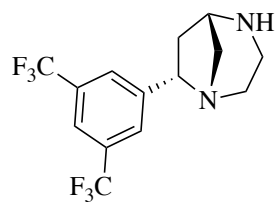


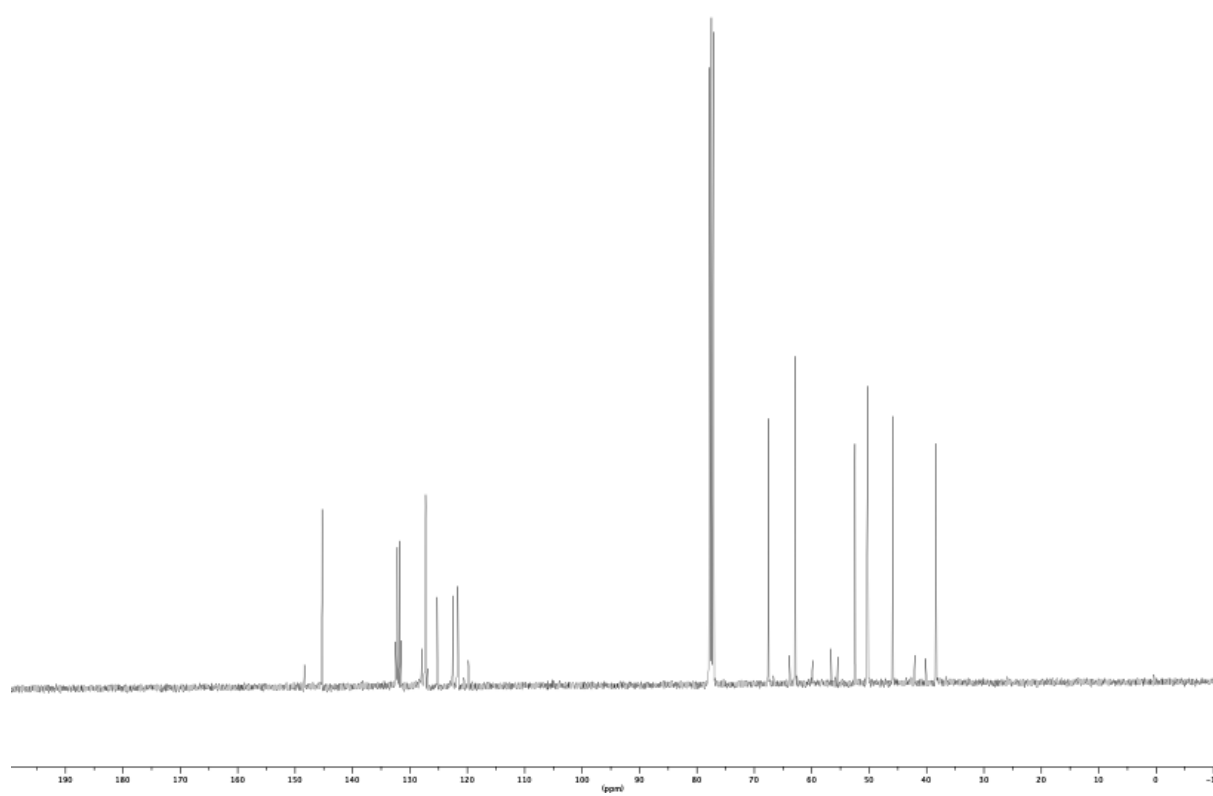
7.1.5. Representative NMR Spectra for Decorated 4,6-Fused Scaffold



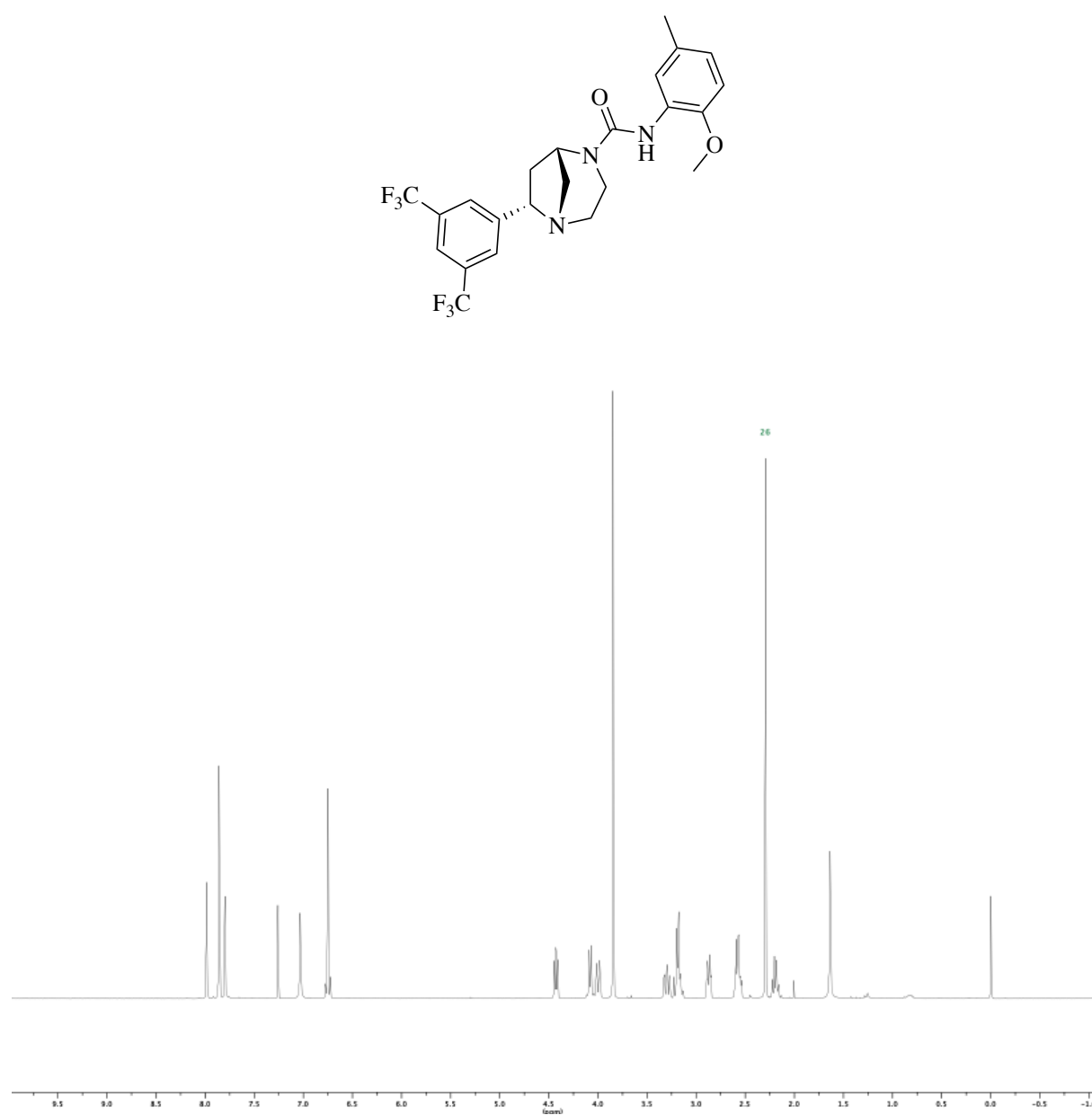


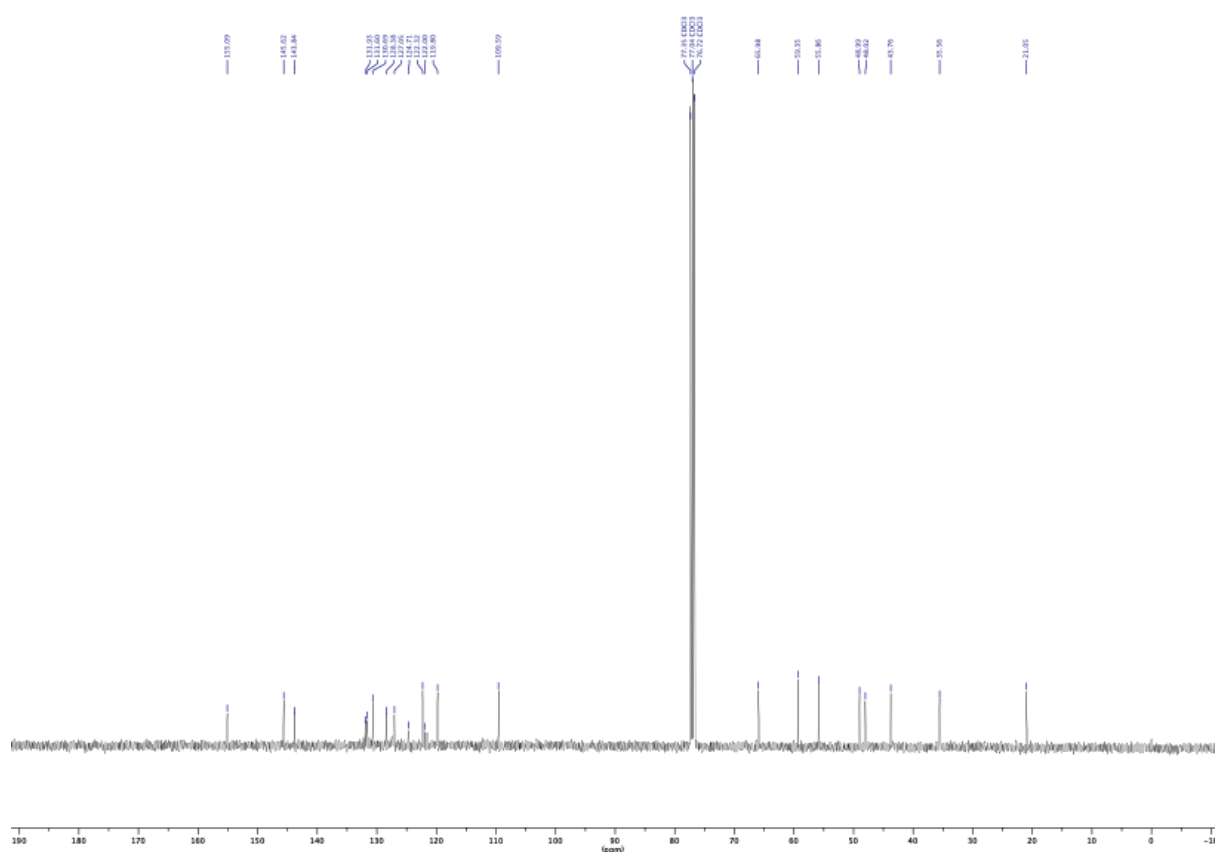
7.1.6. Representative NMR Spectra for 5,6-Bridged Scaffold





7.1.7. Representative NMR Spectra of Decorated 5,6-Bridged Scaffold





7.2. X-Ray Crystallography Tables

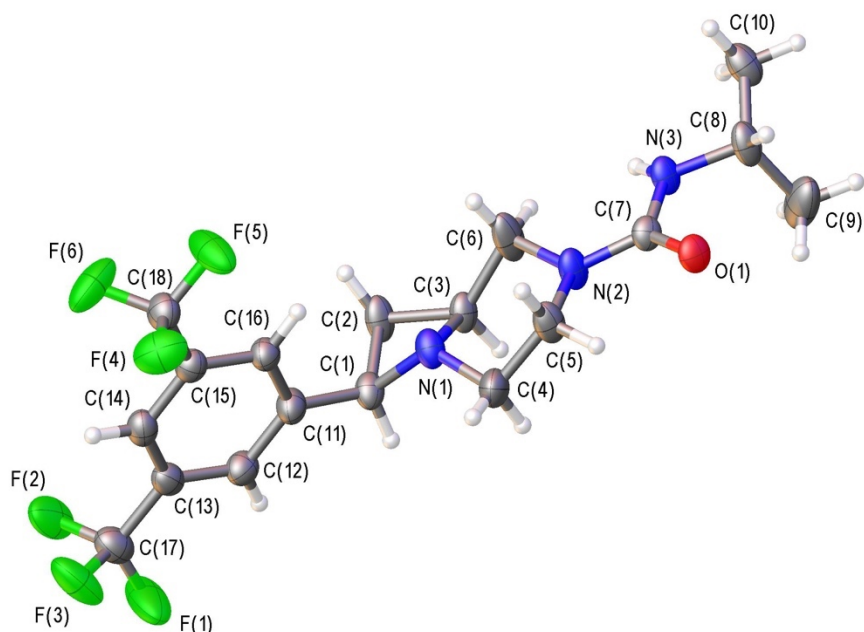


Table 7.5. Crystal data and structure refinement for (SC-5-CF3-3)

Empirical formula	$C_{18}H_{21}F_6N_3O$
Formula weight	409.38
Temperature/K	100.01(10)
Crystal system	monoclinic
Space group	$P2_1/c$
$a/\text{\AA}$	13.8215(8)
$b/\text{\AA}$	15.5380(10)
$c/\text{\AA}$	9.1588(5)
$\alpha/^\circ$	90
$\beta/^\circ$	101.769(5)
$\gamma/^\circ$	90
Volume/ \AA^3	1925.6(2)
Z	4
$\rho_{\text{calc}}/\text{g cm}^{-3}$	1.412
μ/mm^{-1}	1.131
$F(000)$	848.0
Crystal size/ mm^3	$0.178 \times 0.117 \times 0.085$
Radiation	$\text{Cu K}\alpha$ ($\lambda = 1.54184$)
2θ range for data collection/ $^\circ$	8.666 to 148.056
Index ranges	$-17 \leq h \leq 17, -18 \leq k \leq 19, -11 \leq l \leq 10$
Reflections collected	35885

Independent reflections	3832 [$R_{\text{int}} = 0.0361$, $R_{\text{sigma}} = 0.0159$]
Data/restraints/parameters	3832/131/343
Goodness-of-fit on F^2	1.050
Final R indexes [$I \geq 2\sigma(I)$]	$R_1 = 0.0506$, $wR_2 = 0.1289$
Final R indexes [all data]	$R_1 = 0.0601$, $wR_2 = 0.1387$
Largest diff. peak/hole / $e \text{ \AA}^{-3}$	0.41/-0.35

Table 7.6. Fractional Atomic Coordinates ($\times 104$) and Equivalent Isotropic Displacement Parameters ($\text{\AA}^2 \times 103$) for ORCO04-066_D. U_{eq} is defined as 1/3 of of the trace of the orthogonalised UIJ tensor.

Atom	x	y	z	$U(\text{eq})$
C1	2578.5(18)	4886.4(19)	2177(3)	33.3(6)
C2	2787.4(19)	5760.8(18)	1453(2)	40.6(7)
C3	3487(2)	5931(2)	2942(3)	33.6(6)
C1A	2576(6)	4593(6)	2847(11)	36(2)
C2A	3007(7)	4193(4)	4456(9)	40(2)
C3A	3116(9)	6237(8)	2724(12)	37(2)
C4	3436.3(16)	5006.3(14)	4948(2)	48.2(5)
C5	3691.6(15)	5756.2(13)	6004(2)	39.9(4)
C6	3612.2(18)	6764.8(15)	3869(2)	51.3(6)
C7	4797.8(12)	6979.7(11)	6293.8(18)	29.3(4)
C8	5920.0(15)	8210.9(14)	6633(2)	41.1(5)
C9	6907.4(17)	7773.9(19)	6662(4)	70.1(8)
C10	5892.5(16)	9108.8(14)	5984(2)	43.5(5)
C11	1545.3(13)	4498.0(13)	1906(2)	36.5(4)
C12	1322.3(14)	3791.2(13)	976(2)	36.4(4)
C13	364.1(14)	3470.6(12)	625.1(19)	35.5(4)
C14	-375.6(14)	3852.8(12)	1215(2)	36.3(4)
C15	-154.5(13)	4561.1(12)	2136(2)	32.9(4)
C16	798.1(13)	4886.4(12)	2488(2)	33.0(4)
C17	117.3(18)	2718.4(14)	-403(2)	47.4(5)
C18	-954.1(14)	4956.4(13)	2792(2)	41.1(4)
F1	858(4)	2274(4)	-609(10)	95(2)
F2	-424(5)	2952.2(19)	-1741(3)	69.7(12)
F3	-510(5)	2162(3)	78(5)	72.2(12)
F1A	850(12)	2164(7)	-204(17)	77(3)
F2A	213(14)	2967(5)	-1786(8)	84(3)
F3A	-673(8)	2383(9)	-454(19)	89(3)
F4	-1253(6)	4409(5)	3802(10)	62.0(16)
F5	-698(3)	5650(5)	3637(12)	67(2)
F6	-1765(7)	5108(7)	1869(9)	72(2)

F4A	-994(7)	4687(8)	4062(8)	71(2)
F5A	-873(4)	5826(3)	2787(13)	64.0(16)
F6A	-1836(6)	4843(8)	1865(11)	79(3)
N1	2863.9(11)	5366.6(10)	3571.4(16)	34.6(4)
N2	4142.0(12)	6474.3(11)	5340.2(15)	35.8(4)
N3	5113.9(11)	7714.2(10)	5744.4(16)	32.2(3)
O1	5091.6(9)	6771.1(8)	7617.0(13)	34.5(3)

Table 7.7. Anisotropic Displacement Parameters ($\text{\AA}^2 \times 10^3$) for ORCO04-066_D. The Anisotropic displacement factor exponent takes the form: $-2\pi^2[h^2a^{*2}U_{11}+2hka^*b^*U_{12}+\dots]$.

Atom	U ₁₁	U ₂₂	U ₃₃	U ₂₃	U ₁₃	U ₁₂
C1	28.2(11)	45.8(15)	26.0(14)	-7.4(11)	5.6(10)	-1.6(10)
C2	39.3(13)	60.7(16)	20.1(11)	0.4(10)	1.8(9)	-15.2(11)
C3	30.1(15)	48.7(17)	20.8(12)	1.0(11)	2.3(11)	-7.6(12)
C1A	29(4)	50(6)	29(5)	-5(4)	5(4)	7(4)
C2A	36(4)	49(5)	33(5)	-9(4)	0(3)	2(4)
C3A	27(5)	54(7)	31(5)	19(5)	9(4)	-2(4)
C4	40.6(11)	48.3(12)	47.3(12)	-4.6(9)	-10.8(9)	1.2(9)
C5	47.7(11)	45.3(11)	23.9(8)	5.6(8)	0.4(7)	-13.6(8)
C6	65.8(14)	56.6(13)	23.7(9)	10.9(9)	-9.5(9)	-27.3(11)
C7	30.3(8)	38.9(9)	19.1(8)	-1.0(6)	5.8(6)	-0.8(7)
C8	44.1(10)	54.0(12)	22.7(8)	-0.6(8)	1.0(7)	-17.9(9)
C9	36.8(12)	75.4(18)	90(2)	28.9(15)	-6.3(12)	-14.7(11)
C10	53.3(12)	48.9(11)	29.6(9)	-7.0(8)	11.4(8)	-17.3(9)
C11	30.4(9)	44.2(10)	33.1(9)	-7.9(8)	2.3(7)	1.4(8)
C12	36.8(9)	41.2(10)	30.1(9)	-3.8(8)	3.9(7)	5.0(8)
C13	43.1(10)	32.4(9)	28.2(8)	1.4(7)	0.7(7)	-1.2(7)
C14	33.7(9)	39.1(10)	34.2(9)	3.5(7)	2.1(7)	-5.7(7)
C15	31.9(9)	35.2(9)	31.5(9)	3.3(7)	5.8(7)	0.0(7)
C16	30.9(9)	36.5(9)	30.1(9)	-3.9(7)	2.6(7)	0.3(7)
C17	61.0(13)	39.7(11)	39.5(11)	-4.2(9)	5.5(9)	-4.7(10)
C18	31.7(9)	46.1(11)	45.0(11)	-2.5(9)	7.1(8)	-3.2(8)
F1	57.2(18)	82(4)	142(5)	-75(3)	12(2)	-2(2)
F2	109(3)	52.8(13)	35.1(11)	-10.2(9)	-14.7(15)	-1.7(16)
F3	114(3)	49.1(17)	54.3(18)	-12.9(12)	18.8(17)	-37.9(17)
F1A	123(7)	24(3)	77(5)	-5(3)	2(4)	11(3)
F2A	147(9)	60(3)	39(3)	-18(2)	6(4)	-13(5)
F3A	61(4)	84(7)	118(8)	-50(6)	13(5)	-34(4)
F4	63(3)	65(3)	69(4)	14(2)	39(3)	11(2)
F5	47.6(18)	59(3)	104(5)	-42(3)	36(2)	-14.5(16)
F6	57(4)	113(5)	43(3)	11(3)	6(2)	45(3)

F4A	78(4)	106(6)	36(2)	14(3)	30(2)	25(3)
F5A	57(2)	48.1(17)	99(5)	-1(2)	44(3)	9.2(15)
F6A	23(2)	131(6)	81(4)	-46(4)	7(2)	-3(3)
N1	30.2(7)	47.4(9)	26.9(7)	-5.2(6)	7.3(6)	-8.3(6)
N2	39.3(8)	46.4(9)	19.7(7)	3.9(6)	1.2(6)	-13.2(7)
N3	36.2(8)	42.0(8)	17.8(7)	-0.7(6)	4.0(6)	-9.2(6)
O1	40.7(7)	43.8(7)	18.1(5)	0.4(5)	3.6(5)	-3.7(5)

Table 7.8. Bond Lengths for (SC-5-CF3-3).

Atom	Atom	Length/Å	Atom	Atom	Length/Å
C1	C2	1.564(4)	C8	N3	1.459(2)
C1	C11	1.523(3)	C11	C12	1.386(3)
C1	N1	1.462(3)	C11	C16	1.392(3)
C2	C3	1.526(3)	C12	C13	1.390(3)
C3	C6	1.539(4)	C13	C14	1.384(3)
C3	N1	1.430(3)	C13	C17	1.496(3)
C1A	C2A	1.599(11)	C14	C15	1.383(3)
C1A	C11	1.514(8)	C15	C16	1.386(2)
C1A	N1	1.391(9)	C15	C18	1.493(3)
C2A	C4	1.429(7)	C17	F1	1.280(6)
C3A	C6	1.396(11)	C17	F2	1.348(4)
C3A	N1	1.632(11)	C17	F3	1.360(5)
C4	C5	1.509(3)	C17	F1A	1.314(14)
C4	N1	1.457(3)	C17	F2A	1.356(8)
C5	N2	1.468(2)	C17	F3A	1.203(11)
C6	N2	1.467(2)	C18	F4	1.380(7)
C7	N2	1.370(2)	C18	F5	1.332(4)
C7	N3	1.355(2)	C18	F6	1.281(8)
C7	O1	1.240(2)	C18	F4A	1.248(8)
C8	C9	1.520(3)	C18	F5A	1.355(5)
C8	C10	1.514(3)	C18	F6A	1.348(8)

Table 7.9. Bond Angles for (SC-5-CF3-3).

Atom	Atom	Atom	Angle/°	Atom	Atom	Atom	Angle/°
C11	C1	C2	121.5(2)	C16	C15	C18	120.17(17)
N1	C1	C2	83.51(17)	C15	C16	C11	119.79(17)
N1	C1	C11	114.91(19)	F1	C17	C13	115.3(3)
C3	C2	C1	84.81(19)	F1	C17	F2	108.9(4)
C2	C3	C6	128.2(3)	F1	C17	F3	106.6(4)

N1	C3	C2	86.01(18)	F2	C17	C13	112.0(2)
N1	C3	C6	107.7(2)	F2	C17	F3	101.2(3)
C11	C1A	C2A	128.1(8)	F3	C17	C13	111.8(3)
N1	C1A	C2A	83.1(5)	F1A	C17	C13	110.7(7)
N1	C1A	C11	120.0(6)	F1A	C17	F2A	95.6(9)
C4	C2A	C1A	90.0(4)	F2A	C17	C13	108.2(4)
C6	C3A	N1	104.4(6)	F3A	C17	C13	116.8(6)
C2A	C4	C5	155.8(4)	F3A	C17	F1A	112.9(10)
C2A	C4	N1	87.1(3)	F3A	C17	F2A	110.4(7)
N1	C4	C5	105.80(16)	F4	C18	C15	111.3(4)
N2	C5	C4	112.66(16)	F5	C18	C15	115.8(2)
C3A	C6	N2	125.9(5)	F5	C18	F4	100.9(4)
N2	C6	C3	103.1(2)	F6	C18	C15	115.5(5)
N3	C7	N2	117.86(14)	F6	C18	F4	102.4(5)
O1	C7	N2	121.02(16)	F6	C18	F5	109.1(5)
O1	C7	N3	121.12(16)	F4A	C18	C15	114.4(4)
C10	C8	C9	111.68(18)	F4A	C18	F5A	110.9(4)
N3	C8	C9	110.77(19)	F4A	C18	F6A	109.7(6)
N3	C8	C10	108.28(15)	F5A	C18	C15	109.9(3)
C12	C11	C1	119.84(18)	F6A	C18	C15	110.0(5)
C12	C11	C1A	119.5(4)	F6A	C18	F5A	101.1(5)
C12	C11	C16	119.30(17)	C3	N1	C1	92.20(17)
C16	C11	C1	120.66(17)	C3	N1	C4	108.61(19)
C16	C11	C1A	115.2(4)	C1A	N1	C3A	123.8(6)
C11	C12	C13	120.54(17)	C1A	N1	C4	97.6(4)
C12	C13	C17	120.64(18)	C4	N1	C1	124.19(19)
C14	C13	C12	120.06(17)	C4	N1	C3A	126.8(4)
C14	C13	C17	119.29(18)	C6	N2	C5	116.07(15)
C15	C14	C13	119.40(17)	C7	N2	C5	116.93(14)
C14	C15	C16	120.90(17)	C7	N2	C6	123.39(16)
C14	C15	C18	118.90(16)	C7	N3	C8	120.39(15)

Table 7.10. Table 6 Hydrogen Bonds for (SC-5-CF3-3)

D	H	A	d(D-H)/Å	d(H-A)/Å	d(D-A)/Å	D-H-A/°
N3	H3A	O1 ¹	0.87(2)	2.12(2)	2.9680(19)	165(2)

¹+X,3/2-Y,-1/2+Z

Table 7.11. Torsion Angles for (SC-5-CF3-3).

A	B	C	D	Angle/°	A	B	C	D	Angle/°
C1	C2	C3	C6	-136.0(3)	C12	C13	C14	C15	0.9(3)
C1	C2	C3	N1	-26.61(19)	C12	C13	C17	F1	17.1(5)
C1	C11	C12	C13	-175.0(2)	C12	C13	C17	F2	-108.1(4)
C1	C11	C16	C15	175.1(2)	C12	C13	C17	F3	139.1(3)
C2	C1	C11	C12	106.0(2)	C12	C13	C17	F1A	36.2(7)
C2	C1	C11	C16	-68.8(3)	C12	C13	C17	F2A	-67.3(9)
C2	C1	N1	C3	-27.9(2)	C12	C13	C17	F3A	167.4(10)
C2	C1	N1	C4	-142.2(2)	C13	C14	C15	C16	-0.7(3)
C2	C3	C6	N2	163.6(2)	C13	C14	C15	C18	-178.73(17)
C2	C3	N1	C1	28.5(2)	C14	C13	C17	F1	-163.6(5)
C2	C3	N1	C4	155.86(19)	C14	C13	C17	F2	71.2(4)
C3	C6	N2	C5	-53.5(2)	C14	C13	C17	F3	-41.6(4)
C3	C6	N2	C7	148.66(19)	C14	C13	C17	F1A	-144.5(7)
C1A	C2A	C4	C5	134.2(7)	C14	C13	C17	F2A	112.0(9)
C1A	C2A	C4	N1	10.5(5)	C14	C13	C17	F3A	-13.3(11)
C1A	C11	C12	C13	151.4(5)	C14	C15	C16	C11	0.1(3)
C1A	C11	C16	C15	-152.4(5)	C14	C15	C18	F4	67.2(5)
C2A	C1A	C11	C12	-85.8(8)	C14	C15	C18	F5	-178.3(6)
C2A	C1A	C11	C16	66.8(9)	C14	C15	C18	F6	-49.0(6)
C2A	C1A	N1	C3A	155.9(6)	C14	C15	C18	F4A	94.0(6)
C2A	C1A	N1	C4	11.0(5)	C14	C15	C18	F5A	-140.5(5)
C2A	C4	C5	N2	-171.6(8)	C14	C15	C18	F6A	-30.0(6)
C2A	C4	N1	C1A	-12.3(6)	C16	C11	C12	C13	-0.1(3)
C2A	C4	N1	C3A	-155.6(7)	C16	C15	C18	F4	-110.8(5)
C3A	C6	N2	C5	-37.5(7)	C16	C15	C18	F5	3.6(7)
C3A	C6	N2	C7	164.6(6)	C16	C15	C18	F6	133.0(6)
C4	C5	N2	C6	50.5(3)	C16	C15	C18	F4A	-84.0(7)
C4	C5	N2	C7	-150.21(17)	C16	C15	C18	F5A	41.5(6)
C5	C4	N1	C1	171.24(18)	C16	C15	C18	F6A	152.0(6)
C5	C4	N1	C3	65.1(2)	C17	C13	C14	C15	-178.41(17)
C5	C4	N1	C1A	-171.5(4)	C18	C15	C16	C11	178.12(17)
C5	C4	N1	C3A	45.2(6)	N1	C1	C2	C3	26.09(18)
C6	C3	N1	C1	157.5(2)	N1	C1	C11	C12	-156.0(2)
C6	C3	N1	C4	-75.2(3)	N1	C1	C11	C16	29.2(3)
C6	C3A	N1	C1A	-164.7(6)	N1	C3	C6	N2	64.6(3)
C6	C3A	N1	C4	-30.1(10)	N1	C1A	C2A	C4	-11.1(5)
C9	C8	N3	C7	75.2(2)	N1	C1A	C11	C12	168.3(6)
C10	C8	N3	C7	-162.01(16)	N1	C1A	C11	C16	-39.2(10)
C11	C1	C2	C3	141.4(2)	N1	C3A	C6	N2	23.0(10)
C11	C1	N1	C3	-149.7(3)	N1	C4	C5	N2	-51.4(2)

C11	C1	N1	C4	95.9(3)	N2	C7	N3	C8	-170.68(17)
C11	C1A	C2A	C4	-134.1(7)	N3	C7	N2	C5	-170.78(17)
C11	C1A	N1	C3A	-73.8(11)	N3	C7	N2	C6	-13.1(3)
C11	C1A	N1	C4	141.3(7)	O1	C7	N2	C5	9.2(3)
C11	C12	C13	C14	-0.5(3)	O1	C7	N2	C6	166.86(19)
C11	C12	C13	C17	178.78(18)	O1	C7	N3	C8	9.4(3)
C12	C11	C16	C15	0.3(3)					

Table 7.12. Hydrogen Atom Coordinates ($\text{\AA}\times 104$) and Isotropic Displacement Parameters ($\text{\AA}^2\times 103$) for (SC-5-CF3-3).

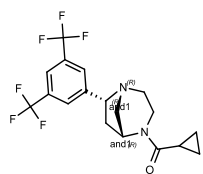
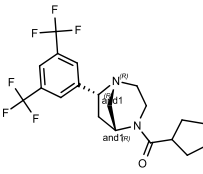
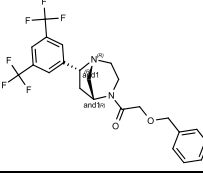
Atom	<i>x</i>	<i>y</i>	<i>z</i>	U(eq)
H1	3075.41	4452.64	2076.11	40
H2A	3110.92	5705.74	611.8	49
H2B	2224.27	6146.01	1231.27	49
H3	4130.32	5661.78	2962.06	40
H1A	3046.7	4463.53	2208.22	43
H2C	2500.21	4008.57	4980.87	48
H2D	3489.41	3741.07	4447.42	48
H3C	3532.67	6106.25	2019.14	44
H3D	2515.36	6510.91	2196.08	44
H4C	4031.99	4732.67	4768.34	58
H4D	3050.37	4582.44	5358.04	58
H4	4072.75	4939.52	4645.91	58
H5A	3095.46	5957.33	6299.11	48
H5B	4146	5563.15	6894.24	48
H6A	3995.19	7187.22	3450.7	62
H6B	2976.22	7011.59	3925.73	62
H6C	3127.42	7179	4059.15	62
H6D	4089.35	7087.57	3446.29	62
H8	5813.79	8250.7	7656.13	49
H9A	7032.4	7751.98	5669.63	105
H9B	6890.38	7199.65	7042.84	105
H9C	7423.28	8094.07	7293.1	105
H10A	6418.72	9445.83	6555.43	65
H10B	5269.84	9373.57	6017.74	65
H10C	5971.55	9076.58	4968.33	65
H12	1817.85	3529.25	582.78	44
H14	-1015.59	3635.08	993.99	44
H16	937.99	5362.66	3110.31	40

Atom	<i>x</i>	<i>y</i>	<i>z</i>	U(eq)
H3A	4997(16)	7819(15)	4790(30)	41(6)

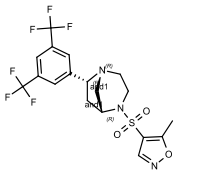
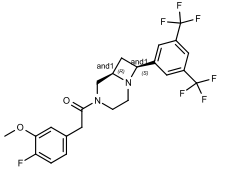
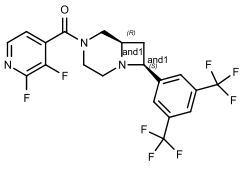
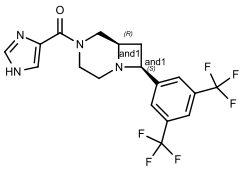
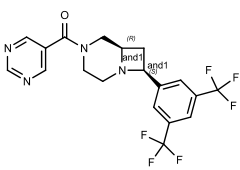
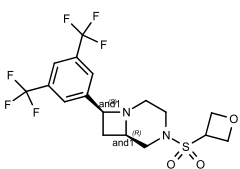
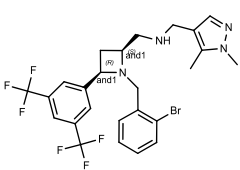
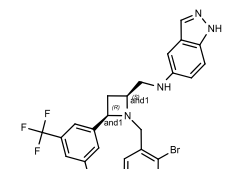
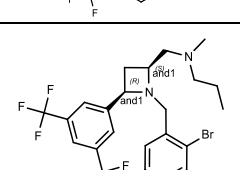
Table 7.13. Atomic Occupancy for (SC-5-CF3-3).

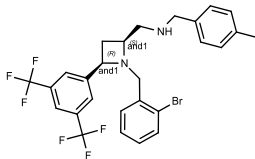
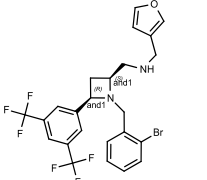
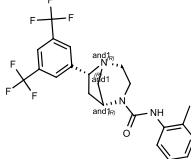
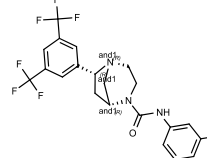
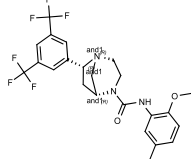
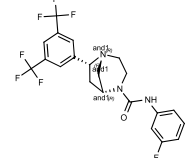
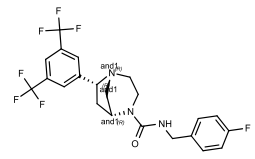
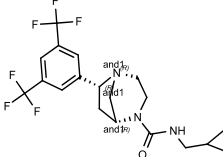
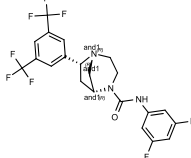
Atom	Occupancy	Atom	Occupancy	Atom	Occupancy
C1	0.784(5)	H1	0.784(5)	C2	0.784(5)
H2A	0.784(5)	H2B	0.784(5)	C3	0.784(5)
H3	0.784(5)	C1A	0.216(5)	H1A	0.216(5)
C2A	0.216(5)	H2C	0.216(5)	H2D	0.216(5)
C3A	0.216(5)	H3C	0.216(5)	H3D	0.216(5)
H4C	0.784(5)	H4D	0.784(5)	H4	0.216(5)
H6A	0.784(5)	H6B	0.784(5)	H6C	0.216(5)
H6D	0.216(5)	F1	0.701(12)	F2	0.701(12)
F3	0.701(12)	F1A	0.299(12)	F2A	0.299(12)
F3A	0.299(12)	F4	0.513(15)	F5	0.513(15)
F6	0.513(15)	F4A	0.487(15)	F5A	0.487(15)
F6A	0.487(15)				

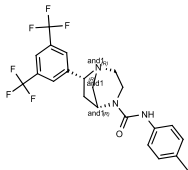
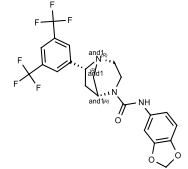
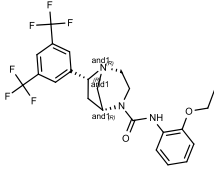
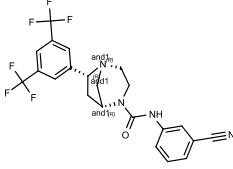
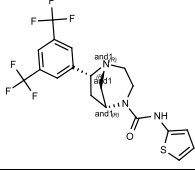
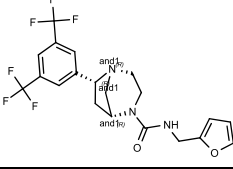
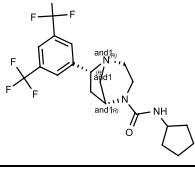
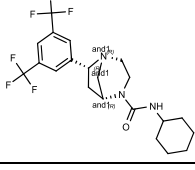
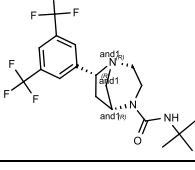
7.3. Compounds Submitted for Biological Screening

Molecule Name	Structure	Molecular weight (g/mol)	log P	pKa	Fsp3	Barcode	% Purity
UoB-DD-0006325		392.345	3.53	6.37	0.61	HCC - 100435	100
UoB-DD-0006324		420.399	4.42	6.37	0.65	HCC - 100433	100
UoB-DD-0006323		472.431	4.3	6.31	0.43	HCC - 100440	99

UoB-DD-0006322		474.42	2.15	5.45	0.61	HCC - 100436	100
UoB-DD-0006321		468.84	5.29	5.43	0.42	HCC - 100431	96
UoB-DD-0006320		429.366	3.39	5.64	0.4	HCC - 100437	92
UoB-DD-0006319		600.403	6.68	5.85	0.3	HCC - 100430	100
UoB-DD-0006318		423.403	3.89	5.45	0.63	HCC - 100338	100
UoB-DD-0006317		408.388	4.34	5.47	0.63	HCC - 100432	100
UoB-DD-0006316		472.387	4.23	6.28	0.41	HCC - 100443	99
UoB-DD-0006315		430.354	2.41	6.16	0.42	HCC - 100439	100
UoB-DD-0006314		432.37	3.1	5.33	0.47	HCC - 100438	100

UoB-DD-0006313		469.4	2.93	4.78	0.5	HCC - 100429	96
UoB-DD-0006312		490.422	4.57	5.79	0.43	HCC - 100441	100
UoB-DD-0006311		465.347	4.07	5.51	0.4	HCC - 100434	100
UoB-DD-0006310		418.343	2.41	5.81	0.44	HCC - 100427	96
UoB-DD-0006309		430.354	2.68	5.55	0.42	HCC - 100428	100
UoB-DD-0006308		444.39	2.39	5.46	0.65	HCC - 100442	94
UoB-DD-0006212		575.397	6.16	8.66	0.4	HCC - 100344	92
UoB-DD-0006211		583.376	7.13	5.85	0.27	HCC - 100337	94
UoB-DD-0006210		523.361	7.07	9.42	0.48	HCC - 100335	93

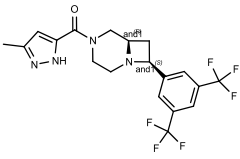
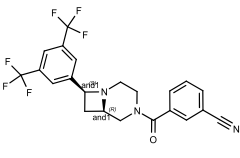
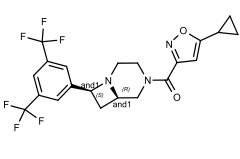
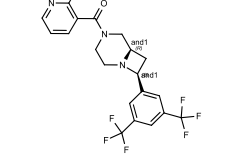
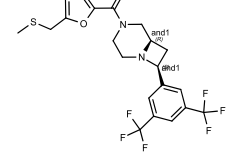
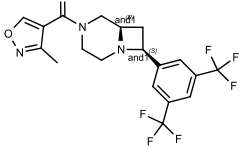
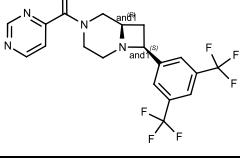
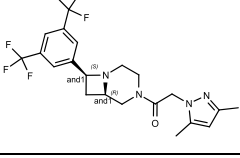
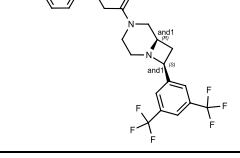
UoB-DD-0006209		571.405	8.05	9.21	0.33	HCC - 100334	95
UoB-DD-0006208		547.339	6.67	8.48	0.33	HCC - 100328	91
UoB-DD-0006207		457.42	5.17	5.45	0.41	HCC - 100341	99
UoB-DD-0006206		457.42	5.17	6.34	0.41	HCC - 100332	100
UoB-DD-0006205		487.446	5.02	5.42	0.43	HCC - 100330	100
UoB-DD-0006204		461.384	4.8	6.33	0.38	HCC - 100325	100
UoB-DD-0006203		475.411	4.51	6.35	0.41	HCC - 100324	100
UoB-DD-0006202		421.387	3.42	6.35	0.63	HCC - 100326	95
UoB-DD-0006201		479.374	4.95	6.32	0.38	HCC - 100342	100

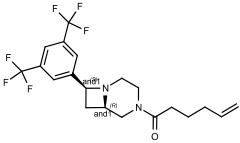
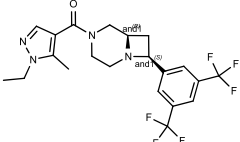
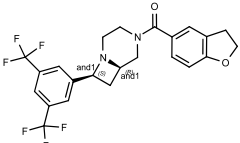
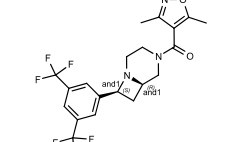
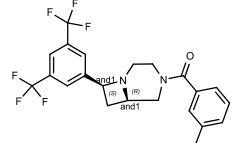
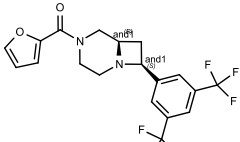
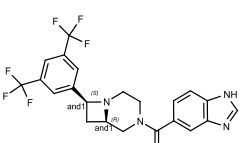
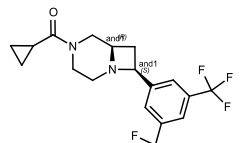
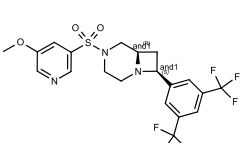
UoB-DD-0006200		457.42	5.17	6.35	0.41	HCC - 100339	100
UoB-DD-0006199		487.402	4.28	6.34	0.41	HCC - 100375	92
UoB-DD-0006198		487.446	4.86	5.42	0.43	HCC - 100361	97
UoB-DD-0006197		468.403	4.52	6.33	0.36	HCC - 100350	100
UoB-DD-0006196		449.42	4.61	6.29	0.42	HCC - 100379	100
UoB-DD-0006195		447.381	3.43	6.35	0.45	HCC - 100353	100
UoB-DD-0006194		435.414	4	6.35	0.65	HCC - 100383	100
UoB-DD-0006193		449.441	4.44	6.35	0.67	HCC - 100373	100
UoB-DD-0006192		423.403	3.7	5.45	0.63	HCC - 100349	100

UoB-DD-0006182		418.343	2.83	6.26	0.44	HCC - 100372	100
UoB-DD-0006181		459.392	2.65	5.53	0.43	HCC - 100370	100
UoB-DD-0006180		446.393	4.15	6.19	0.48	HCC - 100359	95
UoB-DD-0006179		432.37	3.09	5.33	0.47	HCC - 100366	95
UoB-DD-0006178		433.354	2.6	5.15	0.47	HCC - 100348	90
UoB-DD-0006177		459.392	3.83	5.26	0.43	HCC - 100347	100
UoB-DD-0006176		486.414	4.12	6.23	0.43	HCC - 100367	100
UoB-DD-0006175		419.327	3.36	6.11	0.44	HCC - 100384	97
UoB-DD-0006174		418.339	3.67	6.1	0.42	HCC - 100365	99

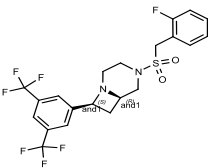
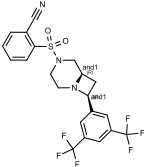
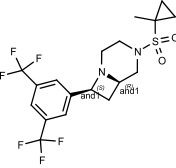
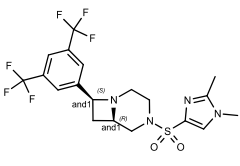
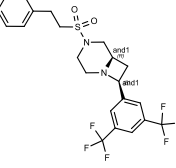
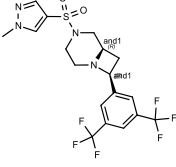
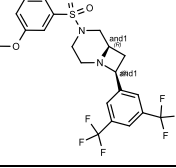
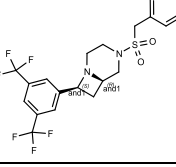
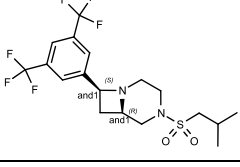
UoB-DD-0006173		449.441	3.24	8.79	0.67	HCC - 100358	100
UoB-DD-0006172		445.365	2.58	6.43	0.4	HCC - 100351	97
UoB-DD-0006171		424.387	2.87	5.47	0.63	HCC - 100374	94
UoB-DD-0006170		432.37	2.85	6.33	0.47	HCC - 100363	100
UoB-DD-0006169		392.345	3.53	6.37	0.61	HCC - 100360	100
UoB-DD-0006168		391.317	2.7	6.26	0.53	HCC - 100385	100
UoB-DD-0006167		496.44	4.27	5.11	0.43	HCC - 100371	100
UoB-DD-0006166		492.48	4.41	6.03	0.45	HCC - 100381	100
UoB-DD-0006165		473.43	2.02	6.02	0.67	HCC - 100345	100

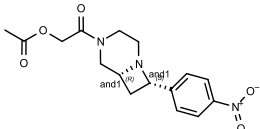
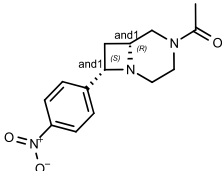
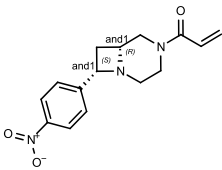
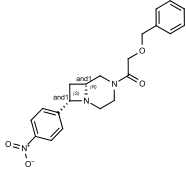
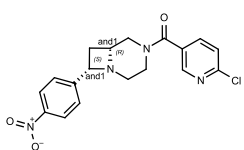
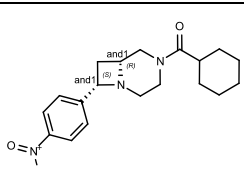
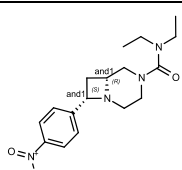
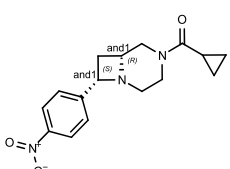
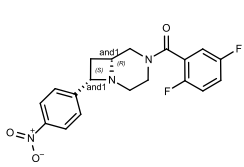
UoB-DD-0006164		470.47	4.35	6.04	0.7	HCC - 100378	100
UoB-DD-0006163		478.45	4.12	6.05	0.43	HCC - 100376	100
UoB-DD-0006162		454.39	2.84	5.87	0.47	HCC - 100382	100
UoB-DD-0006161		444.44	3.64	5.13	0.67	HCC - 100368	100
UoB-DD-0006160		486.414	4.15	5.72	0.43	HCC - 100386	96
UoB-DD-0006159		495.5	4.22	5.6	0.5	HCC - 100387	100
UoB-DD-0006158		449.441	3.49	7.81	0.67	HCC - 100388	100
UoB-DD-0006157		468.403	4.14	5.71	0.36	HCC - 100389	99
UoB-DD-0006156		480.414	4.32	5.6	0.35	HCC - 100390	100

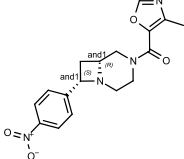
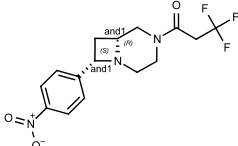
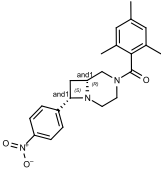
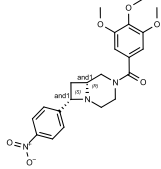
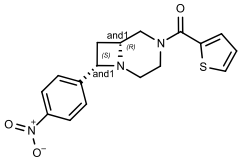
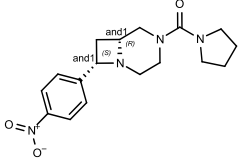
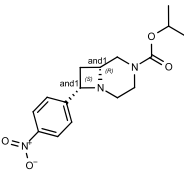
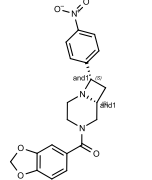
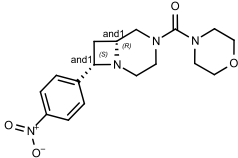
UoB-DD-0006155		432.37	2.96	5.66	0.47	HCC - 100391	100
UoB-DD-0006154		453.388	4.46	5.67	0.36	HCC - 100392	100
UoB-DD-0006153		459.392	3.98	5.52	0.52	HCC - 100393	100
UoB-DD-0006152		443.393	3.52	5.69	0.43	HCC - 100394	100
UoB-DD-0006151		478.45	4.3	5.51	0.48	HCC - 100396	100
UoB-DD-0006150		433.354	3.1	5.44	0.47	HCC - 100397	100
UoB-DD-0006149		430.354	3.07	5.58	0.42	HCC - 100395	100
UoB-DD-0006148		460.424	3.19	5.74	0.52	HCC - 100398	100
UoB-DD-0006147		472.431	4.73	5.78	0.43	HCC - 100400	100

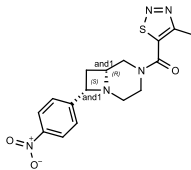
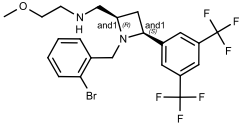
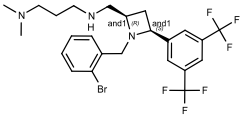
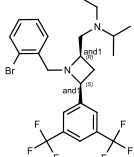
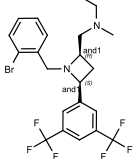
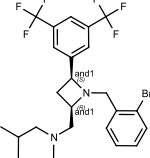
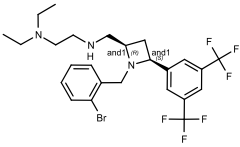
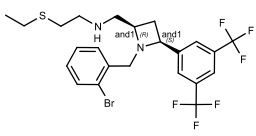
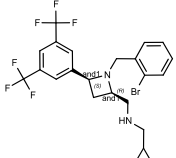
UoB-DD-0006146		420.399	4.48	5.78	0.55	HCC - 100401	100
UoB-DD-0006145		460.424	3.59	5.64	0.52	HCC - 100402	95
UoB-DD-0006144		470.415	4.49	5.73	0.43	HCC - 100403	96
UoB-DD-0006143		447.381	3.3	5.46	0.5	HCC - 100399	98
UoB-DD-0006142		470.415	4.16	5.58	0.39	HCC - 100404	100
UoB-DD-0006141		418.339	3.67	5.51	0.42	HCC - 100405	98
UoB-DD-0006140		468.403	3.89	5.89	0.36	HCC - 100406	96
UoB-DD-0006139		392.345	3.53	5.78	0.61	HCC - 100407	100
UoB-DD-0006138		495.44	2.99	5.24	0.45	HCC - 100408	99

UoB-DD-0006137		479.374	4.95	5.73	0.38	HCC - 100409	97
UoB-DD-0006136		479.374	4.95	5.68	0.38	HCC - 100411	96
UoB-DD-0006135		487.446	4.21	5.76	0.43	HCC - 100412	97
UoB-DD-0006134		487.402	4.28	5.75	0.41	HCC - 100413	100
UoB-DD-0006133		468.403	4.52	5.74	0.36	HCC - 100415	100
UoB-DD-0006132		447.381	3.43	5.76	0.45	HCC - 100410	98
UoB-DD-0006131		449.441	4.44	5.76	0.67	HCC - 100414	96
UoB-DD-0006130		496.44	5.02	5.32	0.43	HCC - 100416	100
UoB-DD-0006129		482.42	4.5	5.29	0.4	HCC - 100417	97

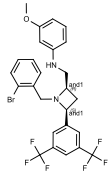
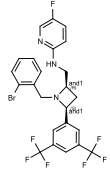
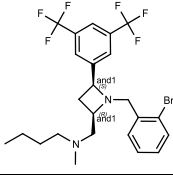
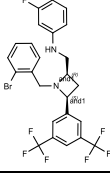
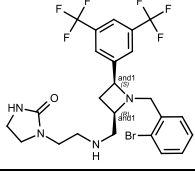
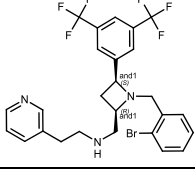
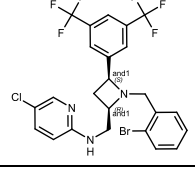
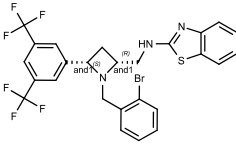
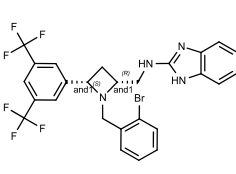
UoB-DD-0006128		496.44	4.27	5.42	0.43	HCC - 100355	92
UoB-DD-0006127		489.44	4.22	5.26	0.38	HCC - 100419	91
UoB-DD-0006126		442.42	3.45	5.47	0.67	HCC - 100420	100
UoB-DD-0006125		482.45	3.18	5.29	0.53	HCC - 100421	100
UoB-DD-0006124		492.48	4.41	5.45	0.45	HCC - 100422	100
UoB-DD-0006123		468.42	2.79	5.25	0.5	HCC - 100423	98
UoB-DD-0006122		494.45	4.2	5.31	0.43	HCC - 100424	95
UoB-DD-0006121		478.45	4.12	5.46	0.43	HCC - 100425	100
UoB-DD-0006120		444.44	3.64	5.45	0.67	HCC - 100426	100

UoB-DD-0004309		333.344	0.56	6.76	0.5		
UoB-DD-0004308		275.308	0.94	6.94	0.5		
UoB-DD-0004307		287.319	1.69	6.93	0.4		
UoB-DD-0004306		381.432	2.49	6.76	0.38		
UoB-DD-0004305		372.81	2.4	6.62	0.33		
UoB-DD-0004304		343.427	3.05	6.81	0.63		
UoB-DD-0004303		332.404	1.76	6.78	0.59		
UoB-DD-0004302		301.346	1.72	6.81	0.56		
UoB-DD-0004301		373.36	3.08	6.54	0.32		

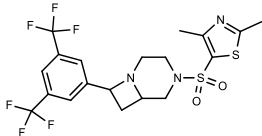
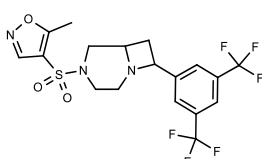
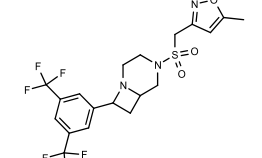
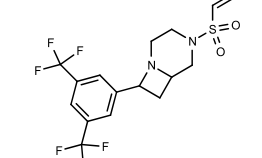
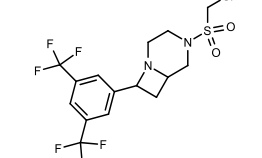
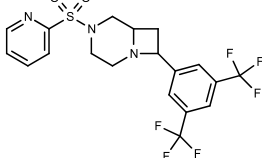
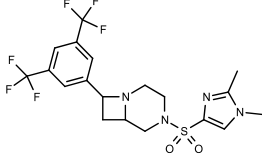
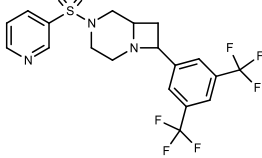
UoB-DD-0004300		342.355	0.78	6.38	0.41		
UoB-DD-0004299		343.306	2	6.87	0.53		
UoB-DD-0004298		379.46	4.33	6.78	0.41		
UoB-DD-0004297		427.457	2.32	6.69	0.41		
UoB-DD-0004296		343.4	2.7	6.36	0.35		
UoB-DD-0004295		330.388	1.46	6.78	0.59		
UoB-DD-0004294		319.361	2.33	6.73	0.56		
UoB-DD-0004293		381.388	2.41	6.7	0.35		
UoB-DD-0004292		346.387	0.83	6.78	0.59		

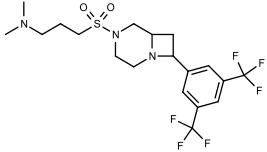
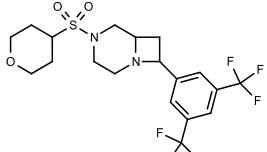
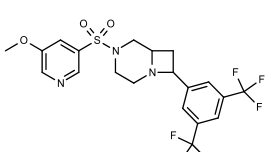
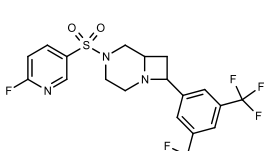
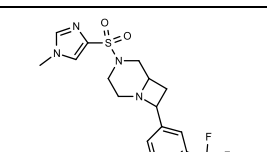
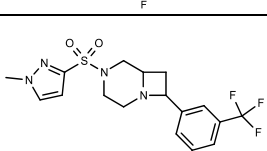
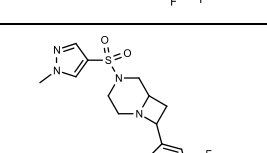
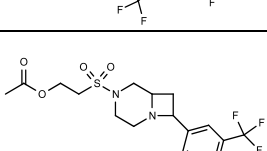
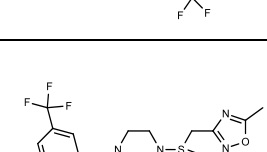
UoB-DD-0004291		359.4	1.64	5.92	0.44		
UoB-DD-0004290		525.333	5.76	9.44	0.45	HCC - 100331	95
UoB-DD-0004289		552.403	5.89	9.76	0.5		
UoB-DD-0004288		537.388	7.32	9.72	0.5		
UoB-DD-0004287		509.334	6.55	9.16	0.45	HCC - 100336	94
UoB-DD-0004286		537.388	7.43	9.69	0.5	HCC - 100340	93
UoB-DD-0004285		566.43	6.54	9.76	0.52		
UoB-DD-0004284		555.42	6.85	9.72	0.48		
UoB-DD-0004283		521.345	6.59	10.3	0.48		

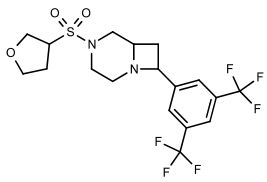
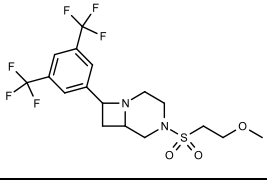
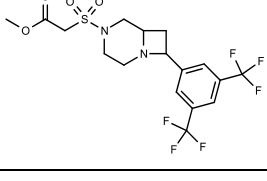
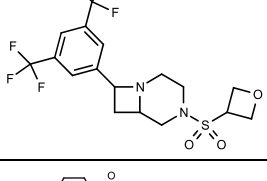
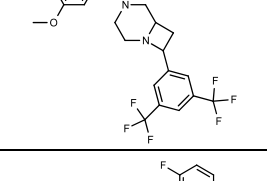
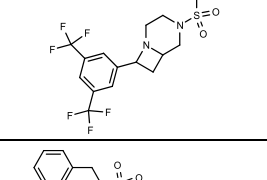
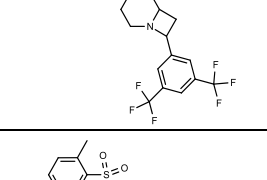
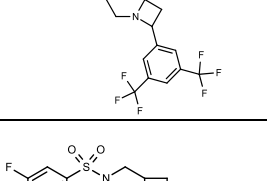
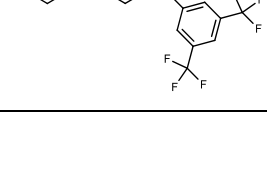
UoB-DD-0004273		567.373	7.6	5.87	0.26		
UoB-DD-0004272		562.354	6.54	5.39	0.38		
UoB-DD-0004271		578.441	6.22	9.6	0.54	HCC - 100333	96
UoB-DD-0004270		578.397	5.46	8.74	0.48		
UoB-DD-0004269		534.344	5.63	10.3	0.43		
UoB-DD-0004268		575.393	7.17	7.8	0.38		
UoB-DD-0004267		564.414	6.39	8.05	0.52	HCC - 100343	93
UoB-DD-0004266		576.425	6.77	7.73	0.46		
UoB-DD-0004265		572.393	6.6	9.74	0.35		

UoB-DD-0004264		573.377	7.29	5.84	0.31		
UoB-DD-0004263		562.33	6.97	5.58	0.29		
UoB-DD-0004262		537.388	7.51	9.44	0.5		
UoB-DD-0004259		561.342	7.59	5.78	0.28		
UoB-DD-0004258		579.385	4.77	9.33	0.46		
UoB-DD-0004257		572.393	6.6	9.71	0.35		
UoB-DD-0004255		578.78	7.43	5.61	0.29		
UoB-DD-0004253		600.42	8.27	5.67	0.27		
UoB-DD-0004252		583.376	7.42	7	0.27		

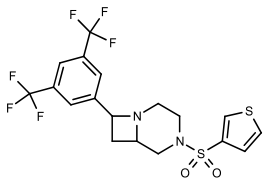
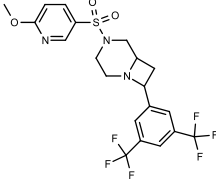
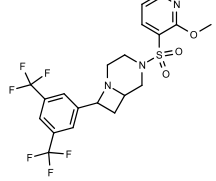
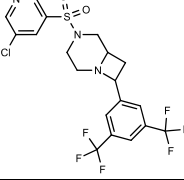
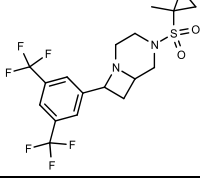
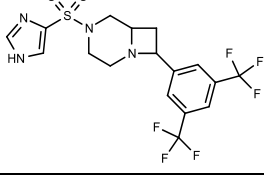
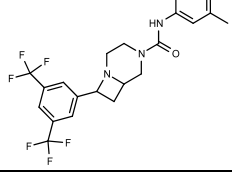
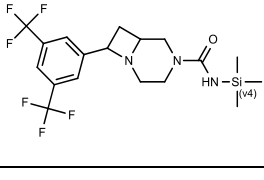
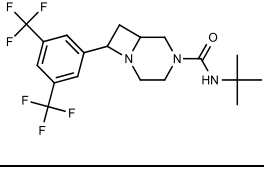
7.4. 4,6 Fused Compound Library

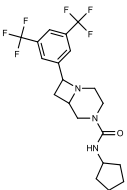
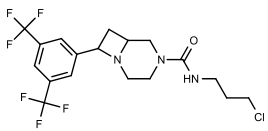
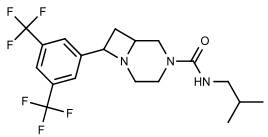
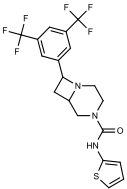
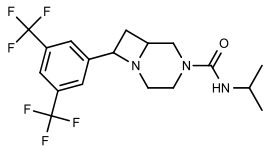
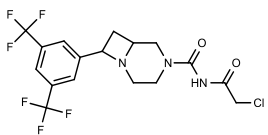
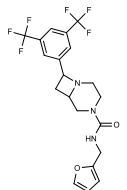
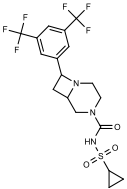
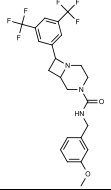
	Structure	Chemical formula	MW (g/mol)	log P	pKa	TPSA (Å ²)	Fsp3
1		C ₁₉ H ₁₉ F ₆ N ₃ O ₂ S ₂	499.49	3.44	5.07	53.51	0.53
2		C ₁₈ H ₁₇ F ₆ N ₃ O ₃ S	469.4	2.93	5.09	66.65	0.5
3		C ₁₉ H ₁₉ F ₆ N ₃ O ₃ S	483.43	3.07	5.38	66.65	0.53
4		C ₁₆ H ₁₆ F ₆ N ₂ O ₂ S	414.37	2.98	5.48	40.62	0.5
5		C ₁₅ H ₁₅ ClF ₆ N ₂ O ₂ S	436.8	3.02	5.14	40.62	0.6
6		C ₁₉ H ₁₇ F ₆ N ₃ O ₂ S	465.41	3.74	5.26	53.51	0.42
7		C ₁₉ H ₂₀ F ₆ N ₄ O ₂ S	482.45	3.18	5.29	58.44	0.53
8		C ₁₉ H ₁₇ F ₆ N ₃ O ₂ S	465.41	3.14	5.25	53.51	0.42

9		C ₁₉ H ₂₅ F ₆ N ₃ O ₂ S	473.48	2.48	8.44	43.86	0.68
10		C ₁₉ H ₂₂ F ₆ N ₂ O ₃ S	472.45	2.51	5.46	49.85	0.68
11		C ₂₀ H ₁₉ F ₆ N ₃ O ₃ S	495.44	2.99	5.24	62.74	0.45
12		C ₁₉ H ₁₆ F ₇ N ₃ O ₂ S	483.4	3.68	5.24	53.51	0.42
13		C ₁₈ H ₁₈ F ₆ N ₄ O ₂ S	468.42	3.06	5.27	58.44	0.5
14		C ₁₈ H ₁₈ F ₆ N ₄ O ₂ S	468.42	3.38	5.25	58.44	0.5
15		C ₁₈ H ₁₈ F ₆ N ₄ O ₂ S	468.42	2.79	5.25	58.44	0.5
16		C ₁₈ H ₂₀ F ₆ N ₂ O ₄ S	474.42	2.15	5.45	66.92	0.61
17		C ₁₈ H ₁₈ F ₆ N ₄ O ₃ S	484.42	3.02	5.34	79.54	0.56

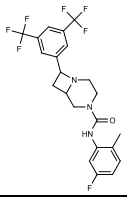
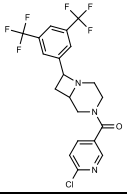
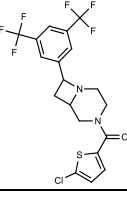
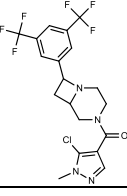
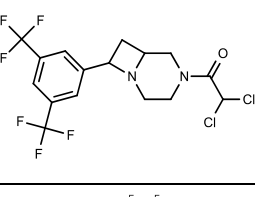
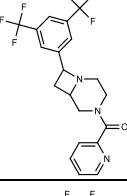
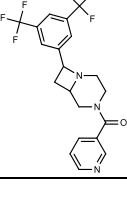
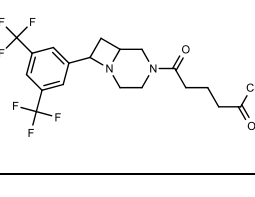
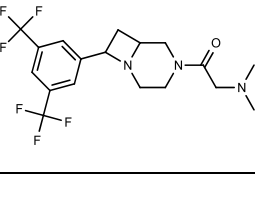
18		C18H20F6N2O3S	458.42	2.45	5.46	49.85	0.67
19		C17H20F6N2O3S	446.41	2.35	5.45	49.85	0.65
20		C17H18F6N2O4S	460.39	2.33	5.47	66.92	0.59
21		C17H18F6N2O3S	444.39	2.39	5.46	49.85	0.65
22		C21H20F6N2O3S	494.45	4.2	5.31	49.85	0.43
23		C21H19F7N2O2S	496.44	5.02	5.3	40.62	0.43
24		C22H22F6N2O2S	492.48	4.41	5.45	40.62	0.45
25		C21H20F6N2O2S	478.45	4.88	5.34	40.62	0.43
26		C20H17F7N2O2S	482.42	4.5	5.29	40.62	0.4

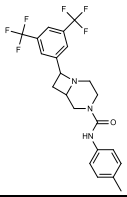
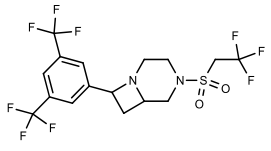
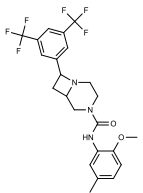
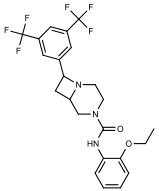
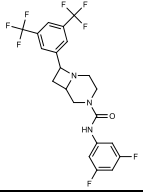
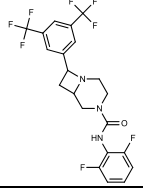
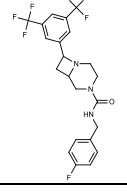
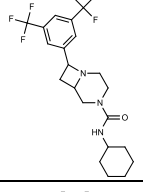
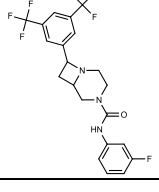
27		C ₂₁ H ₁₉ F ₇ N ₂ O ₂ S	496.44	4.27	5.42	40.62	0.43
28		C ₂₀ H ₂₄ F ₆ N ₂ O ₂ S	470.47	4.35	5.46	40.62	0.7
29		C ₁₉ H ₂₀ F ₆ N ₄ O ₂ S	482.45	3	5.28	69.3	0.53
30		C ₂₁ H ₂₀ F ₆ N ₂ O ₂ S	478.45	4.12	5.46	40.62	0.43
31		C ₂₁ H ₂₀ F ₆ N ₂ O ₃ S	494.45	4.2	5.27	49.85	0.43
32		C ₂₀ H ₁₆ ClF ₆ N ₃ O	463.81	4.21	5.58	36.44	0.4
33		C ₁₇ H ₁₉ ClF ₆ N ₂ O ₂ S	464.85	3.12	5.45	40.62	0.65
34		C ₁₈ H ₂₂ F ₆ N ₂ O ₂ S	444.44	3.64	5.45	40.62	0.67
35		C ₁₉ H ₁₆ ClF ₆ N ₃ O ₂ S	499.86	3.97	5.2	53.51	0.42

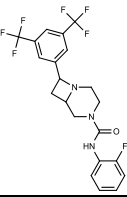
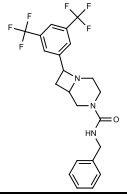
36		C18H16F6N2O2S2	470.45	4.14	5.24	40.62	0.44
37		C20H19F6N3O3S	495.44	3.58	5.25	62.74	0.45
38		C20H19F6N3O3S	495.44	3.58	5.19	62.74	0.45
39		C19H16ClF6N3O2S	499.86	3.75	5.22	53.51	0.42
40		C18H20F6N2O2S	442.42	3.45	5.47	40.62	0.67
41		C17H16F6N4O2S	454.39	2.84	5.28	69.3	0.47
42		C22H21F6N3O	457.42	5.17	5.75	35.58	0.41
43		C18H23F6N3OSi	439.477	4.25	5.52	35.58	0.61
44		C19H23F6N3O	423.403	3.7	5.76	35.58	0.63

45		C ₂₀ H ₂₃ F ₆ N ₃ O	435.414	4	5.76	35.58	0.65
46		C ₁₈ H ₂₀ ClF ₆ N ₃ O	443.82	3.37	5.76	35.58	0.61
47		C ₁₉ H ₂₃ F ₆ N ₃ O	423.403	3.89	5.76	35.58	0.63
48		C ₁₉ H ₁₇ F ₆ N ₃ OS	449.42	4.61	5.7	35.58	0.42
49		C ₁₈ H ₂₁ F ₆ N ₃ O	409.376	3.42	5.76	35.58	0.61
50		C ₁₇ H ₁₆ ClF ₆ N ₃ O ₂	443.77	2.94	5.78	52.65	0.53
51		C ₂₀ H ₁₉ F ₆ N ₃ O ₂	447.381	3.43	5.76	48.72	0.45
52		C ₁₈ H ₁₉ F ₆ N ₃ O ₃ S	471.42	1.52	3.81	69.72	0.61
53		C ₂₃ H ₂₃ F ₆ N ₃ O ₂	487.446	4.21	5.76	44.81	0.43

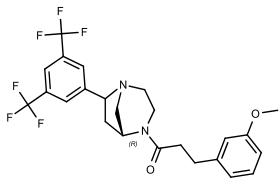
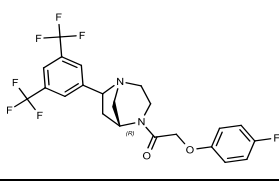
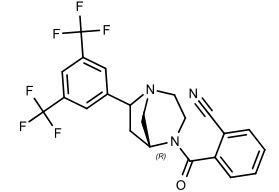
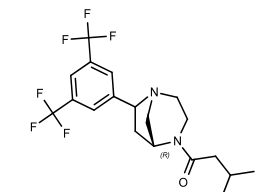
54		C22H20F7N3O	475.411	5.32	5.75	35.58	0.41
55		C22H21F6N3O	457.42	5.17	5.76	35.58	0.41
56		C23H23F6N3O2	487.446	4.21	5.76	44.81	0.43
57		C22H18F6N4O	468.403	4.52	5.74	59.37	0.36
58		C22H19F6N3O3	487.402	4.28	5.75	54.04	0.41
59		C19H26F6N2O2SS i	488.56	4.44	5.45	40.62	0.68
60		C21H17F6N3O2S	489.44	4.22	5.26	64.41	0.38
61		C16H17ClF6N2O2 S	450.82	3.06	5.45	40.62	0.62
62		C21H19F7N2O2S	496.44	5.02	5.32	40.62	0.43

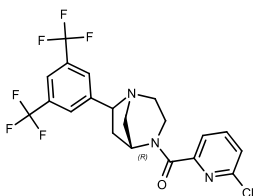
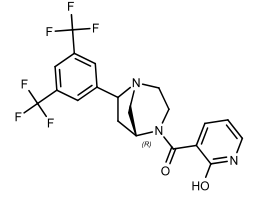
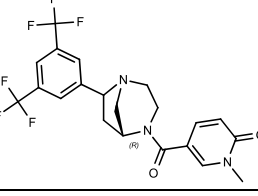
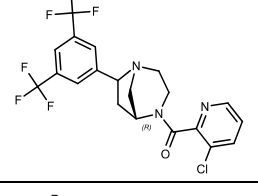
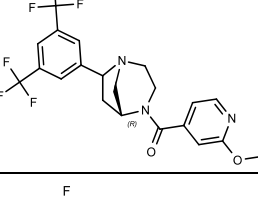
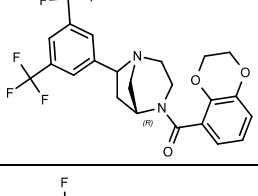
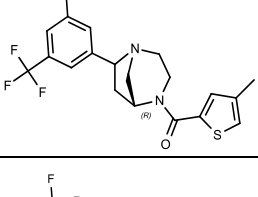
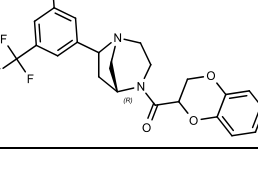
63		C ₂₂ H ₂₀ F ₇ N ₃ O	475.411	5.32	5.74	35.58	0.41
64		C ₂₀ H ₁₆ ClF ₆ N ₃ O	463.81	4.21	5.63	36.44	0.4
65		C ₁₉ H ₁₅ ClF ₆ N ₂ OS	468.84	5.29	5.43	23.55	0.42
66		C ₁₉ H ₁₇ ClF ₆ N ₄ O	466.81	3.35	5.56	41.37	0.47
67		C ₁₆ H ₁₄ Cl ₂ F ₆ N ₂ O	435.19	4.03	5.13	23.55	0.56
68		C ₂₀ H ₁₇ F ₆ N ₃ O	429.366	3.77	5.62	36.44	0.4
69		C ₂₀ H ₁₇ F ₆ N ₃ O	429.366	3.39	5.64	36.44	0.4
70		C ₁₉ H ₁₉ ClF ₆ N ₂ O ₂	456.81	3.56	5.7	40.62	0.58
71		C ₁₈ H ₂₁ F ₆ N ₃ O	409.376	2.64	7.51	26.79	0.61

72		C22H21F6N3O	457.42	5.17	5.76	35.58	0.41
73		C16H15F9N2O2S	470.35	3.35	5.45	40.62	0.62
74		C23H23F6N3O2	487.446	5.02	5.73	44.81	0.43
75		C23H23F6N3O2	487.446	4.86	5.73	44.81	0.43
76		C21H17F8N3O	479.374	4.95	5.73	35.58	0.38
77		C21H17F8N3O	479.374	4.95	5.68	35.58	0.38
78		C22H20F7N3O	475.411	4.51	5.76	35.58	0.41
79		C21H25F6N3O	449.441	4.44	5.76	35.58	0.67
80		C21H18F7N3O	461.384	4.8	5.74	35.58	0.38

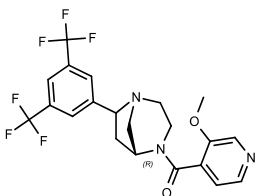
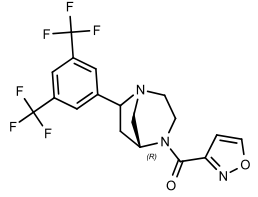
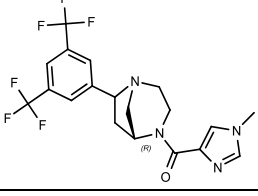
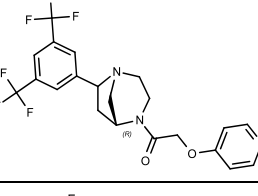
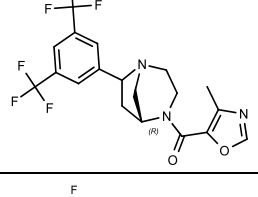
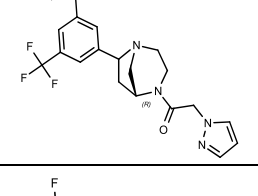
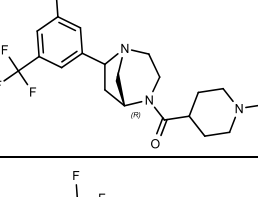
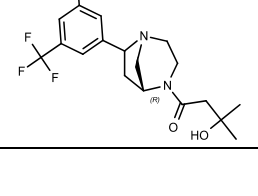
81		C ₂₁ H ₁₈ F ₇ N ₃ O	461.384	4.8	5.71	35.58	0.38
82		C ₂₂ H ₂₁ F ₆ N ₃ O	457.42	4.37	5.76	35.58	0.41

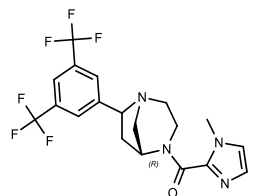
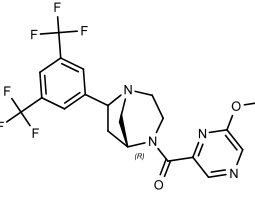
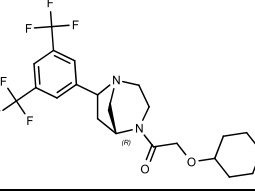
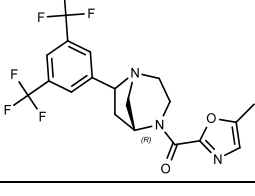
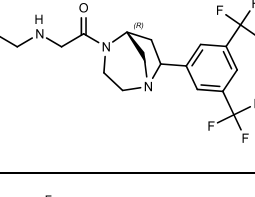
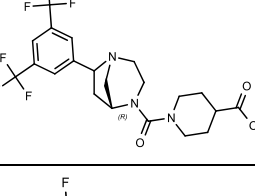
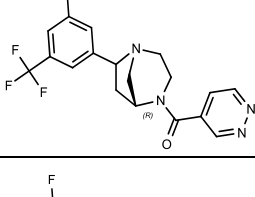
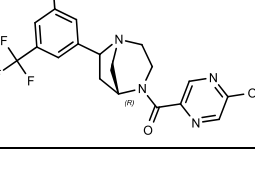
7.5. 5,6-Bridged Compound Library

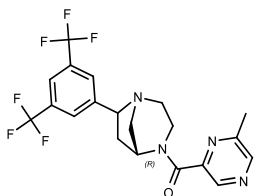
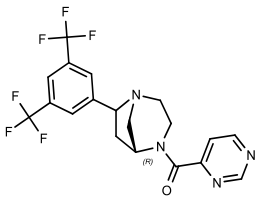
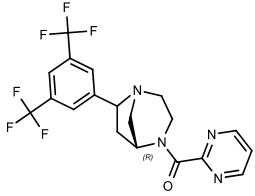
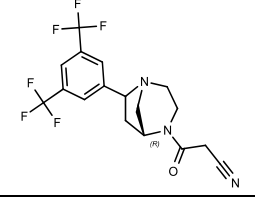
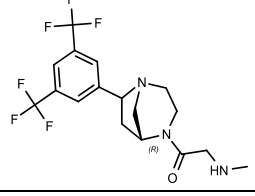
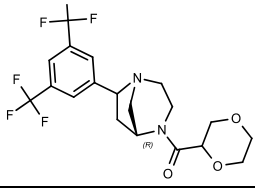
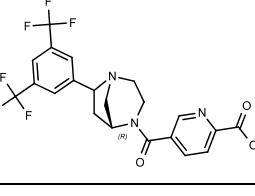
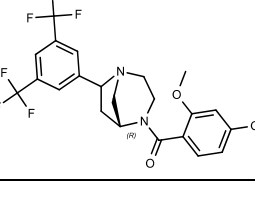
	Structure	Chemical formula	MW (g/mol)	log P	pKa	TPSA (Å ²)	Fsp3
1		C ₂₄ H ₂₄ F ₆ N ₂ O ₂	486.458	4.87	6.37	32.78	0.46
2		C ₂₂ H ₁₉ F ₇ N ₂ O ₂	476.395	4.41	6.31	32.78	0.41
3		C ₂₂ H ₁₇ F ₆ N ₃ O	453.388	4.46	6.23	47.34	0.36
4		C ₁₉ H ₂₂ F ₆ N ₂ O	408.388	4.18	5.47	23.55	0.63

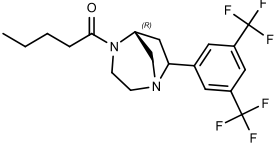
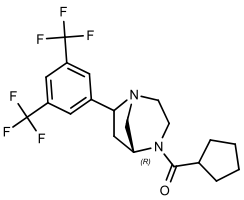
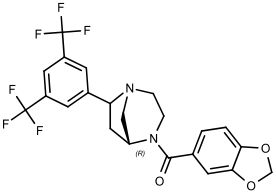
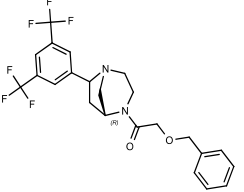
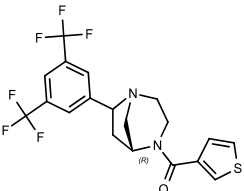
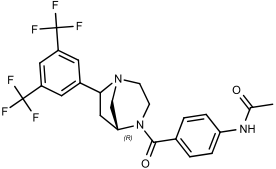
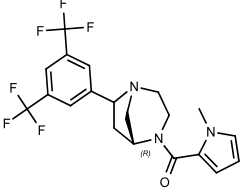
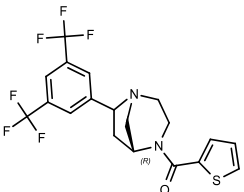
5		C ₂₀ H ₁₆ ClF ₆ N ₃ O	463.81	4.6	6.21	36.44	0.4
6		C ₂₀ H ₁₇ F ₆ N ₃ O ₂	445.365	2.58	6.43	52.65	0.4
7		C ₂₁ H ₁₉ F ₆ N ₃ O ₂	459.392	2.65	5.53	43.86	0.43
8		C ₂₀ H ₁₆ ClF ₆ N ₃ O	463.81	4.38	6.15	36.44	0.4
9		C ₂₁ H ₁₉ F ₆ N ₃ O ₂	459.392	3.83	5.33	45.67	0.43
10		C ₂₃ H ₂₀ F ₆ N ₂ O ₃	486.414	4.12	6.23	42.01	0.43
11		C ₂₀ H ₁₈ F ₆ N ₂ OS	448.43	5.03	5.24	23.55	0.45
12		C ₂₃ H ₂₀ F ₆ N ₂ O ₃	486.414	4.15	6.31	42.01	0.43

13		C ₂₁ H ₁₉ F ₆ N ₃ O	443.393	3.9	5.41	36.44	0.43
14		C ₂₀ H ₁₅ F ₈ N ₃ O	465.347	3.67	5.14	36.44	0.4
15		C ₂₂ H ₁₉ F ₆ N ₃ O ₂	471.403	3.46	5.34	66.64	0.36
16		C ₁₈ H ₁₆ F ₆ N ₄ O	418.343	2.83	6.26	52.23	0.44
17		C ₂₂ H ₁₉ F ₆ N ₃ O ₃	487.402	3.78	5.28	62.74	0.41
18		C ₂₀ H ₂₀ F ₆ N ₄ O	446.397	3.09	6.24	41.37	0.5
19		C ₁₈ H ₁₆ F ₆ N ₄ O	418.343	2.41	6.29	52.23	0.44
20		C ₂₁ H ₂₅ F ₆ N ₃ O	449.441	3.49	7.85	26.79	0.67

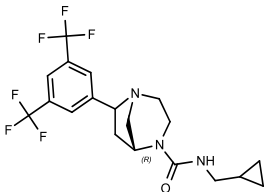
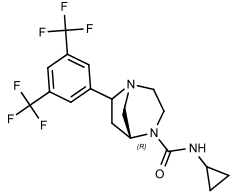
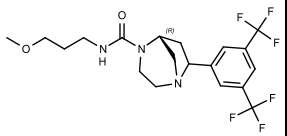
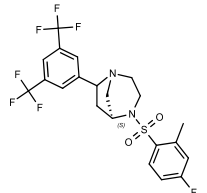
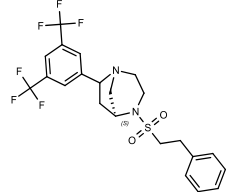
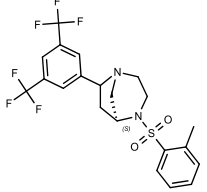
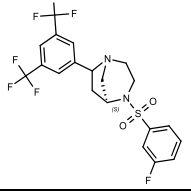
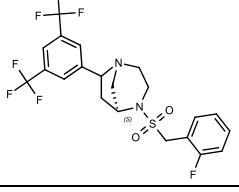
21		C ₂₁ H ₁₉ F ₆ N ₃ O ₂	459.392	3.23	5.28	45.67	0.43
22		C ₁₈ H ₁₅ F ₆ N ₃ O ₂	419.327	3.36	6.11	49.58	0.44
23		C ₁₉ H ₁₈ F ₆ N ₄ O	432.37	3.1	5.33	41.37	0.47
24		C ₂₁ H ₁₉ F ₆ N ₃ O ₂	459.392	3.05	6.67	45.67	0.43
25		C ₁₉ H ₁₇ F ₆ N ₃ O ₂	433.354	2.6	5.15	49.58	0.47
26		C ₁₉ H ₁₈ F ₆ N ₄ O	432.37	2.85	6.33	41.37	0.47
27		C ₂₁ H ₂₅ F ₆ N ₃ O	449.441	3.24	8.79	26.79	0.67
28		C ₁₉ H ₂₂ F ₆ N ₂ O ₂	424.387	2.87	5.47	43.78	0.63

29		C ₁₉ H ₁₈ F ₆ N ₄ O	432.37	3.09	5.33	41.37	0.47
30		C ₂₀ H ₁₈ F ₆ N ₄ O ₂	460.38	2.99	5.25	58.56	0.45
31		C ₂₁ H ₂₄ F ₆ N ₂ O ₃	466.424	2.54	6.31	42.01	0.67
32		C ₁₉ H ₁₇ F ₆ N ₃ O ₂	433.354	3.13	5.17	49.58	0.47
33		C ₁₈ H ₂₁ F ₆ N ₃ O	409.376	2.62	8.9	35.58	0.61
34		C ₂₁ H ₂₃ F ₆ N ₃ O ₃	479.423	1.39	4.05	64.09	0.62
35		C ₁₉ H ₁₆ F ₆ N ₄ O	430.354	2.41	6.16	49.33	0.42
36		C ₁₉ H ₁₆ F ₆ N ₄ O ₂	446.353	2.31	6.37	65.01	0.42

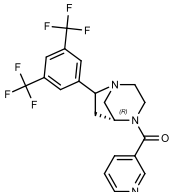
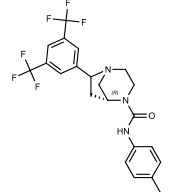
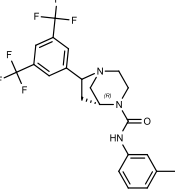
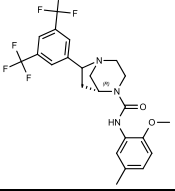
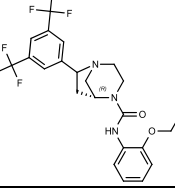
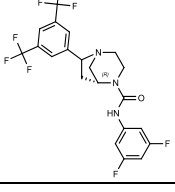
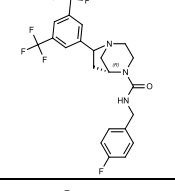
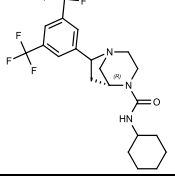
37		C ₂₀ H ₁₈ F ₆ N ₄ O	444.381	2.69	5.25	49.33	0.45
38		C ₁₉ H ₁₆ F ₆ N ₄ O	430.354	3.07	6.17	49.33	0.42
39		C ₁₉ H ₁₆ F ₆ N ₄ O	430.354	3.32	6.15	49.33	0.42
40		C ₁₇ H ₁₅ F ₆ N ₃ O	391.317	2.7	6.26	47.34	0.53
41		C ₁₇ H ₁₉ F ₆ N ₃ O	395.349	2.26	8.81	35.58	0.59
42		C ₁₉ H ₂₀ F ₆ N ₂ O ₃	438.37	2.57	6.31	42.01	0.63
43		C ₂₁ H ₁₇ F ₆ N ₃ O ₃	473.375	1.4	0.81	73.74	0.38
44		C ₂₃ H ₂₂ F ₆ N ₂ O ₃	488.43	4.29	6.24	42.01	0.43

45		C ₁₉ H ₂₂ F ₆ N ₂ O	408.388	4.34	5.47	23.55	0.63
46		C ₂₀ H ₂₂ F ₆ N ₂ O	420.399	4.42	6.37	23.55	0.65
47		C ₂₂ H ₁₈ F ₆ N ₂ O ₃	472.387	4.23	6.28	42.01	0.41
48		C ₂₃ H ₂₂ F ₆ N ₂ O ₂	472.431	4.3	6.31	32.78	0.43
49		C ₁₉ H ₁₆ F ₆ N ₂ OS	434.4	4.39	6.22	23.55	0.42
50		C ₂₃ H ₂₁ F ₆ N ₃ O ₂	485.43	3.84	5.41	52.65	0.39
51		C ₂₀ H ₁₉ F ₆ N ₃ O	431.382	3.83	5.41	28.48	0.45
52		C ₁₉ H ₁₆ F ₆ N ₂ OS	434.4	4.52	6.1	23.55	0.42

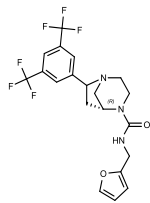
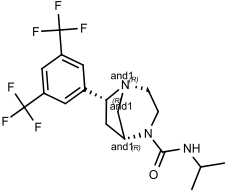
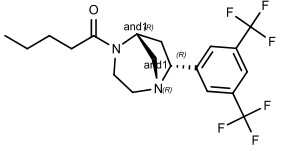
53		C ₂₀ H ₁₉ F ₆ N ₃ O ₂	447.381	3.3	5.15	49.58	0.5
54		C ₁₉ H ₂₂ F ₆ N ₂ O	408.388	4.55	5.48	23.55	0.63
55		C ₂₁ H ₁₉ F ₆ N ₃ O	443.393	3.9	5.37	36.44	0.43
56		C ₁₈ H ₂₀ F ₆ N ₂ O	394.361	4	5.47	23.55	0.61
57		C ₂₀ H ₁₇ F ₆ N ₃ O	429.366	3.39	6.25	36.44	0.4
58		C ₁₉ H ₁₆ F ₆ N ₂ O ₂	418.339	3.67	6.1	36.69	0.42
59		C ₁₈ H ₁₈ F ₆ N ₂ O	392.345	3.53	6.37	23.55	0.61
60		C ₁₉ H ₂₀ F ₆ N ₂ O ₃	438.37	2.72	5.47	49.85	0.58

61		C ₁₉ H ₂₁ F ₆ N ₃ O	421.387	3.42	6.35	35.58	0.63
62		C ₁₈ H ₁₉ F ₆ N ₃ O	407.36	3.11	6.35	35.58	0.61
63		C ₁₉ H ₂₃ F ₆ N ₃ O ₂	439.402	2.66	5.45	44.81	0.63
64		C ₂₁ H ₁₉ F ₇ N ₂ O ₂ S	496.44	5.02	5.01	40.62	0.43
65		C ₂₂ H ₂₂ F ₆ N ₂ O ₂ S	492.48	4.41	6.03	40.62	0.45
66		C ₂₁ H ₂₀ F ₆ N ₂ O ₂ S	478.45	4.88	5.03	40.62	0.43
67		C ₂₀ H ₁₇ F ₇ N ₂ O ₂ S	482.42	4.5	4.97	40.62	0.4
68		C ₂₁ H ₁₉ F ₇ N ₂ O ₂ S	496.44	4.27	5.11	40.62	0.43

69		C20H24F6N2O2S	470.47	4.35	6.04	40.62	0.7
70		C21H20F6N2O2S	478.45	4.12	6.05	40.62	0.43
71		C18H22F6N2O2S	444.44	3.64	5.13	40.62	0.67
72		C17H16F6N4O2S	454.39	2.84	5.87	69.3	0.47
73		C18H17F6N3O3S	469.4	2.93	4.78	66.65	0.5
74		C18H21F6N3O3S	473.43	2.02	6.02	53.09	0.67
75		C19H17ClF6N4O	466.81	3.35	6.15	41.37	0.47
76		C20H17F6N3O	429.366	3.77	6.21	36.44	0.4

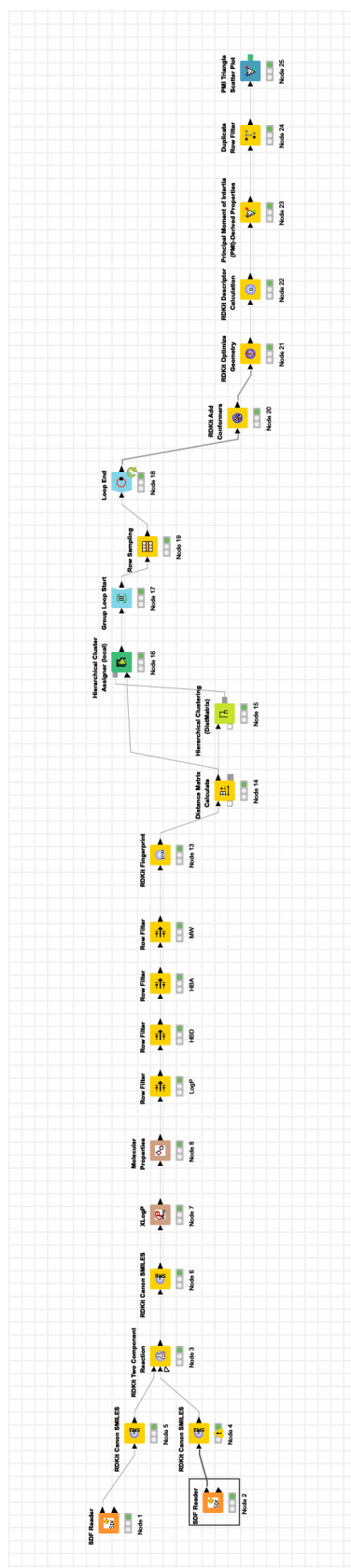
77		C ₂₀ H ₁₇ F ₆ N ₃ O	429.366	3.39	6.23	36.44	0.4
78		C ₂₂ H ₂₁ F ₆ N ₃ O	457.42	5.17	6.35	35.58	0.41
79		C ₂₂ H ₂₁ F ₆ N ₃ O	457.42	5.17	6.34	35.58	0.41
80		C ₂₃ H ₂₃ F ₆ N ₃ O ₂	487.446	5.02	5.42	44.81	0.43
81		C ₂₃ H ₂₃ F ₆ N ₃ O ₂	487.446	4.86	5.42	44.81	0.43
82		C ₂₁ H ₁₇ F ₈ N ₃ O	479.374	4.95	6.32	35.58	0.38
83		C ₂₂ H ₂₀ F ₇ N ₃ O	475.411	4.51	6.35	35.58	0.41
84		C ₂₁ H ₂₅ F ₆ N ₃ O	449.441	4.44	6.35	35.58	0.67

85		C22H21F6N3O	457.42	5.17	5.45	35.58	0.41
86		C21H18F7N3O	461.384	4.8	6.33	35.58	0.38
87		C19H23F6N3O	423.403	3.7	5.45	35.58	0.63
88		C22H18F6N4O	468.403	4.52	6.33	59.37	0.36
89		C20H23F6N3O	435.414	4	6.35	35.58	0.65
90		C19H23F6N3O	423.403	3.89	5.45	35.58	0.63
91		C22H19F6N3O3	487.402	4.28	6.34	54.04	0.41
92		C19H17F6N3OS	449.42	4.61	6.29	35.58	0.42

93		C ₂₀ H ₁₉ F ₆ N ₃ O ₂	447.381	3.43	6.35	48.72	0.45
94		C ₁₈ H ₂₁ F ₆ N ₃ O	409.376	3.42	5.45	35.58	0.61
95		C ₁₉ H ₂₂ F ₆ N ₂ O	408.388	4.34	5.47	23.55	0.63

7.6. Knime Workflows

7.6.1. Amino-Azetidine Library Workflow



7.6.2. 4,6-Fused and 5,6-Bridged Scaffold Decoration Workflow

